



Universitat d'Alacant  
Universidad de Alicante

Useful strategies for the synthesis of 3,3'-  
disubstituted 2-oxindoles and homoallyl alcohols

Cristina Moreno Cabrerizo



Tesis **Doctorales**

UNIVERSIDAD de ALICANTE

Unitat de Digitalització UA

Unidad de Digitalización UA



Universitat d'Alacant  
Universidad de Alicante  
Departament de Química Orgànica  
Departamento de Química Orgánica



## Useful strategies for the synthesis of 3,3'- disubstituted 2-oxindoles and homoallyl alcohols

Manuscript thesis submitted to apply for PhD degree with International  
Mention at the University of Alicante by:

**CRISTINA MORENO CABRERIZO**

Doctoral Program: Organic Synthesis

Scientific advisors:

Carmen Nájera Domingo and José Miguel Sansano Gil

Organic Synthesis Institute (ISO), Science Faculty, University of Alicante

Sant Vicent del Raspeig, 99, E-03080 Alicante, Spain

Tel. +34 965903400. Ext. 2121; +34 5903549; Fax +34 965903549

<http://iso.ua.es> ; iso@ua.es



## Acknowledgments/Agradecimientos

---

Hace cuatro años que empecé esta aventura y desde luego me siento muy agradecida por todo lo que he aprendido durante esta etapa.

En primer lugar, quisiera agradecer a mis directores Carmen y JM por haberme dado la oportunidad de formarme tanto académica como profesionalmente durante este periodo. Me siento afortunada por haber podido trabajar con estos magníficos científicos de los que he podido aprender muchísimo.

Also, I want to thank prof. Cozzi for the knowledge he transmitted to me and PostDoc. Andrea Gualandi for the help in the laboratory, my stay in Bologna was very enriching thanks to you and thanks to Elena to make me feel at home.

Por otra parte, también quiero agradecer a todas las personas que me han acompañado durante esta etapa. A los compañeros de laboratorio, por la ayuda y el compañerismo en el trabajo, pero también por tantas horas de risas, agobios, música del Spotify, espectros ruina, columnas interminables, gritos de "irota treeees!", por escuchar de fondo el reguetón de *Villaabajo*, por toda la gente de otros países que han pasado por *Villaarriba* que me han ayudado a soltarme con el inglés y también, (por qué no decirlo) por todas esas cervezas after-lab. Quiero hacer una especial mención a mi *cuartico*, que me hacía llegar al laboratorio con una sonrisa cada mañana.

Sin duda, no hubiera sido lo mismo sin mis amigos en el laboratorio: Aitor, Alejandro y Marcos, me habéis ayudado y escuchado siempre que lo he necesitado. Al Consejo de Sabios por nuestras terapias semanales y al resto de los Quimicuchos. En 2008 nos juntamos por la Química y 12 años después sigue existiendo química entre nosotros.

A Manu que a pesar de venir de "mundos" distintos, has escuchado todas mis charlas sobre oxindoles. Gracias por tu apoyo y por tu amor.

Por último, pero no menos importante, a mi familia (Sora incluida). A mi padre y a mi madre por acompañarme, ayudarme, apoyarme y quererme en todos los pasos de mi camino. Y a ti Fran, mi hermano, mi amigo, mi persona especial, espero ayudarte en tu camino como tú lo haces en el mío. Os quiero mucho.







*A mis abuelas y abuelos*

Universitat d'Alacant  
Universidad de Alicante



## INDEX

---

<b>PREFACE</b>	<b>13</b>
<b>INTRODUCTION I: OXINDOLES AND DEACYLATIVE ALKYLATION</b>	
<b><i>1. Oxindoles</i></b>	<b>17</b>
1.1. A brief description about oxindole	17
1.2. History of other basic structures in relation with oxindoles	18
1.3. Oxindoles and their pharmaceutical significance	19
1.3.1. Anti-VIH agents	19
1.3.2. Anti-cancer agents	20
1.3.3. Anti-inflammatory agents	21
1.3.4. Sleep-inducers	22
1.3.5. Latest considerations	23
1.4. Synthesis of oxindoles	24
1.4.1. Synthesis by ring construction from 2-substituted nitrobenzene and 2-substituted aniline	24
1.4.2. Synthesis by ring construction from 2-unsubstituted anilines	25
1.4.3. Synthesis from acylated anilines	26
1.4.4. Synthesis of oxindoles by ring contraction	27
1.4.5. Synthesis by reduction of isatins	28
1.4.6. Synthesis of oxidation of indoles	28
1.5. Synthetic strategies for the preparation of 3,3-disubstituted oxindoles	29
1.5.1. Nucleophilic addition to isatins	30
1.5.2. Direct functionalization of 3-substituted oxindoles	32
1.5.2.1. Alkylation reaction	32
1.5.2.2. Fluorination reaction	33



1.5.2.3. Hydroxylation reaction	34
1.5.2.4. Michael-type addition	35
1.5.3. Intramolecular coupling reactions	36
1.5.4. Reaction based on O-substituted oxindoles	38
1.5.5. Methyleneindolinones as substrates	39
1.5.6. Oxindoles as electrophiles	40

## ***2. Deacylative alkylation.*** **41**

2.1. Procedure and description	41
2.2. Application of DaA in oxindoles	44

## **CHAPTER I: Deacylative Alkylation (DaA) of N-methyl-3-acetyl-2-oxindole for the synthesis of symmetrically 3,3-disubstituted 2-oxindoles.**

I.1. Background	53
I.2. Objectives	54
I.3. Results and discussion	55
I.4. Conclusions	63
I.5. Experimental section	64
1. General methods	64
2. Experimental procedure	64
3. Experimental data	66

## **CHAPTER II: Deacylative Bromination (DaB) for the synthesis of 3,3'-bioxindoles and isolation of 3-bromooxindoles.**

II.1. Background	75
II.2. Objectives	79
II.3. Results and discussion	80
II.4. Conclusions	95
II.5. Experimental section	96
1. General methods	96

2. Experimental procedure	96
3. Experimental data	99

## **Introduction II: Photocatalysis and dual catalysis**

### ***1. Photocatalysis.*** **111**

1.1. A brief introduction to this field	111
1.2. Guidelines to understanding photoreactions	112
1.3. Development of photocatalysis in organic synthesis	114
1.4. Activation mechanism in photoredox catalysis	116
1.5. Background about photocatalysis	119
1.5.1. Oxidative process	119
1.5.2. Reductive process	120
1.5.3. Activation via energy transfer	121
1.6. Bioxindoles prepared using photocatalysis	122

### ***2. Dual catalysis*** **125**

2.1. Nickel metallaphotocatalysis	126
2.2. Palladium metallaphotocatalysis	128
2.3. Cobalt metallaphotocatalysis	130
2.4. Latest considerations	131

## **CHAPTER III: Photoredox catalysis in the synthesis of 3,3'-bioxindoles.**

III.1. Background	135
III.2. Objectives	137
III.3. Results and discussion	138
III.4. Conclusions	148
III.5. Experimental section	149
1. General methods	149

2. Experimental procedure	149
3. Experimental data	150
<b>CHAPTER IV: Catalytic photoredox allylation of aldehydes promoted by a cobalt complex.</b>	
IV.1. Background	157
IV.2. Objectives	162
IV.3. Results and discussion	163
IV.4. Conclusions	173
IV.5. Experimental section	174
1. General methods	174
2. Experimental procedure	174
3. Experimental data	175
<b>REFERENCES</b>	<b>185</b>
<b>ABBREVIATIONS</b>	<b>197</b>
<b>SUMMARY IN SPANISH/ RESUMEN EN CASTELLANO</b>	<b>203</b>
<b>BIOGRAPHY</b>	<b>237</b>



**PREFACE**

Universitat d'Alicant  
Universidad de Alicante





## Preface

---

In this doctoral thesis, facile strategies for the synthesis of 3,3-disubstituted 2-oxindoles and homoallyl alcohols are described. The project concerning the oxindole derivatives have been carried out under the supervision of Prof. Carmen Nájera Domingo and Prof. José Miguel Sansano Gil and were developed in the Organic Chemistry Department and the Organic Synthesis Institute at the University of Alicante (Spain). Regarding the preparation of homoallyl alcohols part of this doctoral thesis, it has been developed during my three months stay at the University of Bologna (Italy) under the supervision of Prof. Pier Giorgio Cozzi.

This thesis is divided in two big blocks, the first one includes introduction I, chapter I and chapter II. In which it describes the importance of the oxindoles in synthetic organic chemistry and Deacylative Alkylation as a facile strategy for the synthesis of 3,3'-disubstituted 2-oxindoles.

The second part is formed by introduction II, chapter III and chapter IV and it is referred to photocatalysis and dual catalysis as a methodology for preparation 3,3'-disubstituted 2-oxindoles and homoallyl alcohols respectively.

Most of the results described in this doctoral thesis have been published in the following international peer reviewed journals:

“*Synthesis of 3,3-Disubstituted 2-Oxindoles by Deacylative Alkylation of 3-Acetyl-2-oxindoles*” A. Ortega-Martínez, C. Molina, C. Moreno-Cabrerizo, J. M. Sansano, C. Nájera, *Synthesis* **2017**, 49, 5203–5210.

“*Deacylative alkylation (DaA) of N-methyl-3-acetyl-2-oxindole for the synthesis of symmetrically 3,3-disubstituted 2-oxindoles. An access gate to anticancer agents and natural products*” C. Moreno-Cabrerizo, A. Ortega-Martínez, C. Molina, C. Nájera, J. M. Sansano, *An. Acad. Bras. Cienc.* **2018**, 90, 1089–1099.

“*Deacylative Reactions: Synthetic Applications*” A. Ortega-Martínez, C. Molina, C. Moreno-Cabrerizo, J. M. Sansano, C. Nájera, *European J. Org. Chem.* **2018**, 2394–2405.

"*Deacylative alkylation versus photoredox catalysis in the synthesis of 3,3'-bioxindoles*" C. Moreno-Cabrerizo, A. Ortega-Martínez, M. A. Esteruelas, A. M. López, C. Nájera, J. M. Sansano, *Eur. J. Org. Chem.* **2020**, 3101–3109.

"*Catalytic Photoredox Allylation of Aldehydes Promoted by a Cobalt Complex*" A. Gualandi, G. Rodeghiero, C. Moreno-Cabrerizo, C. Foucher, M. Marchini, P. Ceroni, and P. G. Cozzi, Manuscript in progress.

Furthermore, during my Ph.D time, I collaborated with my research group in these works (not included in this manuscript):

"*4-Amino-3-pentadecyl-3H-1,2,4-triazole-3-thiones and 3-pentadecyl-1,3,4-oxadiazole-2(3H)-thione for the preparation of dimeric palladium(II) complexes and their applications in Tsuji–Trost and Mizoroki–Heck reactions*" M. Chehrouri, A. A. Othman, S. Jiménez-Cecilia, C. Moreno-Cabrerizo, J. M. Sansano, *Synth. Commun.* **2019**, 49, 1301–1307.

"*Synthesis of 5-heptadecyl- and 5-heptadec-8-enyl substituted 4-amino-1,2,4-triazole-3-thiol and 1,3,4-oxadiazole-2-thione from (Z)-octadec-9-enoic acid: preparation of Palladium(II) complexes and evaluation of their antimicrobial activity*" M. Chehrouri, A. A. Othman, C. Moreno-Cabrerizo, M. Gholinejad, J. M. Sansano, *Monatsh. Chem.* **2020**, 151, 173–180.

"*4-Amino-1,2,4-triazoles and 1,3,4-oxadiazoles palladium(II) recoverable complexes as catalysts in the sustainable Suzuki-Miyaura cross-coupling reaction*" M. Chehrouri, C. Moreno-Cabrerizo, A. Othman, I. Chabour, M. Ferrándiz-Saperas, I. Sempere, H. A. Döndaş, J. Sansano, *J. Organomet. Chem.* **2020**, 923, 121353.

*Development of Diels-Alder and aldol condensation-based synthetic methodology with specific application to fragrance ingredients manufacture.* Private project of IFF-BLO and University of Alicante

Finally, I gratefully acknowledge financial support from the Spanish Ministerio de Ciencia e Innovación (MICINN) (projects CTQ2010-20387 and Consolider Ingenio 2010, CSD2007-00006), the Spanish Ministerio de Economía y Competitividad (MINECO) (projects CTQ2013-43446-P and CTQ2014-51912-REDC), the Spanish Ministerio de Economía, Industria y Competitividad, Agencia Estatal de Investigación (AEI) and Fondo Europeo de Desarrollo Regional (FEDER, EU) (projects CTQ2016-76782-P and CTQ2016-81797-REDC), the Generalitat Valenciana (PROMETEO2009/039 and PROMETEOII/ 2014/017) and the University of Alicante.



**INTRODUCTION I:  
OXINDOLES AND DEACYLATIVE ALKYLATION**

Universitat d'Alacant  
Universidad de Alicante

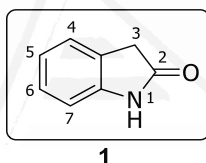




## 1. Oxindoles

### 1.1. A brief description about oxindole

Oxindole is an organic heterocyclic compound having a benzene ring fused with the pyrrole ring with a carbonyl group at 2-position. It is the core structure in a variety of natural products and drugs.



Chemically named 1,3-dihydro-2H-indole-2-one, oxindole exists as two hydroxyl tautomers (**I'** and **I'''**) (Figure 1),<sup>[1]</sup> but nuclear magnetic resonance (NMR) spectra are indicative of an overwhelming predominance of the keto form (**I'**). In the infrared spectrum the stretching of the keto group results in an intense absorption in the 1690-1752  $\text{cm}^{-1}$  region.<sup>[2]</sup> Oxindole is quite acidic and Bordwell has reported a  $\text{pK}_a$  value of 18.2 for the oxindole and 18.5 for *N*-methyloxindole. It was concluded that  $\text{pK}_a$  values for the NH and CH acidic sites in oxindole are about equal.<sup>[3]</sup>

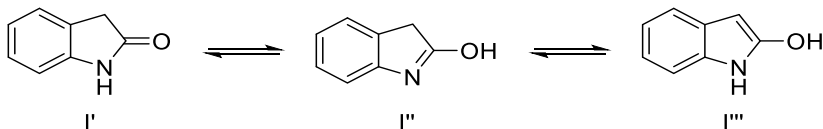


**Figure 1.** Tautomerism in oxindole

The oxindole is the form of alkaloids are extracted from the cat claw's plant *Uncaria tomentosa*, which is a woody, tropical vine indigenous to the Amazon rainforest and other tropical areas of South and Central America.

Being abundant in nature, it has been found in tissues and fluids of mammals as well as natural products produced by a range of plants, bacteria and invertebrates. It can be obtained from synthetic or natural origin and displays a wide range of biological activities. For example, it is used for the treatment of infections, cancer, gastric ulcers, arthritis and other inflammatory processes.

Oxindole and its derivatives are also versatile substrates in multiple kinds of reactions. In this thesis, the focus the attention on the applications of oxindole in various organic reactions on the C-3 site.

## 1.2. History of other basic structures in relation with oxindoles

The early development of oxygenated derivatives of indole **2**, such a oxindole **1** and isatin **3**, was strongly intertwined with the chemistry of the indigo **4** (Figure 2).<sup>[4]</sup>

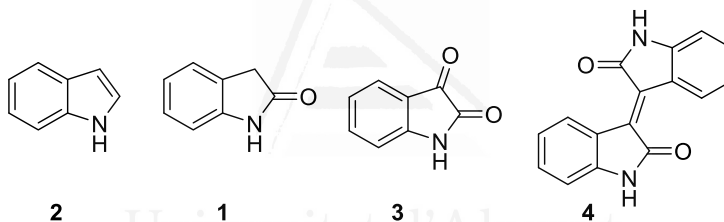


Figure 2. Structures in relation with oxindole

Indole chemistry and its derivatives began to develop with the study of the dye indigo. Adolf Baeyer (later Adolf von Baeyer), was the first to report oxindole structure in 1866 by reduction of isatin. In the 1930s, the interest in indole was intensified when it became known that the indole substituent is present in many important alkaloids for instance, tryptophan and auxins, and it remains as an active area of research today.

In fact, it should be noted that the activity in the field of oxindole chemistry has been intense in recent years. Many scientific articles and reviews, particularly on spirocyclic oxindoles (it will see an example of spirocyclic oxindole in the chapter I) appeared in the literature.

### 1.3. Oxindoles and their pharmaceutical significance

As previously mentioned, oxindole is a skeleton core of multiple pharmaceutical compounds. During this section some examples will be described, thus demonstrating the importance of these molecules and seeing their applicability and benefits for human beings. Below are some structures to exhibit an extensive range of biological effects.

#### 1.3.1. Anti-HIV agents

Acquired Immune Deficiency Syndrome (AIDS) is a global health threat and the leading cause of deaths due to infectious disease. More than 20 million people have died of AIDS since the first reported cases in 1981, with 3.1 million deaths in 2004 alone Joint United Nations Program on HIV and AIDS and World Health Organization (UNAIDS/WHO). Rates of new human immunodeficiency virus (HIV) infections in developing countries continue to climb at an alarming rate, largely due to the high cost of the current drug regimen. More effective, safer, and economical drugs targeting drug-resistant virus are needed in order to control the spread of the disease.<sup>[5]</sup>

Herein it shows the novel synthetic oxindoles (Figure 3) discovered as a potent non-nucleoside reverse transcriptase inhibitor using high throughput screening (HTS). The molecules not only define its structure–activity relationship (SAR), but also lead to the identification of increase antiviral activity targeting the early stages in HIV infection.

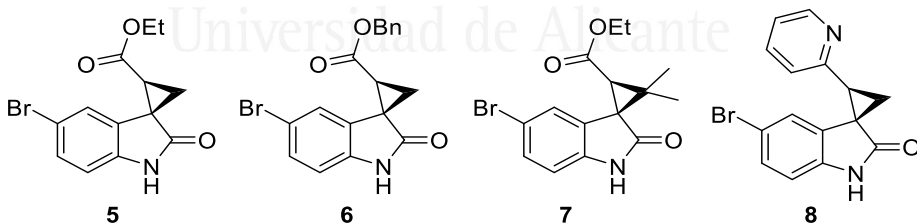


**Figure 3.** Anti-HIV oxindole derivatives structures



### 1.3.2. Anti-cancer agents

Oxindoles have also been credited with antitumor activity by inhibiting tyrosine kinase receptors such as PDGF-R  $\beta$ , VEGF-R or CDK. An important example is the indolin-2-one Sunitinib **9** (Figure 4). This compound has been used in the treatment of gastrointestinal stromal tumors, and metastatic renal cell cancer. Sunitinib is a commercially available medicine that costs 1382 € per 30 pills of 12.5 mg of the oxindole derivative as active ingredient. Due to the high cost of this type of medication, one of the objectives of organic synthesis is to find new strategies to synthesize economically this drug.

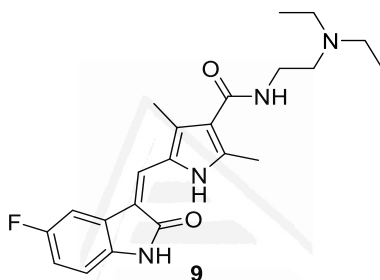


**Figure 4.** Sunitinib structure

On the other hand, the last studies demonstrated that there are a potent aryl-sulfoanilide-oxindole hybrid **10** (Figure 5) that inhibits the growth of cancer cells by partial depletion of intracellular calcium stores and phosphorylation of eIF2 $\alpha$ . These hybrid compounds are used as antiproliferative agents and also inhibits the initiation of translation.<sup>[6]</sup>

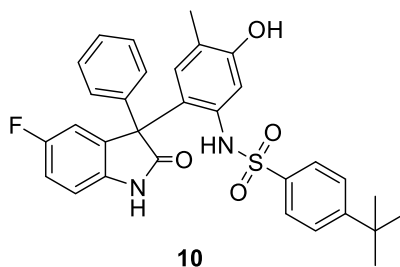


**Figure 5.** Arylsulfoanilide-oxindole hybrid

### 1.3.3. Anti-inflammatory agents

It has been observed that certain ketones containing 1-substituted oxindoles-1-carboxamide **11** (Figure 6) act as analgesic and anti-inflammatory agents. They act by inhibiting the modulating properties of enzymes lipoxygenase (LO) and cyclooxygenase (CO), useful for treating rheumatoid arthritis and osteoarthritis.<sup>[7]</sup>

One example of these type of medical drugs is Tenidap. Tenidap<sup>[8]</sup> is a once-daily, cytokine modulating antirheumatic drug indicated for the treatment of rheumatoid arthritis (RA). In RA patients, Tenidap 120 mg/day is clinically equivalent to the combination of disease-modifying antirheumatic agents plus non-steroidal anti-inflammatory drugs (NSAIDs). The drug had in 1996 a controversial problem due to Pfizer was under the development of these promising potential drug but the FDA rejected the marketing approval because of the liver and kidney toxicity, which was attributed to target metabolites of drug with thiophene moiety that caused oxidative damage.

In the same way, the last studies about some 3-substituted-1-carboxamides and their pharmaceutically active salts are recommended for the prevention and treatment of Alzheimer disease in humans and mammals, and the symptoms of such disease like impairment of memory and Alzheimer's dementia.

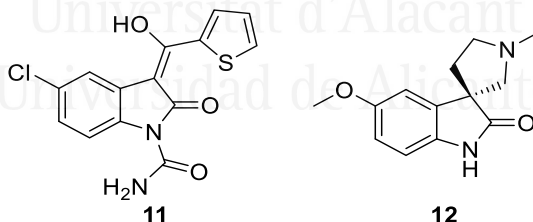


**Figure 6.** Oxindole derivatives with analgesic effects

However, there are also other examples of natural oxindoles derivatives that presents analgesic effects. Is the case of the horsfiline.<sup>[9]</sup> (-)-Horsfiline **12** (Figure 6) was first isolated in 1991 from the leaves of the *Horsfieldia superba* plant. This compound has been a challenge for the synthetic organic chemist during these last years. Nowadays, there are multiple options to synthesize this spirocyclic oxindole and the search of new derivatives.

### 1.3.4. Sleep-inducers

Oxindole itself and certain substituted and/or *N*-alkyl substituted oxindoles have been disclosed in the literature as sedatives and analgesics. For instance, 5-fluorooxindole **9** (Figure 7) is known, which is the motif halo-substituted oxindoles has been associated with pharmaceutical activity.

On the other hand, oxindole itself and certain *N*-alkyl oxindole have been disclosed as possessing CNS depressant activity in mice and other animals. It demonstrated that oxindole has anticonvulsant activity and potentiates hexobarbital anesthesia type effect at moderate dose while causing an anesthetic type effect just prior to death at higher dose. Figure 7 shows some examples of halo-oxindoles employed as sleep inducers:

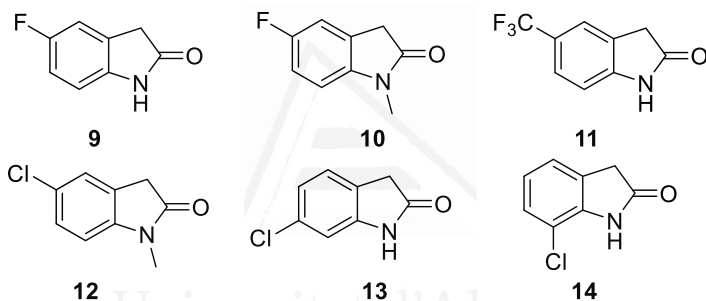


**Figure 7.** Some example of sleep-inducers oxindoles

Our research group are really interested the development of methodologies able to perform new 3-fluorooxindoles.<sup>[10]</sup> We envisaged that 3-acetyl-3-fluoro-2-oxindoles can be easily generated by fluorination of 3-acetyl-2-oxindoles and applied to the synthesis of 3-substituted 3-fluoro-2-oxindoles by base promoted and Pd-catalyzed deaclyative alkylation (DaA).

Further, a new methodology developed for the synthesis and applicability of the 3-bromooxindoles will be described (see Chapter II and III).

### 1.3.5. Latest considerations

To finish this section, it is worth to mention that oxindole has emerged a key nucleus in several natural and synthetic compounds that elicit variety pharmacological responses. As we can see at the (Figure 8) a simple modification in the structure and the substituents bonded to oxindole can modulate the biological activity.

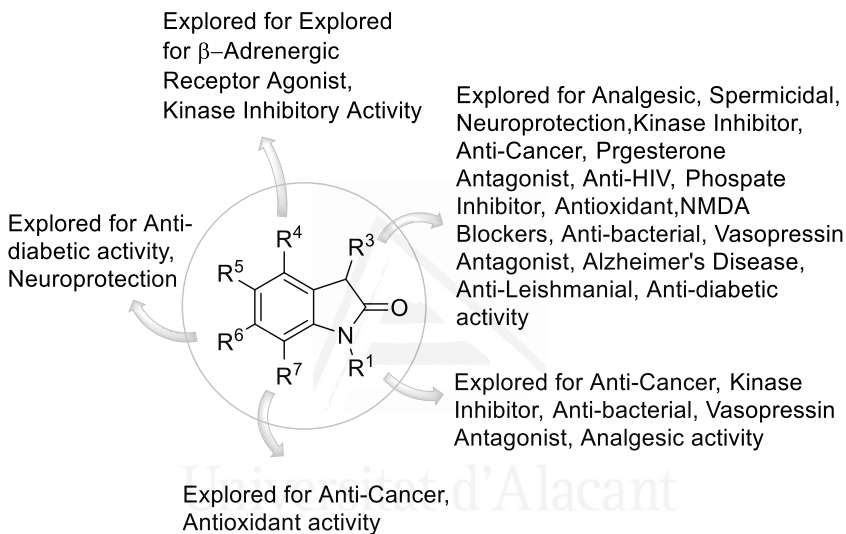
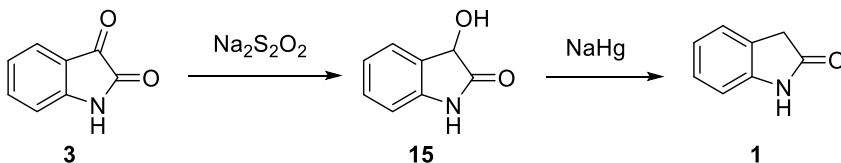


**Figure 8.** Pharmacological profile of oxindole

Although during this introduction only a few effects are described, it is important to know that position C3 of the oxindole has been explored with a multitargeting potential against complex disorders and this is the reason why the major part of this thesis is focused in the reactivity at the 3 position of oxindoles.

## 1.4. Synthesis of oxindoles

In 1866, Baeyer and Knop attempted the synthesis of oxindole nucleus *via* reduction of isatin with sodium dithionite and sodium amalgam in an alkaline medium (Scheme 1).

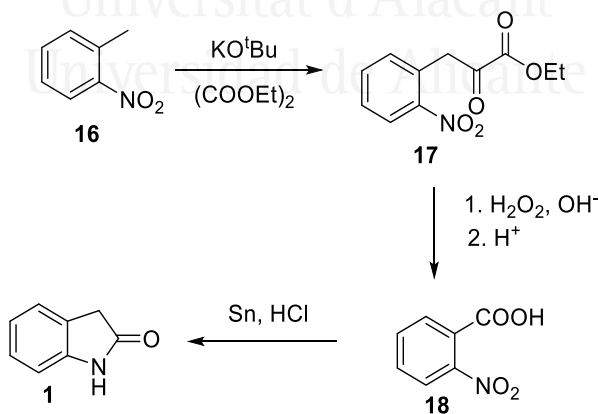


**Scheme 1.** Bayer synthesis of oxindole

Nowadays, there are many ways to prepare oxindoles.<sup>[4]</sup>

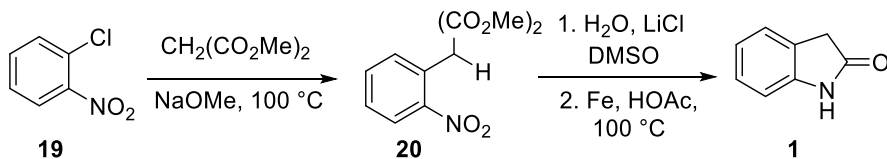
### 1.4.1. Synthesis by ring construction from 2-substituted nitrobenzene and 2-substituted aniline

As shown in (Scheme 2), 2-nitrophenylacetic acid underwent reductive cyclization (**18**→**1**). This method was developed by Baeyer and has remained the most versatile approach to oxindoles, because requires readily available starting materials by condensation according to the Reissert's method (**16**→**17**).<sup>[11]</sup>



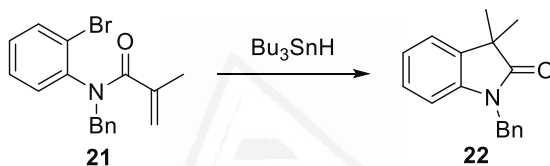
**Scheme 2.** Synthesis from 2-nitrophenylacetic acid

When 2-alkylnitrobenzenes are not available, nucleophilic aromatic substitutions using dialkyl malonates can be employed (Scheme 3).<sup>[12]</sup>



**Scheme 3.** Synthesis from dialkyl malonates

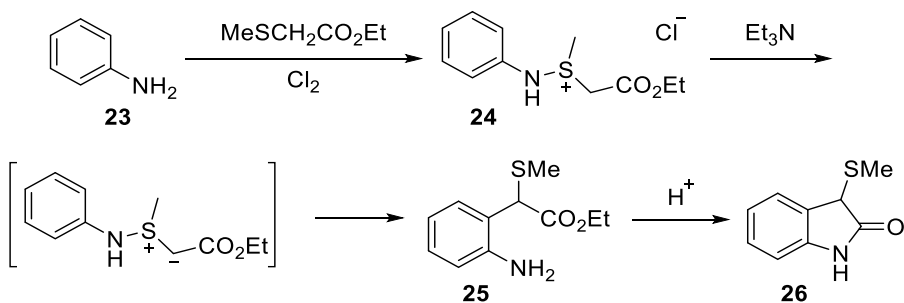
Finally, suitably substituted 2-haloanilines can be cyclized to oxindoles by transformation of the halo substituent to an aryl radical using  $\text{Bu}_3\text{SnH}$  (Scheme 4).<sup>[13]</sup>



**Scheme 4.** Synthesis from 2-haloaniline

### 1.4.2. Synthesis by ring construction from 2-unsubstituted anilines

Gassman introduced in 1973 a method where derivatives based on 2-substituted nitrobenzene were not required instead anilines were used as starting materials (Scheme 5).<sup>[14]</sup>

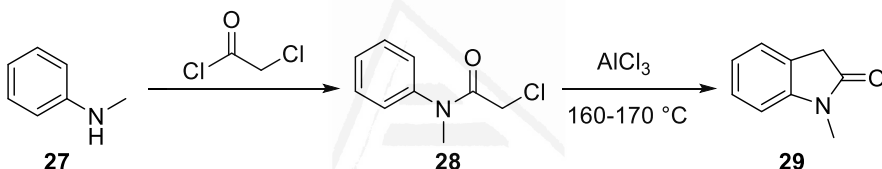


**Scheme 5.** Gassman synthesis

In the first step, the sulfur atom is attacked by chlorine and the S-Cl bond is formed, which is displaced by aniline to give the salt **24**. Abstraction of a proton gave the unstable ylide that can undergo a Sommelet-Hauser rearrangement to **25**, which underwent cyclization to 3-(methylthio)oxindole.

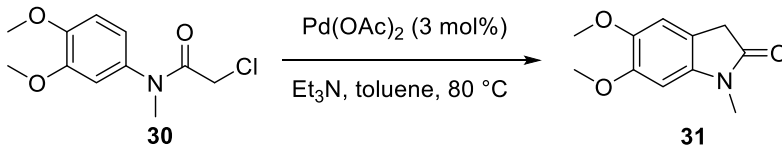
### 1.4.3. Synthesis from acylated anilines

Anilines are easily acylated by chloroacetyl chloride and the amides, formed in a few minutes, cyclized upon heated (160-170 °C) with  $\text{AlCl}_3$  yielding the corresponding oxindole (Stollé reaction). Especially, this route is by far the best synthetic route to *N*-methyloxindole (Scheme 6). However, it is not surprising that methoxy groups do not resist under the severe conditions of the Stollé reaction.<sup>[15]</sup> If an alkoxy substituent is indeed required a final alkylation step is necessary.



**Scheme 6.** Stollé reaction to synthesize *N*-methyloxindole

A way to avoid some of the problems discussed above has been devised by Buchwald using a Pd-catalyzed CH functionalization (Scheme 7).<sup>[16]</sup> With this methodology, several functional groups (e.g., OMe, OTs, TMS,  $\text{CF}_3$ ) will tolerate these conditions in contrast to the Stollé method.



**Scheme 7.** Buchwald reaction using Pd-catalyzed CH functionalization

Buchwald's methodology has also been employed for the synthesis of key intermediates in the route to biologically active molecules, such a serine palmitoyl transferase inhibitor **32** and the key intermediate **33** (Figure 9).<sup>[17]</sup>



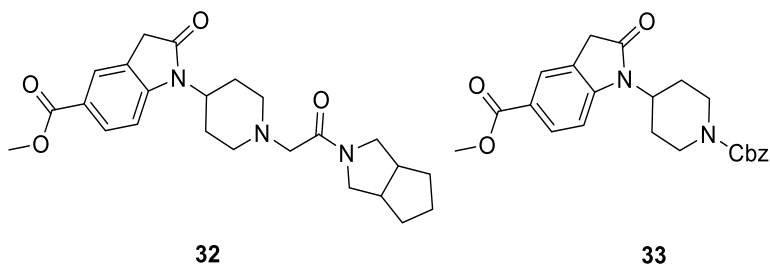
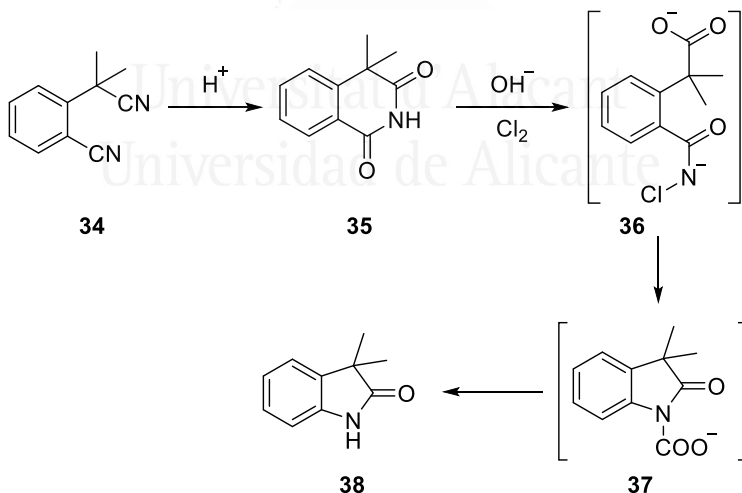


**Figure 9.** Key intermediates for the synthesis of biologically active oxindoles

#### 1.4.4. Synthesis of oxindoles by ring contraction

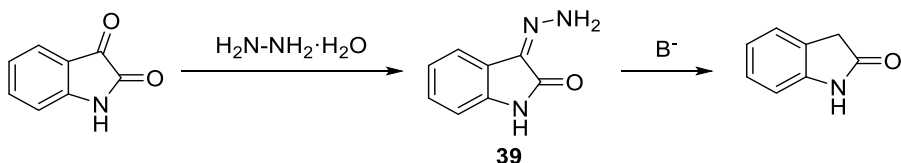
Jönsson and Moses<sup>[18]</sup> reported in 1974 the transformation outlined in Scheme 8, which features a Hoffmann rearrangement (**36**→**37**) as the crucial step leading to the oxindole **38**. Parallely, 3,3-spirocyclohexano-oxindole can be similarly prepared. But this method has been rarely used, probably due to its anonymity and the unavailability of the starting materials. However, the synthesis of 3,3-spirooxindoles should be competitive. During Chapter I, different ways to prepare spirooxindoles, will be covered.



**Scheme 8.** Synthesis of oxindoles by ring contraction

### 1.4.5. Synthesis by reduction of isatins

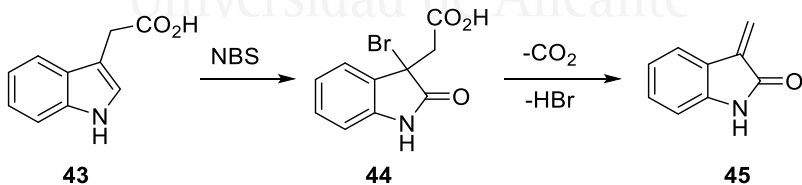
Isatins are often more readily available than oxindoles and hence reductions leading to oxindoles are an attractive synthetic method, particularly Wolff-Kishner reduction using hydrazine hydrate (Scheme 9).<sup>[19]</sup> It produces an intermediate hydrazone, which evolves to the reduced product.



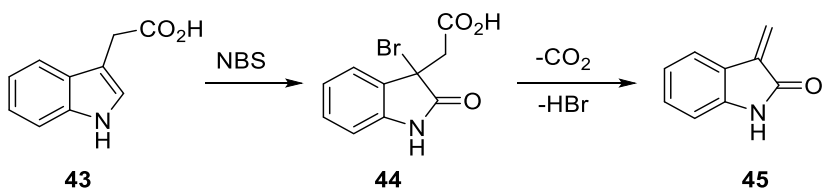
**Scheme 9.** Wolff-Kishner reduction of isatin

### 1.4.6. Synthesis by oxidation of indoles

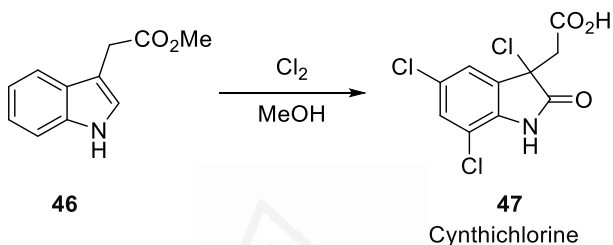
Wiktop introduced *N*-bromosuccinimide (NBS) as an oxidant for indoles, and in many cases oxindoles with intriguing structures are formed as illustrated in Scheme 10. Another example is depicted in Scheme 11 where indole 3-acetic acid (IAA) is converted to 3-methyleneoxindole *via* 3-bromo derivative.<sup>[20]</sup> Also, chlorine in methanol can be used in a similar way to NBS as illustrated by the preparation of the ester to form cynthichlorine (Scheme 12). Cynthichlorine has been identified as the antifungal metabolite isolated from a bacterium infecting the tunicate *Cynthia savignyi*.



**Scheme 10.** Oxidation of indoles with NBS



**Scheme 11.** Oxidation of indole with NBS



**Scheme 12.** Oxidation of indole with chlorine

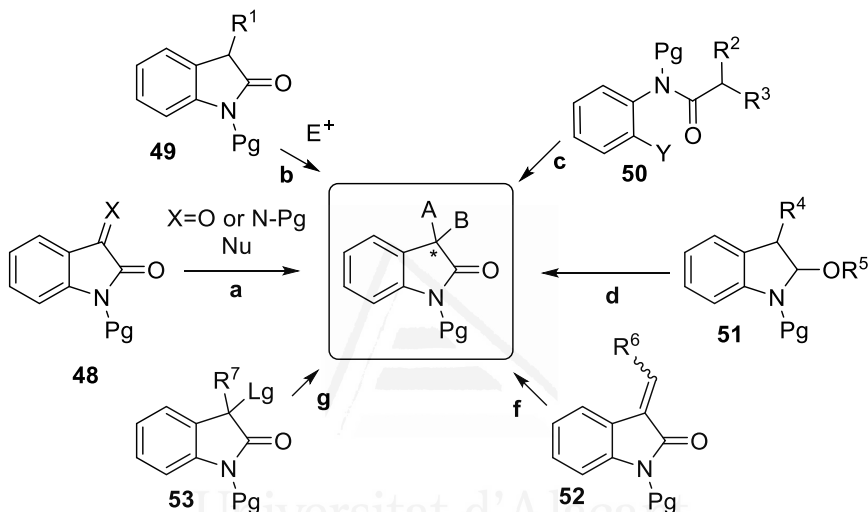
## 1.5. Synthetic strategies for the preparation of 3,3-disubstituted oxindoles

The 3,3-disubstituted oxindoles are a privileged heterocyclic motif that construct the core of a large family of bioactive natural products and a series of pharmaceutically active compounds. Owing to its importance and versatility in the synthesis of these natural products, drugs and analogues, much effort has naturally gone into the asymmetric and symmetric synthesis of 3,3'-disubstituted oxindole framework, which aims to facilitate the synthesis of sufficient quantities of the desired natural products and related analogues for biological evaluation and studies on structure-activity relationships, and finally contributes to the development of new therapeutic agents or important biological tools.

From the synthetic chemistry point of view, during last years, multiple routes to construct the tetrasubstituted carbon a C-3 position of the oxindole framework have been developed.

In summary, these reactions can be classified into the following six categories and they are shown in the next Scheme 13.<sup>[21]</sup>

- Nucleophilic addition to isatins.
- Direct functionalization of 3-substituted oxindoles.
- Intramolecular coupling reactions.
- Reactions based on *O*-substituted oxindoles.
- Methyleneindolinones as substrates.
- Oxindoles as electrophiles.



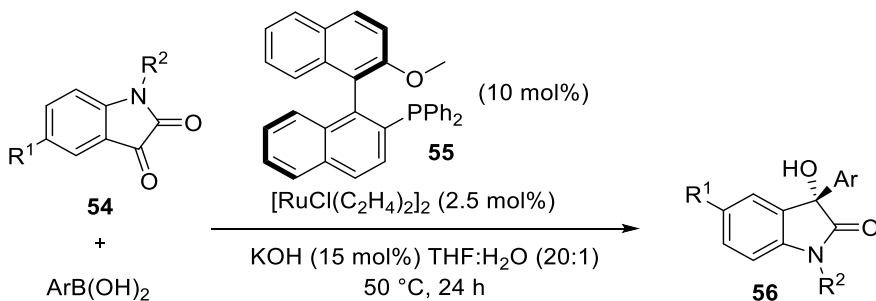
**Scheme 13.** Synthetic strategies for the preparation of 3,3-disubstituted oxindoles

### 1.5.1. Nucleophilic addition to isatins

Isatins are easily available starting materials, so the addition to isatins or related keto imines provides a straightforward method for the preparation of 3-substituted 3-hydroxy or 3-amino-2-oxindoles.

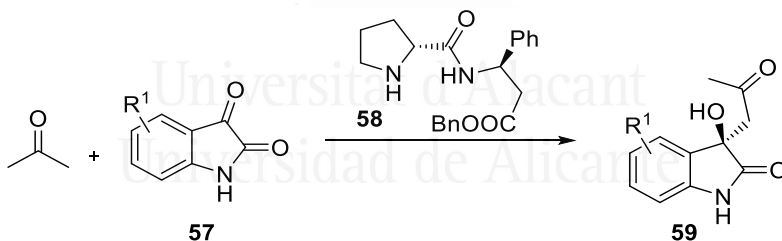
In 2006, Hayashi<sup>[22]</sup> developed the first example of a highly enantioselective addition of arylboronic and alkenylboronic acids to isatins to produce 3-aryl-3-hydroxy-2-oxindoles in high yield (Scheme 14).

In 2009, Krische reported an enantioselective allylation, crotylation and reverse prenylation of isatins via *i*-PrOH-mediated transfer hydrogenation.<sup>[23]</sup>



**Scheme 14.** Hayashi reaction

With the development of asymmetric enamine organocatalysis, the direct cross-aldol reaction of donor carbonyl compounds with highly reactive isatins, in the presence of a chiral enamine catalyst, received much attention and turned out to be a facile method for the construction of the quaternary carbon at the C-3 position of oxindoles. In 2005, Tomasini pioneered the reaction of acetone and isatin, and found that under the catalysis of prolinamide **58**, up to 77% *ee* could be obtained albeit with a limited substrate scope.<sup>[24]</sup>



**Scheme 15.** Cross-aldol reaction

Later, this method was employed for the total synthesis of (*R*)-convolutamydine A,<sup>[25][26]</sup> starting from 4,6-dibromoisatin. Convolutamydine A (Figure 10) is an oxindole alkaloid isolated in low yields from the Floridian marine bryozoan species *Amathia convolute*. The latest investigations highlight the possible pharmacological potential of convolutamydine A as a nociception in mice.

## 1.5.2. Direct functionalization of 3-substituted oxindoles

---

Maybe this section could be the most extensive about the general introduction. This methodology allowed the generation of the desired tetrasubstituted carbon stereocenter with all carbon substituents, or with a heteroatomic substituent. Another merit of this methodology is that 3-substituted oxindoles can be readily prepared by a two-step synthesis from different substituted oxindoles with aldehydes *via* condensation and reduction, from substituted triphenylphosphorane and isatins *via* Wittig reaction and reduction, or from Grignard reagents and isatins *via* nucleophilic addition and reductive deoxygenation. There are multiple routes like Mannich reaction, arylation, amination, etc., but in this case, it describes four categories of reactions that our research group have been able to develop with our methodology.

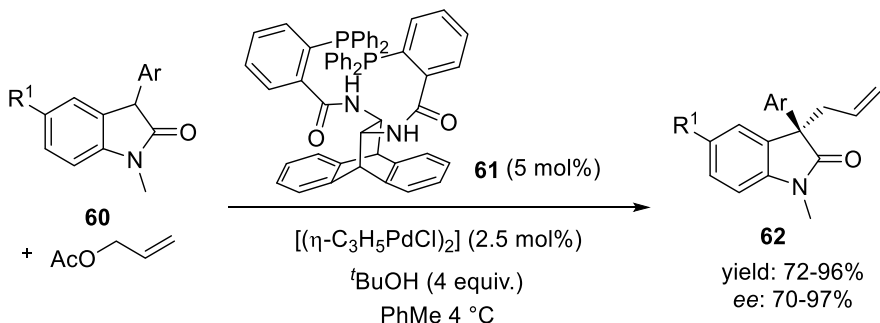
### 1.5.2.1. Alkylation reaction

---

One of the strategies to preparation of 3,3-dialkylated-2 oxindoles was explained in section 1.5.4 preparation of oxindoles by ring contraction (see Scheme 8).

In 1991, Wong reported the probably first example of catalytic asymmetric alkylation of a 3-prochiral oxindole via phase-transfer catalysis, with a yield of 83% and 77% *ee*.<sup>[27]</sup>

Later in 2005, Trost reported a highly enantioselective synthesis of 3-allyl-3-aryloxindole via the Pd-catalyzed asymmetric allylic alkylation (AAA) reaction<sup>[28]</sup>. They found that the ligand **61** derived chiral palladium catalyst could promote the alkylation of several 3-aryloxindoles **60** using allyl acetates to afford the desired products **62** in good to excellent yield and enantioselectivity (Scheme 16).



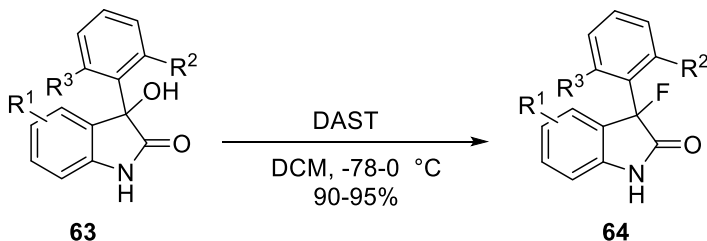
**Scheme 16.** Asymmetric allylic alkylation reaction (AAA)

AAA reaction was applied for the synthesis of (-)-esermethole. Esermethole is an important precursor of the naturally occurring anticholinesterase agent physostigmine (Figure 10) and both compounds are useful in the treatment of glaucoma.

### 1.5.2.2. Fluorination reaction

The fluorination at C-3 position of the oxindole has attracted increasing interest since it was found to be able to enhance the bioactivity of oxindoles derivatives.

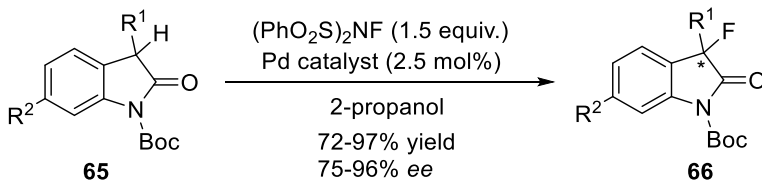
One of the descriptions of the preparation of 3-fluorooxindoles was reported by Starrett in 2002. Starting from 3-aryl-3-hydroxyindol-2-ones **63** as starting material, the fluorination of the tertiary alcohol doing with diethylaminosulfur trifluoride (DAST) in dichloromethane provided the desired 3-aryl-3-fluorooxindol-2-ones **64** in 90–95% yield (Scheme 17).<sup>[29]</sup>



**Scheme 17.** Fluorination of 2-oxindoles at C3 position

In 2005, Sodeoka reported the fluorination of oxindoles under the catalysis of the (*S*)-(-)-2,2'-bis[bis(3,5-dimethylphenyl)phosphino]-1,1'-

binaphthyl [(*S*)-DM-BINAP] derived chiral palladium catalyst. A series of aliphatic or aryl-substituted-*N*-Boc-protected to the desired fluorinated product (Scheme 18) were prepared. *N*-fluorobenzenesulfonamide (NFSI)<sup>[30]</sup> was selected as electrophilic fluorinating agent.

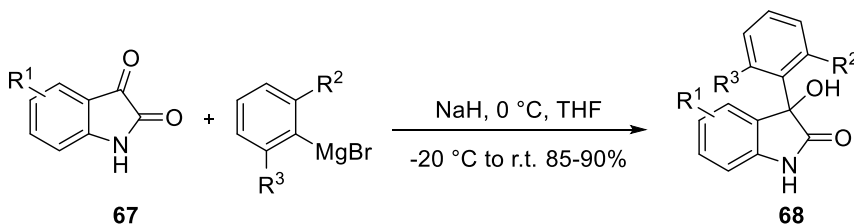


**Scheme 18.** Fluorination at C-3 position

The example with  $R^1=C_7H_7ClO$  and  $R^2=CF_3$  was the key step to the synthesis of BMS 204352 under deprotection of Boc-group with trifluoroacetic acid at 75 °C. BMS 204352 is a promising agent for the treatment of stroke (Figure 10).

### 1.5.2.3. Hydroxylation reaction

Although the nucleophilic addition to isatins provided a facile method for the synthesis of the 3-substituted-3-hydroxy-2-oxindole subunit, the direct hydroxylation of 3-prochiral oxindoles was an alternative useful method. One example of that, was reported by Starret also with the addition of an aryl Grignard reagent to the sodium salt of isatin **67** in THF gave the corresponding 3-aryl-3-hydroxyindol-2-ones **68** in 80–95% yield (Scheme 19).<sup>[29]</sup>



**Scheme 19.** Addition to isatins to prepare 3-hydroxyoxindoles

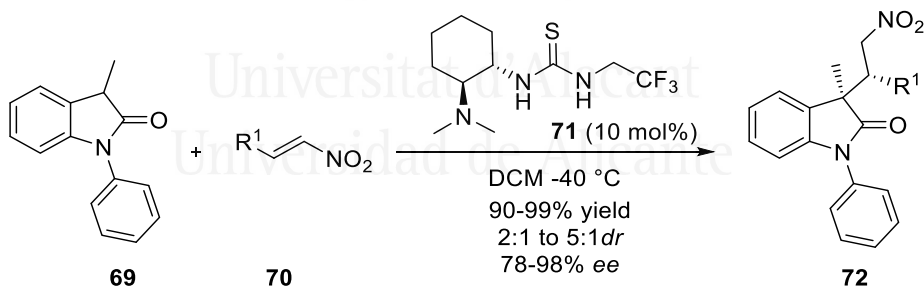
In 2006, Shibata and Toru reported the first example of a highly enantioselective hydroxylation reaction of oxindoles, catalyzed by the DBFOX 60/ $Zn(OAc)_2$  complex, using a racemic oxaziridine in the presence of molecular sieves (MS).<sup>[31]</sup>



In 2008, Itoh developed a highly enantioselective catalytic hydroxylation of 3-prochiral oxindoles using a chiral phase-transfer catalyst with O<sub>2</sub> as an oxidant. It was found that alkyl-, alkenyl-, and alkynyl-substituted oxindoles worked well, affording the desired products in good to excellent enantioselectivities (up to 93%).<sup>[32]</sup> This method was also applied for the formal synthesis of CPC-1. CPC-1 is an alkaloidal constituent in the seeds and rinds of *Chimonanthus praecox* (Figure 10).

#### 1.5.2.4. Michael-type Addition

One of the advantages of the Michael addition at C3-position of the oxindole framework is the possibility of the synthesis of spiral oxindoles or indoline derivatives, because the electron-withdrawing group derived from the Michael-type acceptor in the final Michael adduct, can be further utilized for the ring formation. There are a lot of articles covering this methodology, a recent example was published by Luo and Cheng. They reported the Michael addition of *N*-phenyl-3-methyloxindole to nitroolefins, using a simple bifunctional alkylthiourea catalyst.<sup>[33]</sup> The desired 3,3'-disubstituted oxindole derivatives could be obtained in excellent yield with moderate diastereoselectivity and good to excellent enantioselectivity (Scheme 20).



**Scheme 20.** Michael-type addition with nitroolefins

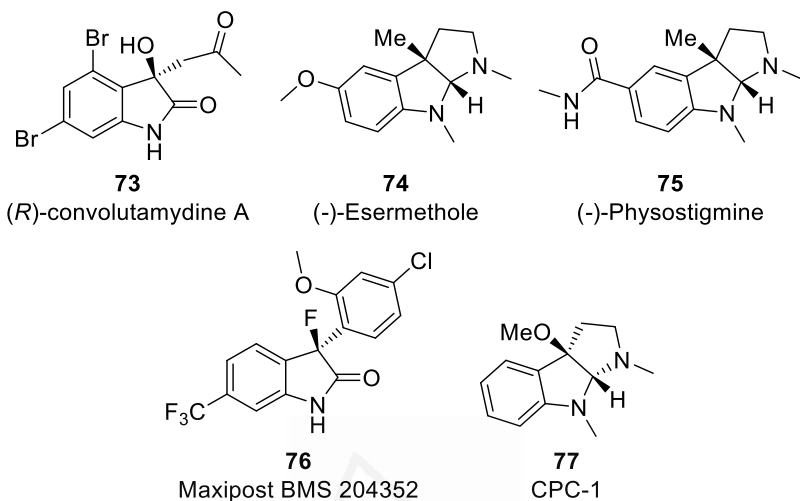
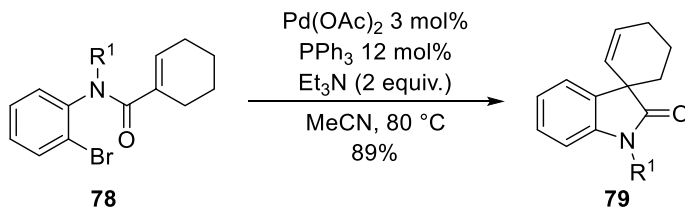


**Figure 10.** Natural and synthetic products prepared by direct functionalization of 3-substituted oxindoles

### 1.5.3. Intramolecular coupling reactions

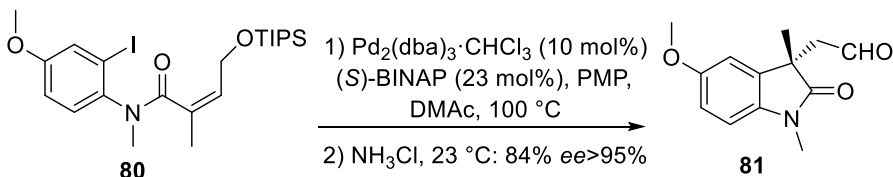
From 1987, Overman's group developed a palladium-catalyzed intramolecular Heck arylations for the synthesis of 3-spiro-2-oxindoles. They observed that the use of 3 mol% of  $\text{Pd}(\text{OAc})_2$ , 12 mol% of triphenylphosphine and 2 equivalents of triethylamine were able to transform the corresponding bromoanilides to the desired 3-spiro-2-oxindole (Scheme 21).<sup>[34]</sup>



**Scheme 21.** Intramolecular Heck reaction

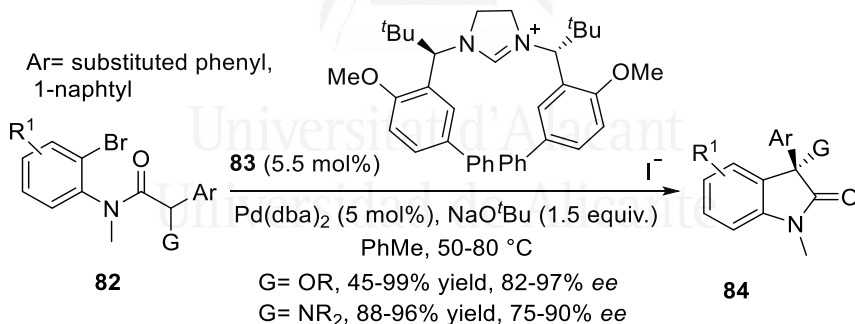
Later in 1993, Overman's group developed a palladium-catalyzed intramolecular Heck reaction of (*Z*)-2-butenoylanilide for the enantioselective version. They found that the use of 20 mol% of a BINAP derived chiral palladium catalyst, in the presence of 1,2,2,6,6-pentamethylpiperidine (PMP), could promote the Heck cyclization of butenoylanilide **80** to form (*S*)-

**81** in good yield and up to 95% *ee* (Scheme 22). This methodology was applied to the total synthesis of (-)-physostigmine and (-)-physovenine. Both bioactive natural products could be synthesized from the same starting material **80** prepared from commercially available 2-butyn-1-ol.<sup>[35]</sup>



**Scheme 22.** Enantioselective intramolecular Heck reaction

Finally, Kündig's group developed the most powerful chiral NHC (*N*-heterocycle carbene) ligand<sup>[36]</sup> in the palladium-catalyzed arylation reaction and could afford products in good to excellent yield and *ee*. Later, Kündig and co-workers applied their new type of ligand **83** in the intramolecular  $\alpha$ -arylation of amides containing heteroatom substituents to furnish chiral 3-substituted, 3-alkoxy- or 3-aminooxindoles in excellent *ee* (Scheme 23).<sup>[37]</sup>



**Scheme 23.** The synthesis of 3-substituted-3-hydroxy or 3-aminooxindoles *via* intramolecular arylation reaction

To conclude with the intramolecular coupling reactions in 2008, Takemoto reported an enantioselective Pd-catalyzed cyanoamidation of olefins which provided a facile method for the synthesis of the 3-alkyl-3-cyanomethyl-2-oxindole subunit.<sup>[38]</sup>

### 1.5.4. Reactions based on *O*-substituted oxindoles

*O*-Substituted oxindoles are versatile building blocks for the catalytic asymmetric construction of quaternary stereocenters at the oxindole framework. Indolyl esters such as indolyl acetates and carbonates are susceptible to undergo nucleophilic intramolecular addition (Figure 11).

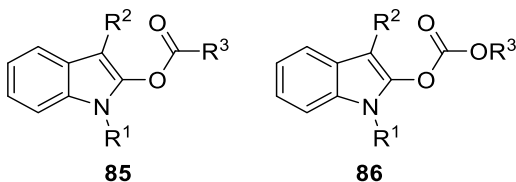
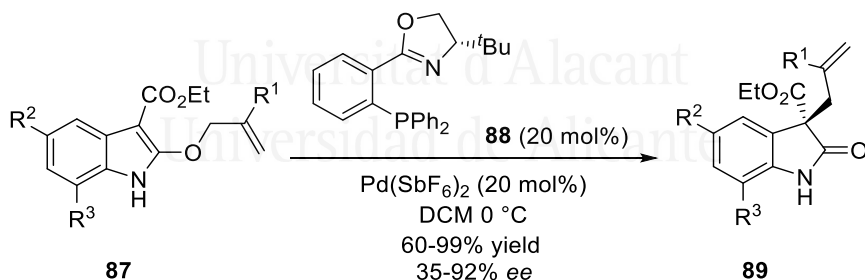


**Figure 11.** *O*-Substituted oxindole structure

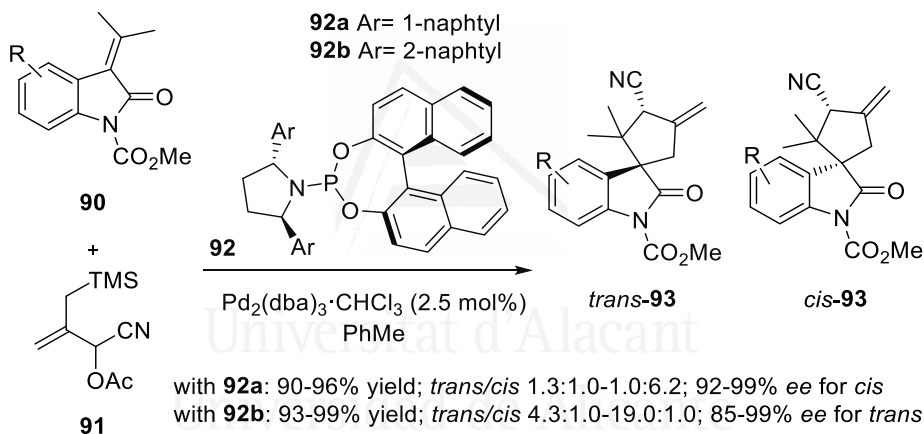
In 2008, Kozłowski reported the first example of catalytic enantioselective Meerwein–Eschenmoser–Claisen rearrangement reaction for the asymmetric synthesis of allyl oxindoles. In the presence of a *t*-BuPHOX **88** derived chiral palladium catalyst, a range of substrates **87** could be readily converted to oxindoles **89** in good to excellent yield and enantioselectivity (Scheme 24).<sup>[39]</sup>



**Scheme 24.** An enantioselective Meerwein–Eschenmoser–Claisen rearrangement reaction

### 1.5.5. Methylideneindolinones as substrates

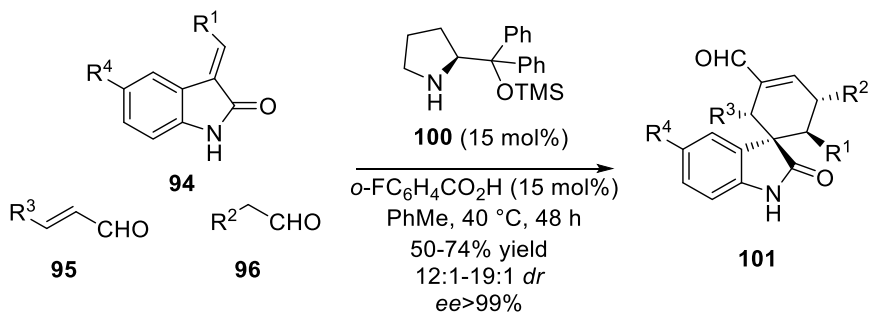
Methylideneindolinones are useful substrates for the synthesis of spirocyclic oxindoles. In 2007, Trost reported an enantioselective palladium-catalyzed [3+2] trimethylenemethane cycloaddition (TMM). They tried trisubstituted or unsymmetrical tetrasubstituted olefins to construct three stereocenters in the cycloadduct, and found that **92a** could promote the reaction to afford the *trans*-product in excellent yields and enantiomeric excess (Scheme 25).<sup>[40]</sup> This method can be potentially used for the asymmetric total synthesis of marcfortine. Marcfortine is one of the indolic alkaloids acting as secondary metabolites isolated from various *Penicillium* species.<sup>[41]</sup>



**Scheme 25.** Pd-catalyzed [3+2] trimethylenemethane cycloaddition

In 2009, Melchiorre reported an organocascade for the construction of spirocyclic oxindoles with multiple stereocenters. Under the catalysis of amine **100**, the three-component cascade reaction involving **94**,  $\alpha$ ,  $\beta$ -unsaturated aldehyde **96** and aldehyde **95** proceeded well to afford spirocyclohexeneoxindoles **101** with good yield and excellent selectivity, *via* a Michael/Michael/aldol condensation sequence (Scheme 26).<sup>[42]</sup>

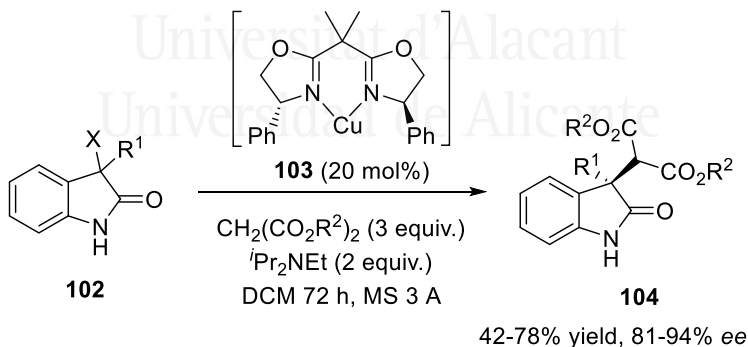
Also, in 2009 Gong reported a novel three-component 1,3-dipolar cycloaddition of a wide variety of different aldehydes, amino esters and methyleneindolinones, catalyzed by a chiral phosphoric acid. This transformation afforded desired spiro[pyrrolidin-3,3'-oxindole] derivatives in excellent yield with unusual regioselectivity and enantioselectivity.<sup>[43]</sup>



**Scheme 26.** Organocascades to spirocyclic oxindoles

### 1.5.6. Oxindoles as electrophiles

While most of the synthetic methods employed 3-substituted oxindoles as nucleophiles, Stoltz used the oxindole moiety as the electrophilic partner to construct the desired quaternary stereocenter. In the presence of a base, 3-halooxindoles might form a highly reactive electrophile, to react with malonate complexed with a chiral Lewis acid. The BOX **103**/Cu(II) complex turned out to be the optimal chiral Lewis acid, and could achieve good yield with up to 94% *ee* (Scheme 27).<sup>[44]</sup>



**Scheme 27.** Oxindole acting as electrophile to generate a quaternary stereocenter

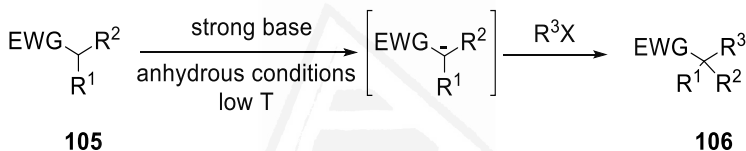
During Chapter II it will show a polar reaction between a mixture of electrophilic and nucleophilic oxindoles.

## 2. Deacylative/decarboxylative alkylation

As it has seen previously, there are several synthetic strategies for the synthesis of 3,3-disubstituted 2-oxindoles which has been developed in the last years. Our research group envisaged that symmetrically and unsymmetrically substituted oxindoles derivatives could be carried out by Deacylative Alkylation (DaA) methodology. In this section, the procedure will be explained in order to review the reported articles.<sup>[45]</sup>

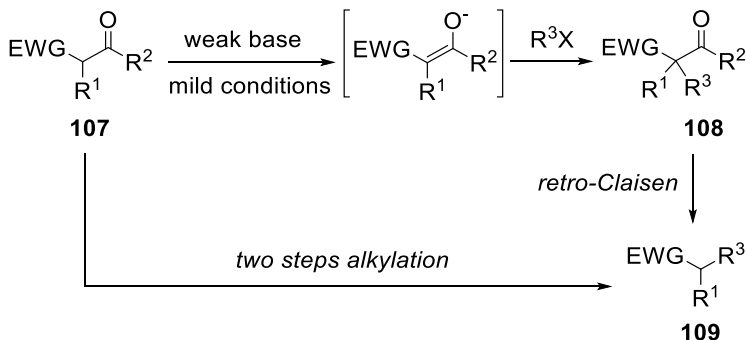
### 2.1. Procedure and description

The classic strategy for the alkylation of enolates requires, usually strict conditions. For the deprotonation step, is necessary the use of strong bases and low temperatures under anhydrous conditions (Scheme 28).



**Scheme 28.** Alkylation of enolates

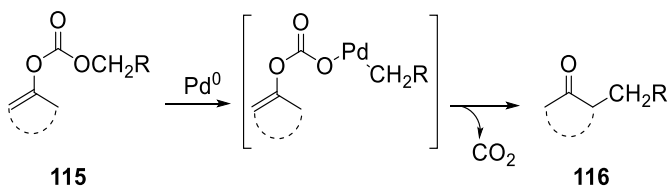
Other methodologies like acetyl acetic and malonic ester syntheses can be performed under mild reaction conditions of base and temperature but, after alkylation and retro-Claisen condensation,<sup>[46]</sup> the corresponding alkylated carbonyl compound can be prepared by means of a two-step procedure (Scheme 29).



**Scheme 29.** Acetyl acetic and malonic ester syntheses



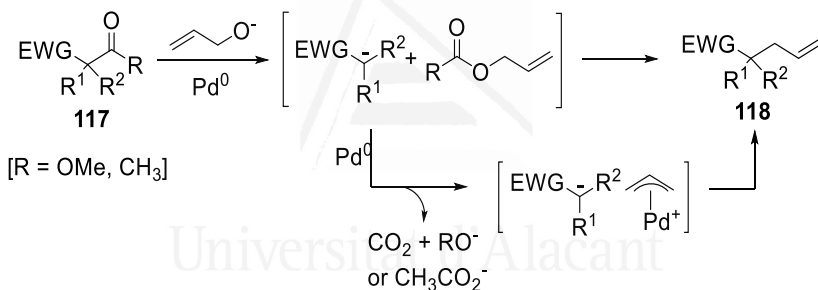




**Scheme 32.** Decarboxylative alkylation (2<sup>nd</sup> mechanism)

These biomimetic decarboxylative reactions (DCA) have been used in aldol, Michael additions and allylic alkylations under neutral conditions and have been applied to the synthesis of natural products.<sup>[48]</sup>

The deacylative allylation (DaA), which is also based on a C-C bond cleavage, can be carried out under palladium-catalysis as well (Scheme 33), and has several advantages *versus* the decarboxylative allylation.

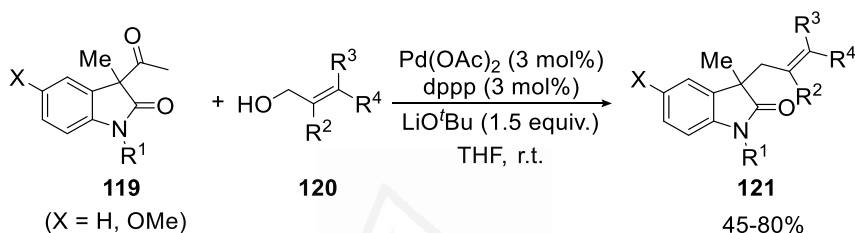


**Scheme 33.** Deacylative allylation

Thus, the synthesis of the acyl derivative can be achieved using simple reaction conditions through a Claisen condensation. In the DaA, the allyl or benzyl group can be introduced using allylic (or benzylic) alcohols and therefore the alkylation takes place directly from the corresponding alcohols. However, the DCA requires the preparation either of the allyl (or benzyl) ester by transesterification or of the allyl (or benzyl) enol ether by means of the corresponding chloroformates.

## 2.2. Applications of DaA in oxindoles

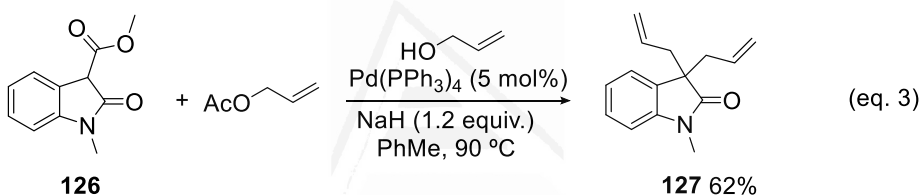
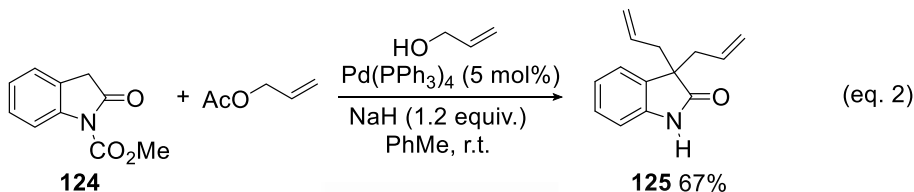
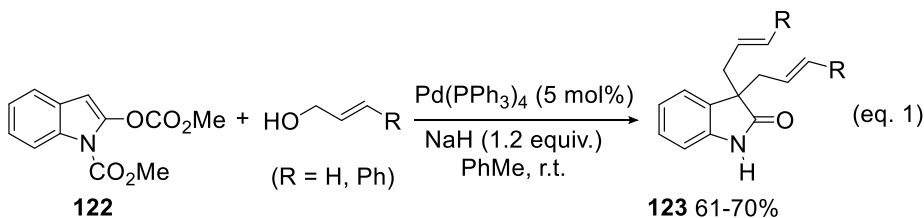
The 2-oxindole unit is present in many natural products and biologically active molecules, specially 3,3-disubstituted 2-oxindoles.<sup>[21,49]</sup> Bisai have reported the Pd-catalyzed deacylative allylation of *N*-alkyl-2-oxindoles bearing a acetyl group at the 3-position with primary allylic alcohols.<sup>[50]</sup> Then, our research group also studied the DaA of 1,3-dimethyl-3-acetyl 2-oxindoles with allylic alcohols (Scheme 34).<sup>[51]</sup>



**Scheme 34.** Pd-catalyzed Deacylative Allylation from 3-acetyl-2-oxindoles

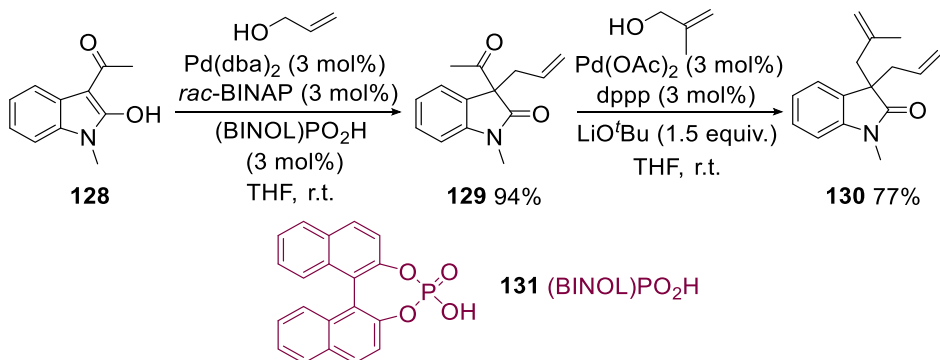
This process took place with 3 mol% of Pd(OAc)<sub>2</sub> and 1,3-bis(diphenylphosphanyl)propane (dppp) using LiO<sup>t</sup>Bu as base at room temperature in tetrahydrofuran (THF) (Scheme 31). Primary and secondary allylic alcohols gave the corresponding 3,3-disubstituted 2-oxindoles in good yields. This process being applied to the synthesis of the precursors of esermethole and horsfiline<sup>[9]</sup> as well as to the access to the acetylcholinesterase inhibitors physostigmine and phenserine.<sup>[7]</sup> This strategy made possible the synthesis of a wide range of 2-oxindoles bearing a quaternary stereocenter at the 3-position. Competitive experiments demonstrated that these alkylation reactions took place through an intermolecular process.

Bisai's group developed *gem*-bisallylation at the 3-position, which has been achieved starting from the *N*-carbamoyl enol acetate with 2.5 equiv. of allylic alcohols giving 3,3-diallylated 2-oxindoles (Scheme 35, eq. 1). A domino process starting from *N*-carbamoyl-2-oxindole (pK<sub>a</sub> ≈ 18–19) or from *N*-methyl-3-methoxycarbonyl-2-oxindole (pK<sub>a</sub> ≈ 16–17), in the presence of both allyl acetate and allyl alcohol, led firstly to Tsuji–Trost allylation and then DaA, giving the corresponding 3,3-diallylated derivatives in 67 % or 62 % yield, respectively (Scheme 35, eq. 2 and eq. 3).<sup>[50]</sup>



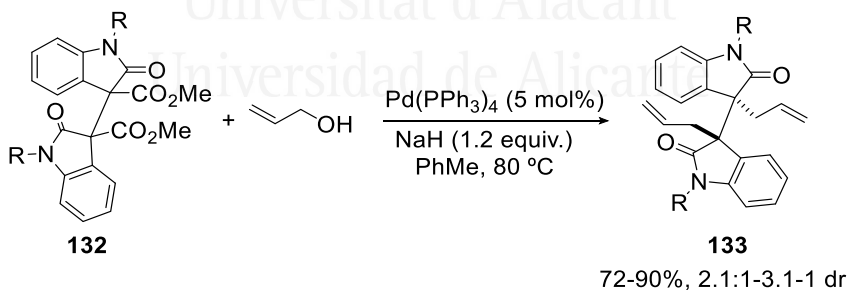
**Scheme 35.** Pd-catalyzed Deaclyative bis-Allylation of 2-oxindoles by Bisai's group

For the bisallylation reaction a two-sequence procedure was reported by our group. The first step, involving the monoallylation of *N*-methyl-3-acetyl-2-oxindole, was carried out under  $\text{Pd}(\text{dba})_2$  and *rac*-BINAP catalysis. In order to avoid the retro-Claisen reaction, acidic conditions were ensured by the employment of the phosphoric acid derived from racemic BINOL as cocatalyst. The second step was performed with a different allylic alcohol using the same DaA reaction conditions affording the corresponding diallylated oxindole in 72 % overall yield (Scheme 36).<sup>[51]</sup>



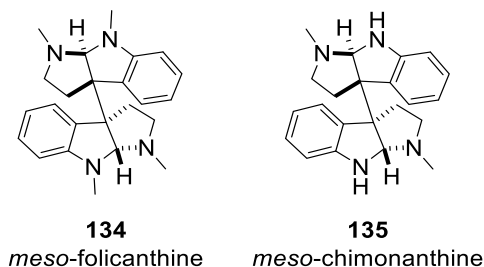
**Scheme 36.** Pd-catalyzed bisallylation of *N*-methyl-3-acetyl-2-oxindole

The former methodology has been applied to the synthesis of dimeric cyclotryptamine alkaloids<sup>[52]</sup> such as *meso*-folicanthine and *meso*-chimonanthine (Figure 12). Dimeric 2-oxindole underwent DaA with allyl alcohol in toluene at 80 °C forming the corresponding diallylated *meso*-bioxindoles in good yields as describes Bisai's group (Scheme 37).<sup>[50]</sup> The *N*-methylated derivative is a useful intermediate for the total synthesis of racemic folicanthine<sup>[53,54]</sup> and the *N*-benzylated dimeric compound was transformed into *meso*-chimonanthine, which is a precursor of *meso*-calycanthine.<sup>[55,56]</sup>

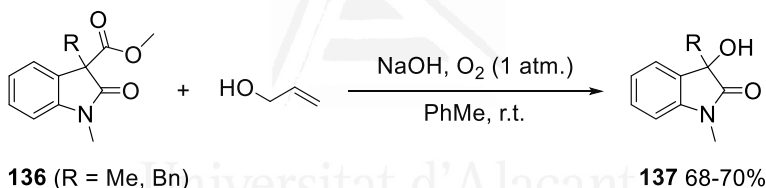


**Scheme 37.** Pd-catalyzed Deacylative Allylation of dimeric 2-oxindoles

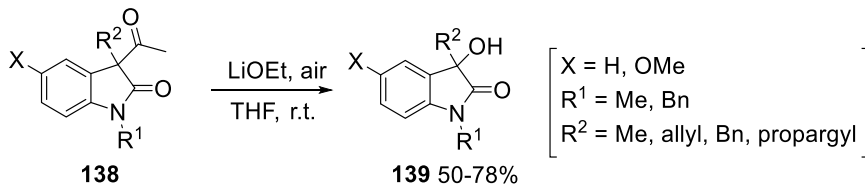
One of the goals of this thesis is improve the synthesis of dimeric 2-oxindoles, during the next chapters it will see new strategies for the preparation of these molecules.

**Figure 12.** Cyclotryptamine alkaloids

Bisai's group also described during their studies on Pd-catalyzed deacylative allylation of methyl 2-oxindole-3-carboxylates the concomitant formation of 3-alkyl-3-hydroxy-2-oxindoles. Then, the deacylative oxidation was performed with two examples in the presence of the sodium allyl alcoholate in the presence of an oxygen balloon at 1 atm at r.t. giving the corresponding 3-hydroxy-2-oxindoles in good yields (Scheme 38).<sup>[50]</sup>

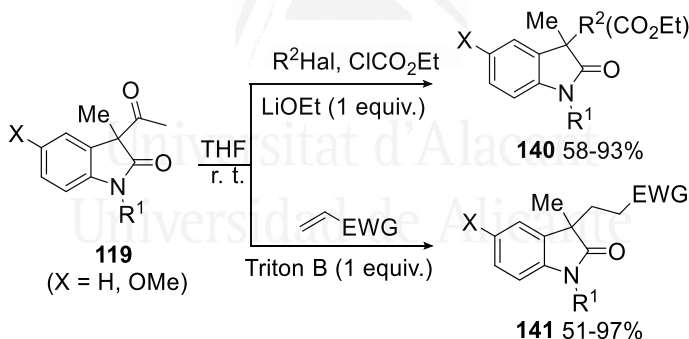
**Scheme 38.** Deacylative oxidation of methyl 2-oxindole-3-carboxylates

In our hands, a similar deacylative oxidation has been achieved in the case of 3-alkyl-3-acetyl-2-oxindoles using 1 equiv. of LiOEt as base in THF under air at room temperature (Scheme 39).<sup>[51]</sup> This base promoted the deacylative oxidation giving the corresponding 3-hydroxyindoles in good yields.

**Scheme 39.** Deacylative oxidation of 3-acetyl-3-alkyl-2-oxindoles

It has been proposed that the *in situ* generated enolate suffered a radical oxidation by oxygen. The former methodology avoided the use of oxidants<sup>[57]</sup> for the synthesis of 3-hydroxy-2-oxindoles.

Leaving aside Pd-catalyzed DaA, our research group has also focused on developing base-promoted deacylative alkylation under mild conditions. Thus, base-promoted deacylative alkylation of 3-alkyl-3-acetyl-2-oxindoles, prepared by acetylation of 2-oxindoles with acetic anhydride,<sup>[58]</sup> has been used for the synthesis of 3,3-disubstituted oxindoles.<sup>[59]</sup> The retro-Claisen condensation has been performed with LiOEt as base in THF at room temperature giving the corresponding carbon nucleophile, which reacted with alkyl and allyl halides as well as with ethyl chloroformate as electrophiles (Scheme 40). When electrophilic alkenes were used as electrophiles benzyltrimethylammonium hydroxide (Triton B) was the best base for achieving the corresponding conjugate addition. This methodology was applied to the synthesis of 1,3-dimethyl-3-(cyanomethyl)-2-oxindole, a precursor of esermethole, which is a precursor of the acetylcholinesterase inhibitors physostigmine and phenserine (see above and Figure 10).<sup>[60]</sup>

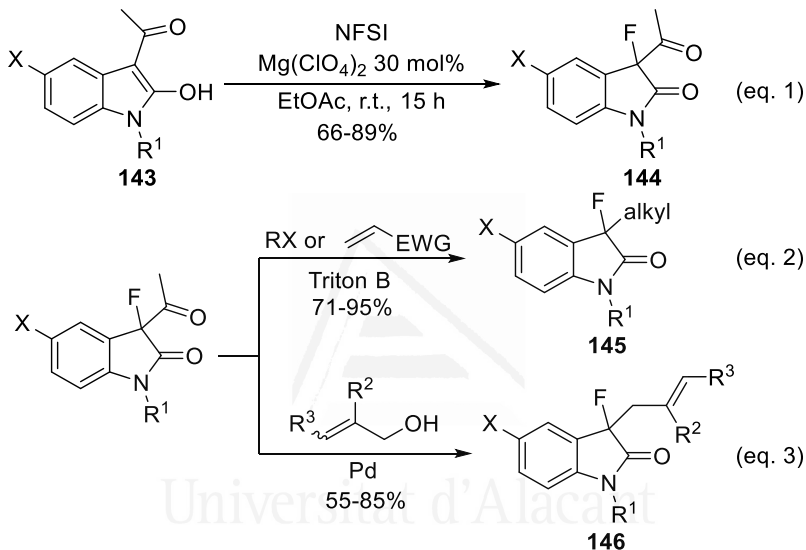


**Scheme 40.** Base-promoted deacylative alkylation of 3-acetyl-2-oxindoles

The most recent publication of our group, dealing with DaA, consisted in the fluorination of 3-acetyl-2-oxindole with *N*-fluorobenzenesulfonimide under Lewis acid catalysis using  $\text{Mg}(\text{ClO}_4)_2$  affording 3-acetyl-3-fluoro-2-oxindoles (Scheme 41, eq.1).<sup>[10]</sup> These compounds are subjected to base-promoted deacylative alkylation (DaA) for the *in-situ* generation of 3-fluoro-2-oxindole enolates under very mild reaction conditions using Triton B (1 equiv.) and alkyl halides or Michael acceptors as electrophilic reagents. The

corresponding 3-alkylated 3-fluoro-2-oxindoles were obtained in good to very high yields (Scheme 41, eq.2).

In addition, the palladium-catalyzed deacylative allylation was carried out with allylic alcohols using  $\text{LiO}^t\text{Bu}$  as base and 6 mol% of  $\text{Pd}(\text{OAc})_2$  and dppp, giving the resulting 3-allylated 3-fluoro-2-oxindoles in good yields (Scheme 41, eq.3).



**Scheme 41.** Synthesis of 3-substituted 3-fluoro-2-oxindoles by deacylative alkylation



Universitat d'Alacant  
Universidad de Alicante





## CHAPTER I:

DEACYLATIVE ALKYLATION (DaA) OF *N*-METHYL 3-ACETYL 2-OXINDOLE FOR THE SYNTHESIS OF SYMMETRICALLY 3,3-DISUBSTITUTED 2-OXINDOLES

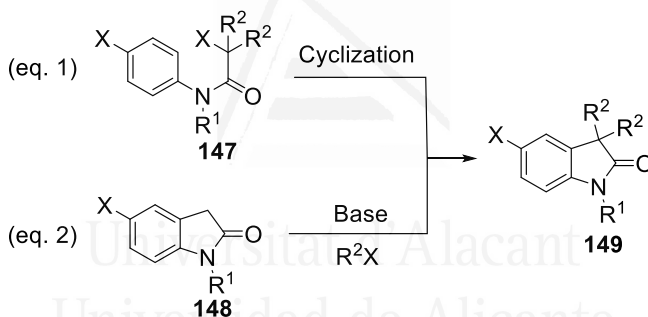
Universitat d'Alacant  
Universidad de Alicante



## CHAPTER I: Deacylative Alkylation (DaA) of *N*-methyl 3-acetyl-2-oxindole for the synthesis of symmetrically 3,3-disubstituted 2-oxindoles.

### I.1. Background

Symmetrically 3,3-disubstitution can be very useful in certain examples. In this sense, there are two main approaches for achieving this last task (compounds **149**); one of them is the cyclization of acylated anilides **147** (see section 1.4.1, 1.4.2 and 1.4.3) (Scheme 42, eq. 1) and, the second (the most frequently used), the direct double alkylation onto 2, which is currently performed employing alkoxides or stronger bases (Scheme 42, eq. 2).

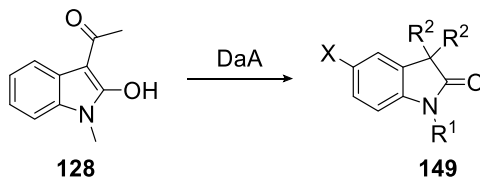


**Scheme 42.** Preparation of symmetrical 3,3-disubstituted-2-oxindoles

According to the previous work of our group, mentioned in the section 2.2 of the introduction, this chapter has been focused on the preparation of symmetrical 3,3-disubstituted-2-oxindole using the methodology of Deacylative Alkylation (DaA).

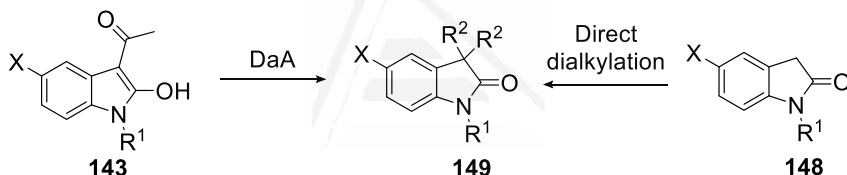
## I.2. Objectives

- ✓ Continuing with our research consisting looking for new applications of this DaA for the synthesis of 3,3-dialkyloxindoles we want to attempt the synthesis of symmetrical 3,3-disubstituted analogues.



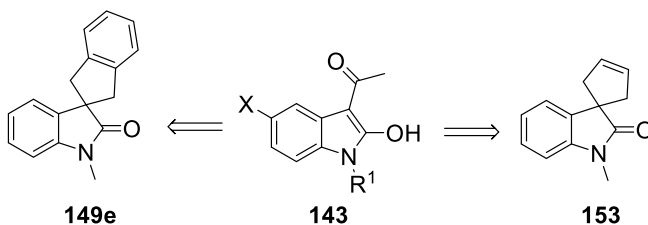
**Scheme 43.** 1<sup>st</sup> target

- ✓ We wish also to compare the results obtained through this DaA methodology *versus* the direct double alkylation of oxindoles.



**Scheme 44.** 2<sup>nd</sup> target

- ✓ The application of some examples for the synthesis of other structurally complex containing this oxindole unit as spiro-oxindoles will be evaluated as well.



**Scheme 45.** 3<sup>rd</sup> target

### I.3. Results and discussion

With the previous work described in section 2.2, and after a deep literature revision our research group envisaged that the new strategy for the synthesis of symmetrical 3,3-disubstituted-2-oxindoles was first monoalkylation step and posterior deacylative alkylation. 3-Acetyl-2-oxindoles derivatives should be appropriate compounds to achieve that goal.

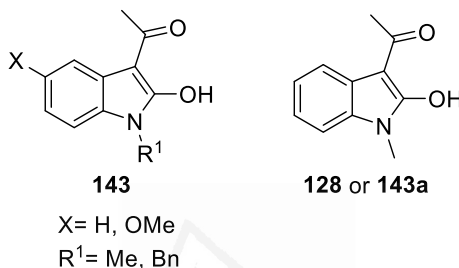
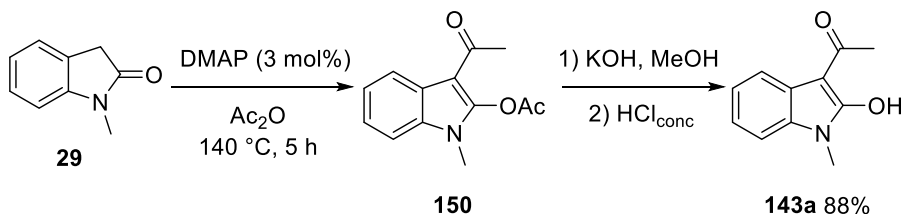


**Figure 13.** 3-Acetyl-2-oxindoles derivatives

The starting material **143a** was prepared from *N*-methyl-2-oxindole **29** by reaction with acetic anhydride in presence of catalytic amounts of 4-(*N,N*-dimethylamino)pyridine (DMAP) at 140 °C for 5 h.<sup>[58]</sup> Afterwards, a hydrolysis with KOH in MeOH, and posterior acidification with concentrated HCl, was required to prepare **143a**, due to the concomitant acylation at oxygen atom in addition to the 3 position of the oxindole, which gave product **150**. After purification by flash chromatography, the target product was obtained in 88% yield.



**Scheme 46.** Synthesis of *N*-methyl-3-acetyl-2-oxindole **143a**

Once prepared the starting material, the reaction conditions for the synthesis of symmetrically 3,3-disubstituted-2-oxindoles were optimized following the previous work published by our group.<sup>[59]</sup> So, THF was selected as the best solvent and room temperature to keep the mild conditions. Then,

it was necessary to know the most appropriate base and the overall procedure of the reaction. The reaction model that it was used for the optimization was with *N*-methyl-3-acetyl-2-oxindole **143a** as starting material and benzyl bromide as electrophile (RHal).

**Table 1.** Reaction conditions study

Entry	Base	Additive	Solvent	Time	T	Product <sup>a</sup> (152/149c)
1	Triton B	-	THF	o.n.	r.t.	79/21
2	Triton B	LiI	THF	o.n.	r.t.	64/36
3	EtOLi	-	THF	o.n.	r.t.	89/11

<sup>a</sup> Conversion of the reaction followed by <sup>1</sup>H NMR.

When benzyl trimethylammonium hydroxide (Triton B or BnNMe<sub>3</sub>OH) was employed in THF as solvent at room temperature the conversion of the reaction was not complete (Table 1, Entry 1). Using additive or another bases, the obtain conversion was not complete.

The direct transformation employing 2.5 equiv. of both organic halide and base was not useful due to the formation of monoalkylated deacylated 2-oxindoles. For this reason, the double alkylation was performed in a one pot sequential process. On it, the first step consisted in the addition of the electrophile and the base (1 equiv. each reagent) in this order. After 4 h another addition of the same electrophile and base (1.5 equiv. each reagent) was performed in order to complete the double alkylation mediated by the deacylative process, allowing the reaction to proceed at room temperature overnight. Products **149** were finally purified and isolated after column chromatography (flash silica gel) in very good to moderate yields (Table 2).

When alkyl iodides were employed (iodomethane and 1-iodoethane) the chemical yields of products **149a** and **149b** were 51 and 33%, respectively (Table 2, entries 1 and 2). This low conversion was caused by the relative low reactivity towards these alkyl halides, and by the competition with the easy oxidation at the benzylic position of the oxindole in presence of air. Thus, the conversion of the reaction and the competition between the product and **149a**: 3-hydroxy-1,3-dimethyloxindole in an 88:12 mixture and **149b**: 3-hydroxy-3-ethyl-1-methyloxindole in a 61:39 mixture was observed by  $^1\text{H}$  NMR analysis of the crude product.

On the other hand, more activated halides such as benzylic bromides, appearing in the three next entries of Table 2, furnished higher chemical yields in a range of 69-85% (compounds **149c**, **149d** and **149e**). In the case of bisbenzylic unit, it was efficiently introduced providing spiranic oxindole derivative **149e**, whose skeleton is present in antitumor agents<sup>[61]</sup> and aldose reductase inhibitors.<sup>[62]</sup>

Allylic bromides such as allyl bromide and cinnamyl bromide also gave good conversions and yields 65 and 84%, respectively and no other byproduct was identified by  $^1\text{H}$  NMR of the crude product (Table 2, entries 6 and 7). Despite of allylic bromides gave good results, the employment of geranyl bromide furnished a complex reaction mixture, which, after flash chromatography, allowed to isolate an inseparable 65:35 mixture of **149h** together with its corresponding deacylated 3-monoalkylated compound (Table 2, entry 8).

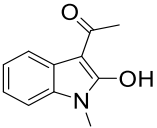
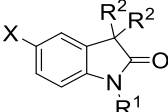
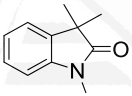
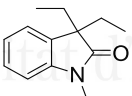
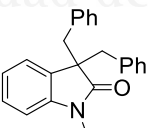
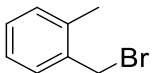
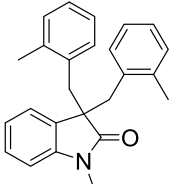
Technical methyl bromocrotonate and ethyl *E*-bromocrotonate gave similar results of **149i** and **149j** after this transformation, the crude compound **149i** being much more complex due to the presence of *Z*- and *E*-stereoisomers (Table 2, entries 9 and 10).

To complete the scope, another three halides with  $\pi$ -extended conjugation were tested. Propargyl bromide gave a 58% yield of the disubstituted product **149k** (Table 2, entry 11), methyl bromoacetate afforded a similar 61% yield (Table 2, entry 12) and finally, bromoacetonitrile furnished the best chemical 82% yield of this series (Table 2, entry 13).

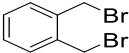
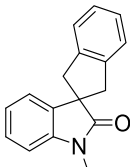
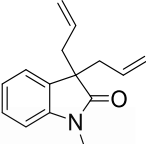
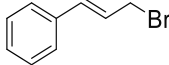
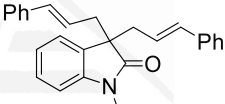
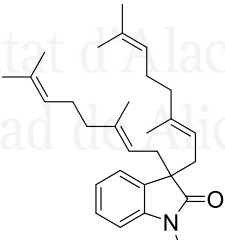
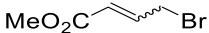
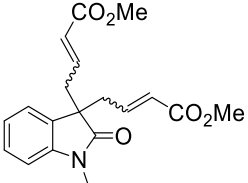
In entries 9 and 12 of the Table 2 a different protocol was employed in order to achieve higher yields. Thus, the addition of the total amount of reagents was performed adding RHal (1 equiv.) and Triton B (1 equiv.) at rt for 4 h, followed by de addition of RHal (1 equiv.) and Triton B (1 equiv.) at rt for 19 h and, finally RHal (0.5 equiv.) and Triton B (0.5 equiv.) at rt for 19

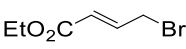
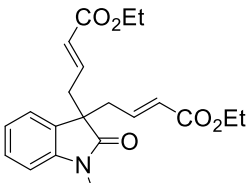
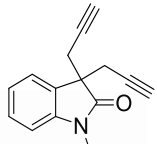
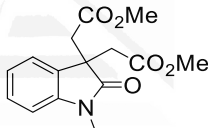
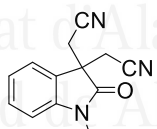
h completed the sequence in three steps. Finally, with these results in hands, we obtained a sequential two steps one-pot reaction. The reaction was studied using several organic halides with moderate to good yields, generating nine new compounds and one example of spirocyclic oxindole.

**Table 2.** Synthesis of 3,3-disubstituted-2-oxindoles by DaA

Entry	RHal	Product	149	Yield (%) <sup>a,b</sup>
<div style="display: flex; align-items: center; justify-content: center;"> <div style="text-align: center;">  <p><b>143a</b></p> </div> <div style="margin: 0 20px;"> <p>1. RHal (1 equiv.) THF 0.1 M, r.t., 4 h BnNMe<sub>3</sub><sup>+</sup>OH (1 equiv.)</p> <p>2. RHal (1.5 equiv.) THF 0.1 M, r.t., 19 h BnNMe<sub>3</sub><sup>+</sup>OH (1.5 equiv.)</p> </div> <div style="text-align: center;">  <p><b>149</b></p> <p>X=H, R<sup>1</sup>=Me</p> </div> </div>				
<b>1<sup>c</sup></b>	MeI		<b>149a</b>	51(65)
<b>2<sup>d</sup></b>	EtI		<b>149b</b>	33
<b>3</b>	PhCH <sub>2</sub> Br		<b>149c</b>	83
<b>4</b>			<b>149d</b>	85(58)

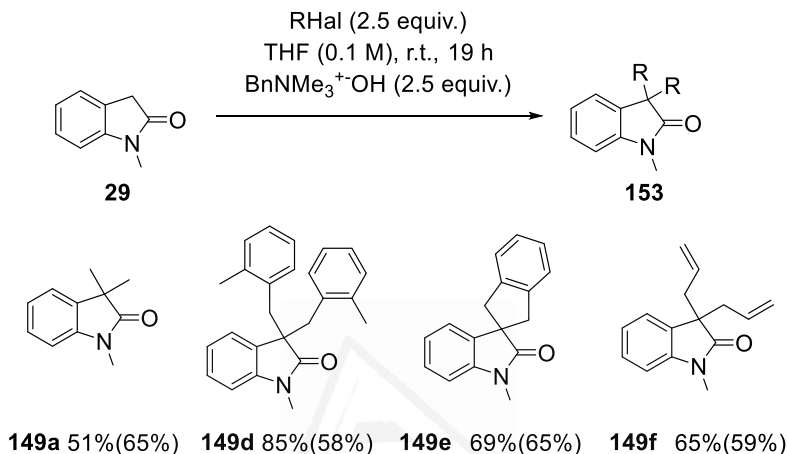


Entry	RHal	Product	149	Yield (%) <sup>a,b</sup>
5			<b>149e</b>	69(65)
6	H <sub>2</sub> C=CHCH <sub>2</sub> Br		<b>149f</b>	65(59)
7			<b>149g</b>	84
8 <sup>e</sup>	Geranyl bromide		<b>149h</b>	48
9 <sup>f,g</sup>			<b>149i</b>	58

Entry	RHal	Product	149	Yield (%) <sup>a,b</sup>
<b>10<sup>h</sup></b>			<b>149j</b>	62
<b>11</b>	HC≡CCH <sub>2</sub> Br		<b>149k</b>	58
<b>12<sup>g</sup></b>	BrCH <sub>2</sub> CO <sub>2</sub> Me		<b>149i</b>	61
<b>13</b>	BrCH <sub>2</sub> CN		<b>149m</b>	82

<sup>a</sup> Isolated yield after column chromatography (flash silica). <sup>b</sup> In brackets, yields obtained from direct dialkylation of *N*-methyloxindole. <sup>c</sup> A 88:12 mixture of **149a**:3-hydroxy-1,3-dimethyloxindole was observed by <sup>1</sup>H NMR (crude product). <sup>d</sup> A 61:39 mixture of **149b**:3-hydroxy-3-ethyl-1-methyloxindole was observed by <sup>1</sup>H NMR (crude product). <sup>e</sup> This compound was obtained as an inseparable 65:35 mixture of **149h** and its corresponding deacylated 3-monoalkylated compound. <sup>f</sup> This compound was obtained as 81:19 mixture of **149i** and its corresponding deacylated 3-monoalkylated compound, but **149i** could be finally separated. <sup>g</sup> In this example, the sequential process was performed using: 1. RHal (1 equiv.) and Triton B (1 equiv.) at rt for 4 h; 2. RHal (1 equiv.) and Triton B (1 equiv.) at rt for 19 h; 3. RHal (0.5 equiv.) and Triton B (0.5 equiv.) at rt for 19 h. <sup>h</sup> This compound was obtained as an inseparable 65:35 mixture of **149j** and its corresponding deacylated 3-monoalkylated compound.

In some examples depicted in Table 2, a comparison of this deacylative route with the direct dialkylation of oxindole **29** with excess of both Triton B and the corresponding halide (Scheme 47) was made.

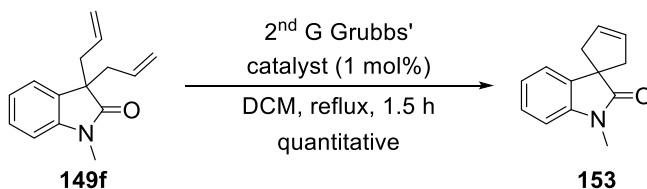


**Scheme 47.** Comparison with direct alkylation of the *N*-methyloxindole

We can observe that, the direct alkylation was much more efficient when methyl iodide was tested (65% *versus* 51%, see Table 2, entry 1, compound **149a**). However, the yield of compound **149d**, using the DaA route, increased manifold (85% *versus* 58%, Table 2, entry 4).

2-(Bromomethyl)benzyl bromide and allyl bromide gave very similar results (compounds **149e** and **149f**) using both reaction sequences such as it was depicted in Table 2 (entries 5 and 6) but the crude of the DaA mediated reactions were cleaner than the corresponding ones for the direct dialkylation way.

Finally, this chapter ends with the application of **149f** for the synthesis of other structurally complex containing this oxindole unit was envisaged. The metathesis reaction employing the 2<sup>nd</sup> generation Grubbs' catalyst produced spirocompound **153** in quantitative yield after 1.5 h under refluxing dichloromethane (Scheme 48). The presence of the residual carbon-carbon double bond would allow the access to core framework of natural compounds citrinadins A and B as well as the preparation of families of mentioned antitumor spirooxindole derivatives.<sup>[63]</sup>



**Scheme 48.** Metathesis reaction employing the 2<sup>nd</sup> generation Grubbs' catalyst

(-)-Citridin A and (+)-citridin B (Figure 14), exhibited notable activity against murine leukemia L1210 (**154**, IC<sub>50</sub> 6.2 µg/mL; **155**, 10 µg/mL) and human epidermoid carcinoma KB cells (**154**, IC<sub>50</sub> 10 µg/mL).<sup>[64]</sup> these natural compounds had been found in marine-derived fungus *Penicillium citrinum*, and in 2004 and 2005 Kobayashi and coworkers reported the isolation of the two related spirooxindole alkaloids.

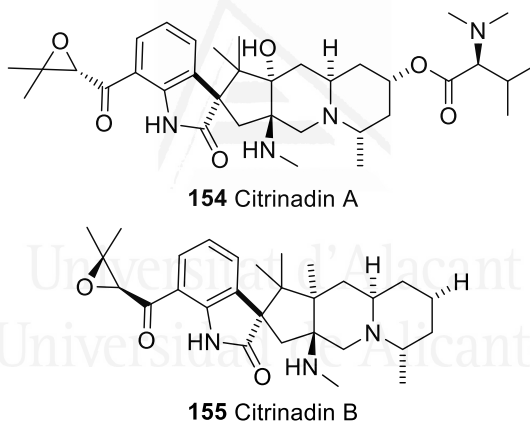


**Figure 14.** Citridin A and B

To summary, thirteen symmetrical 3,3-disubstituted oxindole are obtained in which nine of them are new compounds.

## I.4. Conclusions

- ✓ **1<sup>st</sup> target:** The sequential one-pot monoalkylation of 3-acetyl-1-methyl-2-oxindole, followed by a DaA-second alkylation is an alternative way to obtain symmetrical 3,3-disubstituted oxindole derivatives.
- ✓ **2<sup>nd</sup> target:** The process competes with the direct dialkylation of *N*-methyloxindole because, in many cases, yields are higher and the crude materials cleaner, which are two very strong points in favor of this strategy.

	Yield (%)			
	<b>149a</b>	<b>149d</b>	<b>149e</b>	<b>149f</b>
Direct Alkylation	<b>65</b>	58	65	59
DaA	51	<b>85</b>	<b>69</b>	<b>65</b>

- ✓ **3<sup>rd</sup> target:** Some compounds obtained in this work (specifically **149e** and **153**) were suitable candidates to access interesting antitumor agents and natural compounds.

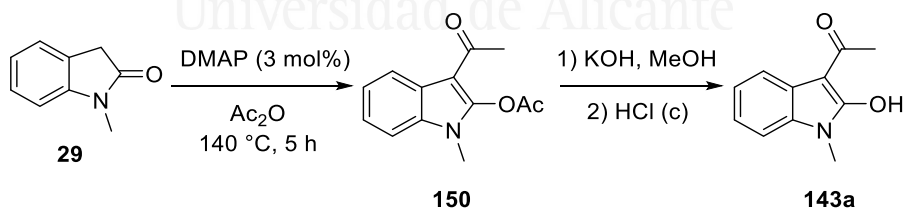
## I.5. Experimental section

### 1. General methods

Melting points were determined with a Marienfeld melting-point meter (MPM-H2) apparatus and are uncorrected. For flash chromatography, silica gel 60 (40–60  $\mu\text{m}$ ) was employed. The structurally most important peaks of the IR spectra (recorded using a Nicolet Avatar 320 FT-IR Spectrometer and JASCO FT/IR-4100 Fourier Transform Infrared Spectrometer) are listed and wave numbers are given in  $\text{cm}^{-1}$ .  $^1\text{H}$  NMR (300, or 400 MHz) and  $^{13}\text{C}$  NMR (75 or 101 MHz) spectra were recorded with Bruker AV300 and Bruker AV400, respectively, with  $\text{CDCl}_3$  as solvent and TMS as internal standard for  $^1\text{H}$  NMR spectra, and the chloroform signal for  $^{13}\text{C}$  NMR spectra; chemical shifts are given in ppm. Low-resolution electron impact (GC-EI) mass spectra were obtained at 70 eV with an Agilent 6890N Network GC system and an Agilent 5973 Network Mass Selective Detector. High-resolution mass spectra (GC-EI) were recorded with a QTOF Agilent 7200 instrument for the exact mass and Agilent 7890B for the GC. Analytical TLC was performed using ALUGRAM® Xtra SIL G/UV254 silica gel plates, and the spots were detected under UV light ( $\lambda=254$  nm).

### 2. Experimental procedures

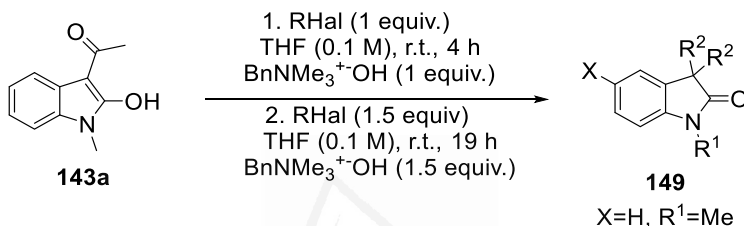
#### Synthesis of *N*-methyl-3-acetyl-2-oxindole (**143a**)



To a round-bottom flask containing a solution of *N*-methyl-2-oxindole (4.85 g, 33 mmol) in acetic anhydride (36 mL, 381 mmol) DMAP (118 mg, 0.96 mmol) was added. The mixture was heated at  $140^\circ\text{C}$  for 5 h. The mixture was evaporated under reduced pressure, the crude residue was dissolved in MeOH (80 mL) and a solution of KOH (18 g, 321 mmol) in MeOH (120 mL) at  $0^\circ\text{C}$  was added. The solution was stirred at r.t. for 22 h then cooled in an ice-bath at  $0^\circ\text{C}$  and 12 M aqueous HCl was added until pH 3.

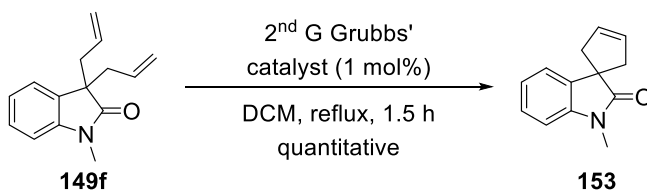
At this point, H<sub>2</sub>O (140 mL) was added and the solution was extracted with EtOAc (3 x 140 mL). the organic layers were dried over MgSO<sub>4</sub>, filtered, and concentrated. The residue was purified by flash chromatography (EtOAc/hexane) to give pure **143a**. Yield: 5.5 g (88%); purple solid; mp 109-110 °C. The spectral data are consisted with the reported data.<sup>[58]</sup>

## Synthesis of symmetrical 3,3-disubstituted oxindoles using DaA (149)



To a solution of *N*-methyl-3-acetyl-2-oxindole **143a** (57 mg, 0.3 mmol) and alkyl halide (0.3 mmol) in THF (3 mL) was added benzyltrimethylammonium hydroxide (Triton B) in MeOH (40wt%, 136 μL, 0.3 mmol) dropwise. The reaction was stirred at r.t. during 4-6 h. The reaction was controlled by gas chromatography until the conversion of 4a to 3-acetyl-3-alkyl-2-oxindole was ≥90%. Then, alkyl halide (0.45 mmol) and base (0.45 mmol) was added to complete the double alkylation, allowing the reaction to proceed at room temperature overnight. H<sub>2</sub>O (10 mL) was added, the mixture was extracted with EtOAc (3 × 10 mL) and the combined organic layers were evaporated and dried over MgSO<sub>4</sub>. After evaporation of the solvents the residue was purified by flash chromatography (EtOAc/hexane).

## Synthesis of spirooxindole (153) through a ruthenium catalyzed metathesis reaction



To a solution of 2<sup>nd</sup> generation Grubbs catalyst (0.002 mmol, 1.7 mg) in dry dichloromethane (20 mL) compound **149f** was added. The mixture was

stirred during 1.5 h at 42°C under Ar atmosphere. The solution was filter off through a short plug of celite. Finally, the solution was concentrated (15 Torr) and the residue was purified by column chromatography (hexane/EtOAc).

### 3. Experimental data

Compounds **143a**, **149c**, **149e**, **149f**, **149k** and **153** are known compounds and experimental data are consist with reported data:

**143a**: 1-(2-hydroxy-1-methyl-1H-indol-3-yl)ethan-1-one.<sup>[58]</sup>

**149c**: 3,3-Dibenzyl-1-methylindolin-2-one.<sup>[65]</sup>

**149e**: 1'-Methyl-1,3-dihydrospiro[indene-2,3'-indolin]-2'-one.<sup>[66]</sup>

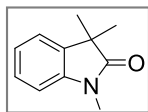
**149f**: 3,3-Diallyl-1-methylindolin-2-one.<sup>[59]</sup>

**149k**: 1-Methyl-3,3-di(prop-2-yn-1-yl)indolin-2-one.<sup>[67]</sup>

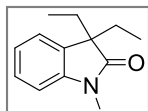
**153**: 1'-methylspiro[cyclopentane-1,3'-indolin]-3-en-2'-one.<sup>[68]</sup>

Following characterization data of new compounds **149a**, **149b**, **149d**, **149g**, **149h**, **149i**, **149j**, **149l** and **149m** will be displayed:

*1,3,3-Trimethylindolin-2-one (149a)*: colorless oil;  $R_F$  0.3 (hexane/EtOAc 8.5:1.5); IR (neat)  $\nu_{\max}$  3053, 2970, 2924, 1704, 1613  $\text{cm}^{-1}$ ; <sup>1</sup>H NMR (300 MHz)  $\delta$  7.27 (1H, td,  $J = 7.7, 1.3$  Hz, ArH), 7.21 (1H, d,  $J = 7.4$  Hz, ArH), 7.07 (1H, td,  $J = 7.5, 0.9$  Hz, ArH), 6.85 (1H, d,  $J = 7.8$  Hz, ArH), 3.22 (3H, s, NCH<sub>3</sub>), 1.37 (6H, s, 2 x CH<sub>3</sub>); <sup>13</sup>C NMR (101 MHz)  $\delta$  181.5 (CO), 142.7 (CH), 135.9 (CH), 127.8 (CH), 122.6 (CH), 122.4 (CH), 108.1 (CH), 44.3 (C), 26.3 (CH<sub>3</sub>), 24.5 (2 x CH<sub>3</sub>); LRMS (EI)  $m/z$  175 (M<sup>+</sup>, 66%), 161 (11), 160 (100), 132 (20), 117 (14), 77(6); HRMS (ESI): calcd. for C<sub>11</sub>H<sub>13</sub>NO [M]<sup>+</sup> 175.0997; found 175.0998.



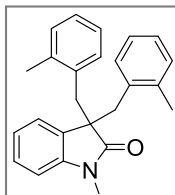
*3,3-Diethyl-1-methylindolin-2-one (149b)*: colorless oil;  $R_F$  0.3 (hexane/EtOAc 9:1); IR (neat)  $\nu$  2963, 2924, 2878, 2852, 1706, 1612  $\text{cm}^{-1}$ ; <sup>1</sup>H NMR (300 MHz)  $\delta$  7.31–7.23 (1H, m, ArH), 7.17–7.04 (2H, m, ArH), 6.84 (1H, d,  $J = 7.7$  Hz, ArH), 3.22 (3H, s, NCH<sub>3</sub>), 2.01–1.68 (4H, m, 2 x CH<sub>2</sub>), 0.56 (6H, t,  $J = 7.4$  Hz, 2 x CH<sub>3</sub>); <sup>13</sup>C NMR (101 MHz)  $\delta$  180.2 (CO), 144.5 (C), 132.1 (C), 127.7 (CH), 122.8 (CH), 122.5 (CH), 107.8 (CH), 54.5 (C), 30.8 (2 x CH<sub>2</sub>), 26.1 (CH<sub>3</sub>), 8.8 (2 x CH<sub>3</sub>); LRMS (EI)  $m/z$  203 (M<sup>+</sup>, 72%), 204 (10), 175 (51), 174



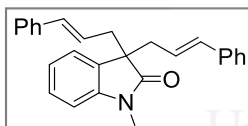


(100), 160 (20), 159 (12), 146 (66), 131 (19), 130 (25); HRMS (ESI): calcd. for  $C_{13}H_{17}NO$   $[M]^+$  203.131; found 203.1313.

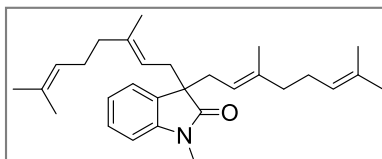
**1-Methyl-3,3-bis(2-methylbenzyl)indolin-2-one (149d)**: pale yellow solid; mp 102–104 °C (hexane/EtOAc);  $R_f$  0.3 (hexane/EtOAc 9:1); IR (neat)  $\nu$  3058, 2963, 2923, 2857, 1709, 1611  $cm^{-1}$ ;  $^1H$  NMR (400 MHz)  $\delta$  7.11 (1H, td,  $J = 7.6, 1.5$  Hz, ArH), 7.02–6.94 (4H, m, ArH), 6.92–6.80 (6H, m, ArH), 6.51 (1H, d,  $J = 7.8$  Hz, ArH), 3.31 (4H, s, 2 x  $CH_2$ ), 2.93 (3H, s,  $NCH_3$ ), 2.11 (6H, s, 2 x  $CH_3$ );  $^{13}C$  NMR (101 MHz)  $\delta$  179.5 (CO), 143.8 (C), 137.19(C), 134.9 (C), 130.4 (C), 130.3 (2 x CH), 130.1 (2 x CH), 128.0 (CH), 126.6 (2 x CH), 125.2 (2 x CH), 124.8 (CH), 121.6 (CH), 107.7 (CH), 55.2 (2 x C), 39.2 (2 x  $CH_2$ ), 26.0 ( $CH_3$ ), 20.3 (2 x  $CH_3$ ); LRMS (EI)  $m/z$  355 ( $M^+$ , 55%), 356 (15), 251 (22), 250 (100), 222 (44), 207 (14), 159 (17), 105 (47); HRMS (ESI): calcd. for  $C_{25}H_{25}NO$   $[M]^+$  355.1936; found 355.1943.



**3,3-Dicinnamyl-1-methylindolin-2-one (149g)**: yellow oil;  $R_f$  0.3 (hexane/EtOAc 9:1); IR (neat)  $\nu$  3053, 3024, 2926, 1701, 1614  $cm^{-1}$ ;  $^1H$  NMR (400 MHz)  $\delta$  7.32–7.12 (12H, m, ArH), 7.08 (1H, t,  $J = 7.0$  Hz, ArH), 6.78 (1H, d,  $J = 7.7$  Hz, ArH), 6.36 (2H, d,  $J = 15.8$  Hz, 2 x CH), 5.86 (2H, dt,  $J = 15.5, 7.5$  Hz, 2 x CH), 3.13 (1H, s,  $NCH_3$ ), 2.75 (4H, d,  $J = 7.4$  Hz, 2 x  $CH_2$ );  $^{13}C$  NMR (101 MHz)  $\delta$  179.0 (CO), 143.8 (C), 137.4 (2 x C), 133.9 (2 x CH), 131.4 (C), 128.5 (4 x CH), 128.1 (CH), 127.3 (2 x CH), 126.3 (4 x CH), 124.1 (2 x CH), 123.6 (CH), 122.5 (CH), 108.1 (CH), 53.4 (C), 40.4 (2 x  $CH_2$ ), 26.3 ( $CH_3$ ); LRMS (EI)  $m/z$  379 ( $M^+$ , 32%) 380 (12), 288 (12), 281 (17), 262 (43), 261 (14), 234 (11), 208 (11), 207 (54), 147 (45), 146 (23), 118 (23), 117 (100), 116 (10), 115 (34), 91 (14); HRMS (ESI): calcd. for  $C_{27}H_{25}NO$   $[M]^+$  379.1936; found 379.1939.

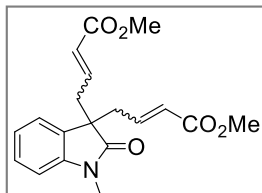


**3,3-Bis((E)-3,7-dimethylocta-2,6-dien-1-yl)-1-methylindolin-2-one (149h)**: yellow oil;  $R_f$  0.2 (hexane/EtOAc 9.5:0.5); IR (neat)  $\nu$  2965, 2921, 2855, 1717, 1612  $cm^{-1}$ ;  $^1H$  NMR (300 MHz)  $\delta$  7.26–7.18 (2H, m, ArH), 7.01 (1H, td,  $J = 7.5, 0.9$  Hz, ArH), 6.77 (1H, d,  $J = 7.7$  Hz, ArH), 4.99–4.88 (2H, m, 2 x CH), 4.80 (2H, t,  $J = 7.0$  Hz, 2 x CH), 3.16 (3H, s,  $NCH_3$ ), 2.53 (4H, d,  $J = 7.5$  Hz, 2 x  $CH_2$ ), 1.90–1.65 (8H, m, 4 x  $CH_2$ ), 1.63 (6H, s, 2 x  $CH_3$ ), 1.53 (6H, s, 2 x  $CH_3$ ), 1.51 (6H, s, 2 x  $CH_3$ );  $^{13}C$  NMR (75 MHz)  $\delta$  180.0 (CO), 144.0 (C),



138.6 (2 x C), 132.3 (C), 131.4 (2 x C), 127.6 (CH), 124.3 (2 x CH), 123.5 (CH), 122.0 (CH), 118.3 (2 x CH), 107.5 (CH), 53.4 (C), 39.9 (2 x CH<sub>2</sub>), 35.3 (2 x CH<sub>2</sub>), 26.8 (2 x CH<sub>2</sub>), 26.1 (CH<sub>3</sub>), 25.8 (2 x CH<sub>3</sub>), 17.7 (2 x CH<sub>3</sub>), 16.5 (2 x CH<sub>3</sub>); LRMS (EI) *m/z* 419 (M<sup>+</sup>, 3%), 283 (35), 214 (10), 198 (18), 161 (11), 160 (91), 159 (100), 147 (24), 146 (14), 81 (12), 69 (39); HRMS (ESI): calcd. for C<sub>29</sub>H<sub>41</sub>NO [M]<sup>+</sup> 419.3188; found 419.3191.

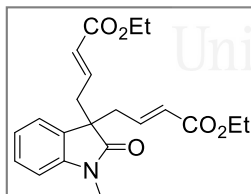
*Dimethyl 4,4'-(1-methyl-2-oxoindoline-3,3-diyl)bis(but-2-enoate)*  
(**149i**): pale oil; *R<sub>f</sub>* 0.25 (hexane/EtOAc 7:3); IR (neat)  $\nu$  2950, 1707, 1611



cm<sup>-1</sup>; <sup>1</sup>H NMR (300 MHz)  $\delta$  7.30 (1H, td, *J* = 7.7, 1.3 Hz, ArH), 7.21–7.17 (1H, m, ArH), 7.09 (1H, td, *J* = 7.5, 0.9 Hz, ArH), 6.85 (1H, d, *J* = 7.8 Hz, ArH), 6.54 (2H, dt, *J* = 15.4, 7.6 Hz, 2 x CH), 5.79 (2H, d, *J* = 15.6 Hz, 2 x CH), 3.65 (6H, s, 2 x OCH<sub>3</sub>), 3.19 (3H, s, NCH<sub>3</sub>), 2.70 (4H, dd, *J* = 7.7, 1.3 Hz, 2 x CH<sub>2</sub>); <sup>13</sup>C NMR (75 MHz)  $\delta$  177.55 (CO), 166.3 (2 x CO),

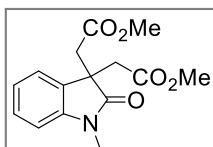
143.4 (C), 142.1 (2 x CH), 129.6 (C), 128.9 (CH), 124.9 (2 x CH), 123.3 (CH), 123.0 (CH), 108.7 (CH), 51.7 (C), 51.6 (2 x CH<sub>3</sub>), 39.5 (2 x CH<sub>2</sub>), 26.4 (CH<sub>3</sub>); LRMS (EI) *m/z* 343 (M<sup>+</sup>, 30%) 312 (14), 245 (14), 244 (88), 212 (46), 185 (23), 184 (100); HRMS (ESI): calcd. for C<sub>19</sub>H<sub>21</sub>NO<sub>5</sub> [M]<sup>+</sup> 343.142; found 343.1424.

*Diethyl 4,4'-(1-methyl-2-oxoindoline-3,3-diyl)(2E,2'E)-bis(but-2-enoate)*  
(**149j**): brown oil; *R<sub>f</sub>* 0.3 (hexane/EtOAc); IR (neat)  $\nu$  2981, 2937, 1716,

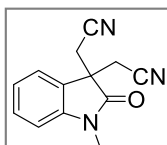


1655 cm<sup>-1</sup>; <sup>1</sup>H NMR (300 MHz)  $\delta$  7.30 (1H, t, *J* = 7.7 Hz, ArH), 7.16–7.07 (2H, m, ArH), 6.84 (1H, d, *J* = 7.8 Hz, ArH), 6.53 (2H, dt, *J* = 15.4, 7.6 Hz, 2 x CH), 5.78 (2H, d, *J* = 15.5 Hz, 2 x CH), 4.34–3.95 (4H, m, 2 x CH<sub>2</sub>), 3.19 (3H, s, NCH<sub>3</sub>), 2.70 (4H, dd, *J* = 7.7, 1.3 Hz, 2 x CH<sub>2</sub>), 1.26 (6H, dt, *J* = 22.4, 7.1 Hz, 2 x CH<sub>3</sub>); <sup>13</sup>C NMR (101 MHz)  $\delta$  177.6 (CO), 165.9 (2 x

CO), 143.4 (C), 141.7 (2 x CH), 129.6 (CH), 128.8 (C), 125.3 (2 x CH), 123.3 (CH), 123.0 (CH), 108.6 (CH), 60.4 (2 x CH<sub>2</sub>), 51.7 (C), 39.4 (2 x CH<sub>2</sub>), 26.3 (CH<sub>3</sub>), 14.2 (2 x CH<sub>3</sub>); LRMS (EI) *m/z* 371 (M<sup>+</sup>, 13%), 258 (54), 230 (10), 212 (24), 186 (14), 185 (27), 184 (100), 158 (11), 156 (14), 147 (11), 144 (12), 130 (10), 128 (13), 77 (13); HRMS (ESI): calcd. for C<sub>21</sub>H<sub>25</sub>NO<sub>5</sub> [M]<sup>+</sup> 371.1733; found 371.1728.



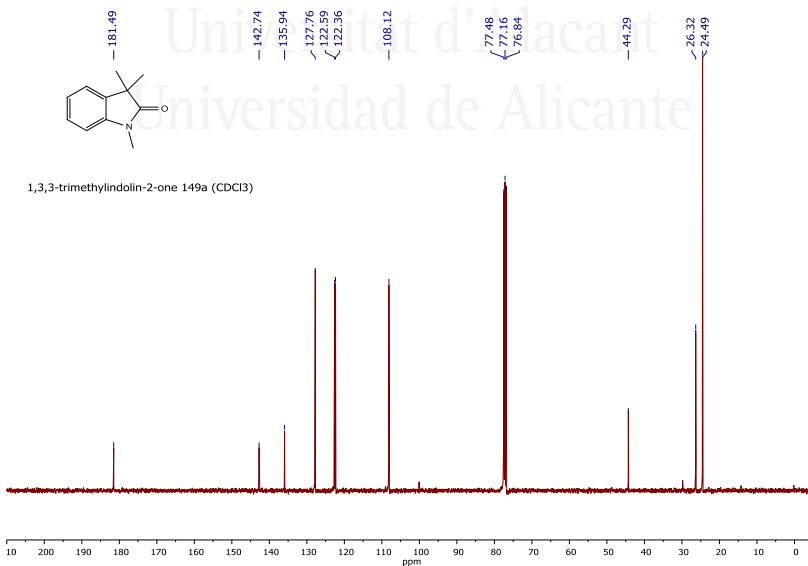
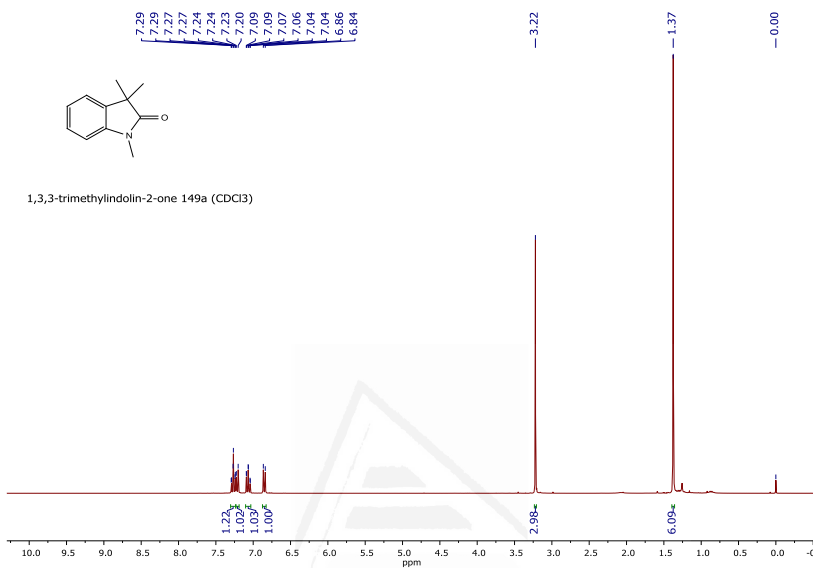
*Dimethyl 2,2'-(1-methyl-2-oxoindoline-3,3'-diyl)diacetate (149l)*: yellow wax;  $R_f$  0.3 (hexane/EtOAc 6.5:3.5); IR (neat)  $\nu$  2997, 2950, 1711, 1612  $\text{cm}^{-1}$ ;  $^1\text{H}$  NMR (300 MHz)  $\delta$  7.30 (2H, t,  $J = 7.0$  Hz, ArH), 7.03 (1H, t,  $J = 7.6$  Hz, ArH), 6.87 (1H, d,  $J = 8.0$  Hz, ArH), 3.50 (6H, s, 2 x OCH<sub>3</sub>), 3.28 (3H, s, NCH<sub>3</sub>), 3.06 (2H, d,  $J = 16.2$  Hz, 2 x C/H), 2.87 (2H, d,  $J = 16.2$  Hz, 2 x CH/H);  $^{13}\text{C}$  NMR (75 MHz)  $\delta$  178.3 (CO), 170.0 (2 x CO), 144.4 (C), 130.0 (C), 128.8 (CH), 123.4 (CH), 122.5 (CH), 108.3 (CH), 51.8 (2 x CH<sub>3</sub>), 46.9 (C), 40.5 (2 x CH<sub>2</sub>), 26.6 (CH<sub>3</sub>); LRMS (EI)  $m/z$  291 ( $\text{M}^+$ , 100%), 292 (17), 232 (29), 218 (13), 200 (13), 186 (21), 176 (51), 174 (21), 159 (43), 144 (16), 130 (25); HRMS (ESI): calcd. for  $\text{C}_{15}\text{H}_{17}\text{NO}_5$  [ $\text{M}$ ]<sup>+</sup> 291.1107; found 291.1103.

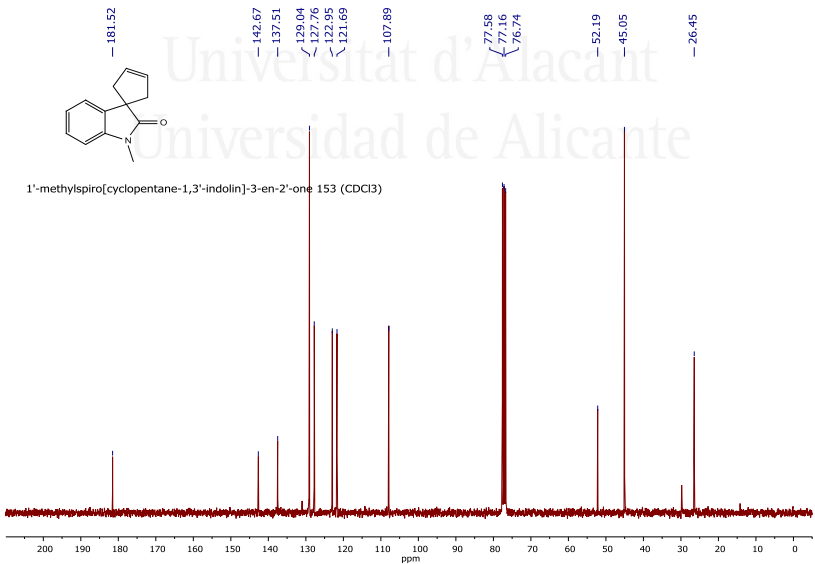
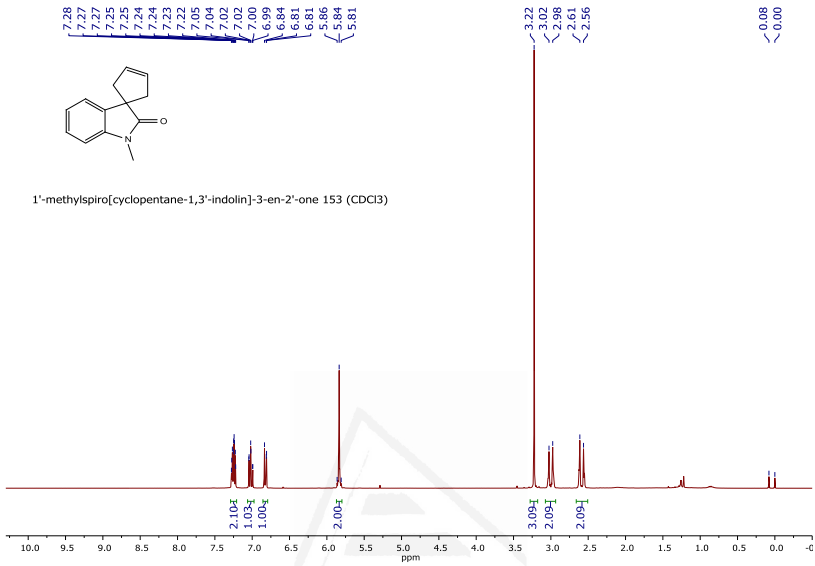


*2,2'-(1-Methyl-2-oxoindoline-3,3'-diyl)diacetonitrile (149m)*: orange solid; mp 104-106 °C;  $R_f$  0.3 (hexane/EtOAc 6.5:3.5); IR (neat)  $\nu$  2964, 2932, 1705, 1615  $\text{cm}^{-1}$ ;  $^1\text{H}$  NMR (400 MHz)  $\delta$  7.58 (1H, d,  $J = 8.0$  Hz, ArH), 7.46 (1H, td,  $J = 7.8, 1.2$  Hz, ArH), 7.22 (1H, td,  $J = 7.7, 0.9$  Hz, ArH), 6.98 (1H, d,  $J = 7.9$  Hz, ArH), 3.29 (3H, s, NCH<sub>3</sub>), 3.02 (2H, d,  $J = 16.7$  Hz, 2 x C/H), 2.82 (2H, d,  $J = 16.7$  Hz, 2 x CH/H);  $^{13}\text{C}$  NMR (101 MHz)  $\delta$  173.9 (CO), 143.2 (C), 130.8 (CH), 124.0 (CH), 126.4 (C), 123.6 (CH), 115.1 (2 x CN), 109.5 (CH), 45.8 (C), 26.9 (CH<sub>3</sub>), 24.8 (2 x CH<sub>2</sub>); LRMS (EI)  $m/z$  225 ( $\text{M}^+$ , 33%), 186 (13), 185 (100), 155 (5), 142 (6), 128 (7); HRMS (ESI): calcd. for  $\text{C}_{13}\text{H}_{11}\text{N}_3\text{O}$  [ $\text{M}$ ]<sup>+</sup> 225.0902; found 225.0907.

Universidad de Alicante

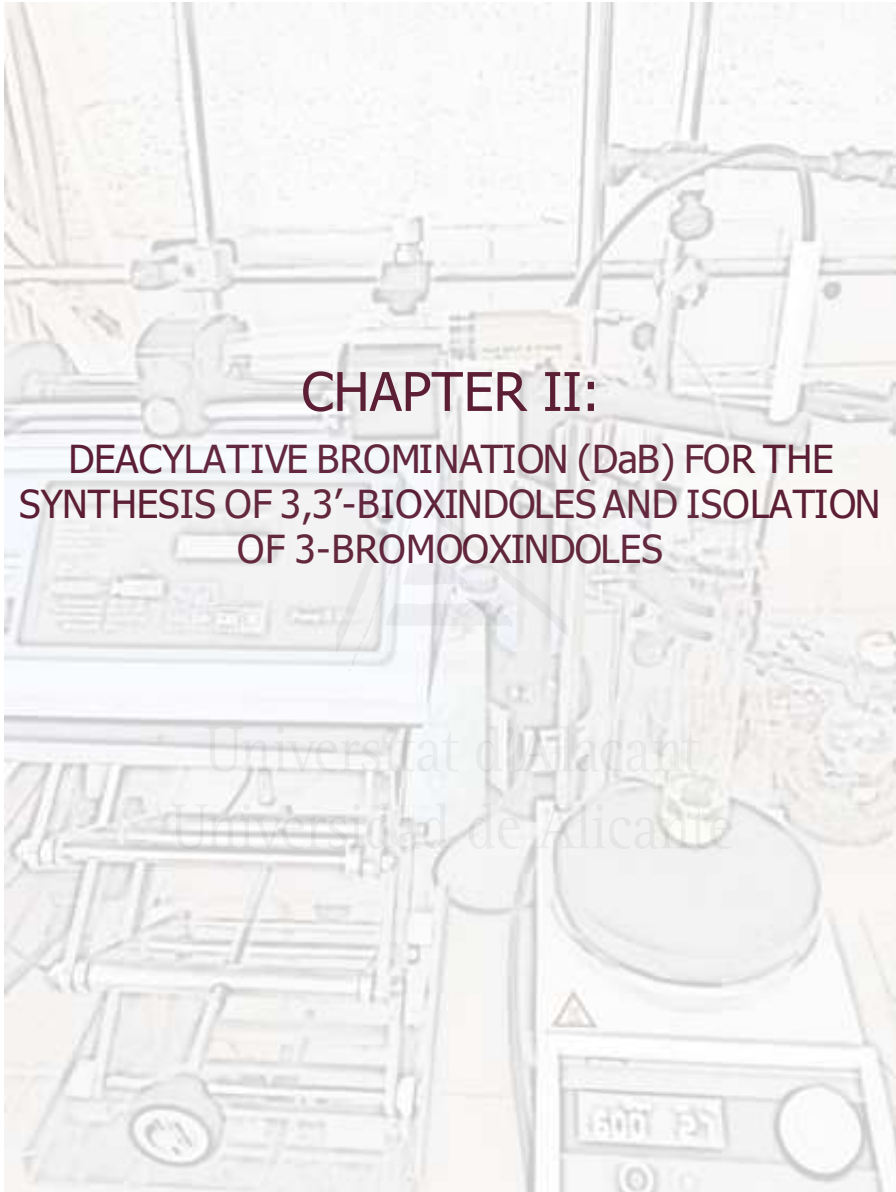
To finalize this experimental section some examples of NMR spectra are shown:







Universitat d'Alacant  
Universidad de Alicante



**CHAPTER II:**  
**DEACYLATIVE BROMINATION (DaB) FOR THE**  
**SYNTHESIS OF 3,3'-BIOXINDOLES AND ISOLATION**  
**OF 3-BROMOOXINDOLES**

Universitat de València  
Universitat de Alicante





## CHAPTER II: Deacylative Bromination (DaB) for the synthesis of 3,3'-bioxindoles and isolation of 3-bromooxindoles.

### II.1. Background

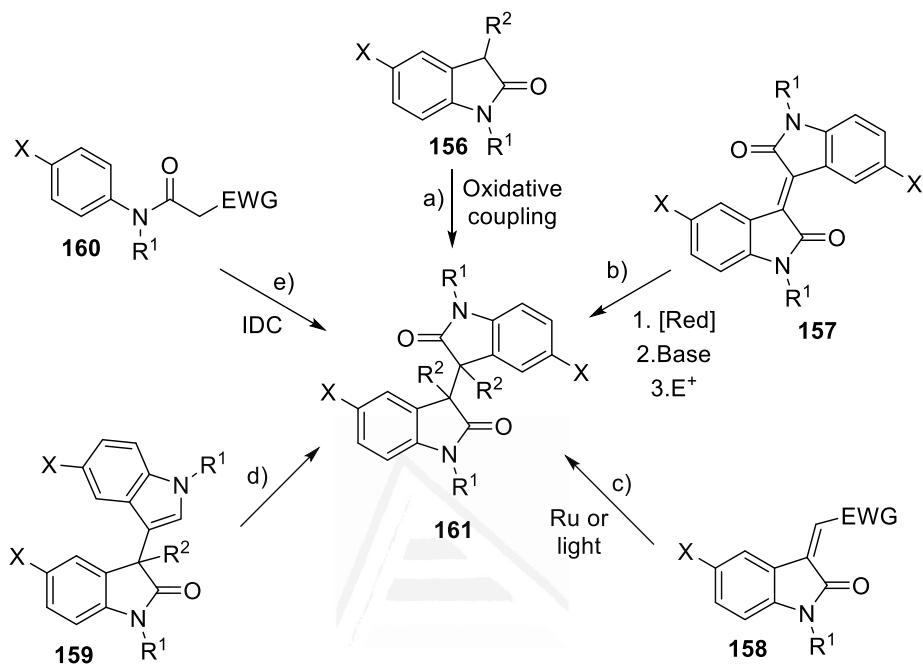
---

There are five general strategies to achieve the synthesis of 3,3'-bis-oxindoles (Scheme 49). The oxidative coupling between two 3-substituted oxindoles **156** allows the preparation of these structures with the same substituents, *via* radical intermediates, employing (or not) transition metal catalysts (Scheme 49a).<sup>[69]</sup>

Isoindigo **157** is a very common starting material for the synthesis of dimeric oxindoles as key step for the construction of complex natural structures. It can be used as electrophilic alkene or a bis-enolate precursor after selective hydrogenation of the carbon-carbon double bond (Scheme 49b).<sup>[70]</sup> Electron-deficient 3-alkylidene oxindoles **158** have been involved in [2+2] photochemical transformations,<sup>[71]</sup> to access finally the desired dimeric unit (Scheme 49c).<sup>[72]</sup>

The synthesis of 3-(3-indolyl)oxindoles **159** and their functional groups transformation allow to obtain non-symmetrically substituted bioxindoles (Scheme 49d).<sup>[73]</sup> The last strategy consists in an intramolecular dehydrogenative coupling (IDC) from the corresponding functionalized *N*-acylanilines **160** in this example a radical C-H bond activation is followed by the coupling with the activated methylene (Scheme 49e).<sup>[74]</sup> The main interest of the synthesis of 3,3'-bisoxindoles is focused on the preparation of very sophisticated natural products (see Figure 12).

The principal goal this chapter was the preparation of 3,3'-bioxindole using a new strategy name Deacylative Bromination (DaB). Before that, it is necessary to obtain 3-bromooxindoles which can be obtained in a similar way that reported one in the case of 3-fluoroindole derivatives using an electrophilic fluorination. In addition, 3-bromooxindoles are excellent starting material for the total synthesis of natural products.<sup>[56][75]</sup>

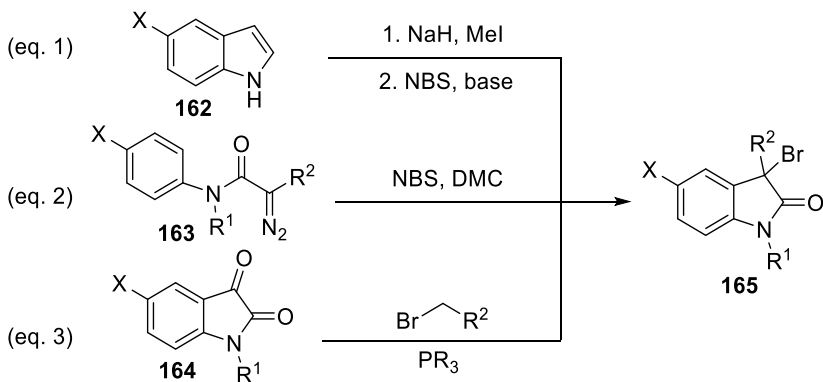


**Scheme 49.** General strategies employed for the synthesis of 3,3'-bis-oxindoles

The literature reported some strategies to the preparation of 3-bromooxindoles. One example of them was published by Wu's group in which starting from the indole a double methylation followed by bromination in strong basic conditions (Scheme 50, eq.1).<sup>[76]</sup>

Hu's group published halogenation of  $\alpha$ -diazocarbonyl compounds with *N*-halosuccinimides. The principal disadvantage of this strategy was the use of halogen solvents and the high toxicity of  $\alpha$ -diazocarbonyl compounds (Scheme 50, eq.2).<sup>[77]</sup>

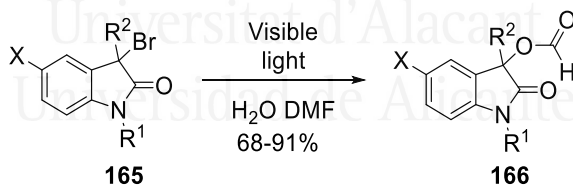
Finally another way to approach the synthesis of 3-bromooxindoles was from isatins using organophosphines (Scheme 50, eq.3).<sup>[78]</sup>



**Scheme 50.** General strategies employed for the synthesis of 3-bromooxindoles

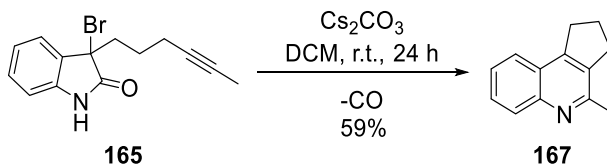
3-Bromooxindole derivatives are interesting compounds because the conversion of the C3-position of the oxindole as electrophilic centre, and also due to the reactivity photoredox reactions. Herein, some examples about the previous work did with 3-bromooxindoles are described:

Firstly, one example of photochemistry, in 2014 Xiao published about visible-light-induced photocatalytic formyloxylation reactions of 3-bromooxindoles with water and DMF (Scheme 51).<sup>[79]</sup>



**Scheme 51.** Use of 3-bromooxindoles as photocatalytic starting material

Another example about the applicability of these molecules was an extensive investigation by Fuchs and Funk in 2004 of the base-promoted reactions of 3-alkyl-3-bromoindolin-2-ones with dienophiles/nucleophiles for the total synthesis of ( $\pm$ )-flustramines A and C (Scheme 52).<sup>[80]</sup>



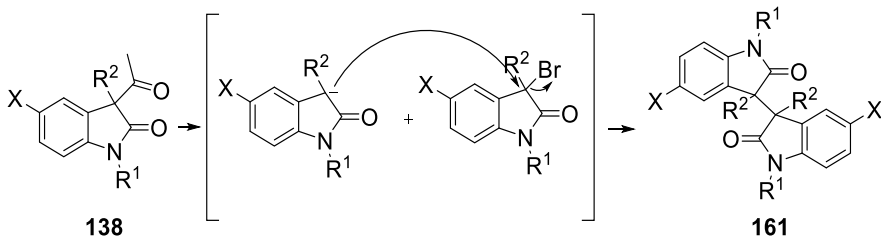
**Scheme 52.** Use of 3-bromoindole as electrophile



Universitat d'Alacant  
Universidad de Alicante

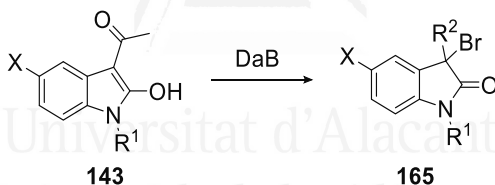
## II.2. Objectives

- ✓ Continuing with our research looking for applications of this DaA we wish study the synthesis of 3,3'-bis-oxindole analogues using Deacylative Bromination as a new methodology.



**Scheme 53.** 1<sup>st</sup> target

- ✓ For achieving this last goal, we would apply Deacylative Bromination (DaB) as a novel strategy to obtain the umpolung 3-alkyl-3-bromooxindoles.



**Scheme 54.** 2<sup>nd</sup> target

### II.3. Results and discussion

Our research group developed other 3-acetyl-2-oxindoles derivatives a part from **143a**<sup>[59]</sup> with the idea to cover wider structural ranges. For example, some synthetic intermediates and/or natural products, such as physostigmine and horsfiline, have a methoxy moiety at the 5 position of the oxindole core. So, it was decided to prepare **143b** and **143d** derivatives, which include this functional group in the structure.

Also, we decided to synthesize **143b** with other different protecting group at the 1 position (see Figure 15).

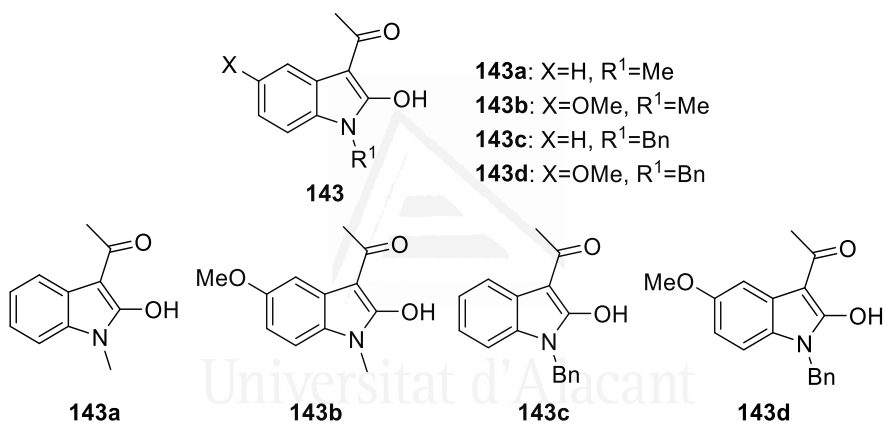
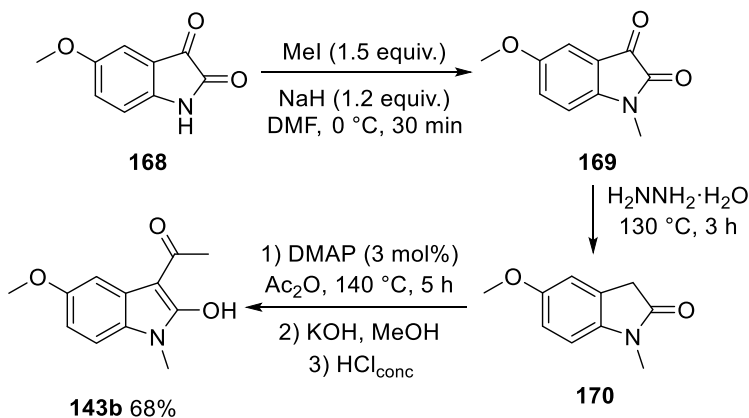


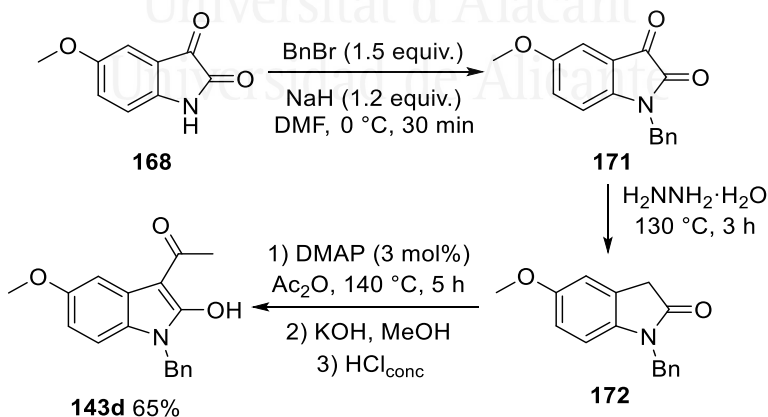
**Figure 15.** 3-Acetyl-2-oxindole derivatives

The selected starting material was 5-methoxyisatin **168**, because 5-methoxy-1-methyl-2-oxindole was not commercially available. Starting from isatin **168**, it was methylated at the 1 position using sodium hydride as base and iodomethane as alkylating agent in dimethylformamide (DMF) at 0 °C for 30 min, giving intermediate **169** (Scheme 55). After that, a Wolff-Kishner reduction was performed in order to obtain the 2-oxindole **170** heating at 130 °C for 3 hours. At this point, the same acetylation procedure for **143a** was carried out, giving the desired product **143b** in 68% overall yield.



**Scheme 55.** Synthesis of *N*-methyl-3-acetyl-5-methoxy-2-oxindole (**143b**)

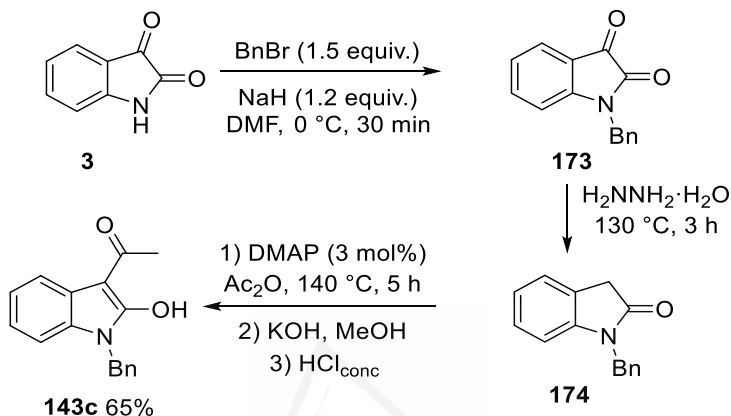
The same synthetic pathway was accomplished for the 1-benzyl-5-methoxy derivative **143d**. The first step involved the benzylation at the N position. Compound **168** was benzylated using benzyl bromide as electrophile and NaH as a base in DMF. After the same Wolf-Kishner reduction, 1-benzyl-5-methoxy-2-oxindole **172** was obtained in 83% yield after this previous two steps. Using the standard acetylation conditions, target product **143d** was obtained in 65% overall yield (Scheme 56).



**Scheme 56.** Synthesis of *N*-benzyl-3-acetyl-5-methoxy-2-oxindole (**143d**)

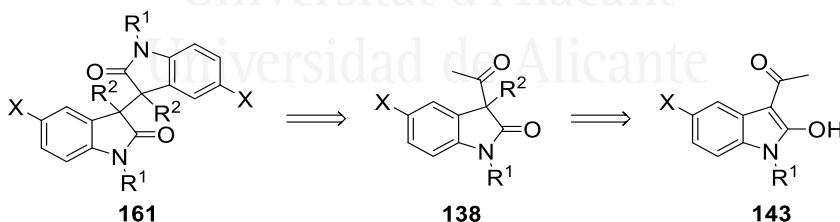
Finally, to improve the scope we decided to prepare *N*-benzyl-3-acetyl-2-oxindole (**143c**), from the commercially available isatin **3**. In this case, we

prepared this product because the benzyl protecting group was more easily removed. The procedure was the same that described one for **143d** (Scheme 57).



**Scheme 57.** Synthesis of *N*-benzyl-3-acetyl-2-oxindole (**143c**)

In order to employ our methodology for the synthesis of 3,3'-bis-oxindoles, the first step was the alkylation of compound **143** followed by the deacylative bromination of compounds **138** using NBS as electrophile (Scheme 58).



**Scheme 58.** Synthetic route for the dimerization of 3-acetyl-2-oxindoles using deacylative bromination

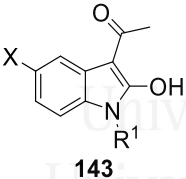
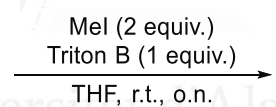
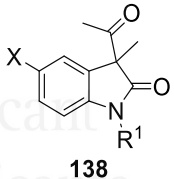
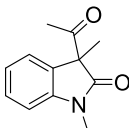
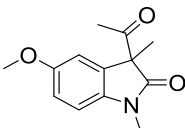


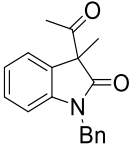
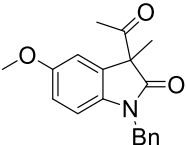
The first step was reported by our group, thus, compounds **138** were obtained with good to excellent yields. We started the investigation obtaining 3-acetyl-3-methyl-2-oxindole derivatives. Next, we studied the possibility to increase the number of substituents at C3 position. So, we discussed the possibility to allylate C3 position in order to promote following reactions for the preparation of sophisticated natural products.<sup>[51,59]</sup> For example, pyrroloindole alkaloids of the *Calycanthaceae* family such as (+)-chimonanthine **134** and (+)-folicanthine **135** (Figure 12), which exhibits diverse therapeutic properties as analgesic, antibacterial, antifungal and antiviral agents.<sup>[81]</sup>

Compounds **138** were prepared from starting material **143** using iodomethane as electrophile, Triton B as a base and THF as a solvent at room temperature and stirring overnight. The synthesis of the intermediate **138** could be scale until 1.2 mmol.

As it can see at Table 3 all the products were prepared with good to excellent yields.

**Table 3.** Methylation of compound **143**

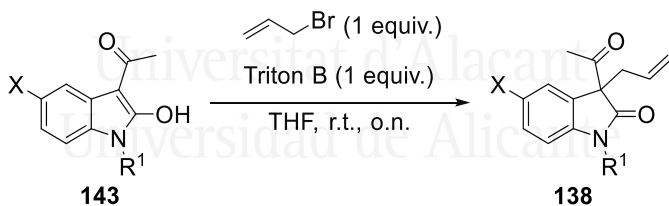
Entry	<b>143</b>	Product	<b>138</b>	Yield (%) <sup>a</sup>
	 <b>143</b>		 <b>138</b>	
<b>1</b>	<b>143a</b>		<b>138a</b>	79
<b>2</b>	<b>143b</b>		<b>138b</b>	80

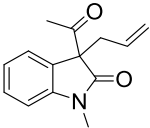
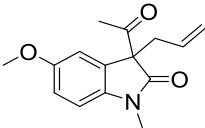
Entry	143	Product	138	Yield (%) <sup>a</sup>
3	143c		138c	65
4	143d		138d	68

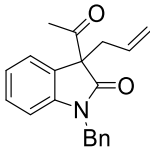
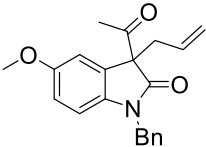
<sup>a</sup> Isolated yield after column chromatography (flash silica).

After, the allylation of compound **143** was using allyl bromide as electrophile, Triton B as a base and THF as a solvent at room temperature stirring overnight.

**Table 4.** Allylation of compound **143**

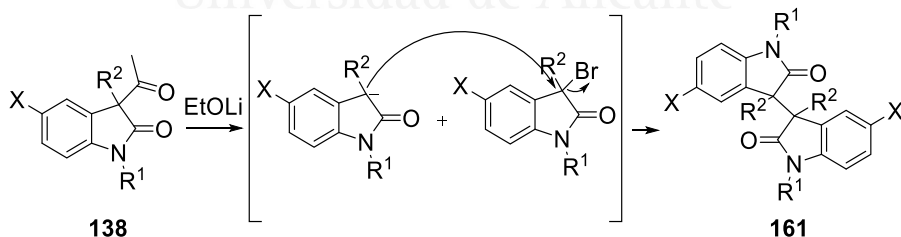


Entry	143	Product	138	Yield (%) <sup>a</sup>
1	143a		138e	80
2	143b		138f	80

Entry	143	Product	138	Yield (%) <sup>a</sup>
3	143c		138g	58
4	143d		138h	94

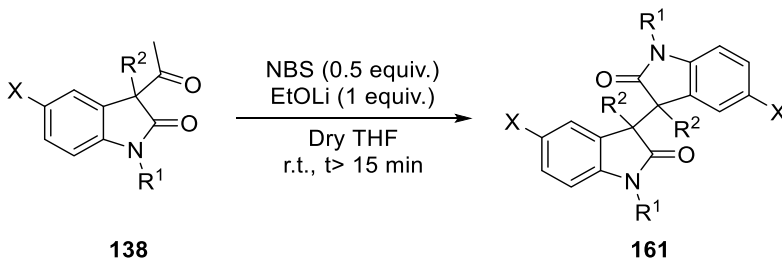
<sup>a</sup> Isolated yield after column chromatography (flash silica).

Originally, we tried to isolate the 3-bromooxindole derivative after reaction of **138** with NBS and EtOLi but we observed important quantities of dimeric species **161**. In order to explain the second step, the plausible mechanism was proposed. In basic conditions and with 0.5 equivalents of *N*-bromosuccinimide (NBS) two species of oxindole were formed *in situ* (Scheme 59). On the one hand, the deacylative oxindole derivative in basic conditions gave a nucleophilic reactivity at C3 position. On the other hand, the bromination of the oxindole ensures the electrophilic character at C3 position.



**Scheme 59.** Proposed mechanism for the dimerization

With the optimal conditions, the reaction was proposed:



**Scheme 60.** Second step of the synthesis of 3,3'-bioxindoles

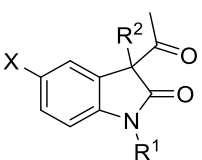
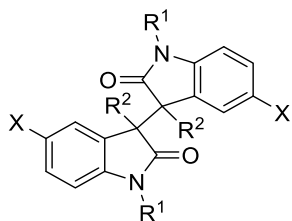
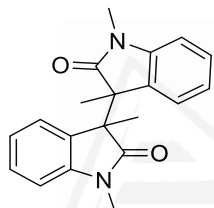
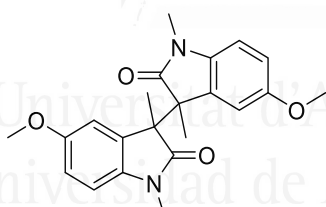
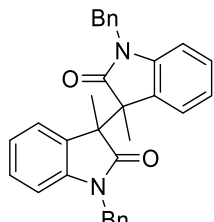
It worth to mention, the reaction took place with *N*-bromosuccinimide (NBS) or with *N*-iodosuccinimide (NIS). Also, dry solvent is necessary due to the presence of water in the media could quench the reaction. On the other hand, freezing- pump was not necessary.

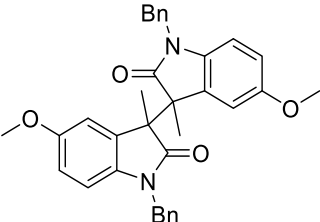
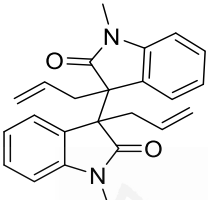
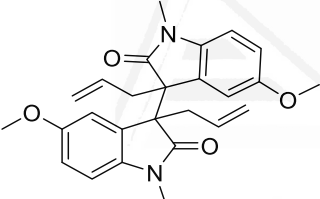
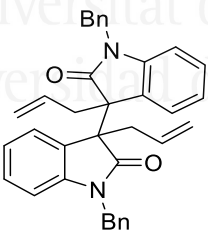
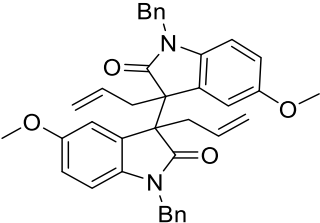
A good point of this methodology was that it is very fast reaction, only a few minutes were enough to produce the dimerization with an excellent conversion. However, in some cases, the reaction took place in 30 minutes. Also, the diastereoselectivity was better in this kind of reactions forming the major ( $R^*,R^*$ )-diastereoisomer. As an inconvenient, in the purification step we only isolated the major diastereoisomer so, the yield of the reaction was moderate, except in one case that it was excellent.

Using this last reaction conditions, the preparation of symmetrically substituted 3,3'-bioxindoles **161** was achieved directly, in a one pot process, where the electrophile was generated *in situ* (it was not necessary to isolate the corresponding iodide or bromide) in the presence of the enolate emulating the classical Barbier conditions. Thus, 3,3'-bioxindoles **161a-h** were isolated in very good and modest yields (90-26%) (Table 5).

In these examples, different substituents at 1, 3 and 5 positions of the heterocycle were evaluated and the diastereoselection was always ( $R^*,R^*$ ):*meso* 3:1 (determined by  $^1\text{H}$  NMR spectroscopy on the crude mixture) and only was isolated the major diastereoisomer after flash chromatography ( $R^*,R^*$ ). It is noticeable that in this cascade reaction two different deacylative processes occurred, the DaI took place and immediately, and the DaA completed the sequence.

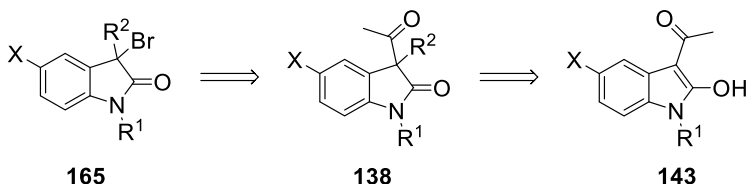
**Table 5.** Scope of the dimerization compound **161** *via* DaA

Entry	<b>138</b>	Product	<b>161</b>	( <i>R*</i> , <i>R*</i> ): <i>meso</i>	Yield (%) <sup>a</sup>
	 <b>138</b>	<p>NBS (0.5 equiv.) EtOLi (1 equiv.)</p> <p>Dry THF r.t., &gt; 15 min</p>	 <b>161</b>		
<b>1</b>	<b>138a</b>		<b>161a</b>	3:1	80
<b>2</b>	<b>138b</b>		<b>161b</b>	3:1	54
<b>3</b>	<b>138c</b>		<b>161c</b>	3:1	48

4	138d		161d	3:1	46
5	138e		161e	3:1	40
6	138f		161f	3:1	40
7	138g		161g	3:1	26
8	138h		161h	3:1	40

<sup>a</sup> Isolated yield after column chromatography (flash silica).

Knowing the procedure of the synthesis of 3,3'-bioxindole, we focused on our second objective of this chapter, the preparation of 3-alkyl-3-bromooxindoles. To achieve this target, the synthetic route was proposed (Scheme 61):



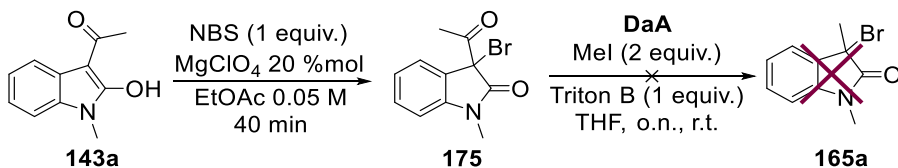
**Scheme 61.** Synthetic route for the preparation of 3-bromooxindoles using deacylative bromination

Although, *a priori* this synthetic route had good results because first step was developed previously, we also propose a second route in order to continue the study of deacylative alkylation as a key methodology. This one, consisted in the bromination of the 3-acetyl-2-oxindole **143** with NBS to produce the intermediate **175** and the second step would be the DaA to form the desired product **165** (Scheme 62).



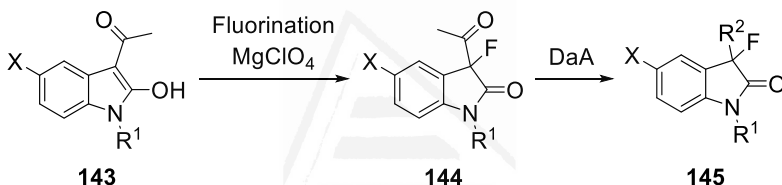
**Scheme 62.** Second hypothetical route using deacylative alkylation

So, we tried the reaction mixing the oxindole **143a**, 1 equiv. of NBS and 0.05 M of ethyl acetate as a solvent and 20 mol% of magnesium perchlorate as a catalyst. After stirring for 40 minutes at room temperature, the work up after reaction was the principal advantage. It was not necessary any purification and  $\text{MgClO}_4$  and succinimide was removed with washing. On the other hand, we discarded the hypothesis because the second step *via* DaA did not occur. The intermediate **175** was decomposed under basic conditions.



**Scheme 63.** Second hypothesis based in deacylative alkylation discarded

Fortunately, the possible halogenation with  $\text{MgClO}_4$  as a catalyst was useful for our research group. This hypothesis had been applied and improved the first step of the preparation of 3-fluorooxindoles. The electronegativity of the fluorine group kept the nucleophilia of C3 of oxindole core and the compound **144** allowed the second step *via* Deacylative Alkylation (Scheme 64). This work was published in 2019.<sup>[10]</sup>

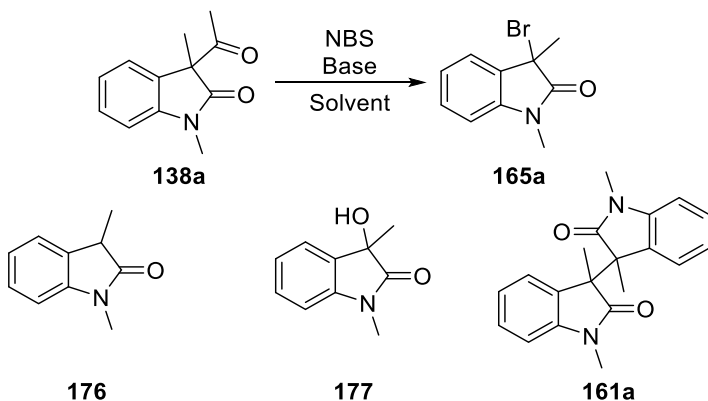


**Scheme 64.** Fluorination of 3-acetyl-2-oxindoles

According to the results of deacylative alkylation to promote the synthesis of 3-bromooxindoles, we came back to the principal route for the preparation of 3-bromooxindoles using deacylative bromination (DaB) (Scheme 61).

With the **138** compounds in hands, we were decided to optimize the conditions of the second step, the Deacylative Bromination. In the previous work, we already knew that the best base for this step were Triton B or lithium ethoxide. We tried both and the best results were obtained with  $\text{EtOLi}$ . The  $^1\text{H}$  NMR spectra of the crude was very complex due to the enormous number of byproducts of the reaction.



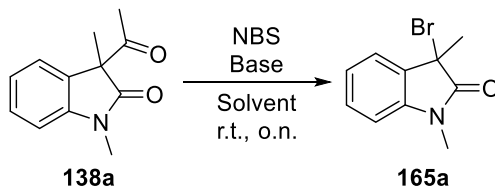


**Scheme 65.** Reaction and byproducts of bromination

Trying to optimize the reaction we concluded that it was necessary more than one equivalent of *N*-bromosuccinimide because in some experiments we obtained unreacted starting material **138a**. Compound **176** was formed in the presence of water, so we changed anhydrous THF (Table 5, entries 3-4). Compound **177** was generated by the oxidation of the starting material with the oxygen of the air, to remove this byproduct we did three cycle of freezing-pump (f.p.) (Table 5, entries 5-9). Finally, we observed of the bioindole derivative **161a** (Table 5, entry 8).

Entry 6 and 7 of Table 5 demonstrated that the reproducibility of the reaction was variable. This is the reason why we tried different ways to do the addition of the reagents. Entry 9 of the Table 5 verified that slowly addition of the mixture between **138** and EtOLi was necessary under NBS solution.

The optimal conditions of the process resulted in preparing two solutions, one of them with the NBS in THF and the other with the anion oxindoles (**138** in basic conditions), followed the second solution was added slowly under NBS solution. This methodology allowed to obtain 3-bromooxindoles with full conversions and good yields. It was a fast reaction and was very simple to follow up by TLC. Also, the reaction was scaled to 2.4 mmol (0.5 g).

**Table 6.** Optimization of the preparation compound **165**

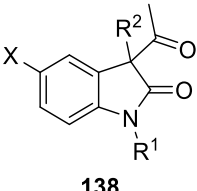
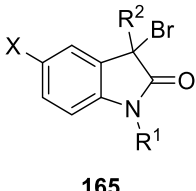
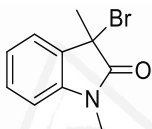
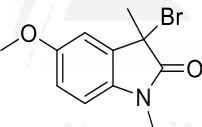
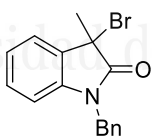
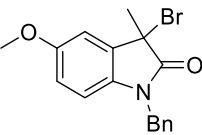
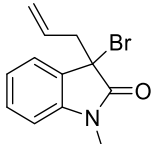
Entry	NBS (equiv.)	EtOLi (equiv.)	Solvent (0.1 M)	Products <sup>b</sup> (165a/176/177/161a)
<b>1<sup>a</sup></b>	1	1	THF	Traces
<b>2</b>	1	1	THF	3/19/14/54
<b>3</b>	1.5	1	Dry THF	15/9/12/50
<b>4<sup>c</sup></b>	1.5	1.2	Dry THF	58/-/7/11
<b>5<sup>c,d</sup></b>	1	1.1	Dry THF	58/-/-/42
<b>6<sup>c,d</sup></b>	2	1	Dry THF	88/-/-/12
<b>7<sup>c,d,e</sup></b>	2	1	Dry THF	75/-/-/25
<b>8<sup>c,d</sup></b>	0.5	1	Dry THF	8/-/-/92
<b>9<sup>c,d,f</sup></b>	2	1	Dry THF	99/-/-/-

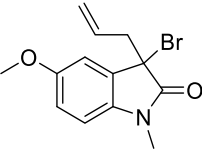
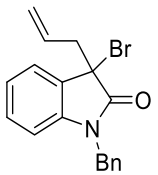
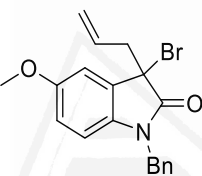
<sup>a</sup> Triton B as a base. <sup>b</sup> Conversion of the crude followed by <sup>1</sup>H NMR. <sup>c</sup> Under argon atmosphere. <sup>d</sup> Three cycle of freezing pump. <sup>e</sup> Scale to 0.6 mmol. <sup>f</sup> Slow addition and quenched after 15 minutes.

In order to minimize the generation of the oxidized compound **177**, three cycles of freezing-pump were necessary. The competition between the formation of the bioindole **161a** and bromoindole **165a** was controlled by the order of addition of the reagents. With the optimal conditions in hands, in a solution containing compound **138**, one equivalent of lithium ethoxide as a base in dry THF, a solution of NBS was added slowly to control the synthesis of the bromoindole. Only 15 minutes are necessary to complete the reaction. After purification by flash chromatography, bromides **165** were isolated as pure compounds in good chemical yields (Table 7). These results were completely reproducible, even the synthesis of compound **165a** was scaled up to 0.5 g (2.4 mmol). This new procedure did not

required strong basic conditions,<sup>[76]</sup> the employment of diazocompounds<sup>[82]</sup> or hazardous tris(dimethylamino)phosphine.<sup>[78]</sup>

**Table 7.** Scope of 3-bromooxindoles (**165**)

Entry	<b>138</b>	Product	<b>165</b>	Yield (%) <sup>a</sup>
	 <b>138</b>	<p>NBS (1.1 equiv.) EtOLi (1 equiv.)</p> <p>Dry THF 0.1M t&gt;15 min, r.t., Ar atm., freezing-pump</p>	 <b>165</b>	
<b>1</b>	<b>138a</b>		<b>165a</b>	70
<b>2</b>	<b>138b</b>		<b>165b</b>	65
<b>3</b>	<b>138c</b>		<b>165c</b>	52
<b>4</b>	<b>138d</b>		<b>165d</b>	45
<b>5</b>	<b>138e</b>		<b>165e</b>	45

<b>6</b>	<b>138f</b>		<b>165f</b>	60
<b>7</b>	<b>138g</b>		<b>165g</b>	51
<b>8</b>	<b>138h</b>		<b>165h</b>	83

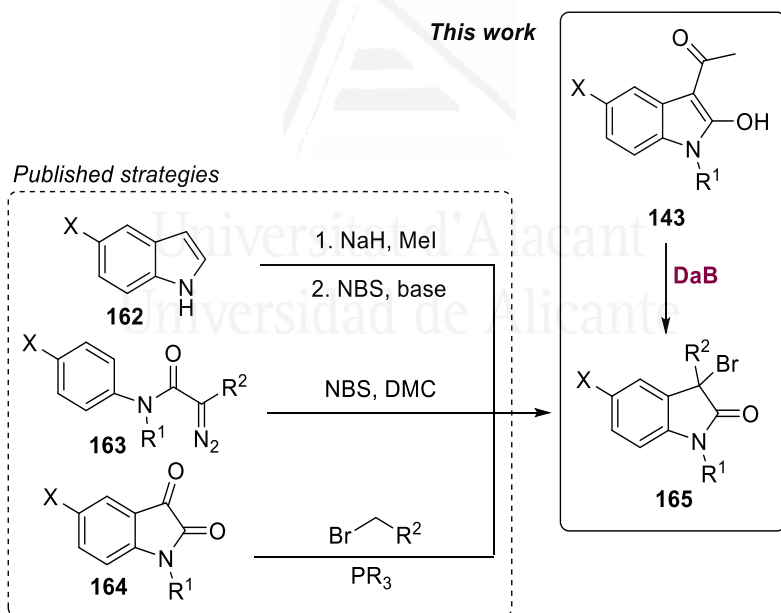
<sup>a</sup> Isolated yield after column chromatography (flash silica).

This protocol allows the preparation of 3-bromooxindoles with moderate (Table 7, entries 2-7) to good and very good yields (Table 7, entries 1 and 8). Also, it is a robust methodology which can be scale up to 0.5 g in a short time (about  $\approx$ 30 minutes).

It worth to mentioning, **165d**, **165f** and **165h** are new compounds.

## II.4. Conclusions

- ✓ **1<sup>st</sup> target:** Deacylative Bromination (DaB) is a good methodology to prepare 3,3'-bioxindole analogues. It is only necessary a few minutes to produce the dimerization with an excellent conversion and good diastereoselectivity forming the major (*R*\*,*R*\*)-diastereoisomer. The yield of the reaction was moderate, except in one case that it was excellent.
- ✓ **2<sup>nd</sup> target:** Deacylative Bromination (DaB) as a novel strategy to obtain the umpolung 3-alkyl-3-bromooxindoles. This protocol can scale up to 0.5 g in a short time. Comparing with the previous work of preparation 3-bromooxindoles (see Scheme 50), this new procedure did not require strong basic conditions, the employment of diazocompounds or hazardous tris(dimethylamino)phosphine.



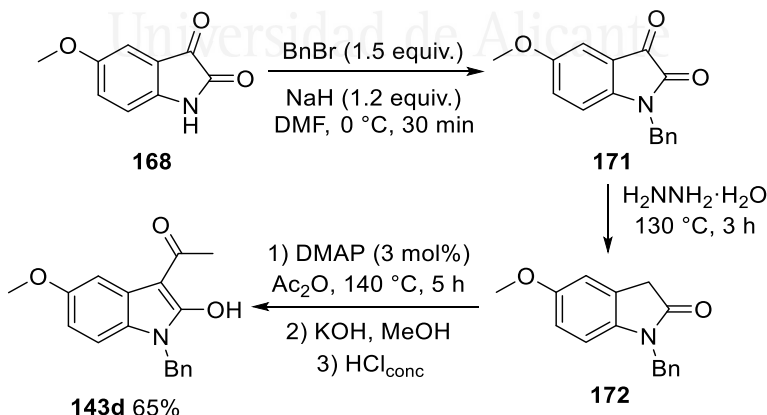
## II.5. Experimental section

### 1. General methods

Melting points were determined with a Marienfeld melting-point meter (MPM-H2) apparatus and are uncorrected. For flash chromatography, silica gel 60 (40–60  $\mu\text{m}$ ) was employed.  $^1\text{H}$  NMR (300, 400 MHz or 500 MHz) and  $^{13}\text{C}$  NMR (75, 101 or 126 MHz) spectra were recorded with Bruker AV300, Bruker AV400, and Bruker ADVANCE DRX500, respectively, with  $\text{CDCl}_3$  as solvent and TMS as internal standard for  $^1\text{H}$  NMR spectra, and the chloroform signal for  $^{13}\text{C}$  NMR spectra; chemical shifts are given in ppm. Low-resolution electron impact (DIP-EI) mass spectra were obtained at 70 eV with an Agilent 6890N Network GC system and an Agilent 5973 Network Mass Selective Detector. High-resolution mass spectra (DIP-EI) were recorded with a QTOF Agilent 7200 instrument for the exact mass and Agilent 7890B for the GC. Analytical TLC was performed using ALUGRAM® Xtra SIL G/UV<sub>254</sub> silica gel plates, and the spots were detected under UV light ( $\lambda=254$  nm).

### 2. Experimental procedures

#### Synthesis of 3-acetyl-2-oxindole derivatives **143b**, **143c** and **143d**



A round-bottom flask containing a solution of isatin (20 mmol) in anhydrous DMF (40 mL) was cooled to 0 °C, then sodium hydride (606 mg,

24 mmol) was added in one portion and the mixture was stirred for 5 minutes. Benzyl bromide was added (30 mmol) and the mixture was stirred at 0 °C for 30 minutes. The mixture was poured in saturated aqueous NH<sub>4</sub>Cl (20 mL) and extracted with dichloromethane (3 x 40 mL). The organic layer was washed with water (3 x 15 mL) and brine (20 mL), dried over MgSO<sub>4</sub> filtered and concentrated.<sup>[83]</sup> To the resulting residue, acetic anhydride (22.5 mL, 238 mL) was added. Then, DMAP (73.3 mg, 0.6 mmol) was added and the mixture was heated at reflux (140 °C) for 5 h and then evaporated under reduced pressure. The residue was dissolved in MeOH (50 mL) and a solution of KOH (11g, 196 mmol) in MeOH (70 mL) was added at 0 °C. The solution was stirred at room temperature overnight. After that, the mixture was cooled in an ice-bath at 0 °C. A solution of 12 M aqueous HCl was added until pH 3. The organic solvent was evaporated, and the residue was extracted with EtOAc (3 x 100 mL), washed with water (100 mL), dried over MgSO<sub>4</sub>, filtered and concentrated. The residue was purified by flash chromatography (hexane/EtOAc) to give pure compounds **143**.

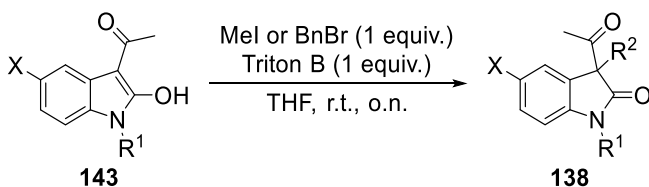
Compounds **143b** and **143d** are described by our research group and the spectral data are consistent with reported data:

**143b**: 1-(2-Hydroxy-5-methoxy-1-methyl-1H-indol-3-yl)ethan-1-one.<sup>[84]</sup>

**143c**: 1-(1-Benzyl-2-hydroxy-1H-indol-3-yl)ethan-1-one.<sup>[84]</sup>

**143d**: 1-(1-Benzyl-2-hydroxy-5-methoxy-1H-indol-3-yl)ethan-1-one.<sup>[85]</sup>

### Synthesis of compounds **138** by monoalkylation (methylation or allylation) of 3-acetyl-2-oxindoles **143**



To a solution of 3-acetyl-2-oxindole **143** (1.2 mmol) and alkyl halide (iodomethane or benzyl bromide) (1.2 mmol) in THF (7 mL) was added Triton B in MeOH (40 wt%, 0.545 mL, 1.2 mmol). The reaction was stirred at room temperature overnight. Water was added (20 mL) and the mixture was extracted with EtOAc (3 x 20 mL) and the combined organic layers were dried over MgSO<sub>4</sub>, filtered and evaporated. The corresponding residue was

purified by flash chromatography (hexane/EtOAc) to afford the corresponding product **138** (see Tables 3 and 4).

**138a**: 3-Acetyl-1,3-dimethylindolin-2-one.<sup>[59]</sup>

**138b**: 3-Acetyl-5-methoxy-1,3-dimethylindolin-2-one.<sup>[59]</sup>

**138c**: 3-Acetyl-1-benzyl-3-methylindolin-2-one.<sup>[86]</sup>

**138d**: 3-Acetyl-1-benzyl-5-methoxy-3-methylindolin-2-one.<sup>[59]</sup>

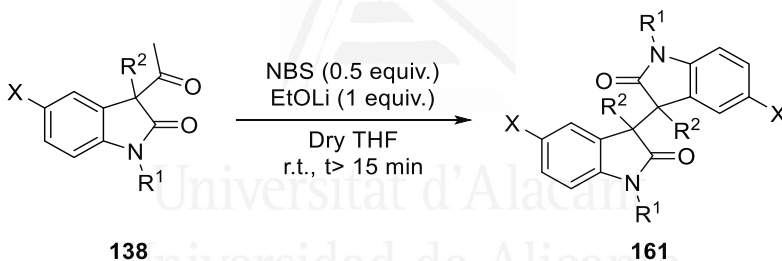
**138e**: 3-Acetyl-3-allyl-1-methylindolin-2-one.<sup>[59]</sup>

**138f**: 3-Acetyl-3-allyl-5-methoxy-1-methylindolin-2-one.<sup>[51]</sup>

**138g**: 3-Acetyl-3-allyl-1-benzylindolin-2-one.<sup>[87]</sup>

**138h**: 3-Acetyl-3-allyl-1-benzyl-5-methoxyindolin-2-one.<sup>[51]</sup>

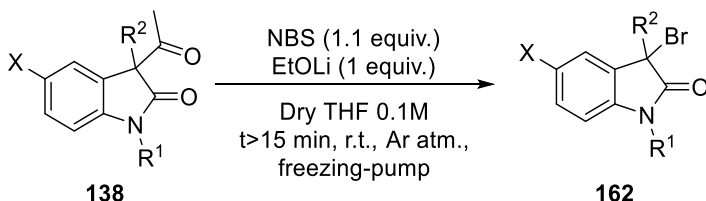
### Synthesis of 3,3'-bioxindoles **161** via DaA



In a Schlenk tube containing 3-acetyl-1,3-dimethylindolin-2-one **138a** (1 equiv., 0.3 mmol, 61 mg) was added in 3mL of dry THF, then lithium ethoxide in THF 1M (1 equiv., 0.3 mmol, 0.3 mL) was added dropwise under Ar atmosphere. Then, *N*-iodosuccinimide (0.5 equiv., 0.15 mmol, 33 mg) was added, and the reaction was stirred a least 15 minutes at room temperature. Work-Up. H<sub>2</sub>O (10 mL) was added, the mixture was extracted with EtOAc (3 × 10 mL) and the combined organic layers were washed (5x10mL H<sub>2</sub>O) and brine. The organic layer was dried over MgSO<sub>4</sub>. Finally, the solution was concentrated (15 Torr) and the residue was purified by column chromatography (hexane/ EtOAc).



## Synthesis of 3-bromooxindole derivatives, compounds **165**

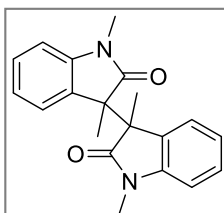


Separately, two solutions were prepared. Solution a) Under Ar atmosphere, *N*-bromosuccinimide (1.1 equiv., 0.33 mmol, 58.7 mg) was added in 1.5 mL of dry THF. This solution was protected from light. Solution b) Under Ar atmosphere **138** (1 equiv., 0.3 mmol) was added in 1.5 mL of dry THF, then lithium ethoxide in THF 1M (1 equiv., 0.3 mmol, 0.3 mL) was added dropwise.

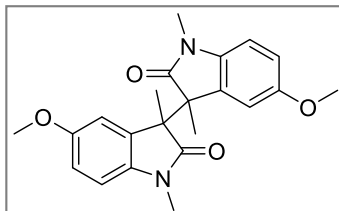
Finally, solution b was added over solution a slowly ( $v=0.6$  mL/min). To complete the reaction, allowing the reaction to proceed at room temperature during at least 10 min. Work-Up was performed as follows: H<sub>2</sub>O (10 mL) was added, the mixture was extracted with EtOAc (3 × 10 mL) and the combined organic layers were washed (5×10mL H<sub>2</sub>O) and brine. Dried the organic layer over MgSO<sub>4</sub>. Finally, the solution was concentrated (15 Torr) and the residue was purified by column chromatography (hexane/ EtOAc).

### 3. Experimental data

Characterization data of compounds described in this chapter will be displayed, it is worth to mention compounds **161d**, **161f**, **161h**, **165d**, **165f** and **165h** are new compounds:

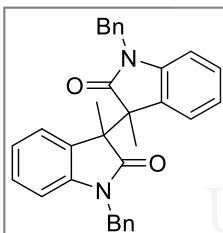


*1,1',3,3'*-Tetramethyl-[3,3'-biindoline]-2,2'-dione (*R*\*,*R*\*-**161a**).<sup>[76]</sup> pale yellow solid; mp 166-167 °C; R<sub>f</sub> 0.70 (hexane/EtOAc 5:5); IR (neat)  $\nu$  2925, 1697, 1609, 1348, 1096, 740, 695 cm<sup>-1</sup>; <sup>1</sup>H NMR (300 MHz, CDCl<sub>3</sub>)  $\delta$  7.08–6.97 (4H, m, ArH), 6.82 (2H, t,  $J = 7.6$  Hz, ArH), 6.45 (2H, d,  $J = 7.7$  Hz, ArH), 3.09 (6H, s, 2 × NCH<sub>3</sub>), 1.75 (6H, s, 2 × CH<sub>3</sub>); <sup>13</sup>C NMR (75 MHz, CDCl<sub>3</sub>)  $\delta$  178.2 (2 × CO), 142.7 (2 × C), 131.2 (2 × C), 128.2 (2 × CH), 122.9 (2 × CH), 121.8 (2 × CH), 107.4 (2 × CH), 51.2 (2 × C), 25.8 (2 × NCH<sub>3</sub>), 16.2 (2 × CH<sub>3</sub>); LRMS(EI)  $m/z$  320 (M<sup>+</sup>, 19%) 161 (61), 160 (100), 130 (12), 117 (13); HRMS(ESI): calcd. for C<sub>20</sub>H<sub>20</sub>N<sub>2</sub>O<sub>2</sub> [M]<sup>+</sup> 320.1529; found 320.1534.

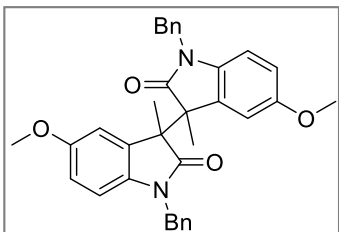


*5,5'-Dimethoxy-1,1',3,3'-tetramethyl-[3,3'-biindoline]-2,2'-dione* ( $R^*,R^*$ -**161b**).<sup>[76]</sup> pale orange solid; mp 213–214 °C;  $R_F$  0.8 (hexane/EtOAc 4.5:5.5); IR (neat)  $\nu$  2940, 1686, 1493, 1215, 1039, 802  $\text{cm}^{-1}$ ;  $^1\text{H}$  NMR (300 MHz,  $\text{CDCl}_3$ )  $\delta$  6.73 (2H, d,  $J = 2.5$  Hz, ArH), 6.58 (2H, dd,  $J = 8.5, 2.6$  Hz, ArH), 6.39 (2H, d,  $J = 8.5$  Hz, ArH), 3.69 (6H, s, 2 x

$\text{OCH}_3$ ), 3.10 (6H, s, 2 x  $\text{NCH}_3$ ), 1.74 (6H, s, 2 x  $\text{CH}_3$ );  $^{13}\text{C}$  NMR (75 MHz,  $\text{CDCl}_3$ )  $\delta$  177.9 (2 x CO), 155.7 (2 x C), 136.1 (2 x C), 132.5 (2 x C), 113.1 (2 x CH), 110.1 (2 x CH), 107.8 (2 x CH), 55.9 (2 x  $\text{OCH}_3$ ), 51.5 (2 x C), 26.0 (2 x  $\text{NCH}_3$ ), 16.6 (2 x  $\text{CH}_3$ ); LRMS (EI)  $m/z$  380 ( $\text{M}^+$ , 10%), 192 (2), 191 (16), 190 (100), 176 (2), 175 (6), 174 (3), 162 (2), 160 (2), 159 (2), 147 (5), 119 (2), 118 (3); HRMS (ESI): calcd. for  $\text{C}_{22}\text{H}_{24}\text{N}_2\text{O}_4$  [ $\text{M}$ ]<sup>+</sup> 380.1736; found 380.1749.

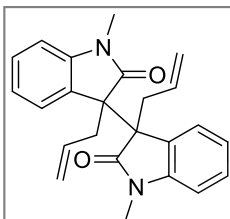


*1,1'-Dibenzyl-3,3'-dimethyl-[3,3'-biindoline]-2,2'-dione* ( $R^*,R^*$ -**161c**).<sup>[76]</sup> yellow solid; mp 189–190 °C;  $R_F$  0.70 (hexane/EtOAc 6:4); IR (neat)  $\nu$  2970, 1697, 1606, 1371, 1181, 741, 694  $\text{cm}^{-1}$ ;  $^1\text{H}$  NMR (300 MHz,  $\text{CDCl}_3$ )  $\delta$  7.31–7.18 (10H, m, ArH), 7.05 (2H, d,  $J = 7.5$  Hz, ArH), 6.94 (2H, td,  $J = 7.7, 1.2$  Hz, ArH), 6.66 (2H, td,  $J = 7.6, 1.0$  Hz, ArH), 6.46 (1H, d,  $J = 7.6$  Hz, ArH), 5.01 (2H, d,  $J = 15.6$  Hz, 2 x CHH), 4.68 (2H, d,  $J = 15.6$  Hz, 2 x CHH), 1.84 (6H, s, 2 x  $\text{CH}_3$ );  $^{13}\text{C}$  NMR (75 MHz,  $\text{CDCl}_3$ )  $\delta$  178.6 (2 x CO), 142.0 (2 x C), 135.8 (2 x C), 131.5 (2 x C), 128.8 (4 x CH), 128.0 (2 x CH), 127.7 (4 x CH), 127.7 (2 x CH), 123.7 (2 x CH), 122.3 (2 x CH), 108.7 (2 x CH), 50.8 (2 x C), 43.8 (2 x  $\text{CH}_2$ ), 17.9 (2 x  $\text{CH}_3$ ); LRMS (EI)  $m/z$  472 ( $\text{M}^+$ , 3%), 238 (6), 237 (43), 236 (100), 235 (6), 91 (61); HRMS (ESI): calcd. for  $\text{C}_{32}\text{H}_{28}\text{N}_2\text{O}_2$  [ $\text{M}$ ]<sup>+</sup> 472.2151; found 472.2169.

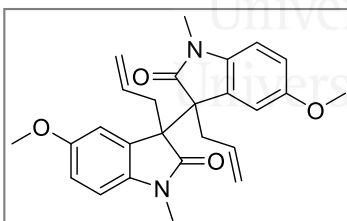


*1,1'-Dibenzyl-5,5'-dimethoxy-3,3'-dimethyl-[3,3'-biindoline]-2,2'-dione* ( $R^*,R^*$ -**161d**). yellow solid; mp 193–194 °C;  $R_F$  0.70 (hexane/EtOAc 6:4); IR (neat)  $\nu$  2967, 1698, 1453, 1180, 1036, 730, 700  $\text{cm}^{-1}$ ;  $^1\text{H}$  NMR (300 MHz,  $\text{CDCl}_3$ )  $\delta$  7.29–7.22 (6H, m, ArH), 7.14 (4H, dd,  $J = 7.4, 2.0$  Hz, ArH), 6.86 (2H, d,  $J = 2.5$  Hz, ArH), 6.50 (2H, dd,  $J = 8.5, 2.6$  Hz, ArH), 6.32 (2H, d,  $J = 8.5$  Hz, ArH), 5.07 (2H, d,  $J = 15.8$  Hz, 2 x CHH),

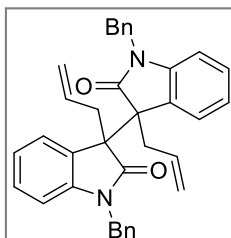
4.66 (2H, d,  $J = 15.8$  Hz, 2 x CHH), 3.58 (6H, s, OCH<sub>3</sub>), 1.86 (6H, s, CH<sub>3</sub>); <sup>13</sup>C NMR (75 MHz, CDCl<sub>3</sub>) δ 178.4 (2 x CO), 155.8 (2 x C), 135.8 (2 x C), 135.4 (2 x C), 132.9 (2 x C), 128.9 (4 x CH), 127.5 (2 x CH), 127.1 (4 x CH), 112.9 (2 x CH), 110.9 (2 x CH), 109.4 (2 x CH), 55.6 (2 x OCH<sub>3</sub>), 51.3 (2 x C), 43.8 (2 x CH<sub>2</sub>), 18.4 (2 x CH<sub>3</sub>); LRMS (EI)  $m/z$  532 (M<sup>+</sup>, 6%), 267 (25), 266 (100), 265 (7), 91 (47); HRMS (ESI): calcd. for C<sub>34</sub>H<sub>32</sub>N<sub>2</sub>O<sub>4</sub> [M]<sup>+</sup> 532.2362; found 532.2361.



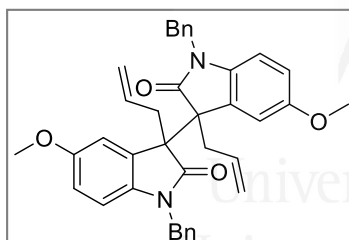
*3,3'-Diallyl-1,1'-dimethyl-[3,3'-biindoline]-2,2'-dione (R\*,R\*-**161e**)*.<sup>[76]</sup> yellow solid; mp 215–216 °C; R<sub>F</sub> 0.70 (hexane/EtOAc 6:4); IR (neat) ν 2932, 1686, 1491, 1353, 1096, 924, 757 cm<sup>-1</sup>; <sup>1</sup>H NMR (300 MHz, CDCl<sub>3</sub>) δ 7.07–6.96 (4H, m, ArH), 6.82 (2H, td,  $J = 7.6, 0.9$  Hz, ArH), 6.41 (2H, d,  $J = 7.8$  Hz, ArH), 5.05–4.98 (4H, m, 2 x HC=CH<sub>2</sub>), 4.74 (2H, dd,  $J = 8.3, 3.9$  Hz, 2 x HC=CH<sub>2</sub>), 3.64 (2H, dd,  $J = 12.6, 5.0$  Hz, 2 x CHH), 3.06 (6H, s, NCH<sub>3</sub>), 3.05–2.99 (2H, m, 2 x CHH); <sup>13</sup>C NMR (75 MHz, CDCl<sub>3</sub>) δ 177.0 (2 x CO), 143.4 (2 x C), 132.6 (2 x CH), 128.3 (2 x C), 128.2 (2 x CH), 123.5 (2 x CH), 121.8 (2 x CH), 118.9 (2 x CH), 107.3 (2 x CH<sub>2</sub>), 56.0 (2 x C), 33.3 (2 x NCH<sub>3</sub>), 25.7 (2 x CH<sub>2</sub>); LRMS (EI)  $m/z$  372 (M<sup>+</sup>, 6%), 187 (49), 186 (100), 158 (16), 144 (10), 143 (10); HRMS (ESI): calcd. for C<sub>24</sub>H<sub>24</sub>N<sub>2</sub>O<sub>2</sub> [M]<sup>+</sup> 372.1838; found 372.1862.



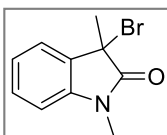
*3,3'-Diallyl-5,5'-dimethoxy-1,1'-dimethyl-[3,3'-biindoline]-2,2'-dione (R\*,R\*-**161f**)*. White solid; mp 201–202 °C; R<sub>F</sub> 0.25 (hexane/EtOAc 9:1); IR (neat) ν 1687, 1498, 1433, 1235, 923, 811, 736 cm<sup>-1</sup>; <sup>1</sup>H NMR (300 MHz, CDCl<sub>3</sub>) δ 6.71 (2H, d,  $J = 2.5$  Hz, ArH), 6.56 (2H, dd,  $J = 8.4, 2.6$  Hz, ArH), 6.35 (2H, d,  $J = 8.5$  Hz, ArH), 5.05–4.99 (2H, m, 2 x HC=CH<sub>2</sub>), 4.76 (2H, dd,  $J = 8.0, 4.2$  Hz, 2 x HC=CH<sub>2</sub>), 3.69 (6H, s, 2 x OCH<sub>3</sub>), 3.62 (2H, dd,  $J = 13.2, 4.9$  Hz, 2 x CHH), 3.07 (6H, s, 2 x NCH<sub>3</sub>), 3.01 (2H, dd,  $J = 13.2, 5.4$  Hz, 2 x CHH); <sup>13</sup>C NMR (75 MHz, CDCl<sub>3</sub>) δ 176.6 (2 x CO), 155.7 (2 x C), 137.0 (2 x C), 132.6 (2 x CH), 129.7 (2 x C), 118.9 (2 x CH<sub>2</sub>), 113.1 (2 x CH), 110.7 (2 x CH), 107.7 (2 x CH), 56.3 (2 x C), 55.9 (2 x OCH<sub>3</sub>), 33.7 (2 x CH<sub>2</sub>), 25.9 (2 x NCH<sub>3</sub>); LRMS (EI)  $m/z$  432 (M<sup>+</sup>, 11%), 217 (22), 216 (100), 174 (12); HRMS (ESI): calcd. for C<sub>26</sub>H<sub>28</sub>N<sub>2</sub>O<sub>4</sub> [M]<sup>+</sup> 432.2049; found 432.2061.



**3,3'-Diallyl-1,1'-dibenzyl-[3,3'-biindoline]-2,2'-dione (*R\*,R\**-**161g**)**.<sup>[76]</sup> Pale yellow solid; mp 201-202 °C;  $R_F$  0.70 (hexane/EtOAc 5:5); IR (neat)  $\nu$  1696, 1606, 1485, 1366, 1178, 919, 753, 695  $\text{cm}^{-1}$ ;  $^1\text{H}$  NMR (300 MHz,  $\text{CDCl}_3$ )  $\delta$  7.31–7.18 (10H, m, ArH), 7.07 (2H, d,  $J = 8.3$  Hz, ArH), 6.91 (2H, td,  $J = 7.7, 1.2$  Hz, ArH), 6.70 (2H, td,  $J = 7.6, 1.0$  Hz, ArH), 6.35 (2H, d,  $J = 7.6$  Hz, ArH), 5.12 (2H, d,  $J = 15.6$  Hz, 2 x CHH), 5.08–5.01 (4H, m, 2 x HC=CH<sub>2</sub>), 4.85–4.75 (2H, m, 2 x HC=CH<sub>2</sub>), 4.47 (2H, d,  $J = 15.6$  Hz, 2 x CHH), 3.80–3.70 (2H, m, 2 x CHH), 3.15–3.06 (2H, m, 2 x CHH);  $^{13}\text{C}$  NMR (75 MHz,  $\text{CDCl}_3$ )  $\delta$  177.2 (2 x CO), 142.9 (2 x C), 135.6 (2 x C), 132.6 (2 x CH), 128.7 (2 x CH), 128.3 (4 x CH), 128.2 (2 x C), 127.7 (2 x CH), 127.6 (4 x CH), 124.1 (2 x CH), 122.1 (2 x CH), 119.3 (2 x CH), 108.6 (2 x CH), 55.8 (2 x C), 43.9 (2 x CH<sub>2</sub>), 34.2 (2 x CH<sub>2</sub>); LRMS (EI)  $m/z$  524 ( $\text{M}^+$ , 2%), 263 (54), 262 (83), 261 (4), 91 (100); HRMS (ESI): calcd. for  $\text{C}_{36}\text{H}_{32}\text{N}_2\text{O}_2$  [ $\text{M}$ ]<sup>+</sup> 524.2464; found 524.2470.

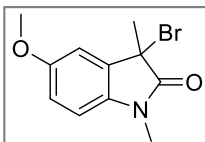


**3,3'-Diallyl-1,1'-dibenzyl-5,5'-dimethoxy-[3,3'-biindoline]-2,2'-dione (*R\*,R\**-**161h**)**. red solid; mp 152-153 °C;  $R_F$  0.70 (hexane/EtOAc 5:5); IR (neat)  $\nu$  1697, 1494, 1434, 1198, 1043, 906, 727  $\text{cm}^{-1}$ ;  $^1\text{H}$  NMR (300 MHz,  $\text{CDCl}_3$ )  $\delta$  7.32-7.13 (10H, m, ArH), 6.84 (2H, d,  $J = 2.5$  Hz, ArH), 6.48 (2H, dd,  $J = 8.5, 2.6$  Hz, ArH), 6.23 (2H, d,  $J = 8.5$  Hz, ArH), 5.18 (2H, d,  $J = 15.7$  Hz, 2 x CHH), 5.13–5.04 (4H, m, 2 x HC=CH<sub>2</sub>), 4.87–4.78 (2H, m, 2 x HC=CH<sub>2</sub>), 4.45 (2H, d,  $J = 15.7$  Hz, 2 x CHH), 3.82–3.70 (2H, m, 2 x CHH), 3.62 (6H, s, 2 x OCH<sub>3</sub>), 3.11 (2H, dd,  $J = 15.4, 4.3$  Hz, 2 x CHH);  $^{13}\text{C}$  NMR (75 MHz,  $\text{CDCl}_3$ )  $\delta$  176.9 (2 x CO), 155.7 (2 x C), 136.3 (2 x C), 135.6 (2 x CH), 132.6 (2 x CH), 129.7 (2 x CH), 128.7 (2 x C), 127.5 (4 x CH), 127.4 (4 x CH), 119.4 (2 x CH<sub>2</sub>), 113.0 (2 x CH), 111.2 (2 x CH), 109.2 (2 x CH), 56.2 (2 x C), 55.7 (2 x OCH<sub>3</sub>), 43.9 (2 x CH<sub>2</sub>), 34.5 (2 x CH<sub>2</sub>); LRMS (EI)  $m/z$  584 ( $\text{M}^+$ , 8%), 293 (33), 292 (96), 188 (13), 91 (100); HRMS (ESI): calcd. for  $\text{C}_{38}\text{H}_{36}\text{N}_2\text{O}_4$  [ $\text{M}$ ]<sup>+</sup> 584.2675; found 584.2682.

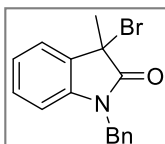


**3-Bromo-1,3-dimethylindolin-2-one (**165a**)**.<sup>[77]</sup> yellow solid; mp 83-85 °C;  $R_F$  0.25 (hexane/EtOAc 9:1); IR (neat)  $\nu$  1719, 1611, 1470, 1345, 749, 663  $\text{cm}^{-1}$ ;  $^1\text{H}$  NMR (300 MHz,  $\text{CDCl}_3$ )  $\delta$  7.44 (1H, dd,  $J = 7.5, 1.1$  Hz, ArH), 7.33 (1H, td,

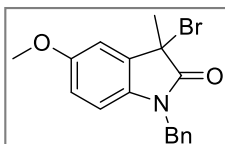
$J = 7.8, 1.3$  Hz, ArH), 7.12 (1H, td,  $J = 7.6, 0.9$  Hz, ArH), 6.84 (1H, d,  $J = 7.8$  Hz, ArH), 3.24 (3H, s, NCH<sub>3</sub>), 2.03 (3H, s, CH<sub>3</sub>); <sup>13</sup>C NMR (101 MHz, CDCl<sub>3</sub>)  $\delta$  174.8 (CO), 141.8 (C), 131.7 (C), 130.2 (CH), 124.2 (CH), 123.5 (CH), 108.9 (CH), 52.5 (C), 26.8 (NCH<sub>3</sub>), 26.5 (CH<sub>3</sub>); LRMS (EI)  $m/z$  240 (M<sup>+</sup>, 10%), 238 (M<sup>+</sup>, 10%), 161 (13), 160 (30), 159 (41), 158 (11), 146 (10), 131 (17), 130 (42), 118 (12), 71 (14), 70 (22), 61 (15), 57 (14), 45 (13), 43 (100); HRMS (ESI): calcd. for C<sub>10</sub>H<sub>10</sub>BrNO [M]<sup>+</sup> 238.9946; found 238.9950.



**3-Bromo-5-methoxy-1,3-dimethylindolin-2-one (165b):**<sup>[77]</sup> brown solid; mp 107-108 °C; R<sub>F</sub> 0.25 (hexane/EtOAc 8.5:1.5); IR (neat)  $\nu$  1717, 1497, 1265, 1109, 1036, 732, 702 cm<sup>-1</sup>; <sup>1</sup>H NMR (300 MHz, CDCl<sub>3</sub>)  $\delta$  7.04 (1H, d,  $J = 2.5$  Hz, ArH), 6.86 (1H, dd,  $J = 8.5, 2.6$  Hz, ArH), 6.74 (1H, d,  $J = 8.5$  Hz, ArH), 3.82 (3H, s, OCH<sub>3</sub>), 3.22 (3H, s, NCH<sub>3</sub>), 2.02 (3H, s, CH<sub>3</sub>); <sup>13</sup>C NMR (75 MHz, CDCl<sub>3</sub>)  $\delta$  174.6 (CO), 156.6 (C), 135.2 (C), 132.8 (C), 114.9 (CH), 111.2 (CH), 109.4 (CH), 56.0 (OCH<sub>3</sub>), 52.8 (C), 26.9 (NCH<sub>3</sub>), 26.5 (CH<sub>3</sub>); LRMS (EI)  $m/z$  271 (M<sup>+</sup>, 4%), 269 (M<sup>+</sup>, 4%), 191 (48), 190 (100), 189 (71), 176 (44), 175 (26), 174 (96), 148 (21), 146 (16), 118 (17), 117 (12), 90 (11), 43 (22); HRMS (ESI): calcd. for C<sub>11</sub>H<sub>12</sub>BrNO<sub>2</sub> [M]<sup>+</sup> 269.0051; found 269.0053.

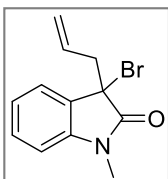


**1-Benzyl-3-bromo-3-methylindolin-2-one (165c):**<sup>[77]</sup> orange wax; R<sub>F</sub> 0.25 (hexane/EtOAc 9.5:0.5); IR (neat)  $\nu$  2359, 1720, 1610, 1486, 1468, 1356, 1182, 751 cm<sup>-1</sup>; <sup>1</sup>H NMR (400 MHz, CDCl<sub>3</sub>)  $\delta$  7.45 (1H, d,  $J = 8.2$  Hz, ArH), 7.34–7.25 (5H, m, ArH), 7.19 (1H, t,  $J = 7.8$  Hz, ArH), 7.07 (1H, t,  $J = 8.0$  Hz, ArH), 6.69 (1H, d,  $J = 7.8$  Hz, ArH), 5.02 (1H, d,  $J = 15.7$  Hz, CHH), 4.84 (1H, d,  $J = 15.7$  Hz, CHH), 2.09 (3H, s, CH<sub>3</sub>); <sup>13</sup>C NMR (101 MHz, CDCl<sub>3</sub>)  $\delta$  175.1 (CO), 141.0 (C), 135.3 (C), 131.8 (C), 130.1 (CH), 129.0 (2 x CH), 127.9 (CH), 127.3 (2 x CH), 124.3 (CH), 123.5 (CH), 109.9 (CH), 52.6 (C), 44.1 (CH<sub>2</sub>), 26.4 (CH<sub>3</sub>); LRMS (EI)  $m/z$  317 (M<sup>+</sup>, 1%), 315 (M<sup>+</sup>, 1%), 237 (33), 236 (34), 235 (49), 91 (100); HRMS (ESI): calcd. for C<sub>16</sub>H<sub>14</sub>BrNO [M]<sup>+</sup> 315.0259; found 315.0257.



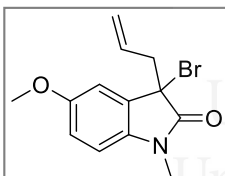
**1-Benzyl-3-bromo-5-methoxy-3-methylindolin-2-one (165d):** brown wax; R<sub>F</sub> 0.25 (hexane/EtOAc 9:1); IR (neat)  $\nu$  1720, 1495, 1264, 1041, 895, 732, 702 cm<sup>-1</sup>; <sup>1</sup>H NMR (300 MHz, CDCl<sub>3</sub>)  $\delta$  7.34–7.25 (5H, m, ArH), 7.04 (1H, d,  $J = 2.6$  Hz, ArH), 6.72 (1H, dd,  $J = 8.6, 2.6$  Hz, ArH), 6.58 (1H, ArH), 5.00 (1H, d,  $J = 15.8$  Hz, CHH), 4.81 (1H, d,  $J = 15.7$  Hz, CHH), 3.77 (3H, s, OCH<sub>3</sub>), 2.08 (3H, s, CH<sub>3</sub>); <sup>13</sup>C NMR (101 MHz,

$\text{CDCl}_3$   $\delta$  174.9 (CO), 156.6 (C), 135.4 (C), 134.2 (C), 132.8 (C), 129.0 (2 x CH), 127.9 (CH), 127.2 (2 x CH), 114.9 (CH), 111.1 (CH), 110.5 (CH), 56.0 (OCH<sub>3</sub>), 52.9 (C), 44.2 (CH<sub>2</sub>), 26.5 (CH<sub>3</sub>); LRMS (EI)  $m/z$  347 (M<sup>+</sup>, 1%), 345 (M<sup>+</sup>, 1%), 267 (27), 266 (31), 265 (97), 146 (14), 91 (100); HRMS (ESI): calcd. for C<sub>17</sub>H<sub>16</sub>BrNO<sub>2</sub> [M]<sup>+</sup> 345.0364; found 345.0356.



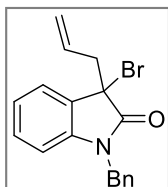
*3-Allyl-3-bromo-1-methylindolin-2-one* (**165e**):<sup>[79]</sup>

yellow solid; mp 76–77 °C; R<sub>F</sub> 0.25 (hexane/EtOAc 9:1); IR (neat)  $\nu$  1723, 1612, 1471, 1265, 930, 732, 702 cm<sup>-1</sup>; <sup>1</sup>H NMR (300 MHz, CDCl<sub>3</sub>)  $\delta$  7.42 (1H, dd,  $J$  = 7.5, 1.2 Hz, ArH), 7.33 (1H, td,  $J$  = 7.8, 1.3 Hz, ArH), 7.10 (1H, td,  $J$  = 7.6, 1.0 Hz, ArH), 6.83 (1H, d,  $J$  = 7.8 Hz, ArH), 5.60–5.44 (1H, m, HC=CH<sub>2</sub>), 5.17–5.03 (2H, m, HC=CH<sub>2</sub>), 3.23 (3H, s, NCH<sub>3</sub>), 3.18–2.97 (2H, m, CH<sub>2</sub>); <sup>13</sup>C NMR (101 MHz, CDCl<sub>3</sub>)  $\delta$  173.9 (CO), 142.5 (C), 131.1 (CH), 130.2 (CH), 129.7 (C), 125.0 (CH), 123.4 (CH), 120.8 (CH), 108.8 (CH<sub>2</sub>), 55. (C), 43.5 (CH<sub>2</sub>), 26.8 (NCH<sub>3</sub>); LRMS (EI)  $m/z$  267 (M<sup>+</sup>, 2%), 265 (M<sup>+</sup>, 3%), 187 (12), 186 (19), 185 (33), 184 (32), 158 (12), 146 (24), 71 (10), 70 (18), 61 (17), 57 (13), 45 (15), 43 (100); HRMS (ESI): calcd. for C<sub>12</sub>H<sub>12</sub>BrNO [M]<sup>+</sup> 265.0102; found 265.0115.



*3-Allyl-3-bromo-5-methoxy-1-methylindolin-2-one* (**165f**):

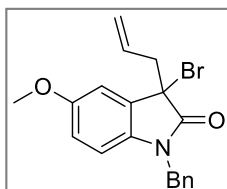
yellow wax; R<sub>F</sub> 0.25 (hexane/EtOAc 9:1); IR (neat)  $\nu$  1719, 1496, 1288, 1265, 1034, 733, 702 cm<sup>-1</sup>; <sup>1</sup>H NMR (300 MHz, CDCl<sub>3</sub>)  $\delta$  7.02 (1H, d,  $J$  = 2.5 Hz, ArH), 6.86 (1H, dd,  $J$  = 8.5, 2.6 Hz, ArH), 6.73 (1H, d,  $J$  = 8.5 Hz, ArH), 5.64–5.44 (1H, m, HC=CH<sub>2</sub>), 5.17–5.03 (2H, m, HC=CH<sub>2</sub>), 3.81 (3H, s, OCH<sub>3</sub>), 3.20 (3H, s, NCH<sub>3</sub>), 3.06 (2H, qd,  $J$  = 13.9, 7.1 Hz, CH<sub>2</sub>); <sup>13</sup>C NMR (101 MHz, CDCl<sub>3</sub>)  $\delta$  174.0 (CO), 156.8 (C), 136.2 (C), 131.3 (CH), 131.1 (C), 121.2 (CH<sub>2</sub>), 115.1 (CH), 112.3 (CH), 109.6 (CH), 56.3 (OCH<sub>3</sub>), 55.7 (C), 43.8 (CH<sub>2</sub>), 27.2 (NCH<sub>3</sub>); LRMS (EI)  $m/z$  297 (M<sup>+</sup>, 4%), 295 (M<sup>+</sup>, 4%), 217 (46), 216 (52), 215 (100), 214 (20), 200 (36), 188 (11), 184 (11), 176 (75), 174 (17), 173 (11), 172 (40), 144 (14), 115 (40), 43 (45); HRMS (ESI): calcd. for C<sub>13</sub>H<sub>14</sub>BrNO<sub>2</sub> [M]<sup>+</sup> 295.0208; found 295.0214.



*3-Allyl-1-benzyl-3-bromoindolin-2-one* (**165g**):<sup>[88]</sup>

orange wax; R<sub>F</sub> 0.25 (hexane/EtOAc 9.7:0.3); IR (neat)  $\nu$  2362, 1721, 1610, 1486, 1468, 1355, 1174, 927, 749 cm<sup>-1</sup>; <sup>1</sup>H NMR (400 MHz, CDCl<sub>3</sub>)  $\delta$  7.45–7.41 (1H, m, ArH), 7.33–7.24 (5H, m, ArH), 7.19 (1H, td,  $J$  = 7.8, 1.3 Hz, ArH), 7.06 (1H, td,  $J$  = 7.6, 0.9 Hz, ArH), 6.67 (1H, d,  $J$  = 7.8 Hz, ArH),

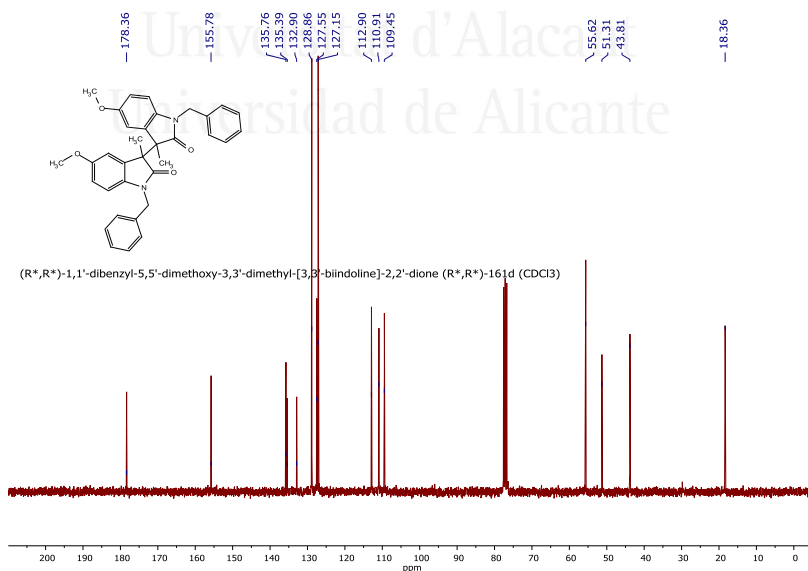
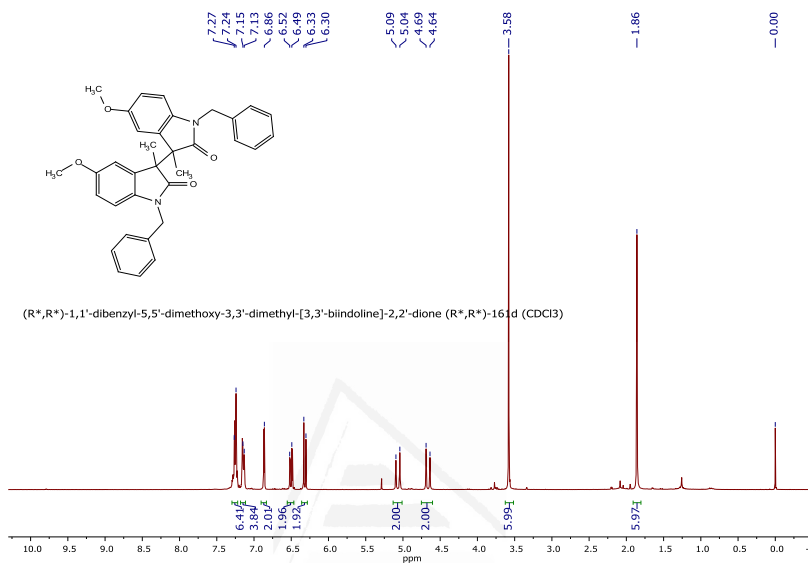
5.59–5.45 (1H, m, HC=CH<sub>2</sub>), 5.20–5.05 (2H, m, HC=CH<sub>2</sub>), 4.97 (1H, d, *J* = 15.8 Hz, CHH), 4.88 (1H, d, *J* = 15.8 Hz, CHH), 3.26–3.09 (2H, m, CH<sub>2</sub>); <sup>13</sup>C NMR (101 MHz, CDCl<sub>3</sub>) δ 174.1 (C), 141.6, 135.3 (C), 131.1 (CH), 130.1 (CH), 129.6 (C), 128.9 (2 x CH), 127.9 (CH), 127.3 (2 x CH), 124.9 (CH), 123.4 (CH), 121.1 (CH), 109.9 (CH<sub>2</sub>), 55.1 (C), 44.2 (CH<sub>2</sub>), 43.5 (CH<sub>2</sub>); LRMS (EI) *m/z* 343 (M<sup>+</sup>, 2%), 341 (M<sup>+</sup>, 2%), 263 (34), 262 (28), 261 (48), 232 (15), 222 (40), 218 (13), 91 (100); HRMS (ESI): calcd. for C<sub>18</sub>H<sub>16</sub>BrNO [M]<sup>+</sup> 341.0415; found 341.0415.



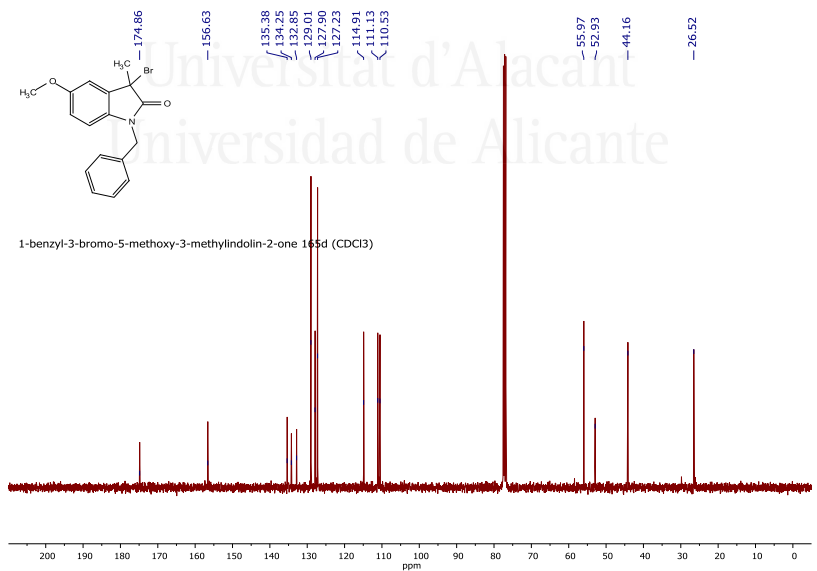
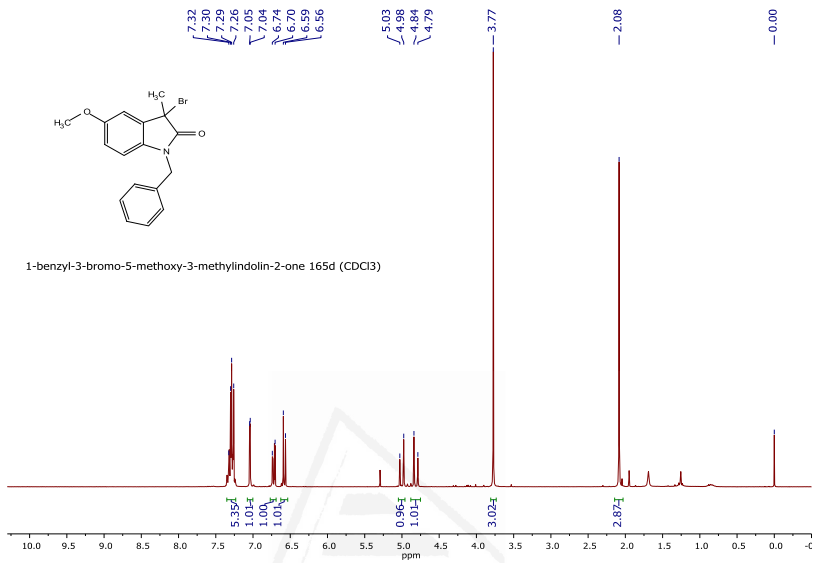
*3-Allyl-1-benzyl-3-bromo-5-methoxyindolin-2-one*

**(165h)**: yellow oil; R<sub>F</sub> 0.25 (hexane/EtOAc 9:1); IR (neat) ν 1717, 1492, 1435, 1178, 1042, 733, 695 cm<sup>-1</sup>; <sup>1</sup>H NMR (300 MHz, CDCl<sub>3</sub>) δ 7.33–7.24 (5H, m, ArH), 7.02 (1H, d, *J* = 2.5 Hz, ArH), 6.71 (1H, dd, *J* = 8.6, 2.6 Hz, ArH), 6.55 (1H, d, *J* = 8.6 Hz, ArH), 5.62–5.43 (1H, m, HC=CH<sub>2</sub>), 5.23–5.04 (2H, m, HC=CH<sub>2</sub>), 4.94 (1H, d, *J* = 15.8 Hz, CHH), 4.85 (1H, d, *J* = 15.8 Hz, CHH), 3.76 (3H, s, OCH<sub>3</sub>), 3.22–3.10 (2H, m, CH<sub>2</sub>); <sup>13</sup>C NMR (101 MHz, CDCl<sub>3</sub>) δ 173.8 (CO), 156.4 (C), 135.3 (C), 134.9 (C), 131.1 (CH), 130.7 (C), 128.9 (2 x CH), 127.8 (CH), 127.3 (2 x CH), 121.1 (CH<sub>2</sub>), 114.8 (CH), 111.8 (CH), 110.4 (CH), 55.9 (OCH<sub>3</sub>), 55.4 (C), 44.2 (CH<sub>2</sub>), 43.5 (CH<sub>2</sub>); LRMS (EI) *m/z* 373 (M<sup>+</sup>, 1%), 371 (M<sup>+</sup>, 1%), 292 (23), 291 (100), 200 (14), 172 (15), 91 (64); HRMS (ESI): calcd. for C<sub>19</sub>H<sub>18</sub>BrNO<sub>2</sub> [M]<sup>+</sup> 371.0521; found 371.0529

To finalize this experimental section some examples of NMR spectra are shown:









Universitat d'Alacant  
Universidad de Alicante



## INTRODUCTION II: PHOTOCATALYSIS AND DUAL CATALISYS

Universitat d'Alacant  
Universidad de Alicante



## **1. Photocatalysis**

---

### **1.1. A brief introduction to this field**

---

Deep environmental impact of the use of fossil resources as a main source of energy makes it essential to develop and improve new systems and processes that allow to obtain which energy from renewable sources like wind, tides or sun.

Photochemistry is the branch of the chemistry that deals with the study of the physical and chemical effects of light under molecules, allowing the use of the light as a source of energy to carry out chemical reaction. However, most part of described reactions are focused on the direct excitation of the molecules and such excitation requires the irradiation at shorter wavelengths between  $\lambda = 200\text{-}400\text{ nm}$  (UV light). Due to the ozone layer blocks the passage of most of the ultraviolet solar radiation ( $\lambda = 200\text{-}320\text{ nm}$ ) the use of sunlight in this kind of reactions is not very efficient. On the other hand, the radiation of the solar spectrum that arrives with great intensity corresponds to the region blue, green and red to area of the visible spectrum ( $\lambda = 400\text{-}650\text{ nm}$ ).

So, photocatalysis is the area responsible for the development of new synthetic processes using light as a source of energy. Most molecules are not able to absorb in the visible light spectrum region. Therefore, the use of photocatalysts acting as a transmitter of energy through electron transfer or energy transfer to other molecules, opens the door to the development of new chemical transformations in the region of the solar spectrum that reaches the Earth with greater intensity, thus optimizing the energy resources.<sup>[89]</sup>

In 1912 Giacomo Ciamician already speculated that the employment of high energetic processes through the use of efficient and clean

photochemical reactions would have a drastic, ecological and beneficial impact in our society.<sup>[90]</sup> Nowadays, there are several activation methods offered by photocatalysis giving access to a wide variety of chemical transformations. Indeed, as demonstrated in Figure 16, there has been an exponential increase in the number of publications that employ photoredox catalysis since the late 2000s, giving rise to a diverse and highly active field of research that continues at the present time.<sup>[91]</sup>

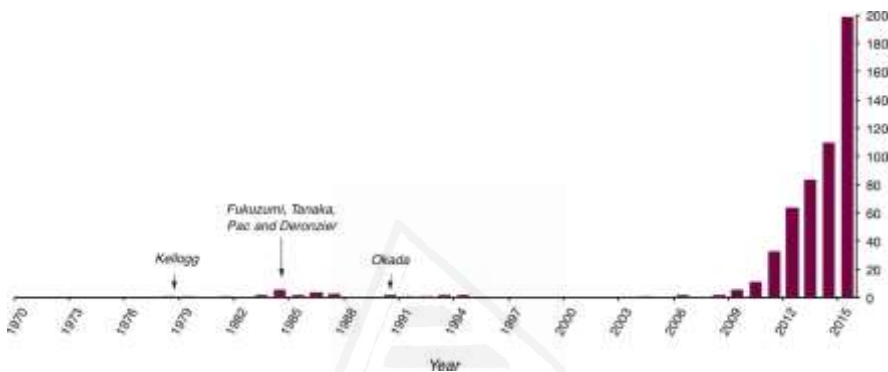


**Figure 16.** Papers published per year in the field of organic photoredox catalysis

## 1.2. Guidelines to understanding photoreactions

The following hypotheses were described to provide a simple and powerful working theory of organic photoreactions:

- i) Light absorption corresponds to the excitation of an electron from a bonding or nonbonding orbital into the lowest unfilled orbital available to the molecule.
- ii) The molecular state which results from excitation of an electron rearranges very rapidly to the state corresponding to the lowest energy (mono) excited electronic configuration.
- iii) Each excited electronic configuration may exist as a singlet state (all electron spins are paired) or a triplet state (two electron spins are parallel).

The consequences of these hypotheses were summarized in an electronic energy diagram (Figure 17). In this diagram the energy of the lowest excited singlet state ( $S_1$ ) is shown relative to the lowest energy triplet state ( $T_1$ ) and the ground (usually singlet) state ( $S_0$ ).

In addition to energy, both  $S_1$  and  $T_1$  possess a characteristic electronic configuration (which determines chemical reactivity) and lifetimes (which limits reaction efficiency). The configuration of a state determines the photoreactions that are possible to run, but the lifetime determines whether these reactions are efficient or can occur at all.

In general,  $S_1$  states are shorter lived ( $\tau$  is the lifetime) than  $T_1$  states ( $\tau_{S_1} = 10^{-7}$  to  $10^{-11}$  second and  $\tau_{T_1} = 10^{-3}$  to  $10^{-6}$  second, respectively) and have higher energies ( $E$ ) [ $E(S_1) = 100$ -50 kcal/mol and  $E(T_1) = 80$  to 30 kcal/mol, respectively]. For comparison the strongest single bonds in molecules have dissociation energies of 100 kcal/mol (for example, C-H and O-H bonds) and the weakest single bonds have dissociation energies of about 35 kcal/mol (for example, O-O bonds). The dissociation energies of most other bonds in organic molecules fall in the range of 80 to 60 kcal/mol.

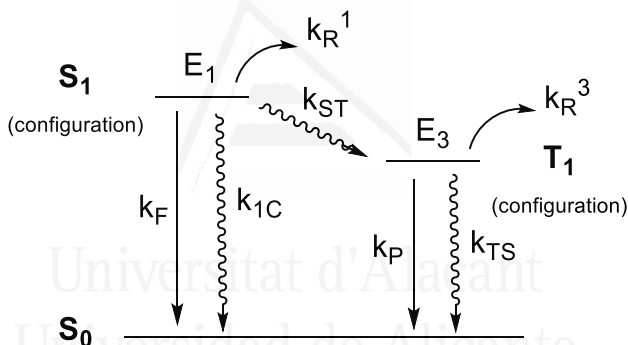


**Figure 17.** Electronic energy diagram. The various  $k$ 's represent the following rate constants:  $k_F$ , fluorescence;  $k_{1c}$ , radiationless deactivation of singlet;  $k_{R^1}$ , chemical reaction from singlet;  $k_P$ , phosphorescence;  $k_{TS}$ , radiationless decay from triplet;  $k_{ST}$ , intersystem crossing; and  $k_{R^3}$ , chemical reactions from triplet.

An important generalization is the state configuration approximation. This principle assumes that  $S_1$  or  $T_1$  (states) can be adequately described in terms of two electrons involved in the  $S_0 \rightarrow S_1$  or  $S_0 \rightarrow T_1$  processes, which determine a configuration of electrons for each state. The chemical reactivity of the  $S_1$  and  $T_1$  states are determined by the specific electronic configurations that can usually be considered to be of either the  $n, n^*$  or  $\pi, \pi^*$  type. The efficiencies of reactions of  $S_1$  and  $T_1$  are determined not only by proclivity toward reaction, but also by lifetimes, since the efficiency of reaction represents a competition between the rate of reaction and other

means of decay. The competition is measured by the quantum efficiency of a reaction, which relates the number of product molecules produced per quantum of light absorbed. This quantity is determined by the ratio of the reaction rate and competing excited state decay rates.

$$\text{Quantum yield (\%)} = \frac{n^{\circ} \text{ reacted electrons}}{n^{\circ} \text{ incident photons}} * 100$$

Fortunately, many photochemical reactions with low quantum efficiency still give a high chemical yield of product.<sup>[92]</sup>

### 1.3. Development of photocatalysis in organic synthesis

---

Recently, photocatalysis has undergone a new renaissance due to a series of new activation modes in which a specifically designed photon-absorbing catalyst (photocatalyst) contribute in a large variety of synthetic methodologies.<sup>[93]</sup>

The most common mechanisms by which photocatalysts are able to convert light into chemical energy and at the same time perform selective molecule activation include:

- i) Energy transfer
- ii) Organometallic excitation
- iii) Light-induced atom transfer
- iv) Photoredox catalysis

However, the discussion will be focused on the utility of photoredox catalysis from a historical viewpoint and the remarkable recent impact of this field in the organic synthesis. Last four decades, photoredox catalysis has found application in the fields of water splitting,<sup>[94]</sup> carbon dioxide reduction,<sup>[95]</sup> and the development of novel solar cells materials.<sup>[96]</sup>

Thus, last years a key factor has been recognized readily accessible metal polypyridyl complexes and organic dyes can facilitate the conversion of visible light into chemical energy under mild conditions (Figure 18). Upon excitation, these molecules can engage in single-electron transfer (SET) events with organic (and organometallic) substrates, providing facile access to open-shell reactive species.<sup>[97]</sup>



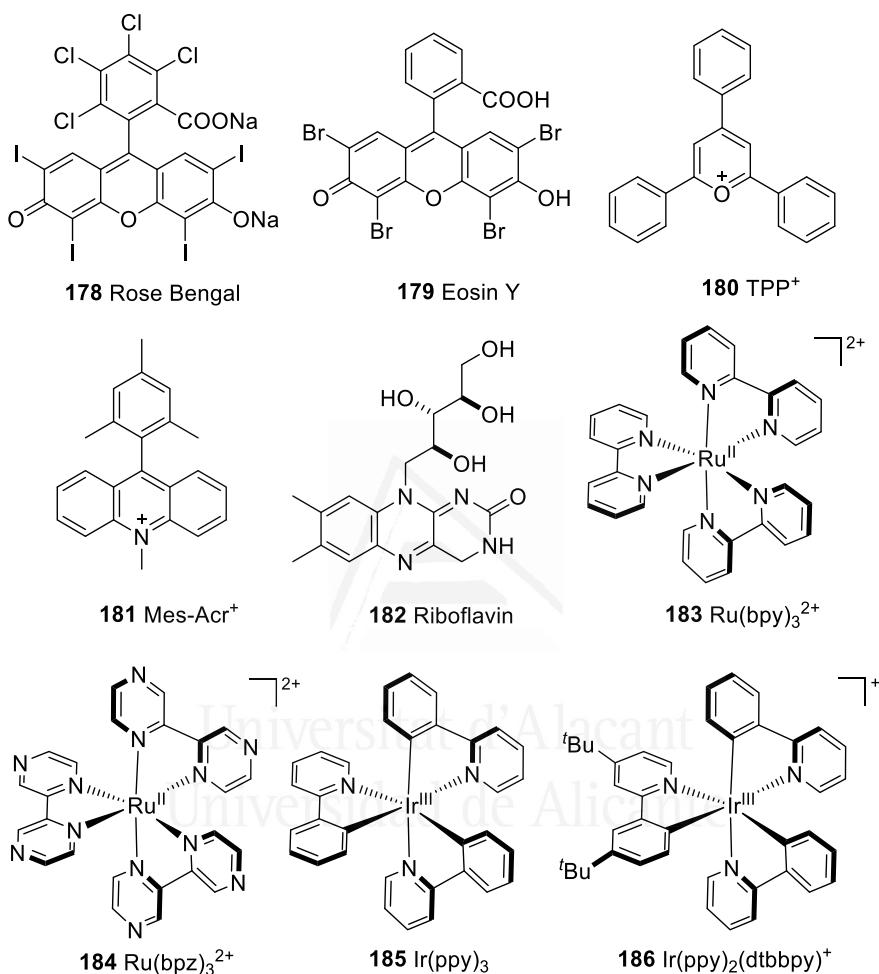


**Figure 18.** Metal polypyridyl complexes and organic dyes in photocatalysis

Here, irradiation with visible light, at wavelengths where common organic molecules do not absorb, effects selective excitation of the photoredox catalyst. Specially in the case of the Ir(ppy)<sub>3</sub>, its maximum absorption is at 375 nm with the capacity to convert into significant levels of chemical energy [the triplet state of Ir(ppy)<sub>3</sub> **185** is 56 kcal/mol]. The resultant excited species can act as both a strong oxidant and a strong

reductant simultaneously, thereby providing access to a reaction environment that is unique for organic chemistry (Figure 19).<sup>[91]</sup>

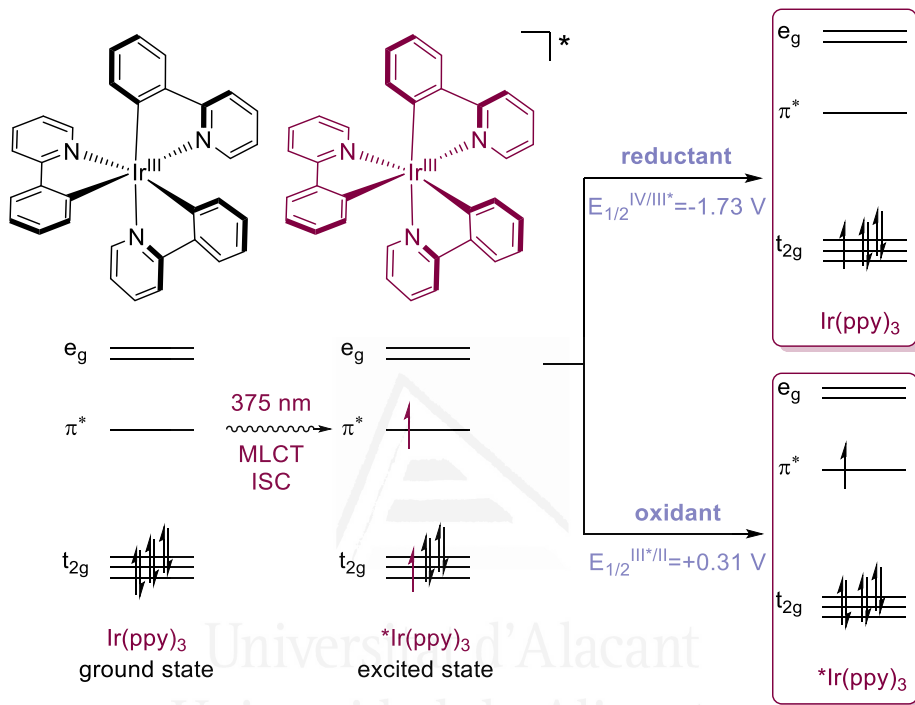


**Figure 19.** Iridium polypyridyl complexes **185**: simplified molecular orbital depiction of Ir(ppy)<sub>3</sub> photochemistry

#### 1.4. Activation mechanisms in photoredox catalysis

Electron transfer is one of the main modes of activation in photocatalysis. The transfer was occurred from excited photocatalyst to give radical species (cations, anions and neutral species when starting material were ionic). This type of processes is described as photoredox catalysis. Radicals can be generated *via* the use of thermal initiators, so that in a theoretical point of view, the photocatalyst could be considered as an initiator of radicals.<sup>[98]</sup>

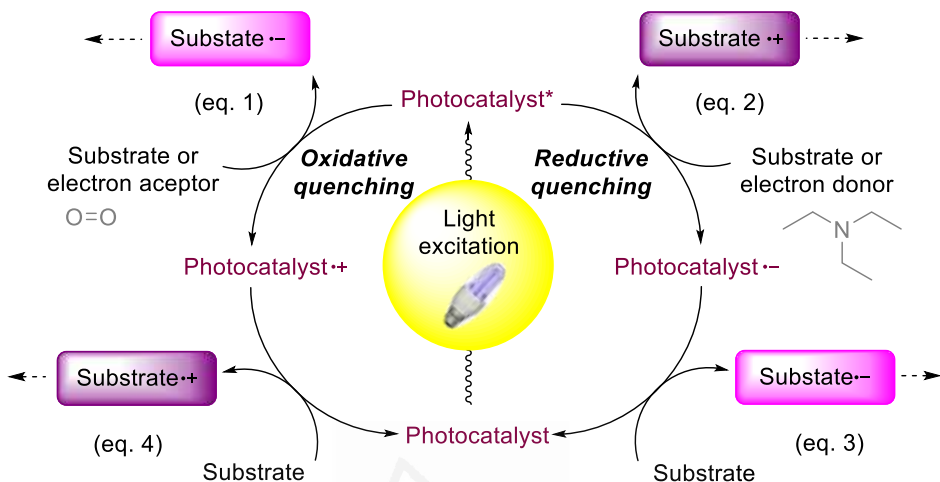
The process is started with the absorption of a photon by the photocatalyst when it is irradiated with visible light. One electron is promoted from HOMO to LUMO and reaching excited state. At this point, the redox

potential is higher than in the fundamental state. From the excited state exists four possible mechanism of electronic transfer (Scheme 66): two of them are named neutral redox because the target substrate reacts immediately with the excited photocatalyst.

Firstly, the oxidative mechanism of the photocatalyst, when the catalyst transfers the electron to the substrate to generate the corresponding radical anion (Scheme 66, eq.1). Secondly, the reductive mechanism of the photocatalyst, when the catalyst takes the electron of the substrate to generate the corresponding radical cation (Scheme 66, eq.2). Both mechanisms are exergonic ( $\Delta G \leq 0$ ), the redox potential of the photocatalyst with the absorbed energy by the excited state it must be enough to oxidize or reduce the substrate.

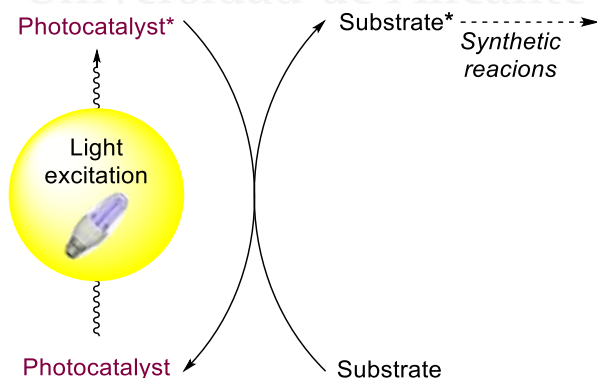
In the rest of the mechanisms, the photocatalyst reacts with a compound that will be an electron donor or recipient. For example, in the third mechanism, the photocatalyst reacts with an electron acceptor (oxygen or peroxodisulfate) to generate the reduced species of catalyst capable of oxidizing the target substrate (Scheme 66, eq.3). Finally, the fourth mechanism, the photocatalyst reacts with an electron donor (like amines, triethylamine or diisopropylamine and ascorbic acid) to generate the oxidized specie of the catalyst capable of reduce the target substrate (Scheme 66, eq.4). Last electronic transfer takes place in the fundamental state of both compounds and followed by an irreversible stage. Therefore, in these cases, the electronic transfers are exergonic reactions ( $\Delta G \geq 0$  until 500 mV).

It worth to mention that the reaction between photocatalyst and substrate (or sacrifice compound) is the photochemical stage of the cycle. The absorbed energy of the photocatalyst is taken advantage to reduce or oxidize. The next step, between radicals is only a thermic process. Also, due to short lifetime of excited state of the photocatalysts kinetic aspects are considered too. It means, if the electronic transfer does not occur during lifetime of the photocatalyst, the reaction will not take place despite being thermodynamically favored.<sup>[99]</sup>



**Scheme 66.** Activation mechanisms in photoredox catalysis

Other mechanism as activation mode in photocatalysis is the energy transfer. This kind of processes, the photocatalyst transfers the energy to the substrate carrying it to the excited state. Finally, from the excited state, the substrate reacts to take place the corresponding synthetic reaction (Scheme 67).<sup>[92]</sup> Although the concept of energy transfer from one molecule in excited state to other molecule in fundamental state has been widely studied in photochemistry, there are few examples in photocatalysis in comparison with reactions that occurs *via* electron transfer.

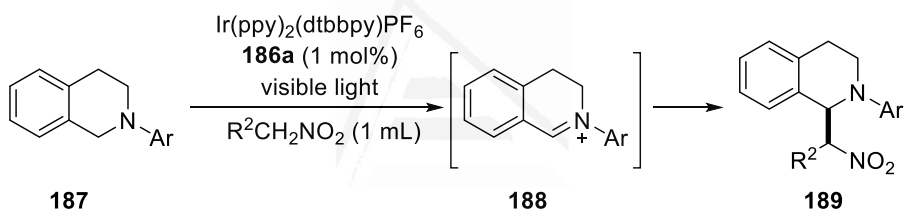


**Scheme 67.** Activation mechanism in photocatalysis *via* energy transfer

## 1.5. Background about photocatalysis

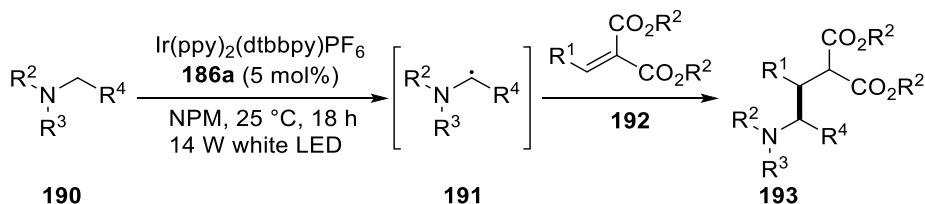
### 1.5.1. Oxidative process

The employment of tertiary amines with low oxidation potential as starting materials have given a wide variety of photocatalytic methods to the formation of C-C bonds in alpha to amino group. Cationic radical is generated focused on the nitrogen (Scheme 66, eq.2) that involves the formation of iminium ion. This ion is capable to react with nucleophiles or losing a proton that it will react with electrophilic compounds. First example of iminium ion was described by Stephenson in 2010, employing iridium catalyst **186a** and different nitroalkanes as a solvent of the reaction, Stephenson's group obtained  $\alpha$ -functionalized isoquinolines with high yields (90-96 %) (Scheme 68).<sup>[100]</sup>



**Scheme 68.** Visible-light photoredox catalysis: Aza-Henry reactions via C-H functionalization

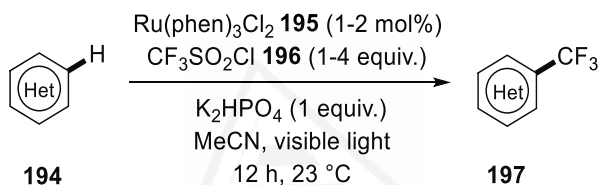
The second type of intermediates from radical cation in nitrogen are radicals in alpha position to an amino group. These radicals have nucleophilic character and they are trapped by an extensive variety of electrophiles. Nishibayashi in 2012 described the capture of these radicals with Michael acceptors to obtain 1,5-aminoesters **193** with low to high yields (36-93 %) (Scheme 69).<sup>[101]</sup> The use of iridium catalysts and the choice of solvent are critical for the formation of intermediate radical **191**.



**Scheme 69.** Photocatalytic addition of  $\alpha$ -amino radicals to Michael acceptors

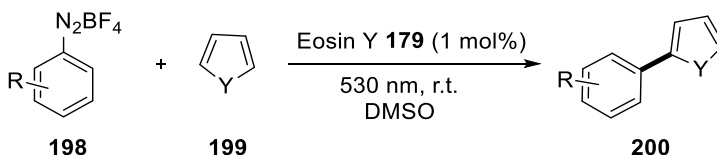
### 1.5.2. Reductive process

In 2012, MacMillan developed a new methodology for the addition of trifluoromethane in aromatic compounds, employing sulphonyl chloride as a source of  $\text{CF}_3$  **196** and a ruthenium(II) complex as a catalyst **195**. The first stage consists in the reduction of **196** by the excited catalyst generating anionic radical (Scheme 67, eq.1) that involves trifluoromethyl radical. Next, the radical will be trapped by the aromatic or heteroaromatic ring (rich of electrons) to give the desired product good to high yields (70-94 %) (Scheme 70).<sup>[102]</sup> The development of this methodology is of great importance in the pharmacological area, since it gives access to compounds with some stability against *in vivo* metabolic oxidation.<sup>[103]</sup>



**Scheme 70.** Photocatalytic trifluoromethylation of aromatic and heteroaromatic compounds

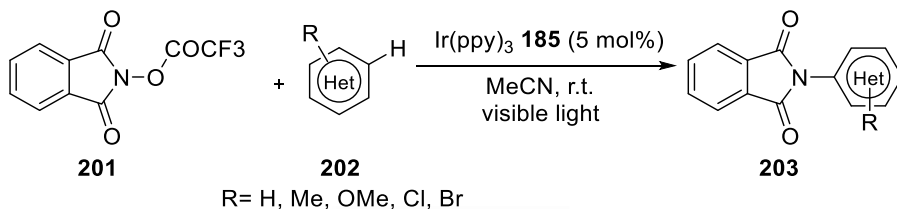
Another transformation studied in the photocatalysis field is the formation of  $\text{Csp}^2\text{-Csp}^2$  bonds. König described the arylation of heteroaromatic compounds. Diazonium salts are suitable to obtain aryl radicals because the low reduction potential. In this way, using 1 mol% of Eosin Y **179** as a catalyst and green light (530 nm), it has been possible the arylation with good yields (51-86 %) (Scheme 71).<sup>[104]</sup>



R = Br,  $\text{NO}_2$ ,  $\text{CO}_2\text{Et}$ , CN  
 Y = O, S, NBoc

**Scheme 71.** C-H photocatalytic arylation from diazonium salts

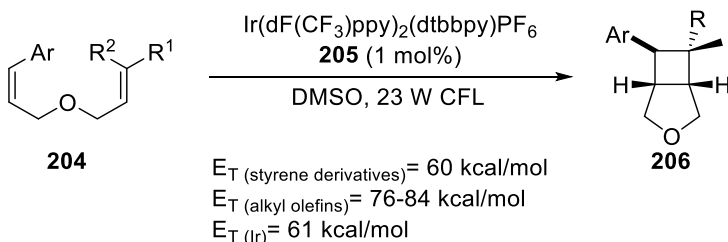
Besides the formation of C-C bond, the formation C-heteroatom bond has been other goal of the photocatalysis. In 2014, Sanford's group have developed a strategy to do the amination of arenes and heteroarenes *via* visible light. Knowing the reduction of alkyl substituted *N*-acyloxiphthalimides promotes the formation of alkyl radical, CO<sub>2</sub> and anionic phthalimide (Scheme 72).<sup>[105]</sup>



**Scheme 72.** Photocatalytic amination of aromatic and heteroaromatic compounds

### 1.5.3. Activation *via* energy transfer

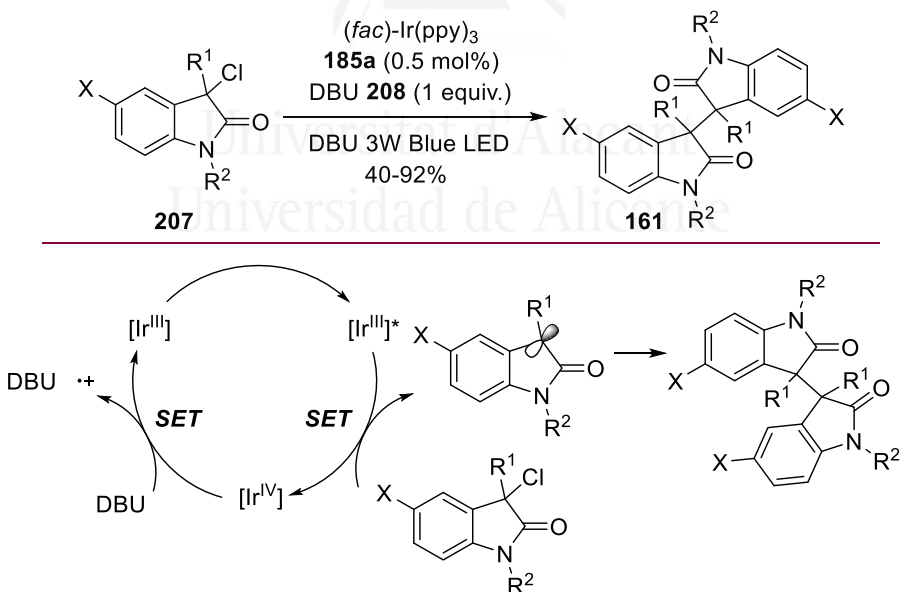
Yoon considered whether it would be possible to develop transformations like those described by electronic transfer but using an energy transfer mechanism (Scheme 67). In 2012 they developed a reaction of intramolecular cycloaddition [2+2] between styrene and alkyl-substituted double bonds employing iridium catalyst XX as a photosensitizer of the reaction (Scheme 73).<sup>[106]</sup> The reaction gives good results regardless of the electronic nature of the substituents in the styrene, but it does not take place with two alkyl-substituted double bonds, due to its high triplet energy.



**Scheme 73.** [2+2] Styrene cycloadditions by energy transfer

## 1.6. Bioindoles prepared using photocatalysis

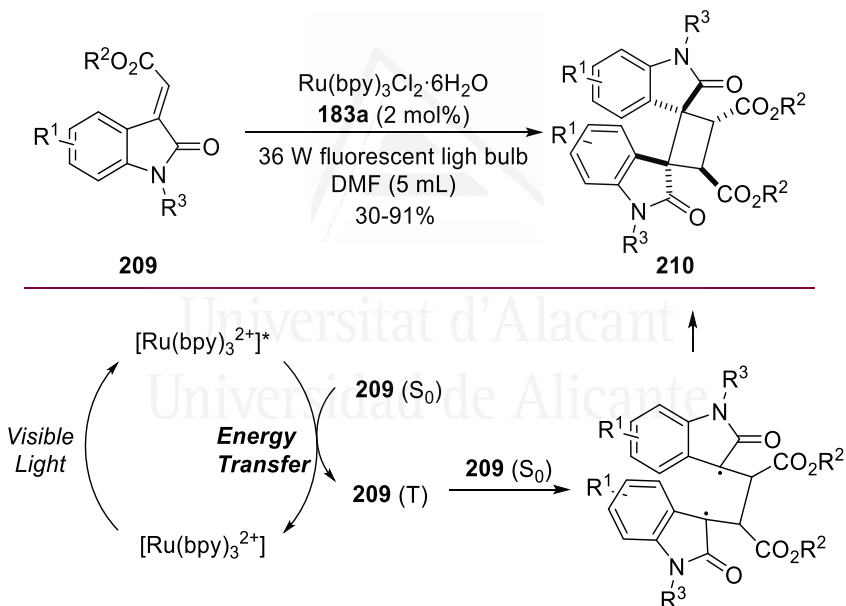
The reactivity of the oxindole in photocatalysis field is evolving day by day. In fact, 3-halooxindoles are the suitable starting materials to take place this target. One example was described in 2016 by Wu's group. They introduced a simple way to the homocoupling of tertiary halides induced by photocatalysis. The advantages of this procedure comparing with other methodologies are mild conditions, excellent group tolerance, high yields and high reactivity. The possible mechanism described starts with the excitation of the photocatalyst  $[\text{Ir}^{\text{III}}] \rightarrow [\text{Ir}^{\text{III}}]^*$ . It is a strong reductant which can be oxidized to  $[\text{Ir}^{\text{IV}}]$  by 3-halooxindole *via* a single electron transfer (SET) process. At the same time, 3-halooxindole was transferred to its radical anion, which can generate 3-alkyl-2-oxindolin-3-yl radical after losing halide anion spontaneously. Successive SET between  $[\text{Ir}^{\text{IV}}]$  and DBU regenerates the photocatalyst and populates DBU radical cation. Further deprotonation of DBU radical cation can produce DBU radical, which should be oxidized to corresponding iminium ion. Finally, the homocoupling of 3-alkyl-2-oxindolin-3-yl radical affords the desired product (Scheme 74).<sup>[76]</sup>



**Scheme 74.** Reaction and mechanism of homocoupling of 3-halooxindole *via* visible light photocatalysis

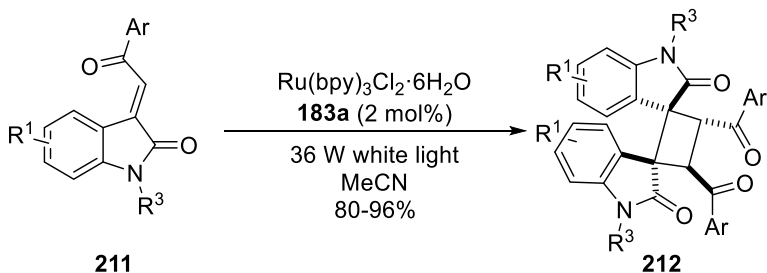


Other possibility to prepare bioindoles was described based on the mechanism energy transfer. Zou's group at 2012 developed an intramolecular [2+2] cycloaddition reactions of 3-ylideneoxindoles through visible light induced. They proposed a reaction which was catalyzed by 2 mol% of ruthenium complex in DMF as a solvent with a 36 W fluorescent light bulb. It was observed the formation of cycloadduct in excellent yields with an excellent level of diastereoselectivity and regioselectivity (Scheme 75).<sup>[107]</sup> In this case, they proposed a plausible catalytic cycle the excited ruthenium complex was able to involving energy transfer from  $\text{Ru}(\text{bpy})_3^{2+*}$  to the ground state **209** ( $S_0$ ). The triplet state **209** (T), formed in this manner, then reacts with other molecule of **209** ( $S_0$ ) to form a biradical intermediate that then undergoes the cyclization.



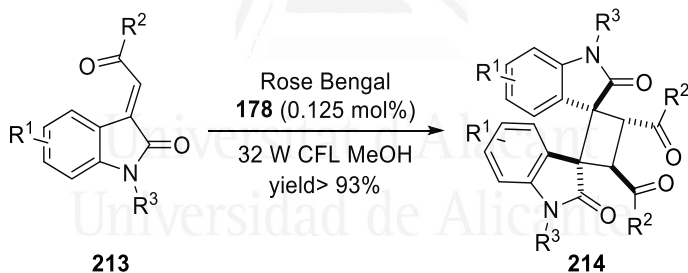
**Scheme 75.** Intramolecular [2+2] cycloaddition of 3-ylideneoxindoles through energy transfer pathway by Zou

Recently, a new version of the reaction was developed by Yan's group in 2016. A protocol was developed for the efficient synthesis of functionalized dispiro[indoline-3,1'-cyclobutane-2',3''-indolines] with high diastereoselectivity. In this case, they used acetonitrile as a solvent and white light (Scheme 76).<sup>[71]</sup>



**Scheme 76.** Visible light catalyzed cyclodimerization of 3-phenacylideneoxindoles by Yan

Even in 2017 it was published the photocatalytic version employing organic dyes. Wu's group described Rose Bengal sensitized intramolecular [2+2] cycloaddition of 3-ylideneoxindoles for the synthesis of spirocyclic oxindoles under visible light irradiation conditions. The cycloaddition products were obtained in good yields (up to 93%) with excellent diastereoselectivity and regioselectivity (Scheme 77).<sup>[108]</sup>



**Scheme 77.** Intramolecular [2+2] cycloaddition of 3-ylideneoxindoles by Wu

## **2. Dual catalysis**

---

Metallocatalysis had produced a deep impact in scientific society. It is exemplified by the last Nobel Prizes awarded in relationship with this topic. In 2001 to Knowles, Noyori and Sharpless for stereoselective catalysis,<sup>[109]</sup> in 2005 to Chauvin,<sup>[110]</sup> Grubbs and Schrock for olefins metathesis and 2010 to Heck, Negishi and Suzuki for palladium-catalyzed cross-coupling.<sup>[111]</sup>

Although they span more than 40 years of research, transition metal chemistry has continually delivered new modes of chemical activation that enable bonding-forming or bonding-cleavage pathways that are often unprecedented within organic chemistry. This capacity for “new reactivity” has made transition metal catalysis a platform for the organic synthesis.

Metallaphotocatalysis, the merger of transition metal catalysis and photocatalysis, has recently emerged as a versatile platform for development of new, highly, enabling synthetic methodologies. Photoredox catalysis provides access to reactive radical species under mild conditions from abundant functional groups, and, when combined with transition metal catalysis, this feature allows direct coupling of nontraditional nucleophile partners. In addition, photocatalysis can aid fundamental organometallic steps through modulation of the oxidation state of transition metal complexes or through energy transfer mediated excitation of intermediate catalytic species. Metallaphotocatalysis provides access to distinct activation modes, which are complementary to those traditionally used in the field of transition metal catalysis, thereby enabling reaction development through new mechanistic paradigms.<sup>[112]</sup>

During this section it will show different examples in the field of metallaphotocatalysis that it demonstrates how the unique mechanistic features permit chemical transformations to be accomplished.

## 2.1. Nickel metallaphotocatalysis

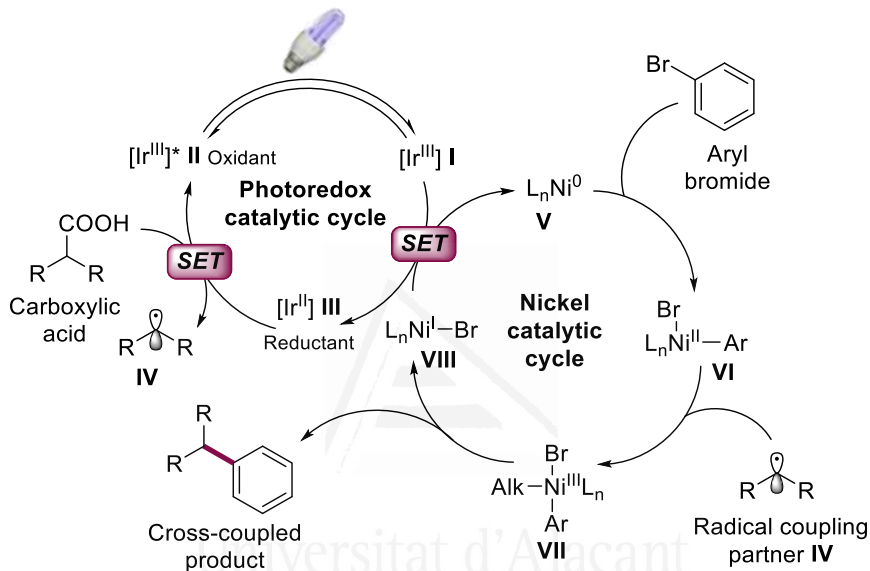
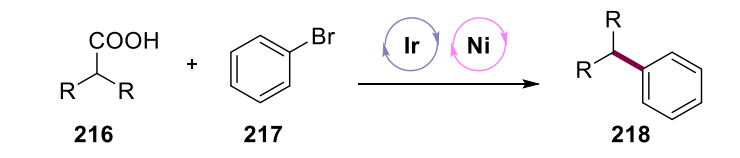
---

Nickel catalysis has provided elegant solutions to the coupling of C( $sp^3$ ) fragments, in part to the ability of nickel complexes to undergo oxidative addition with alkyl electrophiles. Also, the reduced capacity of nickel alkyl species to undergo  $\beta$ -hydride elimination enhances the efficiency of C( $sp^3$ ). Herein, photoredox-mediated radical generation has proved to be a good strategy for activating non-traditional cross-coupling nucleophiles.

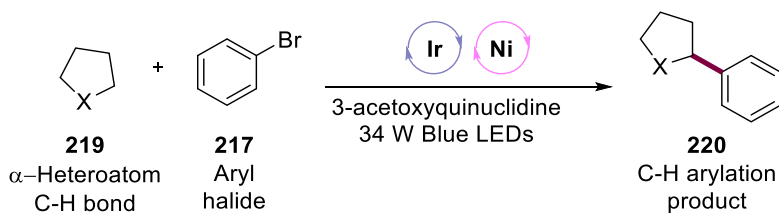
In Scheme 78 Doyle and MacMillan laboratory presents the successful merger of nickel and photoredox catalysis in the decarboxylative coupling of carboxylic acids and aryl halides.<sup>[113]</sup> Upon excitation of photocatalyst **I** by visible light, the highly oxidizing species **II** can facilitate oxidative decarboxylation of a carboxylic acid to yield the corresponding carbon-centered radical **IV**. Concurrently, Ni(0) complex **V** can undergo oxidative addition with an aryl halide to give a Ni(II)-aryl complex **VI**, which can subsequently trap the acid-derived radical **IV**, resulting in formation of Ni(III) complex **VII**. Rapid reductive elimination forges the desired C( $sp^3$ )-C( $sp^2$ ) bond in the cross-coupled product. Finally, the two catalytic cycles are simultaneously closed via a SET event between Ir(II) species **3** and Ni(I) complex **III**.

Continuing this mechanistic structure, Molander and co-workers disclosed a dual nickel photoredox protocol that used benzyl potassium trifluoroborate salts as a radical precursors.<sup>[114]</sup> The mechanism proposed of these dual catalyzed C-C bond-forming protocol has not yet established, the representation in Scheme 78 is only one potential pathway but exists other alternatives. One example is the C-H arylation by dual nickel photoredox catalysis. In this case, the reaction proceeds by means of a hydrogen atom transfer (HAT) event by an amine radical cation, this work was published by Doyle in 2016 (Scheme 79).<sup>[115]</sup>

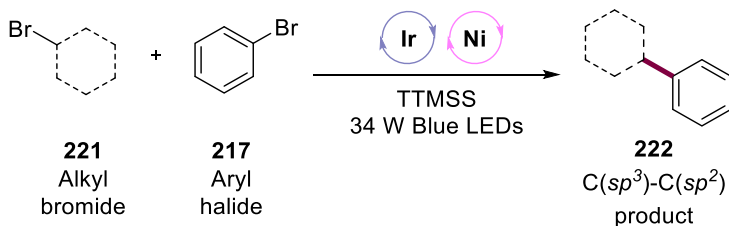
Recently, another alternative was described to implement the dual nickel photoredox catalysis platform in the development of a cross-electrophile coupling between aryl halides and alkyl halides.<sup>[116]</sup> Here, it was necessary selective activation of the aryl and alkyl bromide components was accomplished through the synergistic behavior of a nickel catalyst and a photoredox-generated silyl radical species (Scheme 80).



**Scheme 78.** Nickel metallaphotocatalysis for carbon–carbon bond formation



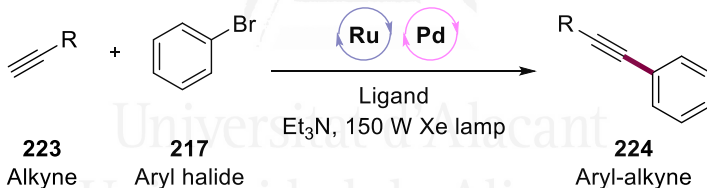
**Scheme 79.** PhotoredoxHAT and Ni-catalyzed C–H arylation



**Scheme 80.** Photoredox Ni-catalyzed cross-electrophile coupling

## 2.2. Palladium metallaphotocatalysis

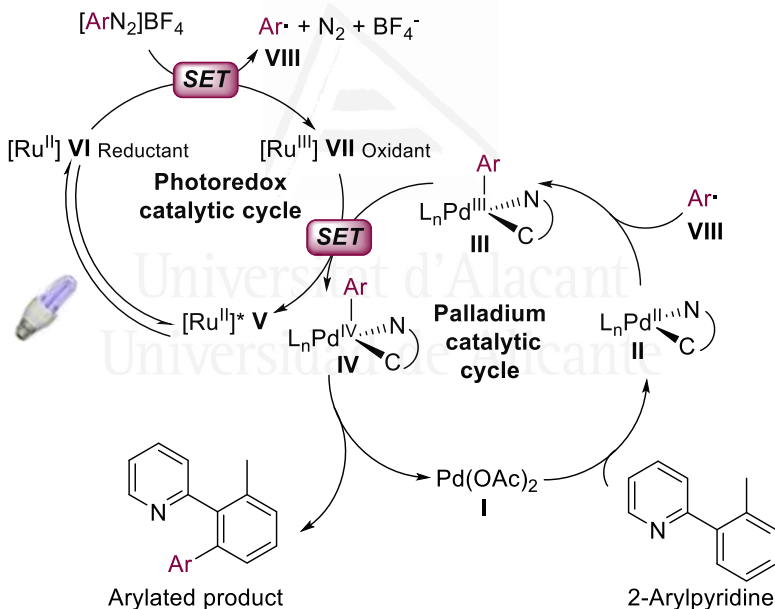
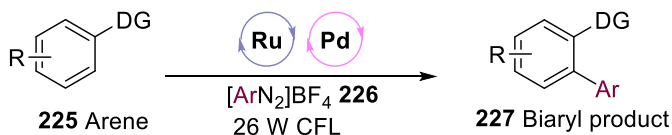
One of the first work about combining light-harvesting catalysis with metal transition catalysis was recognized by Osawa in 2007. In their report, the inclusion of Ru(bpy)<sub>3</sub><sup>2+</sup> and irradiation with visible light was noted to accelerate palladium-catalyzed Sonogashira reactions (Scheme 81).<sup>[117]</sup> The authors of this work postulated that the photocatalyst facilitates the oxidative addition of the palladacycle but the precise mechanism role was not determinate.



**Scheme 81.** Photoredox palladium-catalyzed copper-free Sonogashira coupling by Osawa

Later, Sanford's group in 2011 made the C(sp<sup>2</sup>)-H arylation of 2-arylpyridines with aryl diazonium salts (Scheme 82).<sup>[118]</sup> Normally, palladium catalyzed protocols requires the presence of strong oxidants end/or elevated temperatures. By merging photoredox and palladium catalysis, the outlined C-H arylation could be conducted at ambient temperature and in the absence of strong external oxidants. More important, they proposed a possible mechanism in which the photocatalyst was implicated in both reductive radical generation and the oxidation state of the palladium catalyst.<sup>[118]</sup> This mechanistic key provides an alternative metallaphotoredox platforms and instigated significant growth in the field.

Specifically, Sanford hypothesized that concerted metallation–deprotonation of 2-phenylpyridine **225** by Pd(OAc)<sub>2</sub> **I** delivers palladacycle **II**. Simultaneously, the excited ruthenium photocatalyst **VI** can reduce aryl diazonium salt **226** to afford aryl radical **VII** and dinitrogen upon fragmentation. The aryl radical can then intercept palladacycle **II** to afford the Pd(III) intermediate **III**. Subsequent oxidation of **III** by the Ru(III) complex **VII** generates a high-valent Pd(IV) species **IV** that undergoes rapid reductive elimination to yield the arylated product.



**Scheme 82.** Photoredox-palladium-catalyzed directed C–H arylation by Sanford

### 2.3. Cobalt metallaphotocatalysis

Although principal research in the field of metallaphotocatalysis has focused on nickel, palladium, copper and gold, the merger of cobalt catalysis has been reported.

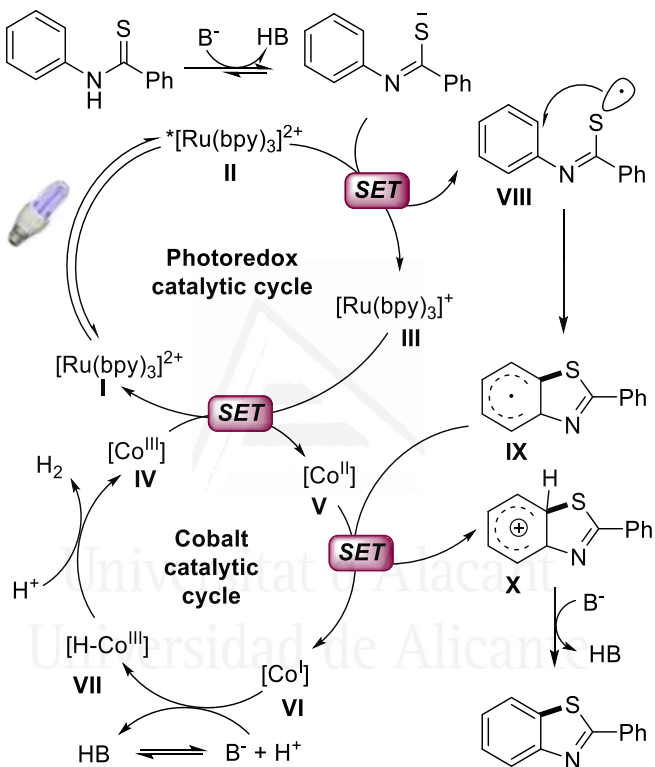
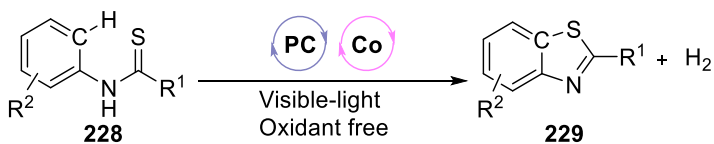
In 2015, Wu and Lei published dehydrogenative C-S bond formation could be achieved through the dual action of a photocatalyst and a 'proton-reducing' cobaloxime catalyst (Scheme 83).<sup>[119]</sup>

Here, benzothiazoles were generated in high yields from thiobenzanilides, with hydrogen gas as the sole by-product. Notably, this dual catalytic strategy avoids the use of a stoichiometric terminal oxidant and has provided a general strategy for achieving 'acceptor-less' dehydrogenative protocols.

Later, Wu's group demonstrated that this dual catalysis is useful for a variety of C-C bond forming reactions.<sup>[120]</sup> This work described an oxidant-free strategy to synthesize indoles, under visible light irradiation ( $\lambda = 450$  nm), catalytic amounts of an iridium(III) photosensitizer and cobaloxime catalyst transform various N-aryl enamines exclusively into indoles.

More recently, the Li group have employed dual photoredox cobalt catalysis to achieve acceptorless dehydrogenation of saturated N-heterocycles.<sup>[121]</sup> Interestingly, extrusion of multiple equivalents of hydrogen could be accomplished and a range of heteroaromatic products could be accessed, including quinolines, quinoxalines, quinazolines, indoles and benzothiazoles.





**Scheme 83.** Proposed mechanism of oxidant-free aromatic C-H thiolation to construct C-S bonds

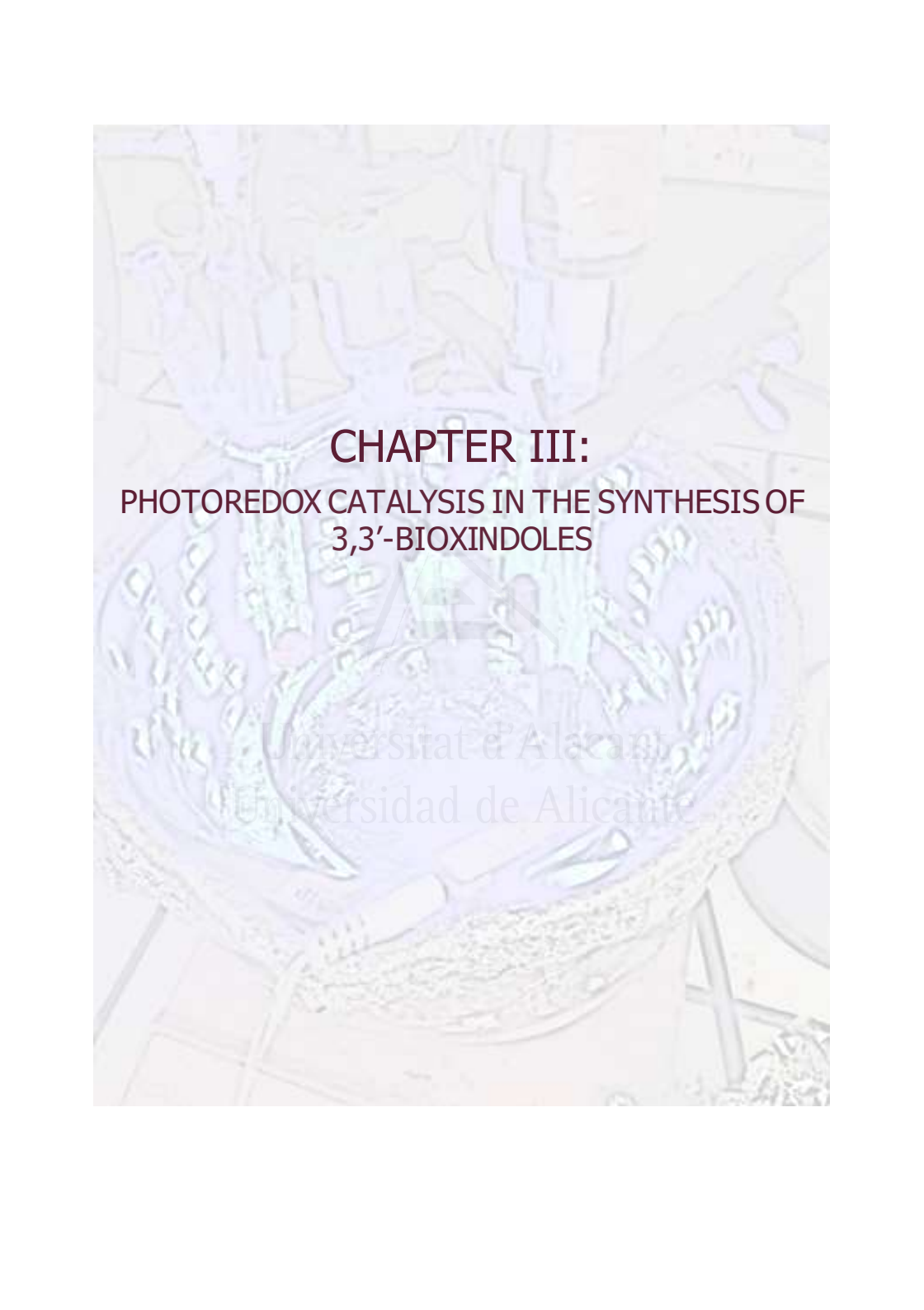
## 2.4. Latest considerations

---

Last decade, visible light photocatalysis has been an attractive field of study in the reactivity of organic chemistry. Many light-harvesting catalysts can promote oxidative or reductive generation of reactive radical species under extremely mild conditions.

Photoredox catalysis provides a unique reaction environment, as the light-harvesting catalysts are simultaneously oxidizing and reducing in nature. By contrast, transition metal-catalyzed protocols are typically oxidative, reductive or neutral, and, consequently, the addition of a photocatalyst and light allows the development of redox-neutral protocols that would be inaccessible under non-irradiative conditions.

That's why, combining these individually powerful catalytic manifolds, synthetic chemists can strive to achieve transformations that are not currently possible using a single catalyst system. Dual catalysis offers access to a broad range of carbon-centered and heteroatom-centered radicals, and these species have been used as a nucleophilic coupling partner in metallaphotocatalysis transformations.<sup>[112]</sup>



**CHAPTER III:**  
**PHOTOREDOX CATALYSIS IN THE SYNTHESIS OF**  
**3,3'-BIOXINDOLES**

Universitat d'Alicant  
Universidad de Alicante

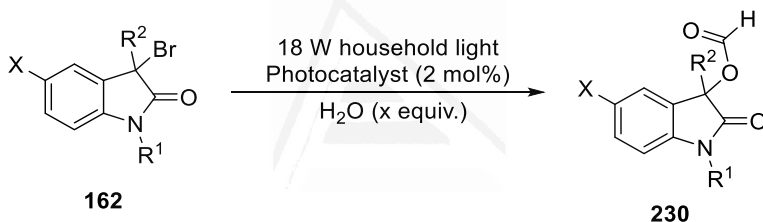


## CHAPTER III: Photoredox catalysis in the synthesis of 3,3'-bioxindoles.

### III.1. Background

It was commented above, 3-halooxindoles are the suitable starting materials to take place reactions *via* photoredox catalysis. One example was described in 2016 by Wu's group (see section 1.6 of Introduction II).<sup>[76]</sup>

More specifically, 3-bromooxindoles were described as a suitable starting material for the visible-light-induced photocatalytic formyloxylation reactions published by Xiao's group in 2014.<sup>[79]</sup>



**Scheme 84.** Visible-light-induced photocatalytic formyloxylation reactions of 3-bromooxindoles

Despite the importance of a good starting material capable of homolytic cleavage, it is worth mentioning that attention should also be paid to the photoredox catalyst. The group of Esteruelas's prepared a new iridium(III) photocatalyst. They described a molecular phosphorescent heteroleptic bis-terdentate iridium(III) emitters have been prepared via  $\eta^1$ -arene intermediates.<sup>[122]</sup>

The magnificent properties of complexes **231** and **232** are green emissive after photoexcitation in solid state at room temperature and in 2-methyltetrahydrofuran (2-MeTHF) at 278 and 77 K, displaying bands centered between 515 and 555 nm. The emissions can be attributed to  $T_1$  excited states originating from HOMO $\rightarrow$ LUMO charge-transfer transitions.

In accordance with this, the lifetimes lie are short in the range 1-10  $\mu\text{s}$ , whereas the quantum yields measured in the solid state in a doped poly(methyl methacrylate) film at 5 % wt are 0.73 for **231** and 0.87 for **232**.

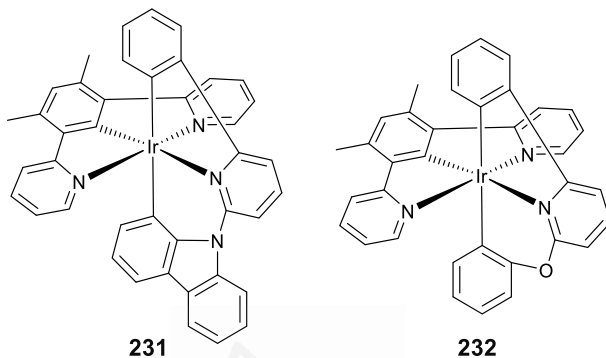
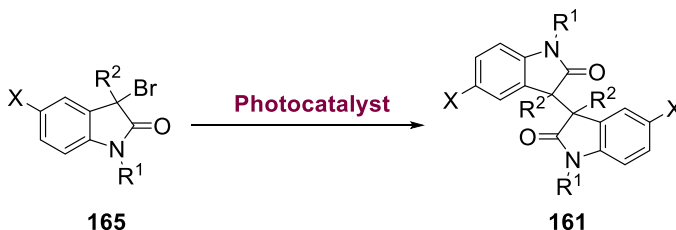


**Figure 20.** Iridium(III) complexes prepared from  $\eta^1$ -arene intermediates by Esteruelas's group

Universitat d'Alacant  
Universidad de Alicante

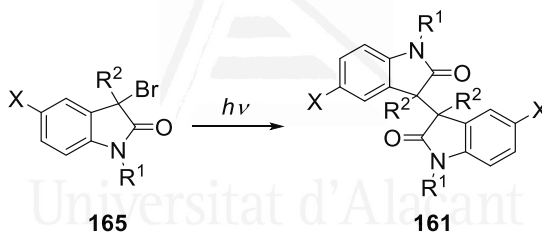
### III.2. Objectives

- ✓ After isolation of 3-bromooxindoles described in the previous chapter, we attempt to find the appropriate photosensitizer for the synthesis of 3,3'-bioxindoles.



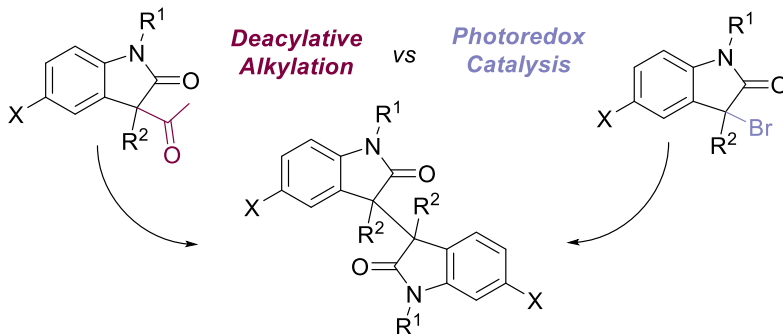
**Scheme 85.** 1<sup>st</sup> target

- ✓ Study of dimerization of 3-bromooxindoles by photoredox catalysis.



**Scheme 86.** 2<sup>nd</sup> target

- ✓ Comparing deacylative alkylation *versus* photoredox catalysis in the synthesis of 3,3'-bioxindoles.

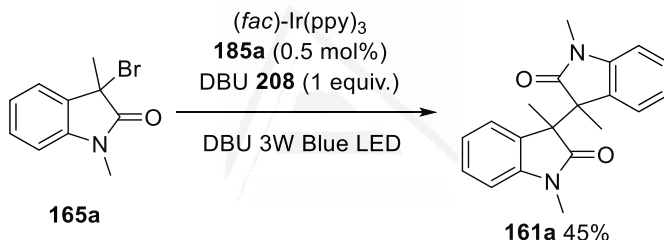


**Scheme 87.** 3<sup>rd</sup> target

### III.3. Results and discussions

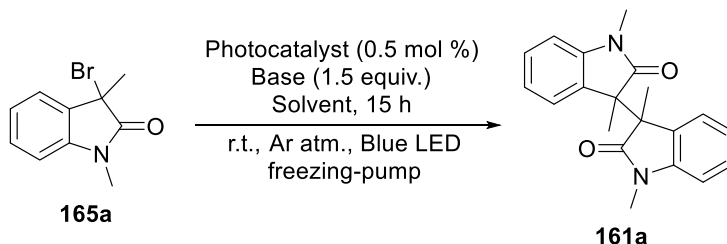
Such as it was described, 3-chloro-3-substituted oxindoles were successfully homocoupled *via* visible light photocatalysis using *fac*-Ir(ppy)<sub>3</sub>.<sup>[76]</sup> So, we envisaged the same transformation but using the bromides **165** instead.

Bromide **165a** (prepared as described in experimental section of chapter II) was submitted to the optimization of solvents, source of light, catalysts, base and electron donor. We initially took the conditions reported previously employing a blue LED source in acetonitrile, with the base DBU as electron donor (see Introduction II, section 1.6) (Scheme 88).<sup>[76]</sup> Under these conditions, photocatalyst **185a** afforded a modest yield (45%) with high amounts of the oxidized product **177** (see Scheme 65).



**Scheme 88.** Homocoupling reaction using 3-bromo-3substituted oxindoles *via* visible light photocatalysis

With the results in hands, we tried to optimize the reaction condition to find better results, we started finding the appropriate photosensitizer, and the screening had been done with the catalysts showed at Figure 21.



**Scheme 89.** General protocol for the synthesis of 3,3'-bioxindoles



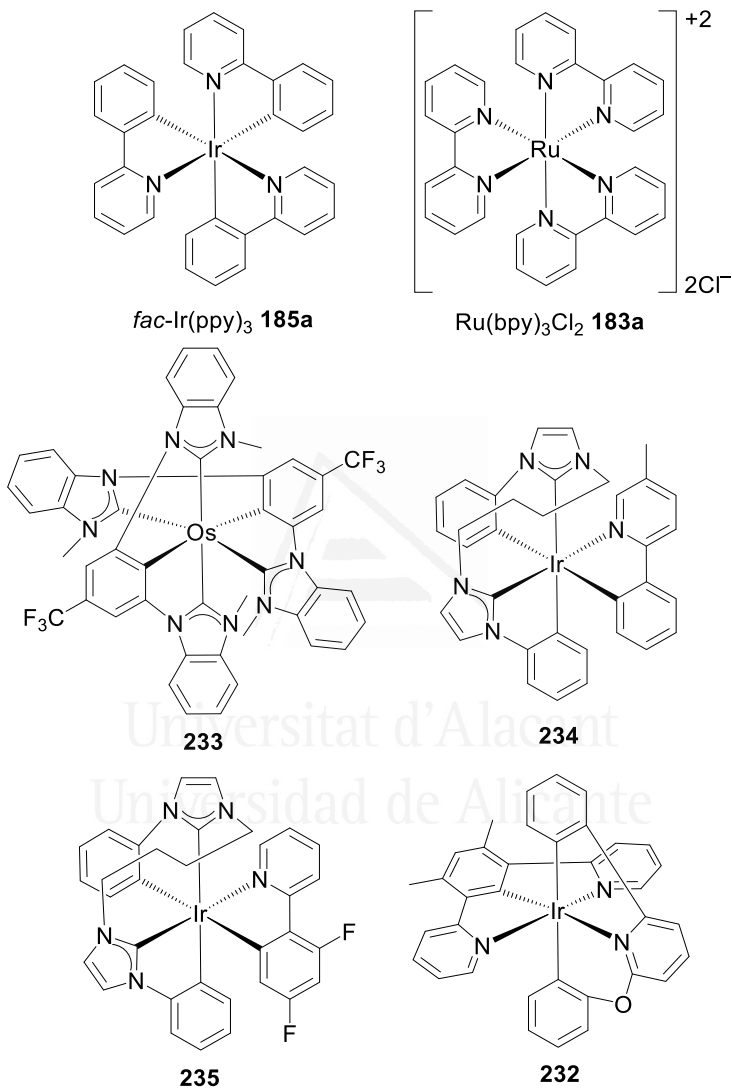


**Figure 21.** Photoredox catalyst used at the optimization of the synthesis of 3,3'-bioxindoles

**Table 8.** Optimization of preparation compound **161a**

Entry	Catalyst	Base	Solvent 0.1 M	161a <sup>a</sup>	165a	177	Yield (%) <sup>b</sup>
1	185a	DBU	MeCN	66	4	30	45
2	183a	DBU	MeCN	trace	85	15	---
3	233	DBU	MeCN	trace	90	10	---
4	234	DBU	MeCN	22	65	13	---
5	235	DBU	MeCN	40	36	24	---
6	232	DBU	MeCN	72	16	12	56
7	232 <sup>c</sup>	DBU	MeCN	78	12	10	58
8	232 <sup>c</sup>	DIPEA	MeCN	25	50	25	---
9	232 <sup>c</sup>	DIPEA	THF	85	---	15	68
10	232 <sup>c</sup>	DBU	THF	88	---	12	69
11	232 <sup>c</sup>	DIPEA <sup>d</sup>	THF	93	---	7	73
12	232 <sup>c,e</sup>	DIPEA <sup>d</sup>	THF	93	---	7	73
13	---	DIPEA <sup>d</sup>	THF	10	67	23	---
14	232 <sup>c,f</sup>	DIPEA <sup>d</sup>	THF	trace	80	10	---
15	232 <sup>c</sup>	---	THF	trace	19	52	---
16	232	DIPEA <sup>d</sup>	THF	79	---	21	---
17	232 <sup>c</sup>	DIPEA <sup>d,g</sup>	THF	trace	80	20	---

<sup>a</sup> A 1:1 (*R\*,R\**):*meso* diastereomeric ratio was determined by <sup>1</sup>H-NMR analysis of the crude mixtures. <sup>b</sup> Isolated yield after flash chromatography. <sup>c</sup> The reaction solution was deoxygenated using freezing-pump technique. <sup>d</sup> Freshly distilled and working under anhydrous conditions. <sup>e</sup> 1 mol% of the catalyst was added. <sup>f</sup> In the absence of Blue LED light. <sup>g</sup> TEMPO (20 mol%) was added.

Ruthenium(II) complex **183a**, as well as organophotocatalyst Eosin B (this last example is not shown at Table 8) did not promote the reaction at all. In view of this situation, we decided to employ recently reported

organometallic phosphorescent compounds as new photocatalysts (Table 8, entries 3-6): the homoleptic osmium(II) complex **233** bearing two equal 5-electron donor C,C,C-pincer ligands based on bis-NHC systems,<sup>[123]</sup> the heteroleptic iridium(III) derivatives **234** and **235**, containing a 6-electron donor C,C,C,C-tetradentate group and a 3-electron donor *ortho*-metallated phenylpyridine,<sup>[124]</sup> and the heteroleptic compound **232** stabilized by a 5-electron donor N,C,N-pincer ligand and a 4-electron donor C,N,C-group.<sup>[122]</sup>

It is worth to know the osmium complex **233** is a blue emitter in 2-methyltetrahydrofuran, which displays a quantum yield of 0.62 in the solid state. Under the same conditions, the iridium complexes **234** and **235** are blue-green emitters with quantum yields close to unity, whereas complex **232** is green emissive with a quantum yield of 0.87.

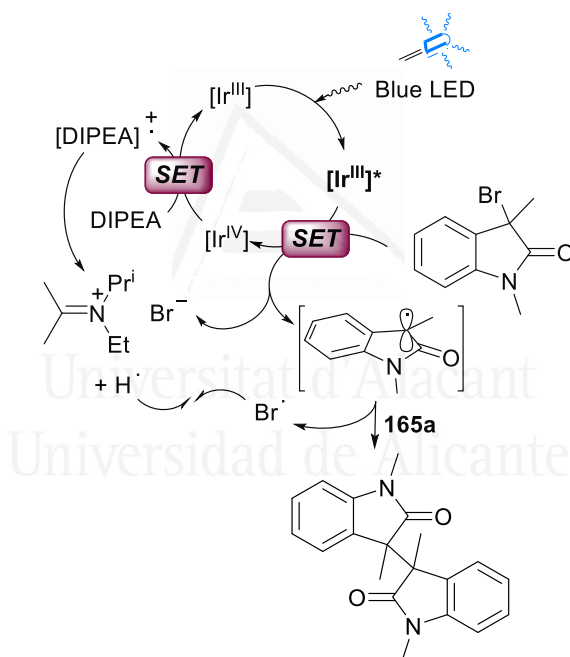
The best conversion and chemical yield of **161a** were achieved by intermediacy of catalyst **232** (Table 8, entry 6). In this context, it should be mentioned that in addition to the lower energy of its emission, complex **232** shows two noticeable differences with regard to **234** and **235**. It displays longer lifetime in 2-methyltetrahydrofuran, at room temperature (2.4 and 1.6  $\mu\text{s}$ , respectively, *versus* 7.7  $\mu\text{s}$ ) and the presence of an oxygen atom between the pyridyl ring and one of the phenyl group of the C,N,C-pincer ligand, which stabilizes the octahedral geometry of the catalyst, due to the increase of a N-Ir-C bite angle.<sup>[125]</sup>

After to notice the suitable photocatalyst other reactions conditions were tried. The 24 W blue LED source afforded better conversions than the visible light, 20 W fluorescent bulb, or 20 W white bulb (not included in Table 8). Despite diisopropylethylamine (DIPEA) did not give satisfactory results in acetonitrile, in THF afforded similar results than the obtained one in the reaction with DBU (compare entries 8-10 of the Table 8). Here, the freezing-pump operation resulted to be crucial to diminish the percentage of the oxidized compound **177**. DIPEA was selected as base because the crude reaction mixture was very clean (detected by  $^1\text{H}$  NMR) unlike the reaction crude generated from DBU. The conversion and the yield of product **161a** were improved employing freshly distilled DIPEA (under anhydrous conditions). The best conditions reactions were shown (Table 8, entry 11).

All **161a** products identified in the crude mixtures or isolated in this Table 8 resulted to be 1:1 mixtures of ( $R^*,R^*$ ):*meso* diastereoisomers according to  $^1\text{H}$  NMR data.

In order to subtract the plausible mechanism, some control experiments were made. In presence of 1 mol% of the catalyst, the reaction occurs with the same conversion and yield that using 0.5 mol% (Table 8, entry 12). The absence of the photocatalyst presented unreacted 3-bromooxindole **165a** as a major product. (Table 8, entry 13).

Without DIPEA, light or freezing-pump cycle, the reaction did not take place, that's reasons emphasize the importance of this elements in the reaction (Table 8, entries 14-16). Finally, TEMPO was added to demonstrate the presence of radical intermediate. With these results, we proposed this plausible mechanism:



**Scheme 90.** Mechanistic proposal for the synthesis of **161a**

The catalysis can be rationalized according to Scheme 90. The excited state of **232** is highly reductant and could be quenched by **165a** faster than by DIPEA through a SET step. The collision should lead to a cation radical iridium(IV) species, a bromide ion, and a radical oxindole. The iridium(III) fundamental state would be regenerated by means of the reaction of DIPEA with the cation radical iridium(IV) species in a second SET stage. The

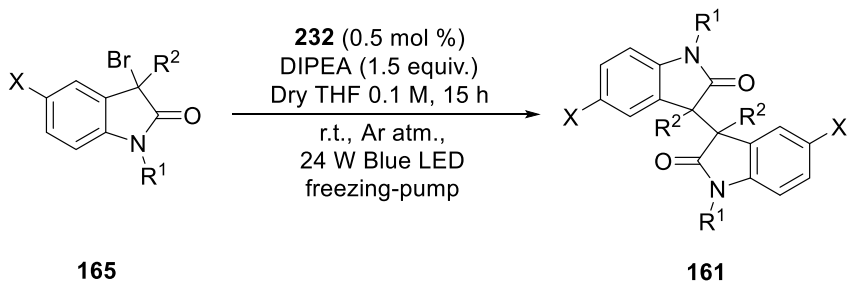
resulting radical cation [DIPEA]<sup>•+</sup> should release a radical H<sup>•</sup>, to afford an iminium cation. Then, the radical H<sup>•</sup> could be trapped by a radical Br<sup>•</sup>, which should be generated in the collision between the radical oxindole and a second molecule of **165a**, to form the carbon-carbon bond of **161a**.

The efficient dimerization took place under anhydrous conditions, under argon atmosphere, with the catalytic complex **232** (0.5 mol%) and DIPEA (1.5 equiv.), after 15 h irradiation with 24 W Blue LED, at room temperature. Previously, all solutions were submitted to the freezing-pump protocol.

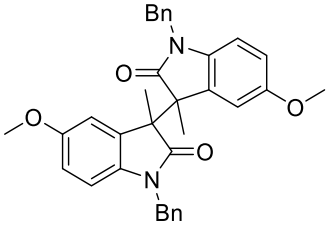
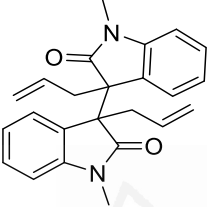
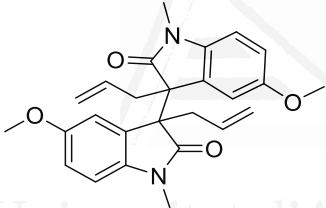
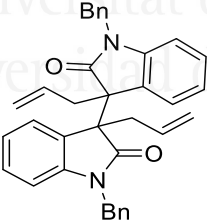
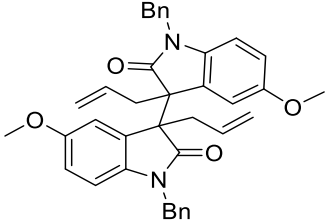
As we can see at Table 9, the reaction presents 1:1 diastereoselectivity in the major part of the cases. The ratio (*R\**,*R\**):*meso* increase in compounds **165b**, **165c** and **165e**. Despite the similar diastereoselectivity between (*R\**,*R\**):*meso* compounds and the good conversion of the reaction, in some cases, *meso* compound could be not isolated. It occurs in compounds **161d**, **161f**, **161h** and **161g**. The yield observed in Table 9 corresponds only to (*R\**,*R\**)-diastereoisomer for these molecules (Table 9, entries 4, 6-8).

Thin Layer Chromatography (TLC) and flash chromatography techniques were used to isolate these compounds, but anyone had not successfully resulted. It is also a remarkable fact that compounds **161d**, **161f** and **161h** (Table 9, entries 4, 6 and 8) corresponding to new compounds and maybe are unstable. The reason why *meso*-**161g** was not isolated was due to low yield.

On the other hand, the yield of the rest entries (Table 9, entries 1-3 and 5) are caused by the contribution of (*R\**,*R\**) and *meso* isolated diastereoisomers.

**Table 9.** Scope of dimerization compound **161** *via* photocatalysis

Entry	<b>165</b>	Product	<b>161</b>	$(R^*, R^*)$ : <i>meso</i> <sup>a</sup>	Yield (%) <sup>b</sup>
<b>1<sup>d</sup></b>	<b>165a</b>		<b>161a</b>	1:1	72
<b>2<sup>d</sup></b>	<b>165b</b>		<b>161b</b>	1.2:1	51
<b>3<sup>d</sup></b>	<b>165c</b>		<b>161c</b>	1.2:1	47

4 <sup>c</sup>	165d		161d	1:1	30
5 <sup>d</sup>	165e		161e	1.2:1	70
6 <sup>c</sup>	165f		161f	1:1	25
7 <sup>c</sup>	165g		161g	1:1	13
8 <sup>c</sup>	165h		161h	1:1	20

<sup>a</sup> Diastereoselectivity ( $R^*,R^*:meso$ ) determined by  $^1\text{H}$  NMR <sup>b</sup> Isolated yield after column chromatography (flash silica) <sup>c</sup> *meso*-diastereoisomer could not be isolated <sup>d</sup> Yield obtained by the sum of  $R^*,R^*$  and *meso* isolated diastereoisomers.

Remarkably, compound *meso*-**161e** is the key building block for the synthesis of (-)-chimonanthine and (+)-calycanthine (see Figure 12 and 22), (-)-WIN 64821 **239**, and (-)-ditryptophenaline **238**,<sup>[126]</sup> and a potential precursor of ( $\pm$ )-dehaloperophoramidines **236**<sup>[127]</sup> and certain communesins **237**.<sup>[128]</sup>

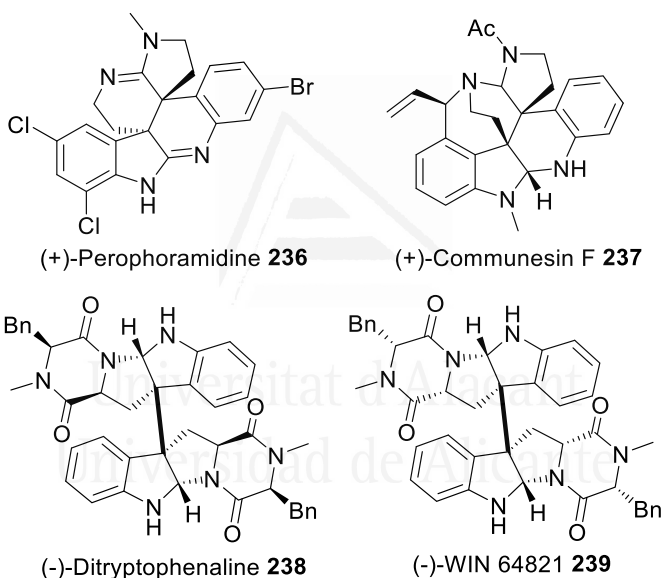


**Figure 22.** Natural products from *meso*-**161e**

As it can be seen at Table 10, comparative study between chapters II and III are shown. As we can observe ratio ( $R^*,R^*$ ): *meso* increase since 1:1 to 3:1 using Deacylative Alkylation (DaA) as a methodology, obtaining ( $R^*,R^*$ )-diastereoisomer after purification with moderate yields.

In some cases, with photoredox catalysis (PC) the yield is lower than with DaA. That is why *meso*-diastereoisomer is lost during purification. On the other hand, employing photoredox catalysis procedure compounds



**161a**, **161b**, **161c** and **161e** has similar or better results because both diastereoisomers has been isolated (compare entries 1-3 and 5 of Table 10).

These results compare well with those obtained from 3-chlorooxindoles (see Scheme 76).<sup>[76]</sup> Compounds **161a**, **161b** and **161c** are obtained with better diastereoselectivity employing DaA methodology.

To synthetize compound **161d**, previous work needs -30 °C and long time to achieve total conversion, meanwhile with our photocatalytic procedure 70 % of yield is obtained at room temperature.

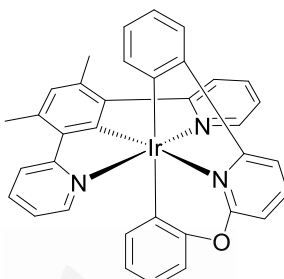
**Table 10.** Comparative study between chapters **II** and **III**

Entry	161	Deacylative Alkylation		Photoredox Catalysis	
		( <i>R*</i> , <i>R*</i> ): <i>meso</i>	Yield (%)	( <i>R*</i> , <i>R*</i> ): <i>meso</i>	Yield (%)
1	<b>161a</b>	3:1	80	1:1	72
2	<b>161b</b>	3:1	54	1.2:1	51
3	<b>161c</b>	3:1	48	1.2:1	47
4	<b>161d</b>	3:1	46	1:1	30
5	<b>161e</b>	3:1	40	1.2:1	70
6	<b>161f</b>	3:1	40	1:1	25
7	<b>161g</b>	3:1	26	1:1	13
8	<b>161h</b>	3:1	40	1:1	20

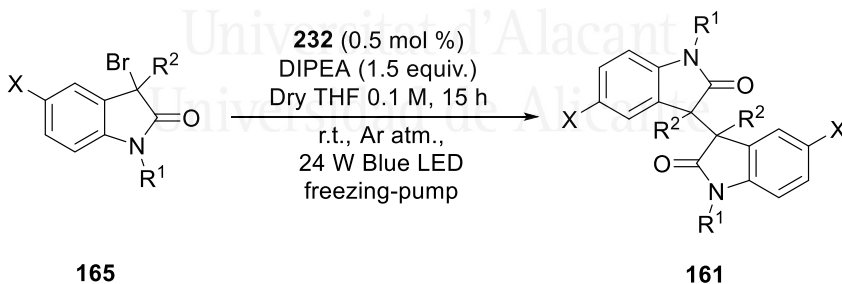
To summary, 8 bioindoles were synthetize using photoredox catalysis with visible light.

### III.4. Conclusions

- ✓ **1<sup>st</sup> target:** The good properties of complex **232** (green emissive after photoexcitation in solid state at room temperature and with good quantum yield 0.87) doing an adequate photocatalyst for the synthesis of 3,3'-bioxindoles.

**232**

- ✓ **2<sup>nd</sup> target:** Photoredox approach achieves a robust procedure using 0.5 mol% of photocatalyst, DIPEA as organic amine reductant and THF as solvent with Blue LED. The ratio of diastereoselectivity is 1:1 and moderate to good yields in the cases that both diastereoisomers are isolated.

**165****161**

- ✓ **3<sup>rd</sup> target:** Similar yields were observed with both methodologies described in chapters II and III for the synthesis of 3,3'-bioxindoles, and better diastereoselectivity was observed under DaA conditions.

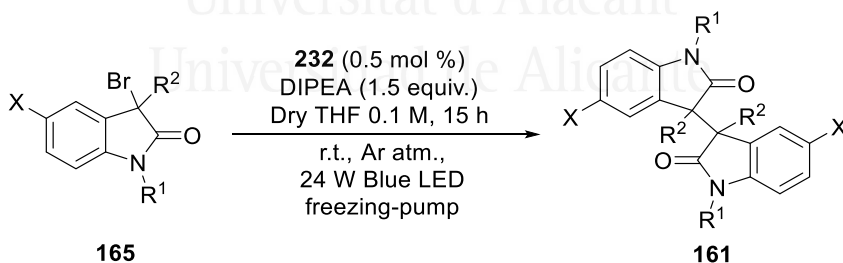
## III.5. Experimental section

### 1. General methods

Melting points were determined with a Marienfeld melting-point meter (MPM-H2) apparatus and are uncorrected. For flash chromatography, silica gel 60 (40–60  $\mu\text{m}$ ) was employed.  $^1\text{H}$  NMR (300, 400 MHz or 500 MHz) and  $^{13}\text{C}$  NMR (75, 101 or 126 MHz) spectra were recorded with Bruker AV300, Bruker AV400, and Bruker ADVANCE DRX500, respectively, with  $\text{CDCl}_3$  as solvent and TMS as internal standard for  $^1\text{H}$  NMR spectra, and the chloroform signal for  $^{13}\text{C}$  NMR spectra; chemical shifts are given in ppm. Low-resolution electron impact (DIP-EI) mass spectra were obtained at 70 eV with an Agilent 6890N Network GC system and an Agilent 5973Network Mass Selective Detector. High-resolution mass spectra (DIP-EI) were recorded with a QTOF Agilent 7200 instrument for the exact mass and Agilent 7890B for the GC. Analytical TLC was performed using ALUGRAM® Xtra SIL G/UV<sub>254</sub> silica gel plates, and the spots were detected under UV light ( $\lambda=254$  nm).

### 2. Experimental procedures

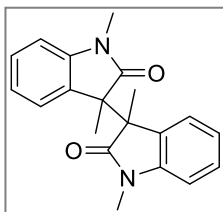
#### Synthesis of 3,3'-bioxindoles **161** via photocatalysis



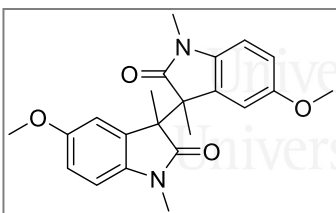
In a Schlenk tube that contained a solution of 3-bromo-1,3-dimethylindolin-2-one **165a**, photocatalyst and DIPEA in dry THF, was degassed by freezing-pump (3 cycles). Then, the reaction was irradiated with Blue LEDs. The reaction was stirring overnight at room temperature. Work-Up.  $\text{H}_2\text{O}$  (10 mL) was added, the mixture was extracted with EtOAc (3  $\times$  10 mL) and the combined organic layers were dried over  $\text{MgSO}_4$ . Finally, the solution was concentrated (15 Torr) and the residue was purified by column chromatography (hexane/EtOAc).

### 3. Experimental data

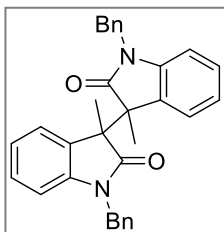
Characterization data of compounds (***R\*,R\****)-**161** were described in Chapter II. In this chapter will be displayed only ***meso***-**161** compounds, it is necessary to mention *meso*-diastereoisomers **161d**, **161f**, **161g** and **161h** could not be isolated after flash chromatography:



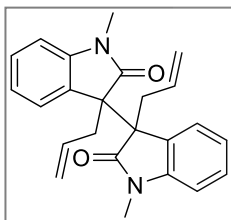
*1,1',3,3'*-Tetramethyl-[3,3'-biindoline]-2,2'-dione (***meso***-**161a**).<sup>[76]</sup> pale yellow solid;  $R_F$  0.30 (hexane/EtOAc 5:5); IR (neat)  $\nu$  1967, 1607, 1374, 1347, 1094, 1026, 757, 736  $\text{cm}^{-1}$ ;  $^1\text{H}$  NMR (300 MHz,  $\text{CDCl}_3$ )  $\delta$  7.24 (2H, t,  $J = 7.7$  Hz, ArH), 6.86 (2H, t,  $J = 7.6$  Hz, ArH), 6.72 (2H, d,  $J = 7.8$  Hz, ArH), 6.61 (2H, d,  $J = 7.3$  Hz, ArH), 2.97 (6H, s,  $\text{NCH}_3$ ), 1.67 (6H, s,  $\text{CH}_3$ );  $^{13}\text{C}$  NMR (75 MHz,  $\text{CDCl}_3$ )  $\delta$  177.81 (2 x CO), 143.89 (2 x C), 131.24 (2 x C), 128.62 (2 x CH), 123.77 (2 x CH), 121.72 (2 x CH), 108.03 (2 x CH), 51.77 (2 x C), 26.03 (2 x  $\text{NCH}_3$ ), 17.51 (2 x  $\text{CH}_3$ ); LRMS (EI)  $m/z$  320 ( $\text{M}^+$ , 8%), 194 (4), 161 (28), 160 (100), 145 (3), 132 (5), 130 (6), 117 (7), 77 (3); HRMS (ESI): calcd. for  $\text{C}_{20}\text{H}_{20}\text{N}_2\text{O}_2$  [ $\text{M}$ ]<sup>+</sup> 320.1525; found 320.1533.



*5,5'*-Dimethoxy-1,1',3,3'-tetramethyl-[3,3'-biindoline]-2,2'-dione (***meso***-**161b**).<sup>[76]</sup> pale yellow solid;  $R_F$  0.30 (hexane/EtOAc 4.5:5.5); IR (neat)  $\nu$  1701, 1497, 1289, 1236, 1035, 732  $\text{cm}^{-1}$ ;  $^1\text{H}$  NMR (300 MHz,  $\text{CDCl}_3$ -d)  $\delta$  6.78 (2H, d,  $J = 10.9$  Hz, ArH), 6.63 (2H, d,  $J = 8.4$  Hz, ArH), 6.29 (2H, s, ArH), 3.65 (6H, s, 2 x  $\text{OCH}_3$ ), 2.96 (6H, s, 2 x  $\text{NCH}_3$ ), 1.66 (6H, s, 2 x  $\text{CH}_3$ );  $^{13}\text{C}$  NMR (75 MHz,  $\text{CDCl}_3$ )  $\delta$  177.23 (2 x CO), 155.15 (2 x C), 137.43 (2 x C), 132.27 (2 x C), 113.04 (2 x CH), 111.19 (2 x CH), 108.07 (2 x CH), 55.78 (2 x  $\text{OCH}_3$ ), 51.88 (2 x C), 26.02 (2 x  $\text{NCH}_3$ ), 17.42 (2 x  $\text{CH}_3$ ); LRMS (EI)  $m/z$  380 ( $\text{M}^+$ , 10%), 192 (2), 191 (15), 190 (100), 176 (2), 175 (6), 174 (2), 162 (2), 160 (2), 159 (2), 147 (5), 119 (2), 118 (3); HRMS (ESI): calcd. for  $\text{C}_{22}\text{H}_{24}\text{N}_2\text{O}_4$  [ $\text{M}$ ]<sup>+</sup> 380.1736; found 380.1756.

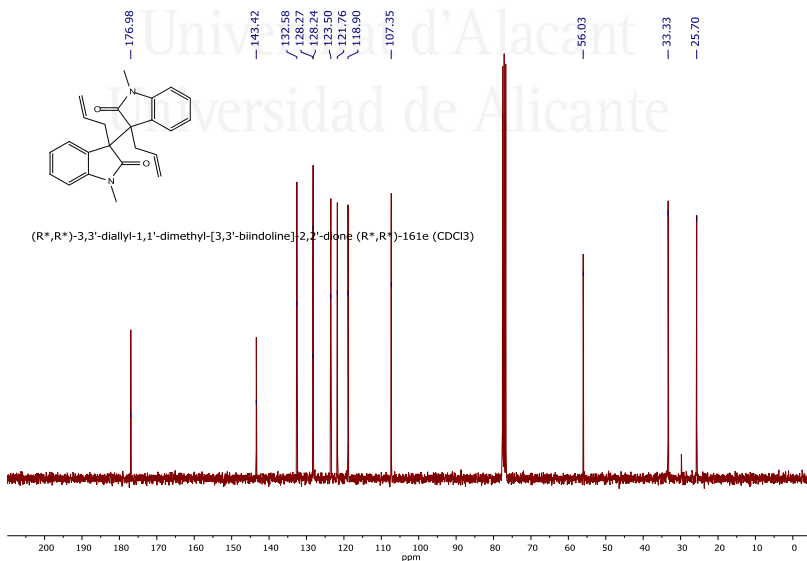
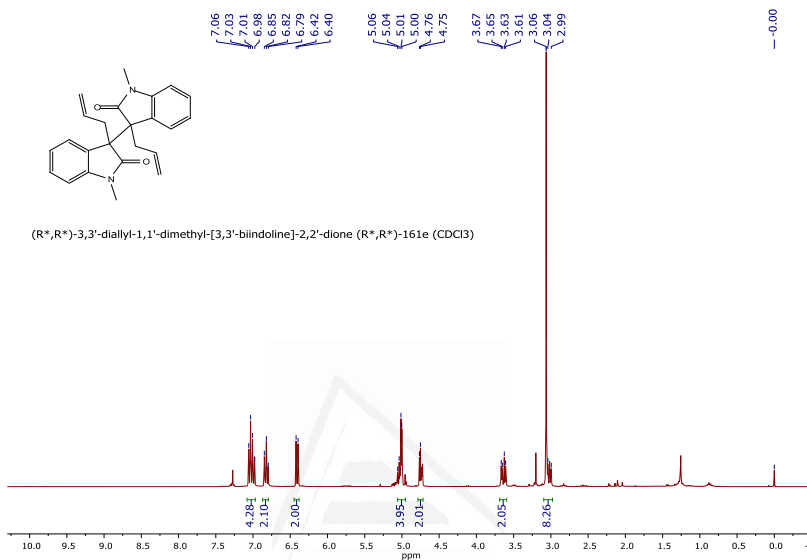


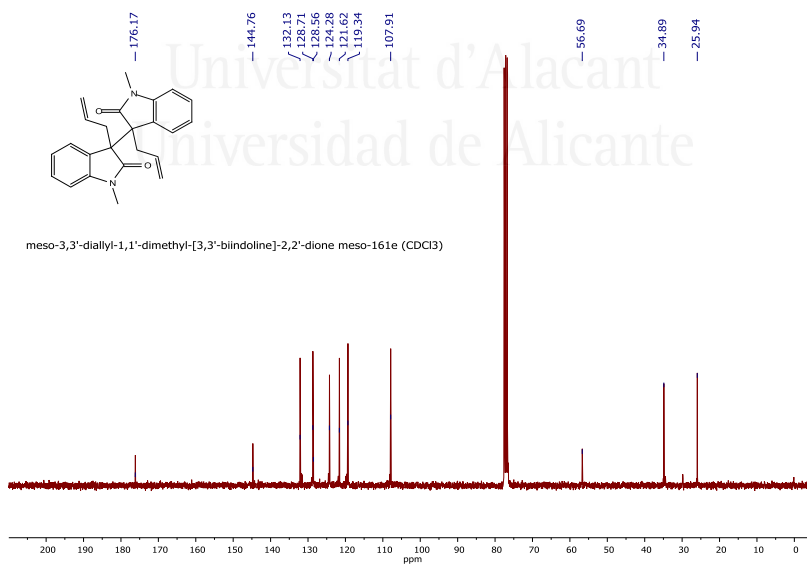
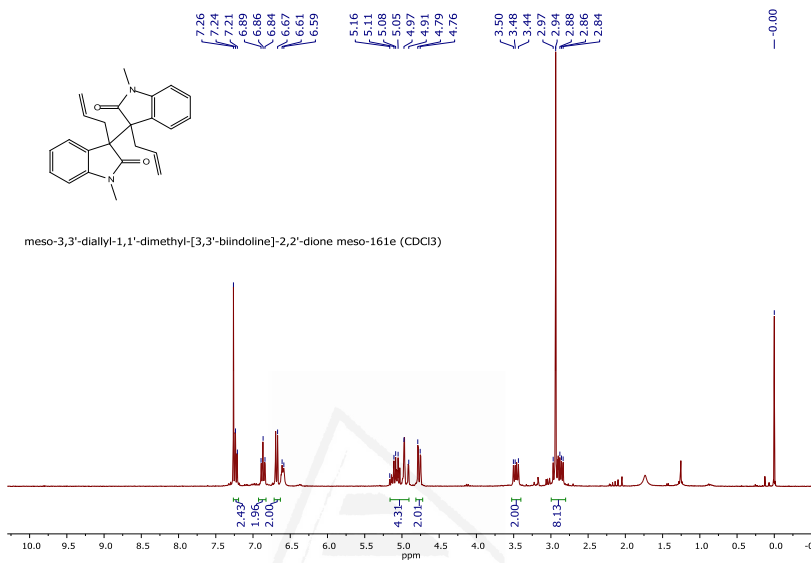
*1,1'-Dibenzyl-3,3'-dimethyl-[3,3'-biindoline]-2,2'-dione (meso-161c)*.<sup>[76]</sup> pale yellow solid;  $R_F$  0.50 (hexane/EtOAc 6:4); IR (neat)  $\nu$  1708, 1608, 1487, 1348, 1183, 731  $\text{cm}^{-1}$ ;  $^1\text{H}$  NMR (300 MHz,  $\text{CDCl}_3$ )  $\delta$  7.20–7.09 (10H, m, ArH), 6.99–6.91 (4H, m, ArH), 6.81 (2H, t,  $J = 7.5$  Hz, ArH), 6.58 (2H, d,  $J = 7.7$  Hz, ArH), 4.93 (2H, d,  $J = 15.8$  Hz, 2 x CHH), 4.65 (2H, d,  $J = 15.9$  Hz, 2 x CHH), 1.80 (3H, s, 2 x  $\text{CH}_3$ );  $^{13}\text{C}$  NMR (75 MHz,  $\text{CDCl}_3$ )  $\delta$  178.18 (2 x CO), 143.06 (2 x C), 135.94 (2 x C), 131.60 (2 x C), 128.74 (4 x CH), 128.57 (2 x CH), 127.31 (2 x CH), 127.22 (4 x CH), 124.07 (2 x CH), 122.12 (2 x CH), 109.40 (2 x CH), 51.48 (2 x C), 44.00 (2 x  $\text{CH}_2$ ), 18.78 (2 x  $\text{CH}_3$ ); LRMS (EI)  $m/z$  472 ( $\text{M}^+$ , 3%), 237 (38), 236 (100), 91 (58); HRMS (ESI): calcd. for  $\text{C}_{32}\text{H}_{28}\text{N}_2\text{O}_2$  [ $\text{M}$ ]<sup>+</sup> 472.2151; found 472.2169.



*3,3'-Diallyl-1,1'-dimethyl-[3,3'-biindoline]-2,2'-dione (meso-161e)*.<sup>[76]</sup> pale yellow solid;  $R_F$  0.30 (hexane/EtOAc 6:4); IR (neat)  $\nu$  1704, 1608, 1469, 1348, 1097, 919, 753  $\text{cm}^{-1}$ ;  $^1\text{H}$  NMR (300 MHz,  $\text{CDCl}_3$ )  $\delta$  7.30–7.19 (2H, m, ArH), 6.87 (2H, t,  $J = 8.0$  Hz, ArH), 6.68 (2H, d,  $J = 7.8$  Hz, ArH), 6.60 (2H, d,  $J = 7.1$  Hz, ArH), 5.18–5.02 (2H, m, 2 x  $\text{HC}=\text{CH}_2$ ), 4.94 (2H, dd,  $J = 17.0, 2.3$  Hz, 2 x  $\text{HC}=\text{CH}$ ), 4.77 (2H, dd,  $J = 9.8, 2.3$  Hz, 2 x  $\text{HC}=\text{CH}$ ), 3.47 (2H, dd,  $J = 13.1, 7.2$  Hz, 2 x CHH), 2.98–2.82 (8H, m, 2 x  $\text{NCH}_3$ , 2 x CHH);  $^{13}\text{C}$  NMR (75 MHz,  $\text{CDCl}_3$ )  $\delta$  176.17 (2 x CO), 144.76 (2 x C), 132.13 (2 x CH), 128.71 (2 x CH), 128.56 (2 x C), 124.28 (2 x CH), 121.62 (2 x CH), 119.34 (2 x CH), 107.91 (2 x  $\text{CH}_2$ ), 56.69 (2 x C), 34.89 (2 x  $\text{NCH}_3$ ), 25.94 (2 x  $\text{CH}_2$ ); LRMS (EI)  $m/z$  372 ( $\text{M}^+$ , 5%), 187 (45), 186 (100), 158 (16), 144 (10), 143 (11); HRMS (ESI): calcd. for  $\text{C}_{24}\text{H}_{24}\text{N}_2\text{O}_2$  [ $\text{M}$ ]<sup>+</sup> 372.1838; found 372.1850.

To finalize this experimental section some examples of NMR spectra are shown:







Universitat d'Alacant  
Universidad de Alicante





## CHAPTER IV:

### CATALYTIC PHOTOREDOX ALLYLATION OF ALDEHYDES PROMOTED BY COBALT COMPLEX

Universitat d'Alacant  
Universidad de Alicante

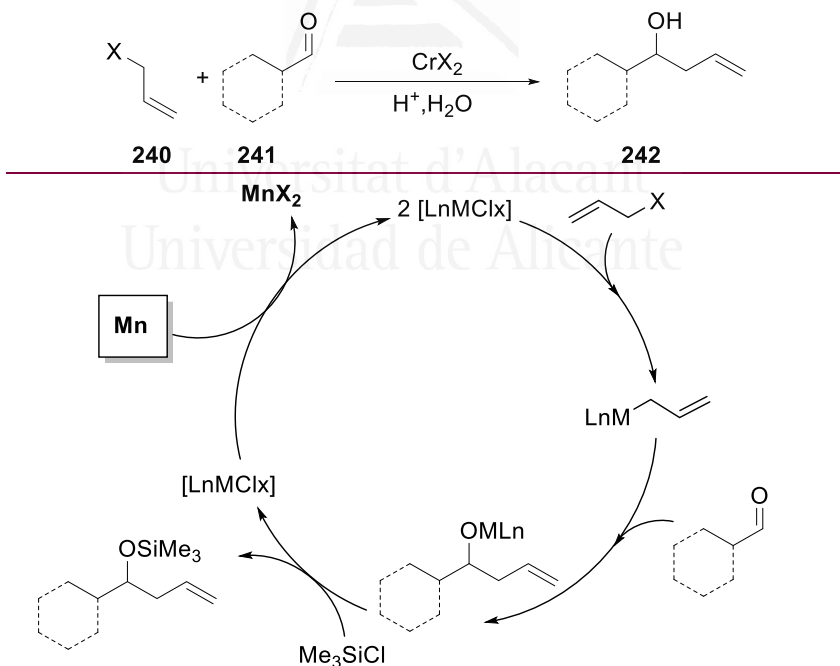


## CHAPTER IV: Catalytic photoredox allylation of aldehydes promoted by a cobalt complex.

### IV.1. Background

The allylation of carbonyl compounds is crucial for the preparation of homoallylic alcohols.<sup>[129][130]</sup> Firstly researches about preparation of homoallyl alcohols was developed by Barbier-Grignard, however the methodology is frequently hazardous, requires cryogenic conditions and, most importantly generates stoichiometric quantities of metallic byproducts, which thwart large scale applications.

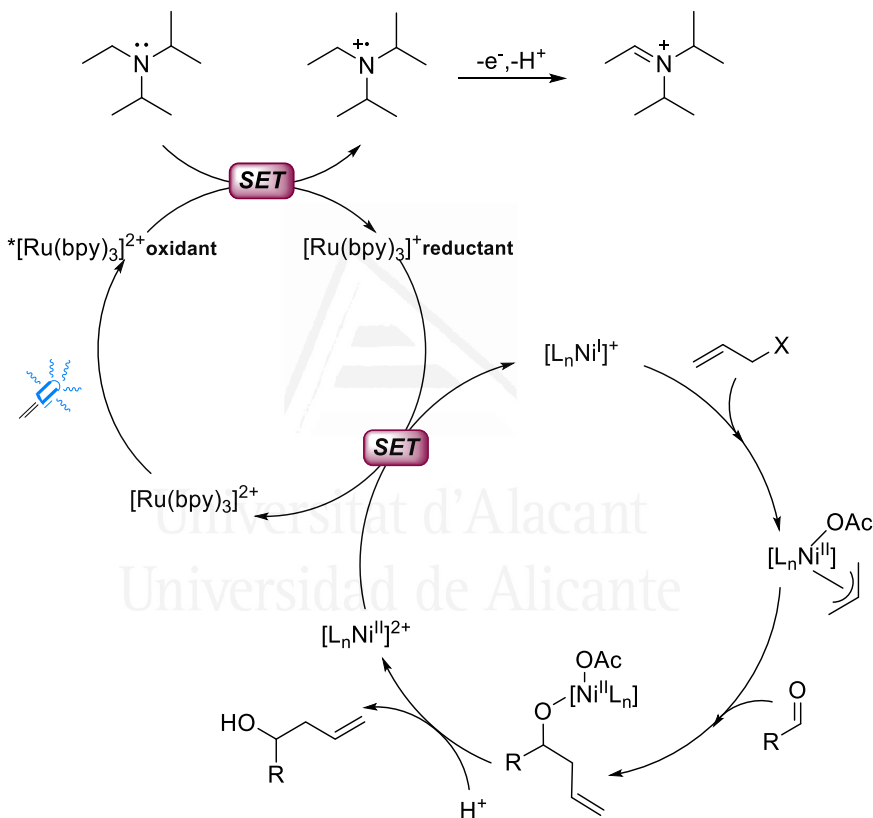
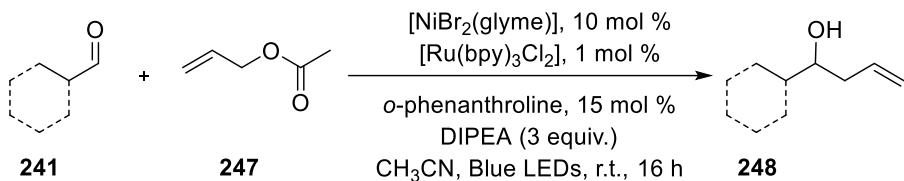
The development of allyl-chromium reactions (Nozaki-Hiyama-Kishi, or NHK)<sup>[131]</sup> and the employment of allyltitanium reagents<sup>[132]</sup> shows the possibility to use a redox cycle, performed under Barbier conditions.



**Scheme 91.** Catalytic allylation *via* redox cycle of NHK reaction





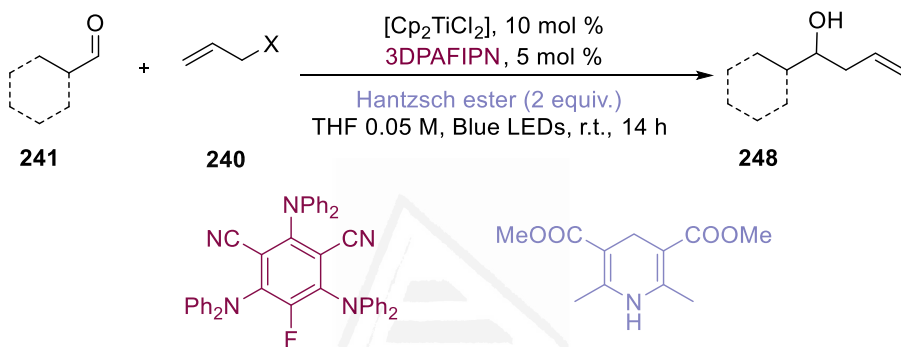


**Scheme 94.** Allylation of aldehydes by dual photoredox and nickel catalysis by Cozzi's group

In this work they developed a novel photoredox nickel catalyzed allylation of aldehydes, using an inexpensive tertiary amine as a sacrificial reductant, and avoiding the use of metals Mg, Zn or Mn. The reaction shows

a broad scope (including aromatic, heterocyclic and aliphatic aldehydes) obtaining more than 25 homoallyl alcohols with moderate to good yields.

Moreover quite recently, they have also reported a novel allylation photoredox methodology based on the use of titanium complex, using an organic dye 1,3-dicyano-5-fluoro-2,4,6-tris(diphenylamino)benzene (3DPAFIPN) to access  $\text{Cp}_2\text{Ti(III)Cl}$  reagent, avoiding the use of stoichiometric metal.<sup>[139]</sup>

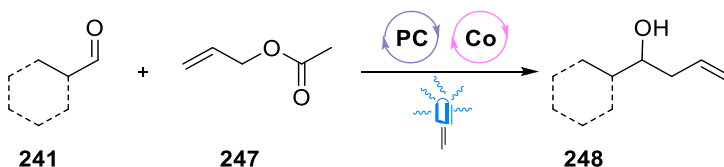


**Scheme 95.**  $\text{Cp}_2\text{TiCl}_2$ -Catalyzed photoredox allylation of aldehydes with visible light by Cozzi's group

In this case, the abundance and low toxicity of the titanium make the procedure attractive for the organic synthesis forming a broad scope of homoallyl alcohols from allyl halides derivatives. Also, this procedure is explained by the mechanism of radical-polar crossover reaction, it will be shown during this chapter.

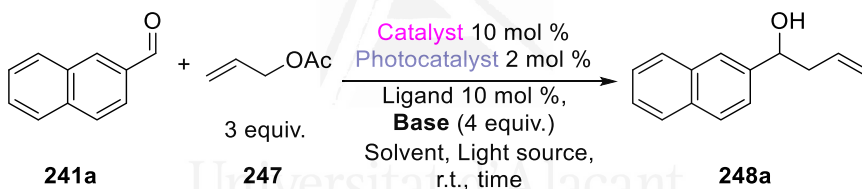
## IV.2. Objectives

- ✓ Continuing last research of Cozzi's group based on radical-polar crossover reaction, a full account of a practical and straightforward allylation methodology of aldehyde based on not toxic and available cobalt salts is reported.



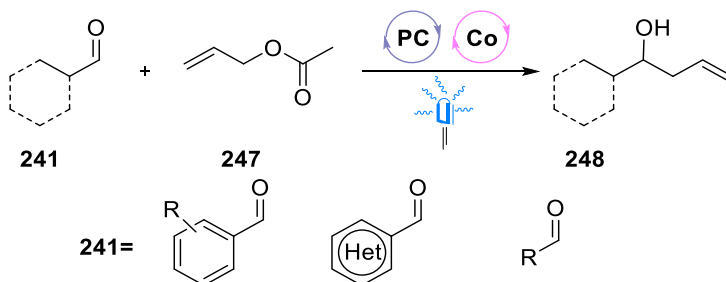
**Scheme 96.** 1<sup>st</sup> target

- ✓ The use of stoichiometric amount of metals, such as manganese or zinc, is avoided due to the merging of photoredox and metal catalyst and it is placed it used an organic available amine.



**Scheme 97.** 2<sup>nd</sup> target

- ✓ Study the scope of the reaction employing aromatic, heterocyclic and aliphatic aldehydes.



**Scheme 98.** 3<sup>rd</sup> target



### IV.3. Results and discussions

---

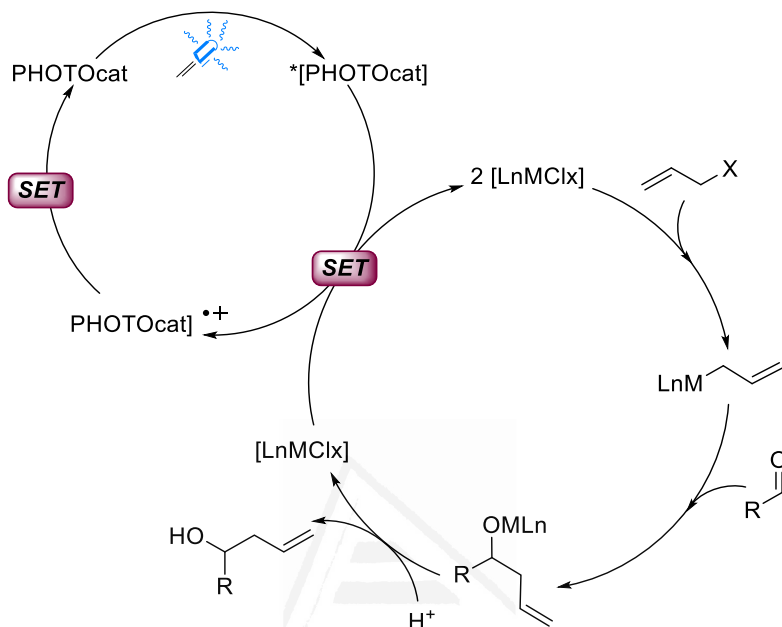
Cobalt is the first and lightest element among the group 9 transition metals, compared with rhodium and iridium is the most abundant element of the group in the Earth.

Co(II) salts are used as precatalysts in many catalytic reactions in the presence of zinc or manganese, in order to reduce cobalt to its active Co(I) state, which is stabilized by appropriate ligand to turn it in a catalytically active species. Gosmini have reported some years ago a cobalt catalyzed coupling reaction of allyl acetates with carbonyl compounds using zinc dust as a reducing agent, leading to homoallylic alcohols.<sup>[140]</sup> This methodology suggested a mechanism for the reaction considered the formation of a low valent cobalt species that undergoes oxidative addition with the allylic acetate.

But before to continue this chapter, is important to know the mechanism which is due to the preparation homoallylic alcohols. Cozzi's group started from the premise effectively recycled by redox (i.e. allylation reactions with redox active metals) cycles can be sustained by photoredox catalysis.

In that hypothesis the combination of radical and polar chemistry, in a so-called reductive radical-polar crossover (RRPC) is realized.<sup>[141][142]</sup> In the design, a metal complex at low oxidation state, generated in the reaction media by SET events is converted in an organometallic nucleophilic specie, thorough a radical-radical combination or by oxidative addition with suitable organic substrates (Scheme 98).

The use of stoichiometric amount of metals, such as manganese or zinc, is avoided, as is the photoredox catalyst, in combination with light, that is maintaining the redox cycle. Of course, the use of other sacrificial reagents is not avoided, as the photocatalyst need to be restored in its fundamental state. Sacrificial agents employed in photoredox reaction are cheap and available organic amines.



**Scheme 99.** Catalytic allylation reaction *via* photoredox cycle

Therefore, it settled a model reaction investigating several reaction parameters and in Table 11 are reported some key experiments for implementing the general reaction conditions. 2-Naphthaldehyde was used in the model reaction. After a preliminary screening of solvent, cobalt catalyst and temperature it was reported the salient observation regarding the photoredox process.

$\text{CoBr}_2$  and  $\text{Co}(\text{OAc})_2$  are appropriate sources of  $\text{Co}(\text{II})$  but  $\text{CoBr}_2$  was chosen because it was not necessary the previous dehydration of the salt and it was the cheapest salt of cobalt. However, the reaction was optimal using 10 mol% of the catalyst, decreasing to 5 mol%, the yield of the reaction was lower (Table 11, entry 2).

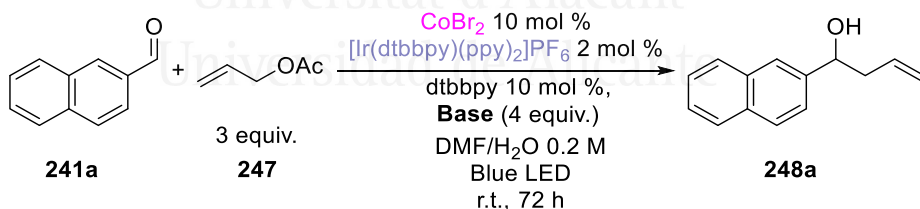
Photocatalyst was limited to  $[\text{Ir}(\text{dtbbpy})(\text{ppy})_2]\text{PF}_6$ , as other photocatalyst tested gave or lower yields (Table 1, entry 5) or no conversion (Table 1, entry 6). Contrary to our nickel mediated process,<sup>[138]</sup>  $[\text{Ru}(\text{bpy})_3]\text{Cl}_2$  is unable to form an active cobalt complex.

The reaction is not occurring in the absence of the photocatalyst or in the dark, so the synergistic approach of metallaphotoredox accomplished to the reaction takes place. Amines are suitable sacrificial agents for the reactions, and we observe just minor conversion by employing TEA (triethylamine) instead than DIPEA (diisopropylethylamine) (Table 11, entry 4).

DMF/H<sub>2</sub>O in a ratio 9:1 is the solvent for this reaction. Although the addition of water slightly improved the isolated yields in the case of naphthyl aldehyde (compare entries 1 and 13, Table 11), in case of other aldehydes we observe a decisive role in the addition of water (it will see at the scope of the reaction).

The chelating di-*tert*-butyl bipyridine is the adapted ligand for the reaction, and other ligand are less effective. Also, a series of different substituted bipyridine were tested. As in many reports on the use of cobalt complexes phosphines are able to stabilize cobalt in low oxidation state (i.e. in Reformatsky reaction,<sup>[143]</sup>) we have also tested mono or chelating phosphines (Table 1, entries 9–12). In some cases, we have observed minor reactivity, but isolated yields and in general, conversion, where in all cases minor to respect N-N chelating ligands. Di-*tert*-butyl bipyridine derivatives will be employed to the enantioselective version of the reaction.

**Table 11.** Modifications of parameters to the preliminary model reaction

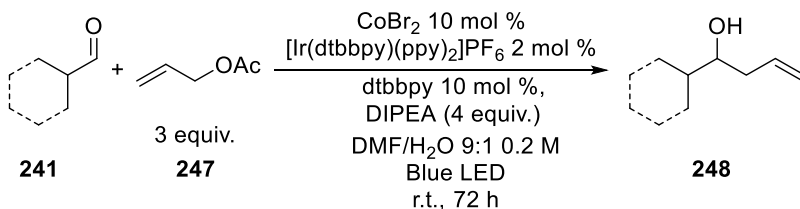


Entry <sup>a</sup>	Deviations from standard conditions	Yield (%) <sup>b</sup>
1	None	97 (76)
2	CoBr <sub>2</sub> 5 mol%	28
3 <sup>c</sup>	Co(OAc) <sub>2</sub>	95 (60)
4 <sup>d</sup>	TEA	85 (53)
5 <sup>e</sup>	{Ir[dF(CF <sub>3</sub> )ppy] <sub>2</sub> (dtbbpy)} <sub>2</sub> (PF <sub>6</sub> )	(25)

<b>6<sup>e</sup></b>	[Ru(bpy) <sub>3</sub> ]Cl <sub>2</sub>	0
<b>7</b>	No photocatalyst	0
<b>8</b>	No light	0
<b>9<sup>f</sup></b>	dppe	0
<b>10<sup>f</sup></b>	dppf	0
<b>11<sup>f</sup></b>	PPh <sub>3</sub>	(23)
<b>12<sup>f</sup></b>	Bpy	38
<b>13<sup>g</sup></b>	DMF	97 (60)
<b>14<sup>g</sup></b>	MeCN	55 (33)
<b>15<sup>g</sup></b>	DCE	(50)
<b>16<sup>g</sup></b>	DMSO	(25)

<sup>a</sup> Reactions were performed on 0.2 mmol of **241a** in DMF (0.2 mL). <sup>b</sup> Determined by <sup>1</sup>H NMR analysis of the reaction crude. Yield in parenthesis are isolated yields after chromatographic purification. <sup>c</sup> Instead of CoBr<sub>2</sub>. <sup>d</sup> Instead of DIPEA. <sup>e</sup> As photocatalyst. <sup>f</sup> As ligand. <sup>g</sup> As solvent.

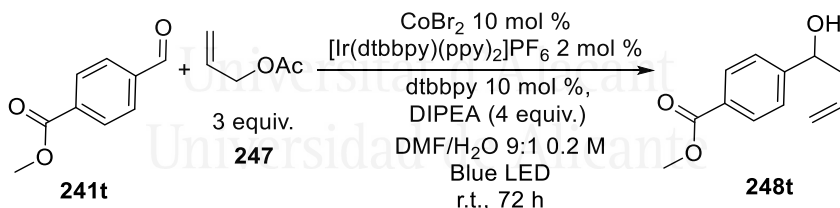
With the optimized conditions we investigated the scope of the reaction with variously substituted aromatic (Table 13), heterocyclic (Table 14), and aliphatic aldehydes (Table 15). The reaction takes place in a solution containing the aldehyde, 3 equivalents of allyl acetate in DMF/H<sub>2</sub>O 9:1. [Ir(dtbbpy)(ppy)<sub>2</sub>]PF<sub>6</sub> was employed as photocatalyst and cobalt bromide as co-catalyst. 10 mol% of dtbbpy was employed as ligand and 4 equivalents of DIPEA as organic basic amine. In order to remove the possible O<sub>2</sub> diluted in the solution 3 cycles of freezing-pump were done. In general, the reaction works effectively with aromatic aldehydes, as specified in Scheme 100.



**Scheme 100.** Optimized cobalt-promoted photoredox allylation reaction with organic aldehydes

Concerning to the scope of the reaction, we found the allylation method particularly adapted to aromatic electron rich aldehydes (Table 13), while electron withdrawing (EWD) group are compromising the reaction outcome (Table 13, entry 10). Methyl 4-formylbenzoate and 4-formylbenzonitrile were tested as example of aldehydes with EWD group at the aromatic ring giving poor results of conversion and yields (not included at Table 13). In order to improve these last results, we tried to modify some conditions of the reaction to improve the yield. In this case, we used methyl 4-formylbenzoate as a reference:

**Table 12.** Optimization of the reaction with aldehydes with EWD groups



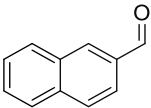
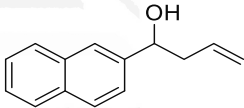
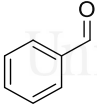
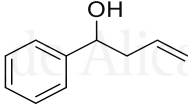
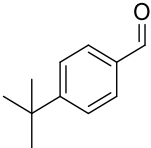
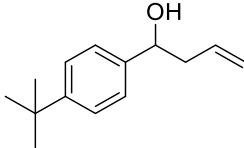
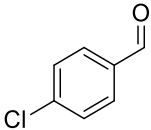
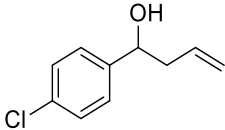
Entry	Deviations from standard conditions	Results
1	None	15 % of yield
2	7 equivalents of allyl acetate	10 % of yield
3	Using dppe as a ligand	Traces of product
4	Using dppe as a ligand and ZnBr <sub>2</sub> as additive	16 % of yield

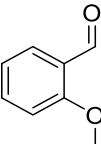
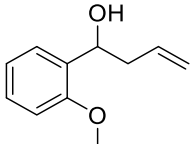
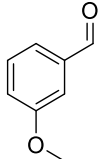
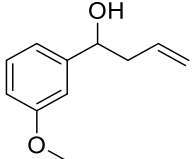
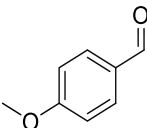
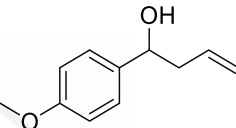
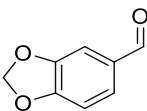
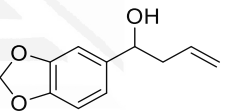
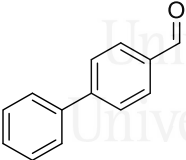
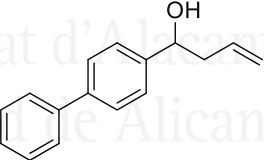
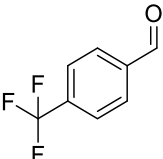
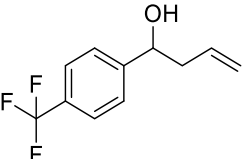
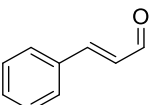
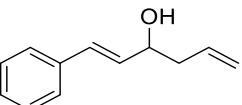
With the results of Table 12, we confirmed that this procedure was not adequate for this kind of reagents. Continuing with the scope of Table 13,

hindrance of the substituent is also affecting the yields, as is possible to evince from the examples with the different methoxy substituted aldehydes (comparing entries 5 to 8 of Table 13). Compounds **241f**, **241g** and **241h** was obtained with similar. Despite to chelating group in *ortho* position is not hampering the reaction, it was observed **241e** had a lower yield than other methoxy derivatives.

Some yields for these substrates were not reduced in absence of water (Table 13, entries 7-9). However, in the case of the major part of products, it has clearly observed the role played by water in the reaction conditions improving the yield. At the present time, given the complexity of the reaction system, can only speculate about the role played by water in enhancing yields and reactivity, and is probably due to the coordination of some cobalt intermediate that can effectively return in the catalytic cycle.

**Table 13.** Scope of the reaction with aromatic aldehydes

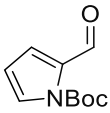
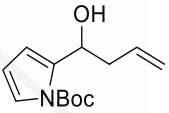
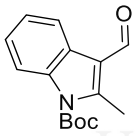
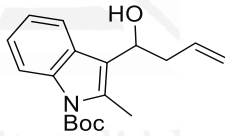
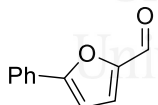
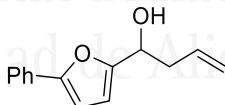
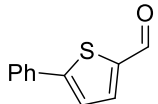
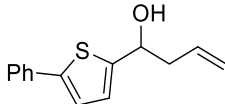
Ent.	Aldehyde	241	Product	248	Yield (%) <sup>a</sup>
1		<b>241a</b>		<b>248a</b>	75 (60)
2		<b>241b</b>		<b>248b</b>	61 (40)
3		<b>241c</b>		<b>248c</b>	70 (33)
4		<b>241d</b>		<b>248d</b>	(66) <sup>b</sup>

<b>5</b>		<b>241e</b>		<b>248e</b>	58
<b>6</b>		<b>241f</b>		<b>248f</b>	73
<b>7</b>		<b>241g</b>		<b>248g</b>	(67)
<b>8</b>		<b>241h</b>		<b>248h</b>	(74)
<b>9</b>		<b>241i</b>		<b>248i</b>	(70)
<b>10</b>		<b>241j</b>		<b>248j</b>	30
<b>11</b>		<b>241k</b>		<b>248k</b>	57 (21)

<sup>a</sup> Yields in parenthesis corresponding to reaction only in DMF as solvent. <sup>b</sup> Aluminum triflate was employed as an additive.

With respect to heterocyclic aldehydes, the reaction took place obtaining moderate yields (Table 14). 1H-pyrrole-2-carbaldehyde and 2-methyl-1H-indole-3-carbaldehyde was firstly protected with di-*tert*-butyl dicarbonate (Boc<sub>2</sub>O) catalyzed by 4-dimethylaminopyridine (DMAP) in order to block the possible allylation at the N position. Also, the compounds **241l** and **241m** were purified by alumina flash chromatography to separate the product and ligand of the reaction correctly. Thiophene and furan derivatives were obtained too with moderate yields (Table 14, entries 3 and 4).

**Table 14.** Scope of the reaction with heterocyclic aldehydes

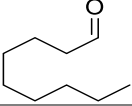
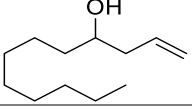
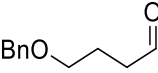
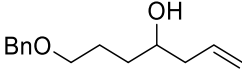
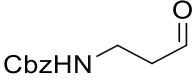
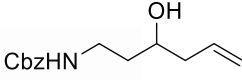
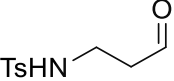
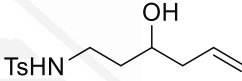
Ent.	Aldehyde	241	Product	248	Yield (%)
1		<b>241l</b>		<b>248l</b>	50 <sup>a</sup>
2		<b>241m</b>		<b>248m</b>	57 <sup>a</sup>
3		<b>241n</b>		<b>248n</b>	50
4		<b>241o</b>		<b>248o</b>	42

<sup>a</sup> Purification by alumina flash chromatography.

In the case of aliphatic aldehydes, the substrates were generally found quite less reactive in comparison to aromatic aldehydes. In the selected examples of many others, in which we can isolate the desired product, the presence of water in the reaction mixture is crucial (Table 15).

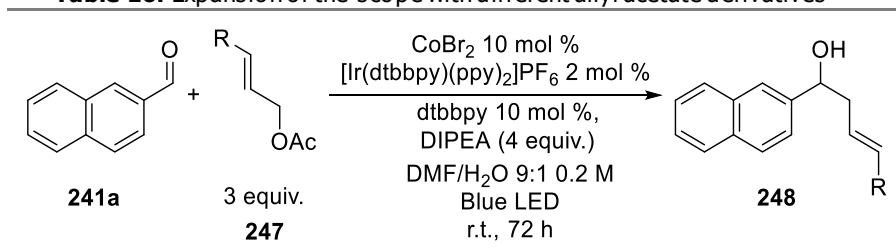


**Table 15.** Scope of the reaction with aliphatic aldehydes

Ent.	Aldehyde	241	Product	248	Yield (%)
1		241p		248p	30
2		241q		248q	34
3		241r		248r	<25 <sup>a</sup>
4		241s		248s	<25 <sup>a</sup>

<sup>a</sup> The reaction presents low conversion and the product was impure after purification.

Finally, to expand the scope different allyl acetates were tried, to do this experiments 2-naphthaldehyde was employed as aldehyde reference (Table 16). When the olefin was substituted, different regioisomers were obtained as product (Table 16, entries 1 and 2). Changing the acylated derivative, allyl *tert*-butanoate, compound 248a was obtained with moderate yield (Table 16, entry 3). To conclude, allyl alcohol was tested as allyl source, but the reaction did not take place.

**Table 16.** Expansion of the scope with different allyl acetate derivatives

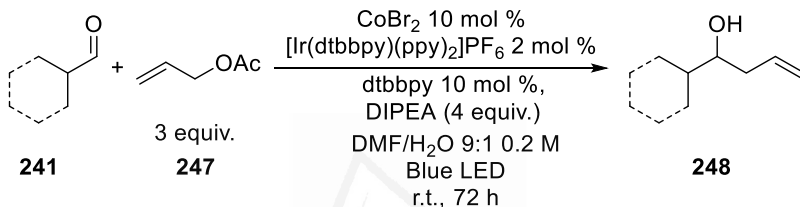
Ent .	Allyl acetate	247	Product	248	Yield (%)
1		<b>247b</b>		<b>248u<sup>b</sup></b>	52 <sup>a</sup>
2		<b>247c</b>		<b>248v<sup>b</sup></b>	43 <sup>a</sup>
3		<b>247d</b>		<b>248a</b>	50

<sup>a</sup>Yield obtained by the sum of both regioisomers <sup>b</sup>d:r 3:1.

To summary, 23 homoallyl alcohols were obtained employing cobalt-promoted photoredox allylation reaction with organic aldehydes.

## IV.4. Conclusions

- ✓ **1<sup>st</sup> target:** A novel photoredox cobalt catalyzed method for the synthesis of homoallyl alcohols has been developed and the reaction conditions optimized for selected substrates.
- ✓ **2<sup>nd</sup> target:** The method requires only catalytic amounts of two transition metal complexes, an amine based stoichiometric reductant and common visible light excitation (Blue LED 450 nm).



- ✓ **3<sup>rd</sup> target:** The reaction is effective for aromatic and heterocyclic substrates, while application of the methodology to aliphatic aldehydes suffer or quite reduced reactivity.

Universitat d'Alacant  
Universidad de Alicante

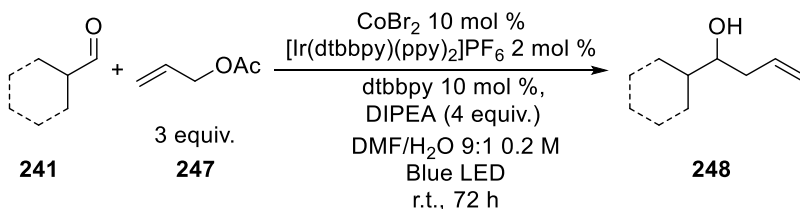
### III.5. Experimental section

#### 1. General methods

All commercial chemicals and dry solvents were purchased from Sigma Aldrich, Alfa Aesar or TCI Chemicals and used without additional purifications.  $^1\text{H}$  and  $^{13}\text{C}$  NMR spectra were recorded on a Varian Inova 400 NMR instrument with a 5 mm probe. All chemical shifts are referenced using deuterated solvent signals; chemical shifts ( $\delta$ ) are reported in ppm from TMS and coupling constants (J) are reported in Hertz. Multiplicity is reported as: s = singlet, d = doublet, t = triplet, q = quartet, sext = sextet, hept = heptet, b = broad, m = multiplet). GC-MS spectra were obtained by EI ionization at 70 eV on a Hewlett-Packard 5971 with GC injection; they are reported as: m/z (rel. intensity). HPLC-MS analyses were performed on an Agilent Technologies HP1100 instrument coupled with an Agilent Technologies MSD1100 single-quadrupole mass spectrometer using a Phenomenex Gemini C18 3  $\mu\text{m}$  (100 x 3 mm) column; mass spectrometric detection was performed in full-scan mode from m/z 50 to 2500, scan time 0.1 s in positive ion mode, ESI spray voltage 4500 V, nitrogen gas 35 psi, drying gas flow rate 11.5 mL  $\text{min}^{-1}$ , fragmentor voltage 30 V. CSP-HPLC analyses were performed on an Agilent Technologies Series 1200 instrument using chiral columns and *n*-hexane/2-propanol (*n*-Hex/IPA) mixtures. The enantiomeric compositions were checked against the corresponding racemic products. Flash chromatography purifications were carried out using VWR or Merck silica gel (40-63  $\mu\text{m}$  particle size). Thin-layer chromatography was performed on Merck 60 F254 plates.

#### 2. Experimental procedures

##### Allylation of aldehydes by photoredox and cobalt catalysis



All the solids (CoBr<sub>2</sub>, photocatalyst, ligand and aldehyde if were solid) were introduced in a 5 mL Schlenk flask, under Ar, followed by 0.9 mL of DMF. The mixture was the degassed using three cycles of freezing-pumping-thawing. The aldehyde (if it were liquid), allyl acetate, 100 µL of H<sub>2</sub>O and the reducing agent were added under Ar, the flask was then sealed and placed under blue LEDs at room temperature for the specified time (3 days). Work-Up. After the reaction, water was added to the mixture, for quench, and then extracted with ethyl acetate (3 x 10mL). The combined organic layers were dried over sodium sulfate, and the solvent was removed under reduced pressure. In some case, was necessary to do a filtration with silica to remove the metal. The product was purified by column chromatography using cyclohexane/acetic acid (100:1) as eluent. The acetic acid is necessary for separate the final product with the ligand because usually two spots exit of the column together. In some case, (heterocycle compounds) the column was done with alumina and without acetic acid.

### 3. Experimental data

---

Compounds **248e**, **248f**, **248n** and **248p** are known compounds and experimental data are consist with reported data:

**248e**: 1-(2-Methoxyphenyl)but-3-en-1-ol.<sup>[144]</sup>

**248f**: 1-(3-Methoxyphenyl)but-3-en-1-ol.<sup>[145]</sup>

**248p**: Dodec-1-en-4-ol.<sup>[146]</sup>

**248ua**: 1-(Naphthalen-2-yl)-2-phenylbut-3-en-1-ol.<sup>[147]</sup>

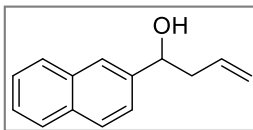
**248ub**: (E)-1-(Naphthalen-2-yl)-4-phenylbut-3-en-1-ol.<sup>[148]</sup>

**248va**: 1-(Naphthalen-2-yl)-2-vinylpentan-1-ol.<sup>[138]</sup>

**248vb**: (E)-1-(Naphthalen-2-yl)hept-3-en-1-ol.<sup>[138]</sup>

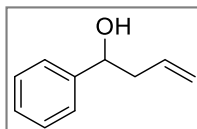
Compound **248n** 1-(5-phenylfuran-2-yl)but-3-en-1-ol is a new compound and its experimental data are in progress, it will be shown when the manuscript will be published.

Following characterization data of compounds **248a**, **248b**, **248c**, **248d**, **248g**, **248h**, **248i**, **248j**, **248k**, **248l**, **248m**, **248o**, **248q**, **248r** and **248s** will be displayed:



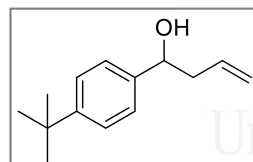
*1-(Naphthalen-2-yl)but-3-en-1-ol* (**248a**).<sup>[138]</sup>

brown oil,  $R_f$  0.20 (cyclohexane/EtOAc 9:1);  $^1\text{H}$  NMR (400 MHz,  $\text{CDCl}_3$ ,  $25^\circ\text{C}$ ):  $\delta$  = 7.85–7.78 (4H, m, ArH), 7.51–7.42 (3H, m, ArH), 5.88–5.77 (1H, m,  $\text{HC}=\text{CH}_2$ ), 5.21–5.12 (2H, m,  $\text{HC}=\text{CH}_2$ ), 4.93–4.86 (1H, m, CH), 2.66–2.52 (2H, m,  $\text{CH}_2$ );  $^{13}\text{C}$  NMR (100 MHz,  $\text{CDCl}_3$ ,  $25^\circ\text{C}$ ):  $\delta$  = 141.2 (C), 134.3 (CH), 133.2 (C), 132.9 (C), 128.2 (CH), 127.9 (CH), 127.6 (CH), 126.1 (CH), 125.8 (CH), 124.4 (CH), 124.0 (CH), 118.5 ( $\text{CH}_2$ ), 73.3 (CH), 43.7 ( $\text{CH}_2$ ); MS (ESI):  $m/z$  = 181.2 [ $\text{M}-\text{OH}$ ] $^+$ .



*1-Phenylbut-3-en-1-ol* (**248b**).<sup>[138]</sup>

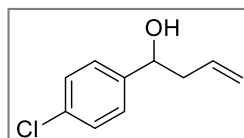
brown oil,  $R_f$  0.40 (cyclohexane/EtOAc 9:1);  $^1\text{H}$ -NMR (400 MHz,  $\text{CDCl}_3$ ,  $25^\circ\text{C}$ ):  $\delta$  = 7.36–7.12 (5H, m, ArH), 5.86–5.74 (1H, m,  $\text{HC}=\text{CH}_2$ ), 5.18–5.11 (2H, m,  $\text{HC}=\text{CH}_2$ ), 4.72 (1H, dd,  $J$  = 7.6, 5.4 Hz, CH), 2.56–2.44 (2H, m,  $\text{CH}_2$ ), 2.06 (1H, br s, OH);  $^{13}\text{C}$ -NMR (100 MHz,  $\text{CDCl}_3$ ,  $25^\circ\text{C}$ ):  $\delta$  = 143.8 (C), 134.4 (CH), 128.4 (2 x CH), 127.5 (CH), 125.8 (2 x CH), 118.4 ( $\text{CH}_2$ ), 73.3 (CH), 43.8 ( $\text{CH}_2$ ); MS (ESI):  $m/z$  = 131.2 [ $\text{M}-\text{OH}$ ] $^+$ .



*1-(4-(Tert-butyl)phenyl)but-3-en-1-ol*

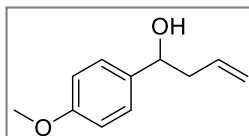
(**248c**).<sup>[138]</sup>

brown oil,  $R_f$  0.20 (cyclohexane/EtOAc 9:1);  $^1\text{H}$ -NMR (400 MHz,  $\text{CDCl}_3$ ,  $25^\circ\text{C}$ ):  $\delta$  = 7.37 (2H, d,  $J$  = 8.3 Hz, ArH), 7.28 (2H, d,  $J$  = 8.4 Hz, ArH), 5.82 (1H, ddt,  $J$  = 17.1, 10.1, 7.1 Hz,  $\text{HC}=\text{CH}_2$ ), 5.20–5.10 (2H, m,  $\text{HC}=\text{CH}_2$ ), 4.70 (1H, t,  $J$  = 6.5 Hz, CH), 2.57–2.44 (2H, m,  $\text{CH}_2$ ), 1.32 (9H, s, 3 x  $\text{CH}_3$ );  $^{13}\text{C}$ -NMR (100 MHz,  $\text{CDCl}_3$ ,  $25^\circ\text{C}$ ):  $\delta$  = 150.4 (C), 140.9 (C), 134.7 (CH), 125.5 (2 x CH), 125.3 (2 x CH), 118.1 ( $\text{CH}_2$ ), 73.1 (CH), 43.6 ( $\text{CH}_2$ ), 34.5 (C), 31.3 (3 x  $\text{CH}_3$ ); MS (ESI):  $m/z$  = 187.2 [ $\text{M}-\text{OH}$ ] $^+$ .

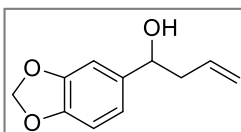


*1-(4-Chlorophenyl)but-3-en-1-ol* (**248d**).<sup>[138]</sup>

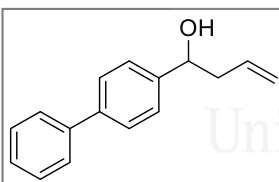
brown oil,  $R_f$  0.20 (cyclohexane/EtOAc 9:1);  $^1\text{H}$ -NMR (400 MHz,  $\text{CDCl}_3$ ,  $25^\circ\text{C}$ ):  $\delta$  = 7.32–7.25 (4H, m, ArH), 5.82–5.71 (1H, m,  $\text{HC}=\text{CH}_2$ ), 5.17–5.14 (1H, m,  $\text{HC}=\text{CH}_2$ ), 5.12 (1H, m,  $\text{HC}=\text{CH}_2$ ), 4.70 (1H, dd,  $J$  = 7.8, 5.1 Hz, CH), 2.53–2.39 (2H, m,  $\text{CH}_2$ );  $^{13}\text{C}$ -NMR (100 MHz,  $\text{CDCl}_3$ ,  $25^\circ\text{C}$ ):  $\delta$  = 142.2 (C), 133.9 (CH), 133.1 (C), 128.5 (2 x CH), 127.2 (2 x CH), 118.8 ( $\text{CH}_2$ ), 72.5 (CH), 43.8 ( $\text{CH}_2$ ); MS (ESI):  $m/z$  = 165.1 [ $\text{M}-\text{OH}$ ] $^+$ .



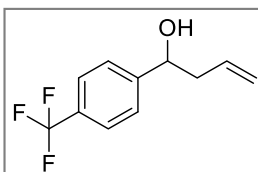
**1-(4-Methoxyphenyl)but-3-en-1-ol (248g)**:<sup>[138]</sup> brown oil,  $R_f$  0.30 (cyclohexane/EtOAc 8:2);  $^1\text{H-NMR}$  (400 MHz,  $\text{CDCl}_3$ ,  $25^\circ\text{C}$ ):  $\delta$  = 7.30–7.23 (2H, m, ArH), 6.90–6.84 (2H, m, ArH), 5.78 (1H, ddt,  $J$  = 17.2, 10.2, 7.1 Hz,  $\text{HC}=\text{CH}_2$ ), 5.17–5.08 (2H, m,  $\text{HC}=\text{CH}_2$ ), 4.67 (1H, t,  $J$  = 6.5 Hz, CH), 3.79 (1H, s,  $\text{CH}_3$ ), 2.51–2.46 (2H, m,  $\text{CH}_2$ );  $^{13}\text{C-NMR}$  (100 MHz,  $\text{CDCl}_3$ ,  $25^\circ\text{C}$ ):  $\delta$  = 159.0 (C), 136.0 (C), 134.6 (CH), 127.0 (2 x CH), 118.2 ( $\text{CH}_2$ ), 113.8 (2 x CH), 73.0 (CH), 55.2 ( $\text{CH}_3$ ), 43.7 ( $\text{CH}_2$ ).



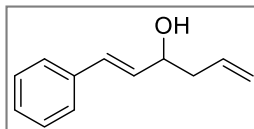
**1-(Benzo[d][1,3]dioxol-5-yl)but-3-en-1-ol (248h)**:<sup>[138]</sup> brown oil,  $R_f$  0.30 (cyclohexane/EtOAc 8:2);  $^1\text{H-NMR}$  (400 MHz,  $\text{CDCl}_3$ ,  $25^\circ\text{C}$ ):  $\delta$  = 6.85 (1H, d,  $J$  = 1.5 Hz, ArH), 6.80–6.72 (2H, m, ArH), 5.92 (2H, s,  $\text{CH}_2$ ), 5.82–5.70 (1H, m,  $\text{HC}=\text{CH}_2$ ), 5.16–5.09 (2H, m,  $\text{HC}=\text{CH}_2$ ), 4.62 (1H, t,  $J$  = 6.5 Hz, CH), 2.48–2.42 (2H, m,  $\text{CH}_2$ );  $^{13}\text{C-NMR}$  (100 MHz,  $\text{CDCl}_3$ ,  $25^\circ\text{C}$ ):  $\delta$  = 147.7 (C), 146.8 (C), 138.0 (C), 134.4 (CH), 119.2 ( $\text{CH}_2$ ), 118.3 (CH), 108.0 (CH), 106.4 (CH), 100.9 ( $\text{CH}_2$ ), 73.2 (CH), 43.8 ( $\text{CH}_2$ ); MS (ESI):  $m/z$  = 175.2 [ $\text{M-OH}$ ] $^+$ .



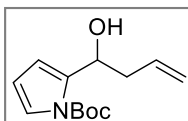
**1-([1,1'-Biphenyl]-4-yl)but-3-en-1-ol (248i)**:<sup>[138]</sup> brown oil,  $R_f$  0.30 (cyclohexane/EtOAc 9:1);  $^1\text{H-NMR}$  (400 MHz,  $\text{CDCl}_3$ ,  $25^\circ\text{C}$ ):  $\delta$  = 7.60–7.56 (4H, m, ArH), 7.45–7.41 (4H, m, ArH), 7.36–7.30 (1H, m, ArH), 5.89–5.79 (1H, m,  $\text{HC}=\text{CH}_2$ ), 5.22–5.15 (2H, m,  $\text{HC}=\text{CH}_2$ ), 4.81–4.75 (1H, m, CH), 2.62–2.48 (2H, m,  $\text{CH}_2$ );  $^{13}\text{C-NMR}$  (100 MHz,  $\text{CDCl}_3$ ,  $25^\circ\text{C}$ ):  $\delta$  = 142.9 (C), 140.8 (C), 140.5 (C), 134.4 (CH), 128.7 (2 x CH), 127.2 (CH), 127.1 (2 x CH), 127.0 (2 x CH), 126.2 (2 x CH), 118.5 ( $\text{CH}_2$ ), 73.02 (CH), 43.8 ( $\text{CH}_2$ ); MS (ESI):  $m/z$  = 207.2 [ $\text{M-OH}$ ] $^+$ .



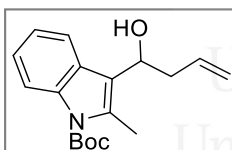
**1-(4-(Trifluoromethyl)phenyl)but-3-en-1-ol (248j)**:<sup>[138]</sup> brown oil,  $R_f$  0.10 (cyclohexane/EtOAc 9:1);  $^1\text{H-NMR}$  (400 MHz,  $\text{CDCl}_3$ ,  $25^\circ\text{C}$ ):  $\delta$  = 7.59 (2H, d,  $J$  = 8.2 Hz, ArH), 7.46 (2H, d,  $J$  = 8.1 Hz, ArH), 5.83–5.71 (1H, m,  $\text{HC}=\text{CH}_2$ ), 5.18 (1H, m,  $\text{HC}=\text{CH}_2$ ), 5.16–5.13 (1H, m,  $\text{HC}=\text{CH}_2$ ), 4.78 (1H, dd,  $J$  = 7.9, 4.8 Hz, CH), 2.57–2.40 (2H, m,  $\text{CH}_2$ ), 2.19 (1H, br s, OH);  $^{13}\text{C-NMR}$  (100 MHz,  $\text{CDCl}_3$ ,  $25^\circ\text{C}$ ):  $\delta$  = 147.7 (C), 133.7 (CH), 129.7 (q,  $J$  = 32.4 Hz, C), 126.1 (2 x CH), 125.3 (q,  $J$  = 3.6 Hz, 2 x CH), 124.3 (q,  $J$  = 272.1 Hz,  $\text{CF}_3$ ), 119.2 ( $\text{CH}_2$ ), 72.5 (CH), 43.9 ( $\text{CH}_2$ );  $^{19}\text{F-NMR}$  (377 MHz,  $\text{CDCl}_3$ ,  $25^\circ\text{C}$ ):  $\delta$  = -61.28; MS (ESI):  $m/z$  = 199.2 [ $\text{M-OH}$ ] $^+$ .



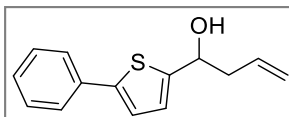
*(E)*-1-Phenylhexa-1,5-dien-3-ol (**248k**).<sup>[138]</sup> yellow oil,  $R_F$  0.10 (cyclohexane/EtOAc 9:1);  $^1\text{H-NMR}$  (400 MHz,  $\text{CDCl}_3$ , 25°C):  $\delta$  = 7.39–7.35 (2H, m, ArH), 7.33–7.27 (2H, m, ArH), 7.25–7.20 (1H, m, CH), 6.60 (1H, d,  $J$  = 16.0 Hz, CH), 6.23 (1H, dd,  $J$  = 15.9, 6.3 Hz, CH), 5.90–5.79 (1H, m,  $\text{HC}=\text{CH}_2$ ), 5.21–5.13 (2H, m,  $\text{HC}=\text{CH}_2$ ), 4.39–4.31 (1H, m, CH), 2.48–2.32 (2H, m,  $\text{CH}_2$ );  $^{13}\text{C-NMR}$  (100 MHz,  $\text{CDCl}_3$ , 25°C):  $\delta$  = 136.6 (C), 134.0 (CH), 131.5 (CH), 130.3 (CH), 128.5 (2 x CH), 127.6 (CH), 126.4 (2 x CH), 118.5 ( $\text{CH}_2$ ), 71.7 (CH), 42.0 ( $\text{CH}_2$ ).



*Tert*-butyl 2-(1-hydroxybut-3-en-1-yl)-1H-pyrrole-1-carboxylate (**248l**).<sup>[138]</sup> brown oil,  $R_F$  0.50 (cyclohexane/EtOAc 9:1);  $^1\text{H-NMR}$  (400 MHz,  $\text{CDCl}_3$ , 25°C):  $\delta$  = 7.14 (1H, dd,  $J$  = 3.4, 1.7 Hz, ArH), 6.20–6.18 (1H, m, ArH), 6.08 (1H, t,  $J$  = 3.4 Hz, ArH), 5.90 (1H, ddt,  $J$  = 17.1, 10.2, 6.9 Hz,  $\text{HC}=\text{CH}_2$ ), 5.17–5.04 (2H, m,  $\text{HC}=\text{CH}_2$ ), 4.93 (1H, t,  $J$  = 6.4 Hz, CH), 3.94 (1H, br s, OH), 2.68–2.62 (2H, m,  $\text{CH}_2$ ), 1.59 (9H, s, 3 x  $\text{CH}_3$ );  $^{13}\text{C-NMR}$  (100 MHz,  $\text{CDCl}_3$ , 25°C):  $\delta$  = 150.2 (CO), 137.5 (C), 135.3 (CH), 121.9 (CH), 116.9 ( $\text{CH}_2$ ), 111.7 (CH), 110.2 (CH), 84.5 (C), 66.2 (CH), 39.2 ( $\text{CH}_2$ ), 28.0 (3 x  $\text{CH}_3$ ); MS (ESI):  $m/z$  = 220.4 [ $\text{M-OH}$ ]<sup>+</sup>.



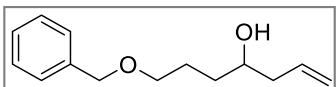
*Tert*-butyl 3-(1-hydroxybut-3-en-1-yl)-2-methyl-1H-indole-1-carboxylate (**248m**).<sup>[138]</sup> brown oil,  $R_F$  0.50 (cyclohexane/EtOAc 9:1);  $^1\text{H-NMR}$  (400 MHz,  $\text{CDCl}_3$ , 25°C):  $\delta$  = 8.10–8.07 (1H, m, ArH), 7.80–7.75 (1H, m, ArH), 7.27–7.15 (2H, m, ArH), 5.84–5.71 (1H, m,  $\text{HC}=\text{CH}_2$ ), 5.18–5.06 (2H, m,  $\text{HC}=\text{CH}_2$ ), 5.04 (1H, dd,  $J$  = 7.9, 6.3 Hz, CH), 2.86–2.57 (2H, m,  $\text{CH}_2$ ), 2.55 (3H, s,  $\text{CH}_3$ ), 1.67 (9H, s, 3 x  $\text{CH}_3$ );  $^{13}\text{C-NMR}$  (100 MHz,  $\text{C}_6\text{D}_{12}$ , 25°C):  $\delta$  = 150.7 (CO), 136.0 (C), 134.6 (CH), 133.6 (C), 127.7 (C), 123.4 (CH), 122.3 (CH), 119.7 (CH), 119.6 ( $\text{CH}_2$ ), 117.9 (CH), 115.4 (CH), 83.8 (C), 67.8 (CH), 41.6 ( $\text{CH}_2$ ), 28.2 (3 x  $\text{CH}_3$ ), 14.1 ( $\text{CH}_3$ ); MS (ESI):  $m/z$  = 284.3 [ $\text{M-OH}$ ]<sup>+</sup>.



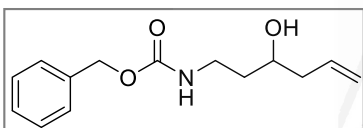
1-(5-Phenylthiophen-2-yl)but-3-en-1-ol (**248o**).<sup>[138]</sup> brown oil,  $R_F$  0.40 (cyclohexane/EtOAc 8:2);  $^1\text{H-NMR}$  (400 MHz,  $\text{CDCl}_3$ , 25°C):  $\delta$  = 7.57 (2H, d,  $J$  = 8.1, ArH), 7.38–7.33 (2H, m, ArH), 7.27 (1H, d,  $J$  = 7.2 Hz, ArH), 7.15 (1H, d,  $J$  = 3.6 Hz, ArH), 6.93 (1H, d,  $J$  = 3.6 Hz, ArH), 5.85 (1H, ddt,  $J$  = 17.2, 10.2, 7.1 Hz,  $\text{HC}=\text{CH}_2$ ), 5.25–5.15 (2H, m,  $\text{HC}=\text{CH}_2$ ), 4.96 (1H, t,  $J$  = 6.3 Hz, CH), 2.70–2.58 (2H, m,  $\text{CH}_2$ ), 2.20 (1H, br s, OH);  $^{13}\text{C-NMR}$



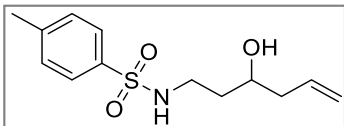
(100 MHz, CDCl<sub>3</sub>, 25°C):  $\delta$  = 147.2 (C), 143.5 (C), 134.4 (C), 133.7 (CH), 128.8 (2 x CH), 127.4 (CH), 125.7 (2 x CH), 124.6 (CH), 122.5 (CH), 118.9 (CH<sub>2</sub>), 69.5 (CH), 43.6 (CH<sub>2</sub>); MS (ESI):  $m/z$  = 213.2 [M-OH]<sup>+</sup>.



*7-(Benzyloxy)hept-1-en-4-ol (248q)*.<sup>[138]</sup>  
yellow oil,  $R_f$  0.30 (cyclohexane/EtOAc 9:1); <sup>1</sup>H-NMR (400 MHz, CDCl<sub>3</sub>, 25°C):  $\delta$  = 7.35–7.25 (5H, m, ArH), 5.87–5.76 (1H, m, HC=CH<sub>2</sub>), 5.13–5.08 (2H, m, HC=CH<sub>2</sub>), 4.50 (2H, s, CH<sub>2</sub>), 3.68–3.62 (1H, m, CH), 3.50 (2H, t,  $J$  = 6.0 Hz, CH<sub>2</sub>), 2.35 (1H, br s, OH), 2.30–2.11 (2H, m, CH<sub>2</sub>), 1.81–1.59 (3H, m, CHH, CH<sub>2</sub>), 1.48 (1H, ddd,  $J$  = 14.3, 11.1, 7.2 Hz, CHH); <sup>13</sup>C-NMR (100 MHz, CDCl<sub>3</sub>, 25°C):  $\delta$  = 138.2 (C), 135.0 (CH), 128.4 (2 x CH), 127.7 (2 x CH), 127.6 (CH), 117.7 (CH<sub>2</sub>), 73.0 (CH<sub>2</sub>), 70.5 (CH<sub>2</sub>), 70.4 (CH<sub>2</sub>), 42.0 (CH), 34.0 (CH<sub>2</sub>), 26.2 (CH<sub>2</sub>); (ESI):  $m/z$  = 221.2 [M+H]<sup>+</sup>, 203.2 [M-OH]<sup>+</sup>.



*Benzyl (3-hydroxyhex-5-en-1-yl)carbamate (248r)*.<sup>[138]</sup> yellow oil,  $R_f$  0.40 (cyclohexane/EtOAc 8:2); <sup>1</sup>H-NMR (400 MHz, CDCl<sub>3</sub>, 25°C):  $\delta$  = 7.36–7.27 (5H, m, ArH), 5.79 (1H, dt,  $J$  = 16.8, 7.3 Hz, HC=CH<sub>2</sub>), 5.21–5.04 (4H, m, HC=CH<sub>2</sub>, CH<sub>2</sub>), 3.72–3.66 (1H, m, CH), 3.52–3.44 (1H, m, CHH), 3.21 (1H, dt,  $J$  = 19.3, 5.3 Hz, CHH), 2.60 (1H, br s, OH), 2.28–2.15 (1H, m, CH<sub>2</sub>), 1.67 (1H, dddd,  $J$  = 14.2, 8.7, 5.6, 3.1 Hz, CHH), 1.52 (1H, ddd,  $J$  = 14.6, 10.6, 5.4 Hz, CHH); <sup>13</sup>C-NMR (100 MHz, CDCl<sub>3</sub>, 25°C):  $\delta$  = 157.0 (CO), 136.5 (C), 134.5 (CH), 128.5 (2 x CH), 128.1 (3 x CH), 118.1 (CH<sub>2</sub>), 68.5 (CH), 66.7 (CH<sub>2</sub>), 41.9 (CH<sub>2</sub>), 38.1 (CH<sub>2</sub>), 36.6 (CH<sub>2</sub>); MS (ESI):  $m/z$  = 272.0 [M+Na]<sup>+</sup>, 250.2 [M+H]<sup>+</sup>.



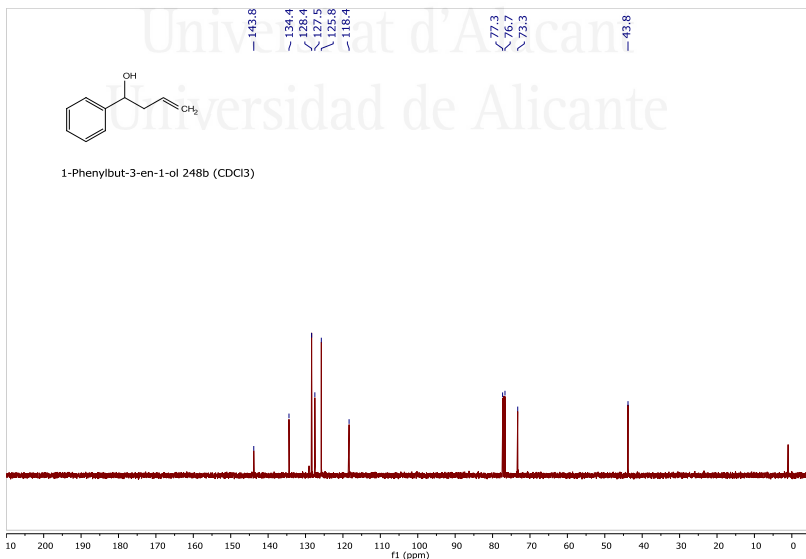
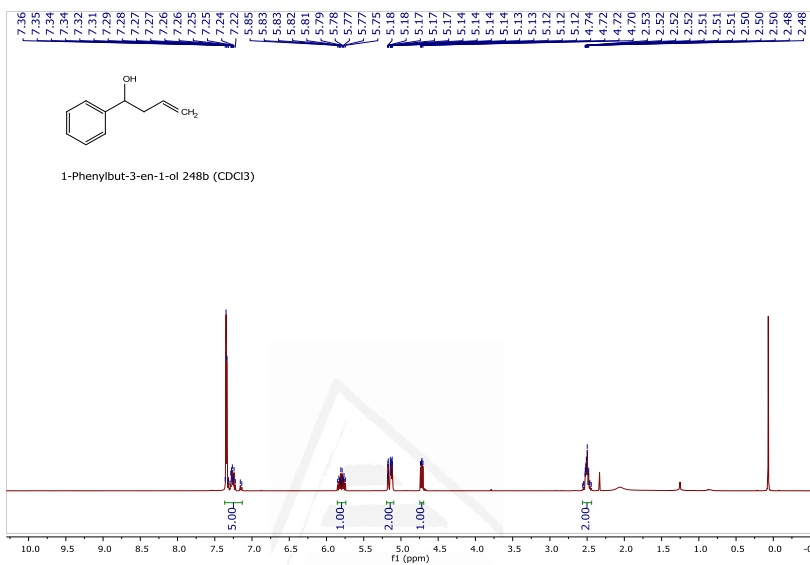
*N-(3-Hydroxyhex-5-en-1-yl)-4-methylbenzenesulfonamide (248s)*.<sup>[138]</sup>  
brown oil,  $R_f$  0.30 (cyclohexane/EtOAc 8:2); <sup>1</sup>H-NMR (400 MHz, CDCl<sub>3</sub>, 25°C):  $\delta$  = 7.72 (2H, d,  $J$  = 8.3 Hz, ArH), 7.32–7.25 (2H, m, ArH), 5.71 (1H, dddd,  $J$  = 16.9, 10.3, 7.9, 6.5 Hz, HC=CH<sub>2</sub>), 5.22 (1H, br s, OH), 5.13–5.05 (2H, m, HC=CH<sub>2</sub>), 3.72 (1H, ddd,  $J$  = 12.3, 7.8, 4.4 Hz, CH), 3.16 (1H, dtd,  $J$  = 12.5, 7.5, 4.9 Hz, CHH), 3.00 (1H, dtd,  $J$  = 12.2, 7.1, 4.9 Hz, CHH), 2.40 (3H, s, CH<sub>3</sub>), 2.25–2.16 (1H, m, CHH), 2.13–2.05 (1H, m, CHH), 2.01 (1H, br s, NH), 1.66 (1H, dddd,  $J$  = 14.4, 7.8, 5.0, 3.0 Hz, CHH), 1.52 (1H, dddd,  $J$  = 14.3, 9.3, 7.1, 4.9 Hz, CHH); <sup>13</sup>C-NMR (100 MHz, CDCl<sub>3</sub>, 25°C):  $\delta$  = 143.3 (C), 136.9 (C), 133.9 (CH), 129.6 (2 x CH), 127.1 (2 x CH),

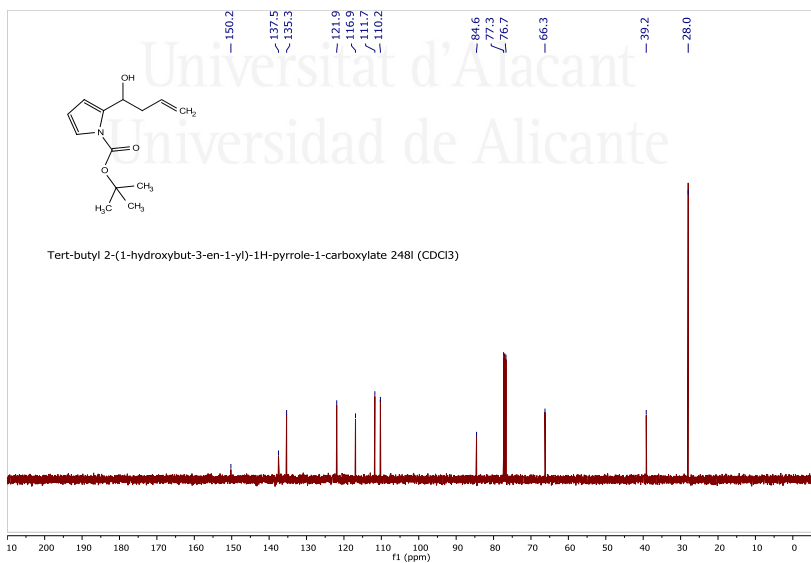
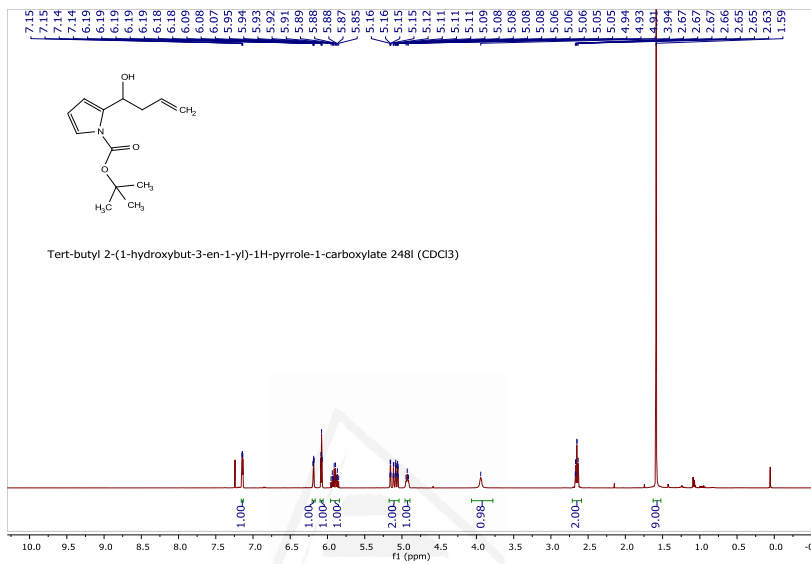
118.8 (CH<sub>2</sub>), 69.5 (CH), 42.0 (CH<sub>2</sub>), 41.0 (CH<sub>2</sub>), 35.2 (CH<sub>2</sub>), 21.5 (CH<sub>3</sub>); MS (ESI):  $m/z = 270.0$  [M+H]<sup>+</sup>, 252.0 [M-H<sub>2</sub>O]<sup>+</sup>.



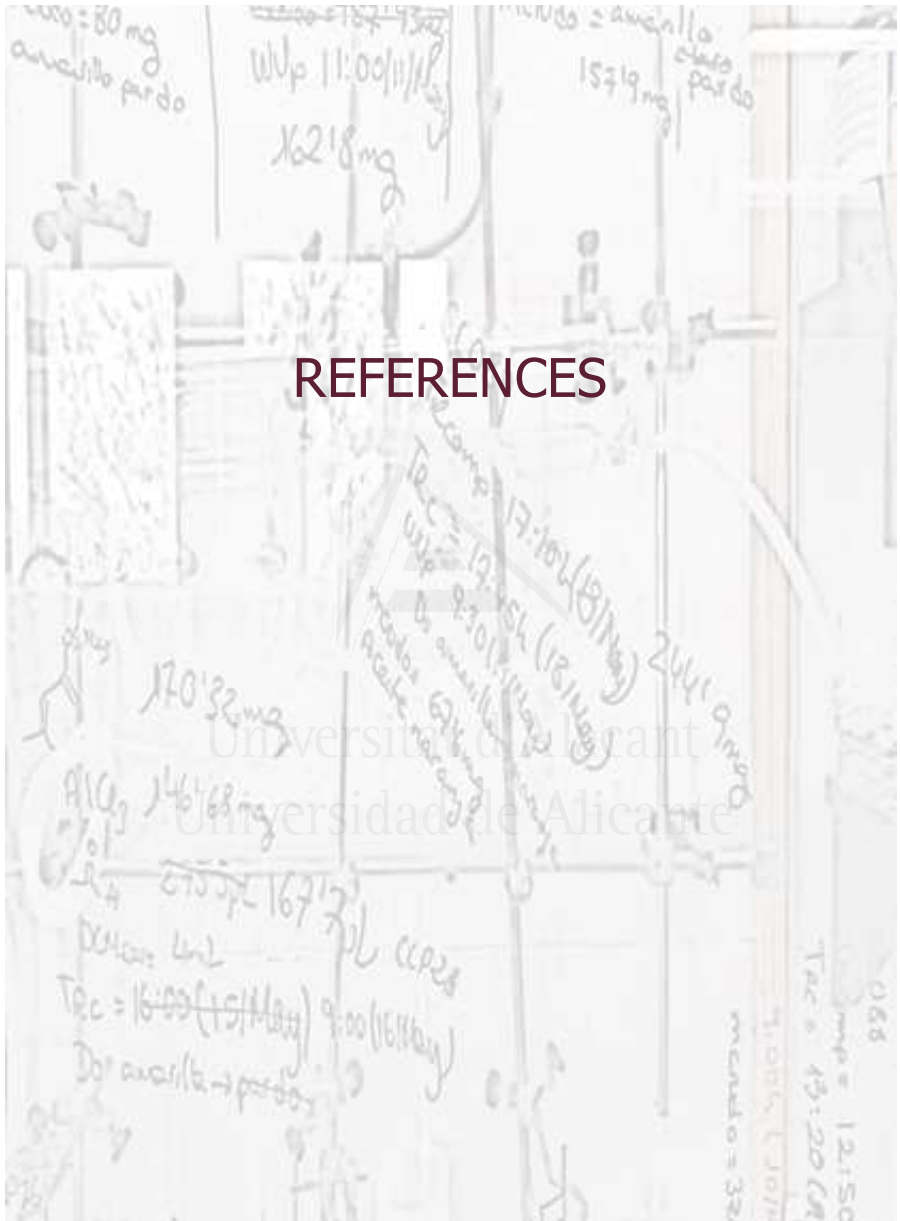
Universitat d'Alacant  
Universidad de Alicante

To finalize this experimental section some examples of NMR spectra are shown:





## REFERENCES





## References

---

- [1] M. Kaur, *Key Heterocycle Cores Des. Multitargeting Mol.* **2018**, 211–246.
- [2] A. H. Beckett, R. W. Daisley, J. Walker, *Tetrahedron* **1968**, *24*, 6093–6109.
- [3] F. G. Bordwell, H. E. Fried, *J. Org. Chem.* **1991**, *56*, 4218–4223.
- [4] J. Bergman, *Adv. Heterocycl. Chem.* **2015**, *117*, 1–81.
- [5] T. Jiang, K. L. Kuhen, K. Wolff, H. Yin, K. Bieza, J. Caldwell, B. Bursulaya, T. Y. H. Wu, Y. He, *Bioorganic Med. Chem. Lett.* **2006**, *16*, 2105–2108.
- [6] A. Natarajan, Y. Guo, F. Harbinski, Y. H. Fan, H. Chen, L. Luus, J. Diercks, H. Aktas, M. Chorev, J. A. Halperin, *J. Med. Chem.* **2004**, *47*, 4979–4982.
- [7] S. R. S. Rudrangi, V. K. Bontha, V. R. Manda, S. Bethi, *Asian J. Res. Chem.* **2011**, *4*, 335–338.
- [8] G. Wylie, T. Appelboom, W. Bolten, F. C. Breedveld, J. Feely, M. R. G. Leeming, X. Le Loët, R. Manthorpe, R. Marcolongo, J. Smolen, *Rheumatology* **1995**, *34*, 554–563.
- [9] S. B. J. Sapi, J. Levy, *Heterocycles* **1994**, *38*, 725–732.
- [10] C. Molina, A. Ortega-Martínez, J. M. Sansano, C. Nájera, *Org. Biomol. Chem.* **2019**, *17*, 482–489.
- [11] A. Reissert, *Berichte der Dtsch. Chem. Gesellschaft* **1897**, *30*, 1030–1053.
- [12] M. P. M. Quallich G.J., *Synthesis (Stuttg)*. **1993**, 51–53.
- [13] K. Jones, J. M. D. Storey, *Tetrahedron* **1993**, *49*, 4901–4906.
- [14] P. G. Gassman, T. J. van Bergen, *J. Am. Chem. Soc.* **1973**, *95*, 2718–2719.
- [15] W. Stollé, R., Bergdoll, R., Luther, M., Auerhahn, A., & Wacker, *J. Für Prakt. Chemie* **1930**, *128*, 1–43.

- [16] S. L. Hennessy, E. J., & Buchwald, *ChemInform* **2004**, *125*, 12085.
- [17] E. J. Hennessy, S. L. Buchwald, *J. Am. Chem. Soc.* **2003**, *125*, 12084–12085.
- [18] P. Jönsson, N. Åke; Moses, **1974**.
- [19] C. Crestini, R. Saladino, *Synth. Commu.* **2012**, 2835–2841.
- [20] R. L. Hlnman, C. P. Bauman, *J. Org. Chem.* **1964**, *29*, 2431–2437.
- [21] F. Zhou, Y. L. Liu, J. Zhou, *Adv. Synth. Catal.* **2010**, *352*, 1381–1407.
- [22] R. Shintani, M. Inoue, T. Hayashi, *Angew. Chem. Int. Ed.* **2006**, *45*, 3353–3356.
- [23] J. Itoh, S. B. Han, M. J. Krische, *Angew. Chem. Int. Ed.* **2009**, *48*, 6313–6316.
- [24] G. Luppi, P. G. Cozzi, M. Monari, B. Kaptein, Q. B. Broxterman, C. Tomasini, *J. Org. Chem.* **2005**, *70*, 7418–7421.
- [25] S. Nakamura, N. Hara, H. Nakashima, K. Kubo, N. Shibata, T. Toru, *Chem. Eur. J.* **2008**, *14*, 8079–8081.
- [26] G. S. M. Figueiredo, R. S. Zardo, B. V. Silva, F. A. Violante, A. C. Pinto, P. D. Fernandes, *Pharmacol. Biochem. Behav.* **2013**, *103*, 431–439.
- [27] T. B. K. Lee, G. S. K. Wong, *J. Org. Chem.* **1991**, *56*, 872–875.
- [28] B. M. Trost, M. U. Frederiksen, *Angew. Chem. Int. Ed.* **2004**, *44*, 308–310.
- [29] P. Hewawasam, V. K. Gribkoff, Y. Pendri, S. I. Dworetzky, N. A. Meanwell, E. Martinez, C. G. Boissard, D. J. Post-Munson, J. T. Trojnacki, K. Yeleswaram, et al., *Bioorg. Med. Chem. Lett.* **2002**, *12*, 1023–1026.
- [30] Y. Hamashima, T. Suzuki, H. Takano, Y. Shimura, M. Sodeoka, *J. Am. Chem. Soc.* **2005**, *127*, 10164–10165.
- [31] T. Ishimaru, N. Shibata, J. Nagai, S. Nakamura, T. Toru, S. Kanemasa, *J. Am. Chem. Soc.* **2006**, *128*, 16488–16489.
- [32] D. Sano, K. Nagata, T. Itoh, *Org. Lett.* **2008**, *10*, 1593–1595.
- [33] X. Li, B. Zhang, Z. G. Xi, S. Luo, J. P. Chenga, *Adv. Synth. Catal.* **2010**, *352*, 416–424.



- [34] M. M. Abelman, T. Oh, L. E. Overman, *J. Org. Chem.* **1987**, *52*, 4130–4133.
- [35] A. Ashimori, T. Matsuura, L. E. Overman, D. J. Poon, *J. Org. Chem.* **1993**, *58*, 6949–6951.
- [36] E. P. Kündig, T. M. Seidel, Y. X. Jia, G. Bernardinelli, *Angew. Chem. Int. Ed.* **2007**, *46*, 8484–8487.
- [37] Y. X. Jia, J. M. Hillgren, E. L. Watson, S. P. Marsden, E. P. Kündig, *Chem. Commun.* **2008**, 4040–4042.
- [38] Y. Yasui, H. Kamisaki, Y. Takemoto, *Org. Lett.* **2008**, *10*, 3303–3306.
- [39] E. C. Linton, M. C. Kozlowski, *J. Am. Chem. Soc.* **2008**, *130*, 16162–16163.
- [40] B. M. Trost, N. Cramer, S. M. Silverman, *Chemtracts* **2010**, *23*, 66–68.
- [41] B. M. Trost, N. Cramer, H. Bernsmann, *J. Am. Chem. Soc.* **2007**, *129*, 3086–3087.
- [42] G. Bencivenni, L. Y. Wu, A. Mazzanti, B. Giannichi, F. Pesciaoli, M. P. Song, G. Bartoli, P. Melchiorre, *Angew. Chem. Int. Ed.* **2009**, *48*, 7200–7203.
- [43] X. H. Chen, Q. Wei, S. W. Luo, H. Xiao, L. Z. Gong, *J. Am. Chem. Soc.* **2009**, *131*, 13819–13825.
- [44] S. Ma, X. Han, S. Krishnan, S. C. Virgil, B. M. Stoltz, *Angew. Chem. Int. Ed.* **2009**, *48*, 8037–8041.
- [45] A. Ortega-Martínez, C. Molina, C. Moreno-Cabrerizo, J. M. Sansano, C. Nájera, *Eur. J. Org. Chem.* **2018**, *2018*, 2394–2405.
- [46] M. Jukic, D. Sterk, Z. Casar, *Curr. Org. Synth.* **2012**, *9*, 488–512.
- [47] J. A. Tunge, E. C. Burger, *Eur. J. Org. Chem.* **2005**, 1715–1726.
- [48] B. M. Trost, D. T. Stiles, *Org. Lett.* **2007**, *9*, 2763–2766.
- [49] C. V. Galliford, K. A. Scheidt, *Angew. Chem. Int. Ed.* **2007**, *46*, 8748–8758.
- [50] N. Kumar, M. K. Das, S. Ghosh, A. Bisai, *Chem. Commun.* **2017**, *53*, 2170–2173.

- [51] A. Ortega-Martínez, R. de Lorenzo, J. M. Sansano, C. Nájera, *Tetrahedron* **2018**, *74*, 253–259.
- [52] P. Ruiz-Sanchis, S. A. Savina, F. Albericio, M. Álvarez, *Chem. Eur. J.* **2011**, *17*, 1388–1408.
- [53] S. Ghosh, S. Chaudhuri, A. Bisai, *Org. Lett.* **2015**, *17*, 1373–1376.
- [54] S. Ghosh, S. Chaudhuri, A. Bisai, *Chem. Eur. J.* **2015**, *21*, 17479–17484.
- [55] J. T. Link, L. E. Overman, *J. Am. Chem. Soc.* **1996**, *118*, 8166–8167.
- [56] C. Menozzi, P. I. Dalko, J. Cossy, *Chem. Commun.* **2006**, 4638–4640.
- [57] K. Ohmatsu, Y. Ando, T. Ooi, *Synlett* **2017**, *28*, 1291–1294.
- [58] M. Jha, T. Y. Chou, B. Blunt, *Tetrahedron* **2011**, *67*, 982–989.
- [59] A. Ortega-Martínez, C. Molina, C. Moreno-Cabrerizo, J. M. Sansano, C. Nájera, *Synth.* **2017**, *49*, 5203–5210.
- [60] A. Pinto, Y. Jia, L. Neuville, J. Zhu, *Chem. Eur. J.* **2007**, *13*, 961–967.
- [61] J. Yang, X. W. Liu, D. D. Wang, M. Y. Tian, S. N. Han, T. T. Feng, X. L. Liu, R. Q. Mei, Y. Zhou, *Tetrahedron* **2016**, *72*, 8523–8536.
- [62] T. B. T. Sarges, R. Howard, H. R. Siegel, *Eur. J. Med. Chem.* **1992**, *2*, 779–789.
- [63] Z. Bian, C. C. Marvin, M. Pettersson, S. F. Martin, *J. Am. Chem. Soc.* **2014**, *136*, 14184–14192.
- [64] T. Mugishima, M. Tsuda, Y. Kasai, H. Ishiyama, E. Fukushi, J. Kawabata, M. Watanabe, K. Akao, J. Kobayashi, *J. Org. Chem.* **2005**, *70*, 9430–9435.
- [65] L. Shi, Y. Wang, H. Yang, H. Fu, *Org. Biomol. Chem.* **2014**, *12*, 4070–4073.
- [66] J. R. Frost, S. M. Huber, S. Breitenlechner, C. Bannwarth, T. Bach, *Angew. Chem. Int. Ed.* **2015**, *54*, 691–695.
- [67] F. Zhou, C. Tan, J. Tang, Y. Y. Zhang, W. M. Gao, H. H. Wu, Y. H. Yu, J. Zhou, *J. Am. Chem. Soc.* **2013**, *135*, 10994–10997.
- [68] S. Kattela, G. Heerdt, C. R. D. Correia, *Adv. Synth. Catal.* **2017**, *359*, 260–267.

- [69] Y. L. Huang, W. H. Bao, W. W. Ying, W. T. Chen, L. H. Gao, X. Y. Wang, G. P. Chen, G. P. Ge, W. T. Wei, *Synlett* **2018**, *29*, 1485–1490.
- [70] W. Chan, X. Tang, F. Zhang, G. Quek, G. Mei, Y. Lu, *Angew. Chemie* **2019**, *131*, 6326–6330.
- [71] Y. H. Jiang, R. Y. Yang, J. Sun, C. G. Yan, *Heterocycl. Commun.* **2016**, *22*, 151–156.
- [72] K. A. P. Lingam, P. Shanmugam, K. Selvakumar, *Synlett* **2012**, 278–284.
- [73] L. K. Kinthada, S. R. Medisetty, A. Parida, K. N. Babu, A. Bisai, *J. Org. Chem.* **2017**, *82*, 8548–8567.
- [74] L. E. Overman, D. A. Watson, *J. Org. Chem.* **2006**, *71*, 2587–2599.
- [75] J. R. Fuchs, R. L. Funk, *J. Am. Chem. Soc.* **2004**, *126*, 5068–5069.
- [76] W. L. Jia, J. He, J. J. Yang, X. W. Gao, Q. Liu, L. Z. Wu, *J. Org. Chem.* **2016**, *81*, 7172–7181.
- [77] C. Ma, D. Xing, W. Hu, *Org. Lett.* **2016**, *18*, 3134–3137.
- [78] R. Zhou, R. Liu, K. Zhang, L. Han, H. Zhang, W. Gao, R. Li, *Chem. Commun.* **2017**, *53*, 6860–6863.
- [79] Y. Q. Zou, W. Guo, F. L. Liu, L. Q. Lu, J. R. Chen, W. J. Xiao, *Green Chem.* **2014**, *16*, 3787–3795.
- [80] J. R. Fuchs, R. L. Funk, *Org. Lett.* **2005**, *7*, 677–680.
- [81] C. R. Jamison, J. J. Badillo, J. M. Lipshultz, R. J. Comito, D. W. C. MacMillan, *Nat. Chem.* **2017**, *9*, 1165–1169.
- [82] C. Ma, D. Xing, W. Hu, *Org. Lett.* **2016**, *18*, 3134–3137.
- [83] T. F. Spande, M. W. Edwards, L. K. Pannell, J. W. Daly, V. Erspamer, P. Melchiorri, *J. Org. Chem.* **1988**, *53*, 1222–1226.
- [84] X. D. Xia, L. Q. Lu, W. Q. Liu, D. Z. Chen, Y. H. Zheng, L. Z. Wu, W. J. Xiao, *Chem. Eur. J.* **2016**, *22*, 8432–8437.
- [85] H. M. Hugel, R. J. Greenwood, M. F. Mackay, *Aust. J. Chem.* **1992**, *45*, 1953–1959.
- [86] X. Ju, Y. Liang, P. Jia, W. Li, W. Yu, *Org. Biomol. Chem.* **2012**, *10*,

- 498–501.
- [87] L. H. Chen, Y. T. Ma, F. Yang, X. Y. Huang, S. W. Chen, K. Ji, Z. S. Chen, *Adv. Synth. Catal.* **2019**, *361*, 1307–1312.
- [88] R. Zhou, R. Liu, K. Zhang, L. Han, H. Zhang, W. Gao, R. Li, *Chem. Commun.* **2017**, *53*, 6860–6863.
- [89] L. Marzo, R. Martínez-Haya, *An. Quím.* **2018**, *114*, 141–148.
- [90] G. Ciamcian, *Science* . **1912**, *XXXVI*, No.926,385-394.
- [91] M. H. Shaw, J. Twilton, D. W. C. MacMillan, *J. Org. Chem.* **2016**, *81*, 6898–6926.
- [92] N. Turro, G. Schuster, *Science* **1975**, *187*, 303–312.
- [93] M. D. Kärkäs, J. A. Porco, C. R. J. Stephenson, *Chem. Rev.* **2016**, *116*, 9683–9747.
- [94] T. J. Meyer, *Acc. Chem. Res.* **1989**, *22*, 163–170.
- [95] H. Takeda, O. Ishitani, *Coord. Chem. Rev.* **2010**, *254*, 346–354.
- [96] K. Kalyanasundaram, M. Grätzel, *Coord. Chem. Rev.* **1998**, *77*, 347–414.
- [97] J. M. R. Narayanam, C. R. J. Stephenson, *Chem. Soc. Rev.* **2011**, *40*, 102–113.
- [98] A. Studer, D. P. Curran, *Angew. Chem. Int. Ed.* **2016**, *55*, 58–102.
- [99] S. P. Pitre, C. D. McTiernan, J. C. Scaiano, *Acc. Chem. Res.* **2016**, *49*, 1320–1330.
- [100] A. G. Condie, J. C. González-Gómez, C. R. J. Stephenson, *J. Am. Chem. Soc.* **2010**, *132*, 1464–1465.
- [101] Y. Miyake, Y. Ashida, K. Nakajima, Y. Nishibayashi, *Chem. Eur. J.* **2014**, *20*, 6120–6125.
- [102] D. A. Nagib, D. W. C. Macmillan, *Nature* **2011**, *480*, 224–228.
- [103] S. Purser, P. R. Moore, S. Swallow, V. Gouverneur, *Chem. Soc. Rev.* **2008**, *37*, 320–330.
- [104] D. P. Hari, P. Schroll, B. König, *J. Am. Chem. Soc.* **2012**, *134*, 2958–2961.

- [105] L. J. Allen, P. J. Cabrera, M. Lee, M. S. Sanford, *J. Am. Chem. Soc.* **2014**, *136*, 5607–5610.
- [106] Z. Lu, T. P. Yoon, *Angew. Chemie* **2012**, *124*, 10475–10478.
- [107] Y. Q. Zou, S. W. Duan, X. G. Meng, X. Q. Hu, S. Gao, J. R. Chen, W. J. Xiao, *Tetrahedron* **2012**, *68*, 6914–6919.
- [108] L. L. Wu, G. H. Yang, Z. Guan, Y. H. He, *Tetrahedron* **2017**, *73*, 1854–1860.
- [109] A. Ault, *J. Chem. Educ.* **2002**, *79*, 572–577.
- [110] C. P. Casey, *J. Chem. Educ.* **2006**, *83*, 192–195.
- [111] C. C. C. Johansson Seechurn, M. O. Kitching, T. J. Colacot, V. Snieckus, *Angew. Chem. Int. Ed.* **2012**, *51*, 5062–5085.
- [112] J. Twilton, C. C. Le, P. Zhang, M. H. Shaw, R. W. Evans, D. W. C. MacMillan, *Nat. Rev. Chem.* **2017**, *1*.
- [113] D. W. . Zuo, Zhiwei; Ahneman, Derek; Chu, Lingling; Terrett, Jack; Doyle, Abigail G; MacMillan, *Science* **2014**, *345*, 437–440.
- [114] J. C. Tellis, D. N. Primer, G. A. Molander, *Science* **2014**, *345*, 433–436.
- [115] D. T. Ahneman, A. G. Doyle, *Chem. Sci.* **2016**, *7*, 7002–7006.
- [116] P. Zhang, C. C. Le, D. W. C. MacMillan, *J. Am. Chem. Soc.* **2016**, *138*, 8084–8087.
- [117] M. Osawa, H. Nagai, M. Akita, *J. Chem. Soc., Dalton Trans.* **2006**, 827–829.
- [118] D. Kalyani, K. B. McMurtrey, S. R. Neufeldt, M. S. Sanford, *J. Am. Chem. Soc.* **2011**, *133*, 18566–18569.
- [119] G. Zhang, C. Liu, H. Yi, Q. Meng, C. Bian, H. Chen, J. X. Jian, L. Z. Wu, A. Lei, *J. Am. Chem. Soc.* **2015**, *137*, 9273–9280.
- [120] C. J. Wu, Q. Y. Meng, T. Lei, J. J. Zhong, W. Q. Liu, L. M. Zhao, Z. J. Li, B. Chen, C. H. Tung, L. Z. Wu, *ACS Catal.* **2016**, *6*, 4635–4639.
- [121] K.-H. He, F.-F. Tan, C.-Z. Zhou, G.-J. Zhou, X.-L. Yang, Y. Li, *Angew. Chemie* **2017**, *129*, 3126–3130.
- [122] M. A. Esteruelas, D. Gómez-Bautista, A. M. López, E. Oñate, J. Y. Tsai,

- C. Xia, *Chem. Eur. J.* **2017**, *23*, 15729–15737.
- [123] R. G. Alabau, B. Eguillor, J. Esler, M. A. Esteruelas, M. Oliván, E. Oñate, J. Y. Tsai, C. Xia, *Organometallics* **2014**, *33*, 5582–5596.
- [124] M. A. Esteruelas, A. M. López, E. Onate, A. San-Torcuato, J. Y. Tsai, C. Xia, *Inorg. Chem.* **2018**, *57*, 3720–3730.
- [125] R. Castro-Rodrigo, M. A. Esteruelas, D. Gómez-Bautista, V. Lezáun, A. M. López, M. Oliván, E. Oñate, *Organometallics* **2019**, *38*, 3707–3718.
- [126] S. Ghosh, S. Bhunia, B. N. Kakde, S. De, A. Bisai, *Chem. Commun.* **2014**, *50*, 2434–2437.
- [127] A. Biswas, U. Karmakar, S. Nandi, R. Samanta, *J. Org. Chem.* **2017**, *82*, 8933–8942.
- [128] J. Park, A. Jean, D. Y. K. Chen, *Angew. Chem. Int. Ed.* **2017**, *56*, 14237–14240.
- [129] M. Yus, J. C. González-Gómez, F. Foubelo, *Chem. Rev.* **2011**, *111*, 7774–7854.
- [130] M. Yus, J. C. González-Gómez, F. Foubelo, *Chem. Rev.* **2013**, *113*, 5595–5698.
- [131] A. Fürstner, *Chem. Rev.* **1999**, *99*, 991–1045.
- [132] A. Kasatkin, T. Nakagawa, S. Okamoto, F. Sato, *J. Am. Chem. Soc.* **1995**, *117*, 3881–3882.
- [133] X. Shen, K. Harms, M. Marsch, E. Meggers, *Chem. Eur. J.* **2016**, *22*, 9102–9105.
- [134] C. K. Prier, D. A. Rankic, D. W. C. MacMillan, *Chem. Rev.* **2013**, *113*, 5322–5363.
- [135] J. A. Milligan, J. P. Phelan, S. O. Badir, G. A. Molander, *Angew. Chem. Int. Ed.* **2019**, *58*, 6152–6163.
- [136] J. L. Schwarz, F. Schäfers, A. Tlahuext-Aca, L. Lückemeier, F. Glorius, *J. Am. Chem. Soc.* **2018**, *140*, 12705–12709.
- [137] H. Mitsunuma, S. Tanabe, H. Fuse, K. Ohkubo, M. Kanai, *Chem. Sci.* **2019**, *10*, 3459–3465.

- [138] A. Gualandi, G. Rodeghiero, A. Faraone, F. Patuzzo, M. Marchini, F. Calogero, R. Perciaccante, T. P. Jansen, P. Ceroni, P. G. Cozzi, *Chem. Commun.* **2019**, 55, 6838–6841.
- [139] A. Gualandi, F. Calogero, M. Mazzarini, S. Guazzi, A. Fermi, G. Bergamini, P. G. Cozzi, *ACS Catal.* **2020**, 10, 3857–3863.
- [140] P. Gomes, C. Gosmini, J. Périchon, *Synthesis* **2003**, 1909–1915.
- [141] L. Pitzer, J. L. Schwarz, F. Glorius, *Chem. Sci.* **2019**, 10, 8285–8291.
- [142] R. J. Wiles, G. A. Molander, *Isr. J. Chem.* **2020**, 1–14.
- [143] M. Lombardo, A. Gualandi, F. Pasi, C. Trombini, *Adv. Synth. Catal.* **2007**, 349, 465–468.
- [144] J. Pogula, S. Laha, B. Sreedhar, P. R. Likhar, *Adv. Synth. Catal.* **2020**, 362, 1176–1183.
- [145] T. Hamaguchi, Y. Takahashi, H. Tsuji, M. Kawatsura, *Org. Lett.* **2020**, 22, 1124–1129.
- [146] R. Tomifuji, S. Masuda, T. Kurahashi, S. Matsubara, *Org. Lett.* **2019**, 21, 3834–3837.
- [147] Y. Gan, H. Hu, Y. Liu, *Org. Lett.* **2020**, 22, 4418–4423.
- [148] L. M. Zhao, H. S. Gao, D. F. Li, J. Dong, L. L. Sang, J. Ji, *Org. Biomol. Chem.* **2017**, 15, 4359–4366.



Universitat d'Alacant  
Universidad de Alicante





## ABBREVIATIONS

Universitat d'Alacant  
Universidad de Alicante



## Abbreviations

---

3DPAFIPN: 1,3-dicyano-5-fluoro-2,4,6-tris(diphenylamino)benzene

AAA: asymmetric allylic alkylation

AIDS: acquired Immune Deficiency Syndrome

BINAP: 2,2'-bis(diphenylphosphino)-1,1'-binaphthyl

BINOL: 1,1'-bi-2-naphthol

Boc<sub>2</sub>O: di-*tert*-butyl decarbonate

BOX: bis(oxazoline)

Bpy: bipyridine

CFL: compact fluorescent lamp

DaA: deacylative alkylation

DaB: deacylative bromination

DaI: deacylative iodination

DBU: diazabicycloundecene

DcA: decarboxylative allylation

DCE: dichloroethane

DCM: dichloromethane

DIPEA: diisopropylethylamine

DMAP: 4-(*N,N*-dimethylamino)pyridine

DMF: dimethylformamide

DMSO: dimethyl sulfoxide

Dppp: 1,3-Bis(diphenylphosphino)propane

Dtbbpy: di-*tert*-butyl bipyridine

E: energy

Equiv.: Equivalents  
ET: energy transfer  
EtOAc: Ethyl acetate  
EWD: electron withdrawing group  
f.p.: freezing-pump  
GC: gas chromatography  
HAT: hydrogen atom transfer  
HIV: human immunodeficiency virus  
HOMO: highest occupied molecular orbital  
HTS: high throughput screening  
IDC: intramolecular dehydrogenative coupling  
IR: infrared  
LED: Light Emitting Diode  
LUMO: lowest unoccupied molecular orbital  
MeCN: acetonitrile  
Mes: mesyl  
NBS: *N*-bromosuccinimide  
NFSI: *N*-fluorobenzenesulfonimide  
NIS: *N*-iodosuccinimide  
NMR: nuclear magnetic resonance  
o.n.: over night  
PC: photocatalyst  
PhMe: toluene  
PHOX: Phosphinooxazoline  
PPh<sub>3</sub>: triphenylphosphine  
r.t.: room temperature

RHal: alkyl halide

RRPC: radical-polar crossover reaction

SAR: structure–activity relationship

SET: single-electron transfer

T: temperature

TEA: trimethylamine

TEMPO: (2,2,6,6-Tetramethylpiperidin-1-yl)oxyl

THF: tetrahydrofuran

TLC: Thin-layer chromatography

TMM: trimethylenemethane

TMS: trimethylsilane

Triton B: benzyltrimethylammonium hydroxide

UV: ultraviolet

W: watts

WHO: World Health Organization

Universitat d'Alacant  
Universidad de Alicante



Universitat d'Alacant  
Universidad de Alicante



**SUMMARY IN SPANISH/RESUMEN EN  
CASTELLANO**

Universitat d'Alicant  
Universidad de Alicante





## Resumen en castellano

---

### Prefacio

---

En la presente tesis se describen estrategias útiles y sencillas para las síntesis de 2-oxindoles 3,3'-disustituídos y alcoholes homoalílicos. Estos proyectos se han llevado a cabo bajo la supervisión de Prof. Carmen Nájera Domingo y Prof. José Miguel Sansano Gil en el Departamento de Química Orgánica y el Instituto de Síntesis Orgánica de la Universidad de Alicante. La parte relacionada con la preparación de alcoholes homoalílicos se desarrolló en la Universidad de Bolonia (Italia) bajo la supervisión de Prof. Pier Giorgio Cozzi.

Esta memoria se divide en dos grandes bloques: el primero referido a la alquilación desactivada como método para la síntesis de 2-oxindoles 3,3'-disustituídos que engloba la introducción I, capítulo I y capítulo II. La segunda parte se refiere a fotocatálisis y metalofotocatálisis como nuevos métodos de síntesis orgánica y engloba la introducción II, capítulo III y capítulo IV de esta tesis.

Durante este apartado, se describirá un breve resumen de cada uno de los apartados nombrados. Además, la mayoría de los resultados descritos en esta tesis han sido publicados en las siguientes revistas internacionales:

"*Synthesis of 3,3-Disubstituted 2-Oxindoles by Deacylative Alkylation of 3-Acetyl-2-oxindoles*" A. Ortega-Martínez, C. Molina, C. Moreno-Cabrerizo, J. M. Sansano, C. Nájera, *Synthesis* **2017**, *49*, 5203–5210.

"*Deacylative alkylation (DaA) of N-methyl-3-acetyl-2-oxindole for the synthesis of symmetrically 3,3-disubstituted 2-oxindoles. An access gate to anticancer agents and natural products*" C. Moreno-Cabrerizo, A. Ortega-Martínez, C. Molina, C. Nájera, J. M. Sansano, *An. Acad. Bras. Cienc.* **2018**, *90*, 1089–1099.

"*Deacylative Reactions: Synthetic Applications*" A. Ortega-Martínez, C. Molina, C. Moreno-Cabrerizo, J. M. Sansano, C. Nájera, *European J. Org. Chem.* **2018**, 2018, 2394–2405.

"*Deacylative alkylation versus photoredox catalysis in the synthesis of 3,3'-bioxindoles*" C. Moreno-Cabrerizo, A. Ortega-Martínez, M. A. Esteruelas,

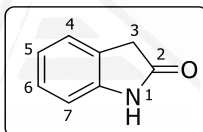
A. M. López, C. Nájera, J. M. Sansano, *European J. Org. Chem.* **2020**, 3101–3109.

“Catalytic Photoredox Allylation of Aldehydes Promoted by a Cobalt Complex” A. Gualandi, G. Rodeghiero, C. Moreno-Cabrerizo, C. Foucher, M. Marchini, P. Ceroni, and P. G. Cozzi, Manuscrito en progreso.

## Introducción I

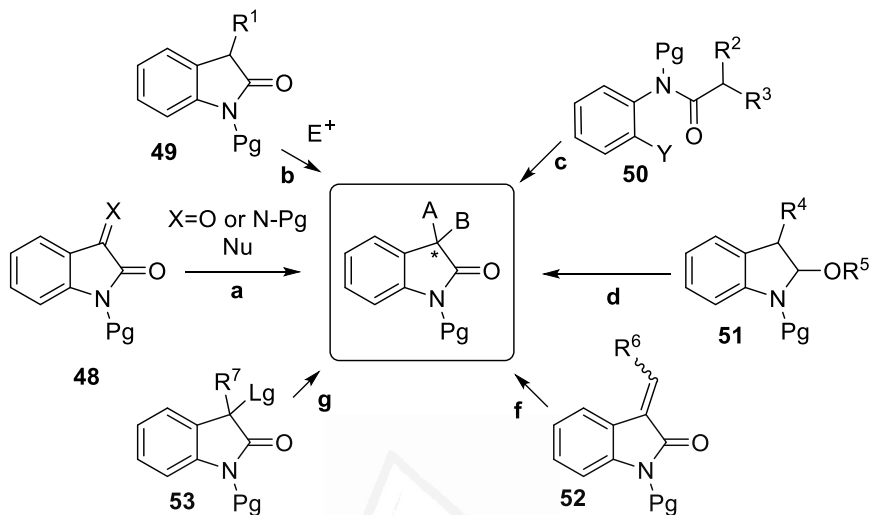
El oxindol es una molécula orgánica que puede obtenerse de manera sintética o natural y presenta una amplia gama de actividades biológicas. Por ejemplo, se utiliza para el tratamiento de infecciones, cáncer, úlceras gástricas, artritis y otros procesos inflamatorios.

También, el oxindol y sus derivados también son sustratos versátiles en múltiples reacciones orgánicas. En esta tesis, la atención se centra en las aplicaciones del oxindol en diversas reacciones afectando a su posición C-3.



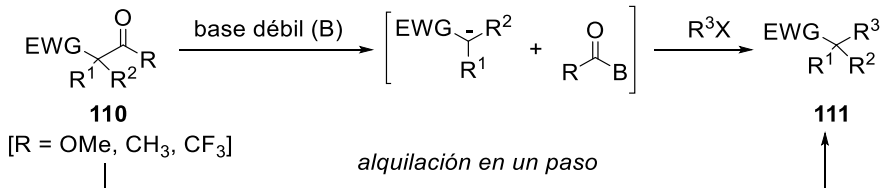
Desde el punto de vista de la química sintética, durante los últimos años, se han desarrollado múltiples rutas para obtener 2-oxindoles 3,3'-disustituídos. Estas rutas se pueden clasificar en seis categorías y se ven desarrolladas en el siguiente esquema (Esquema 1):

- Adición nucleofílica a isatinas.
- Funcionalización directa de oxindoles 3-sustituídos.
- Reacciones de acoplamiento intramolecular.
- Reacciones basadas en oxindoles O-sustituídos.
- Metilenindolinonas como sustratos.
- Oxindoles como electrófilos.



**Esquema 1.** Estrategias sintéticas para la preparación de 2-oxindoles 3,3'-disustituídos

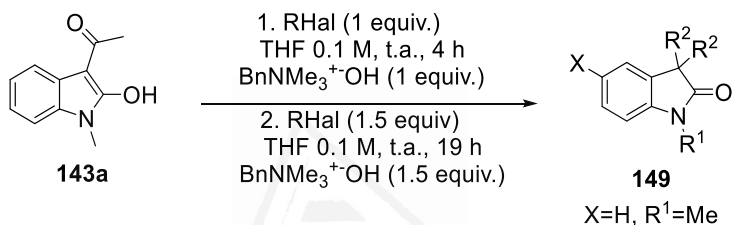
En la presente memoria se propone la alquilación desacilativa como método para la síntesis de 2-oxindoles 3,3'-disustituídos. La alquilación desacilativa (ADa) tiene lugar en condiciones promovidas por bases de tal manera que el enolato resultante reacciona con un electrófilo (E<sup>+</sup>) ya presente en el medio de reacción en un procedimiento de un paso (Esquema 2). Asimismo, el grupo acilo se puede utilizar como grupo director "sin trazas" en la condensación *retro*-Claisen para la generación de enolatos y otros nucleófilos de carbono, que también pueden ser atrapados por diferentes electrófilos.



**Esquema 2.** Alquilación Desacilativa (ADa)

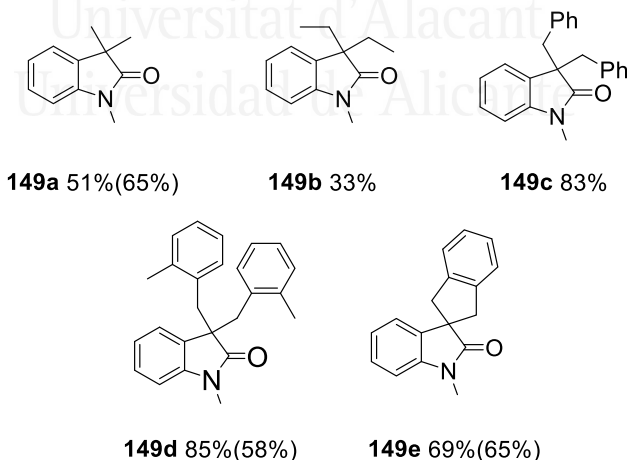
## Capítulo I: Alquilación Desacilativa (ADa) de *N*-metil-3-acetil-2-oxindoles para la síntesis simétrica de 2-oxindoles 3,3'-disustituídos

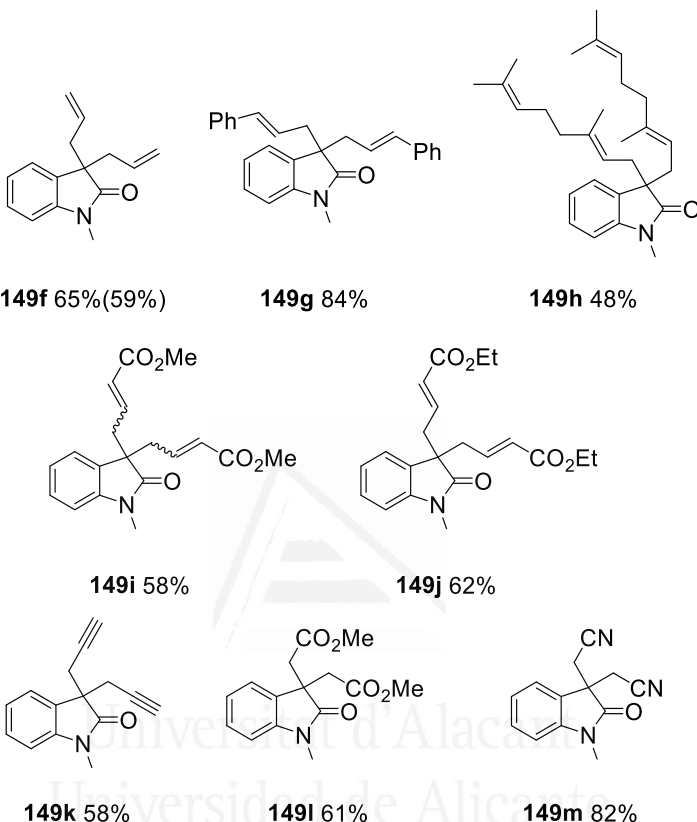
En este capítulo, se estudia la síntesis de *N*-metiloxindoles 3,3'-disustituídos partiendo de 3-acetil-2-hidroxi-1-metiloxindoles empleando una reacción secuencial. El proceso se desarrolla con una primera alquilación en presencia de un equivalente de haloalcano y otro más de Tritón B como base, en la segunda etapa de la reacción 1.5 equivalentes más de los reactivos anteriormente nombrados obteniendo de moderados a altos rendimientos.



### Esquema 3. Síntesis de simétrica de 2-oxindoles 3,3'-disustituídos por ADA

Una vez optimizadas las condiciones de reacción, se estudió el alcance de ésta dando los siguientes resultados (Esquema 4):





Esquema 4. Alcance de la reacción

Como se observa en los compuestos **149a** y **149b**, el rendimiento de las reacciones es 51 y 33% respectivamente. Esto se debe a la baja reactividad de los halobencenos y con la fácil oxidación de la posición bencílica del oxindol en condiciones básicas y en presencia de aire.

Por otra parte, con el uso de haluros más activados como el bromuro de bencilo se obtienen rendimientos más altos (compuestos **149c-e**). De hecho, en el caso de 1,2-bis(bromometil)benceno se introduce una manera de formar un oxindol espiránico, el cual está presente en agentes antitumorales o en inhibidores de a aldosa reductasa.

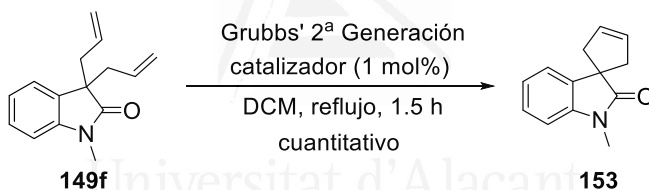
Respecto a los bromuros alílicos como bromuro de alilo o bromuro de cinamilo se alcanzaron buenas conversiones y rendimientos (ver **149f** y

**149g**). Sin embargo, cuando se empleó bromuro de geranilo como electrófilo se obtuvo una mezcla inseparable del producto deseado y del correspondiente oxindol desacilado 3-monosustituído.

En lo que se refiere al bromocrotonato de metilo y etilo se obtienen resultados similares, aunque para el compuesto **149i**, el crudo presenta un espectro  $^1\text{H}$  RMN mucho más complejo debido a la presencia de los *Z*- y *E*-estereoisómeros.

Finalmente, para completar este heterogéneo alcance de la reacción otros haluros *n*-conjugados se probaron dando de buenos a muy buenos rendimientos (ver compuestos **149k-m**).

A lo largo del capítulo, además, se hace una comparativa entre este método y la alquilación directa partiendo de *N*-metiloxindol (rendimientos entre paréntesis del Esquema 4) y finalmente se procede a la metátesis del compuesto **149f** ya que el producto obtenido es un espirooxindol con gran interés sintético.



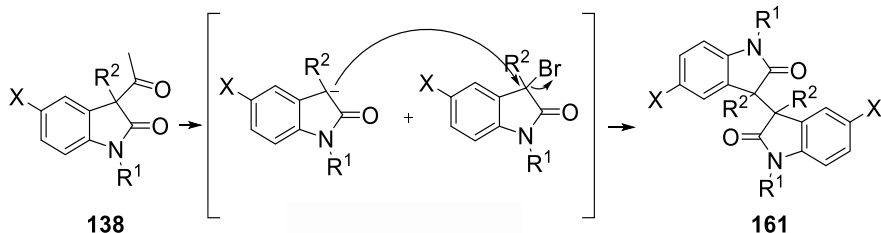
**Esquema 5.** Metátesis empleando el catalizador de Grubbs de 2<sup>a</sup> generación

Este capítulo se resume con las siguientes conclusiones:

- La reacción secuencial para la monoalquilación de 3-acetil *N*-metiloxindoles, seguida de ADA para la segunda alquilación es una buena alternativa para obtener derivados de oxindol simétricamente 3,3'-disustituídos.
- Este proceso compite con la alquilación directa del *N*-metiloxindol porque en muchos casos, se obtienen rendimientos más altos y el crudo de las reacciones presenta menos subproductos, dos fuertes motivos para usar este método.
- Algunos de los compuestos sintetizados en este capítulo (específicamente los compuestos **149e** y **153**) son candidatos adecuados para acceder a interesantes agentes tumorales y compuestos naturales.

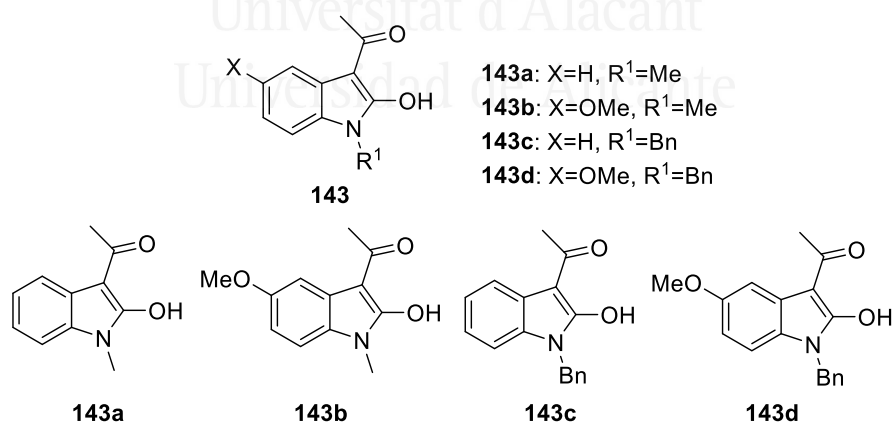
## Capítulo II: Bromación desactivada para la síntesis de 3,3'-bioxindoles y aislamiento de 3-bromooxindoles

Continuando con la metodología descrita en el capítulo anterior. Este capítulo estudia la ADA para la formación *in situ* de 3,3'-bioxindoles formando un intermedio electrofílico: un derivado de 3-bromooxindol.



**Esquema 6.** Mecanismo para la preparación de 3,3'-bioxindoles

Para ello, se partió de distintos 3-acetil oxindoles como sustratos principales para esta metodología. Se tuvo en cuenta que estuvieran protegidos en la posición del nitrógeno para que no hubiera competitividad en posteriores reacciones y también se tuvo en cuenta que la posición 5 del oxindol estuviera sustituida por un grupo metoxi- ya que es de gran interés sintético para la obtención de precursores de productos naturales.

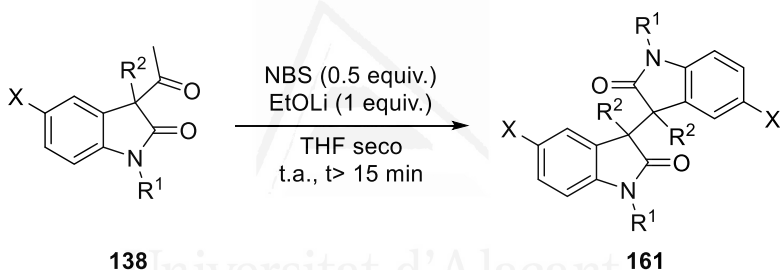


**Esquema 7.** Sustratos de partida

Para obtener dichos sustratos se usan estrategias descritas en la literatura y se escalan fácilmente hasta 5 g en alguno de los casos. La síntesis

total de estos compuestos se basa principalmente en tres pasos: Partiendo de la isatina correspondiente, el primer paso es la protección del grupo amino con una base fuerte y yodometano o bromuro de bencilo en nuestros casos. El segundo paso sería una reducción de Wolf-Kishner y por último la acilación en posición tres en presencia de DMAP y anhídrido acético. Una vez obtenidos estos sustratos se pasará a la consiguiente metilación o alilación de la posición 3 para conseguir los correspondientes compuestos **138** deseados (ya descritos por nuestro grupo de investigación) que serán los materiales de partida adecuados para la dimerización de éstos.

Observando el mecanismo del Esquema 6 se encuentran las condiciones óptimas para conseguir la dimerización de nuestros sustratos. Para ello, se empleará un equivalente de etóxido de litio como base y 0.5 equivalentes de *N*-bromosuccinimida:



**Esquema 8.** Síntesis de 3,3'-bioxindoles

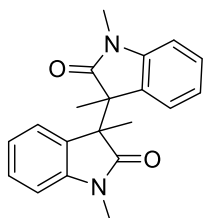
Cabe destacar que la reacción se puede llevar a cabo tanto con NBS como con NIS. Además, es necesario usar un disolvente seco ya que la presencia de agua en el medio podría parar la reacción. Por otra parte, la presencia de aire en la disolución no afecta a los resultados obtenidos, por lo tanto, no es necesario desoxigenar.

Una buena ventaja de esta metodología es que esta reacción ocurre en muy poco tiempo obteniendo una muy buena conversión. También la diastereoselectividad es mejor en este tipo de reacciones obteniendo como mayoritario el (*R*<sup>\*</sup>,*R*<sup>\*</sup>)-diastereoisómero. Como inconveniente, solo se pudo purificar el diastereoisómero mayoritario con rendimientos moderados y en un caso excelente.

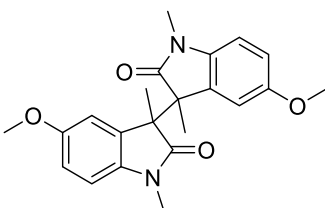
Con estas condiciones y usando los correspondientes 3-acetil oxindoles, se estudia el alcance de la reacción. Como se ha descrito anteriormente, esta



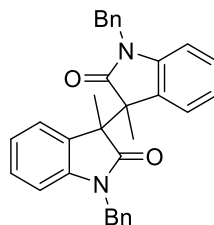
reacción es muy rápida y con relación diastereomérica de 3:1 para ( $R^*,R^*$ ):*meso*.



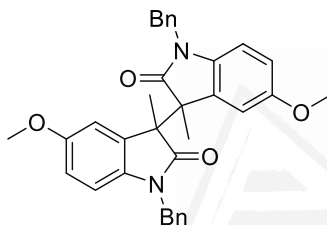
161a 3:1 80%



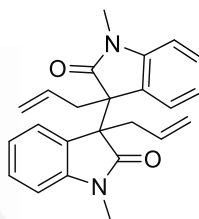
161b 3:1 54%



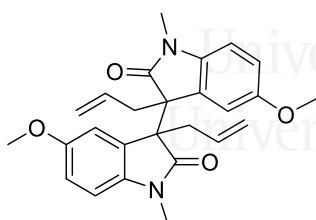
161c 3:1 48%



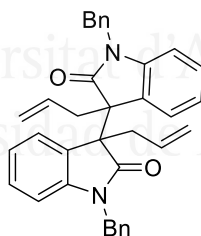
161d 3:1 46%



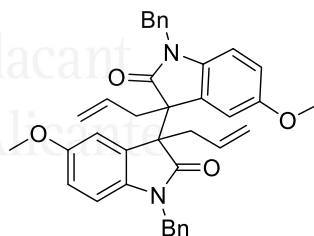
161e 3:1 40%



161f 3:1 40%



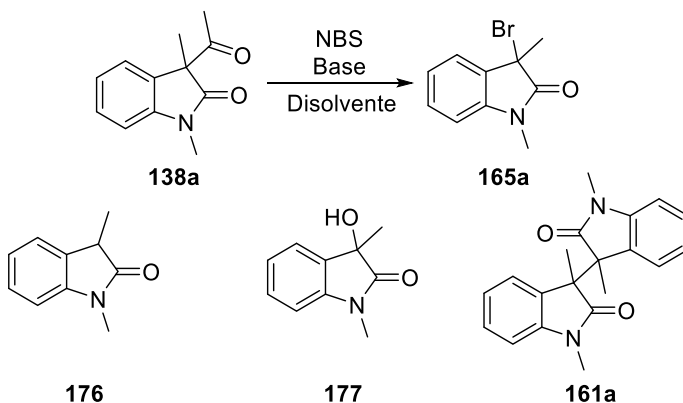
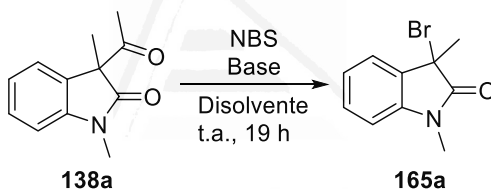
161g 3:1 26%



161h 3:1 40%

### Esquema 9. Alcance de la reacción

Una vez obtenidos los productos de dimerización, el siguiente objetivo del capítulo es la obtención de los intermedios electrofílicos de esta reacción, los derivados de 3-bromooxindoles. De manera que, partiendo de los mismos sustratos, pero variando los equivalentes de base y la fuente de bromo (NBS), se consigue optimizar las condiciones para aislar estos intermedios.

**Esquema 10.** Subproductos obtenidos durante la optimización de la reacción**Tabla 1.** Optimización para la preparación de 3-bromooxindoles

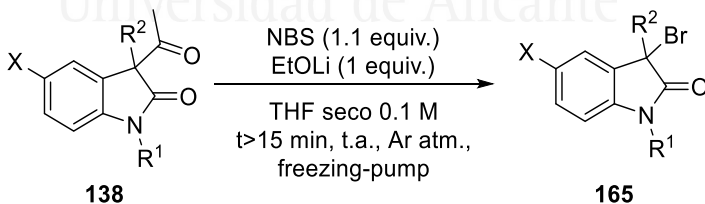
Entr	NBS (equiv.)	EtOLi (equiv.)	Disolvente (0.1 M)	Productos <sup>b</sup> (165a/176/177/161a)
<b>1<sup>a</sup></b>	1	1	THF	Trazas
<b>2</b>	1	1	THF	3/19/14/54
<b>3</b>	1.5	1	THF seco	15/9/12/50
<b>4<sup>c</sup></b>	1.5	1.2	THF seco	58/-/7/11
<b>5<sup>c,d</sup></b>	1	1.1	THF seco	58/-/-/42
<b>6<sup>c,d</sup></b>	2	1	THF seco	88/-/-/12
<b>7<sup>c,d,e</sup></b>	2	1	THF seco	75/-/-/25
<b>8<sup>c,d</sup></b>	0.5	1	THF seco	8/-/-/92
<b>9<sup>c,d,f</sup></b>	2	1	THF seco	99/-/-/-

<sup>a</sup> Triton B como base. <sup>b</sup> Conversión del crudo seguido por <sup>1</sup>H RMN. <sup>c</sup> Bajo atmósfera de argón. <sup>d</sup> Tres ciclos de freezing-pump. <sup>e</sup> Escalado a 0.6 mmol. <sup>f</sup> Adición lenta después de 15 minutos.

Una vez optimizadas las condiciones de reacción se concluyó que era necesario añadir más de 1 equivalente de NBS ya que en algunos experimentos se obtenía material de partida sin reaccionar **138a**. El compuesto **176** se formaba en presencia de agua, de manera que cambiamos a THF anhidro. (Tabla 1, entradas 3-4). El compuesto **177** se generaba por la oxidación del sustrato de partida en presencia de aire así que para eliminar este subproducto se hicieron tres ciclos de freezing-pump (Tabla 1, entradas 5-9). Finalmente, se observó que con las condiciones de la entrada 8 de la Tabla 1, se formaba el derivado de bioxindol.

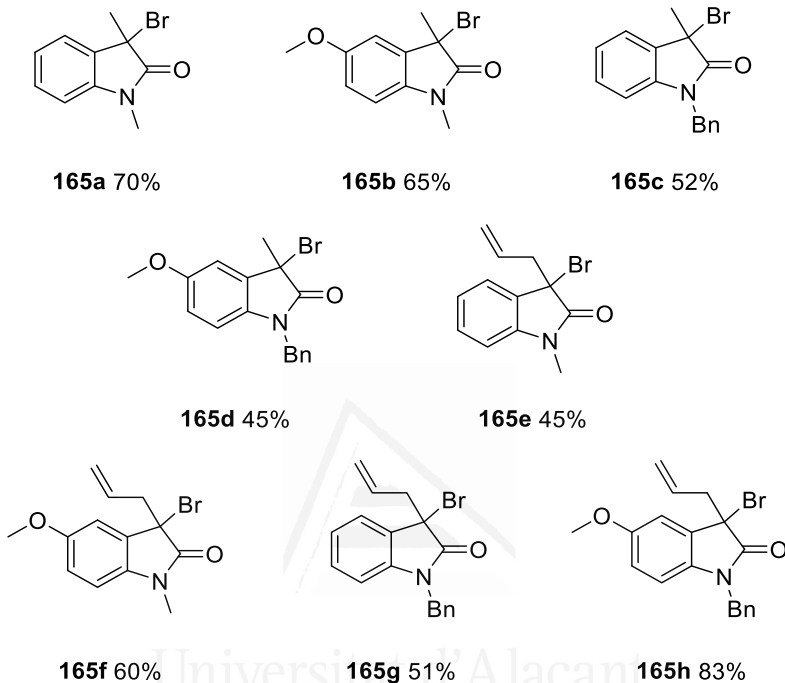
En las entradas 6 y 7 de la Tabla 1 se demostró que la reproducibilidad de la reacción era variable. Es por ello por lo que se probaron distintas formas de adición de los reactivos. En la entrada 9 se verifica que es las condiciones correctas son la adición lenta de una disolución de **138** con etóxido de litio, sobre una segunda disolución de NBS en THF.

Esta metodología es válida para obtener 3-bromooxindoles con conversión completa y buenos rendimientos. Es una reacción rápida y que se puede seguir fácilmente por TLC. Además, la reacción se ha podido escalar hasta 2.4 mmol (0.5 g).



**Esquema 11.** Preparación de derivados de 3-bromooxindol

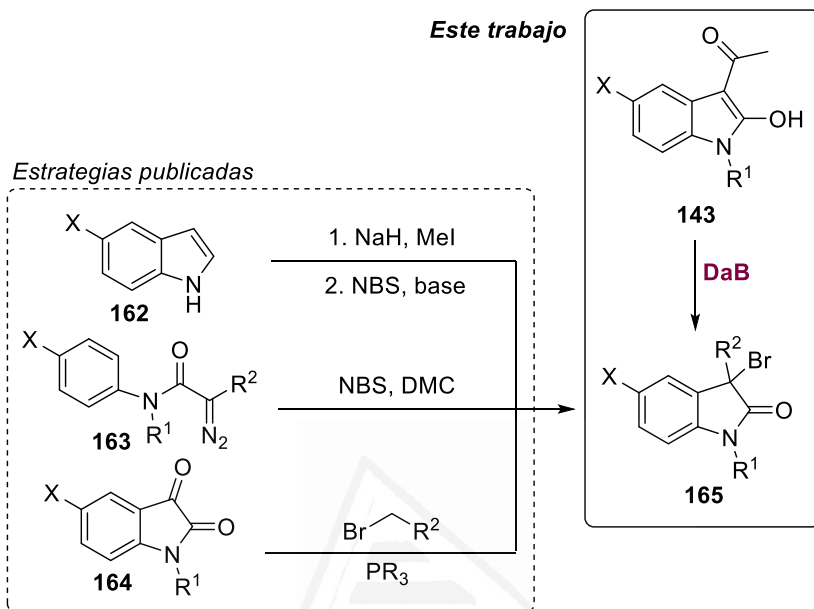
Seguidamente, se procede a estudiar el alcance de la reacción:



**Esquema 12.** Alcance de la reacción

Finalmente, este capítulo se resume con las siguientes conclusiones:

- La Bromación Desacilativa (BDa) es una buena metodología para preparar análogos de 3,3'-bioxindoles. Para ello, solamente es necesario unos pocos minutos para producir la dimerización con excelentes conversiones y buena diastereoselectividad, formando mayoritariamente el ( $R^*,R^*$ )-diastereoisómero. Los rendimientos de la reacción son moderados, excepto en un caso que es excelente.
- La Bromación Desacilativa (BDa) es una novedosa estrategia para obtener 3-alkil-3-bromooxindoles. Este protocolo se puede escalar hasta 0.5 g en un corto plazo de tiempo. Comparando con los trabajos previos para la preparación de 3-bromooxindoles, este nuevo procedimiento no requiere condiciones fuertes de base, ni el empleo de diazocompuestos o peligrosos tris(dimetilamino)fosfinas.



## Introducción II: Fotocatálisis y catálisis dual

La fotocatalisis es el área responsable del desarrollo de nuevos procesos sintéticos usando la luz como fuente de energía. A pesar de que muchas moléculas no son capaces de absorber en la región del espectro visible, el uso de fotocatalizadores permite la transmisión de dicha energía bien a través de transferencia de electrón o transferencia de energía a otras moléculas. De este modo, se abre una puerta al desarrollo de nuevas transformaciones químicas en la región del espectro solar.

En 1912, Giacomo Ciamician ya especuló que el empleo de procesos de alta energía mediante el uso de reacciones fotoquímicas limpias y eficientes tendría un impacto drástico, ecológico y beneficioso en nuestra sociedad. Hoy en día, existen varios métodos de activación ofrecidos por la fotocatalisis que dan acceso a una amplia variedad de transformaciones químicas. De hecho, como se demuestra en la Ilustración 1, ha habido un aumento exponencial en el número de publicaciones que emplean catálisis foto-redox

desde finales de los 2000, dando lugar a un campo de investigación diverso y muy activo que continúa en la actualidad.

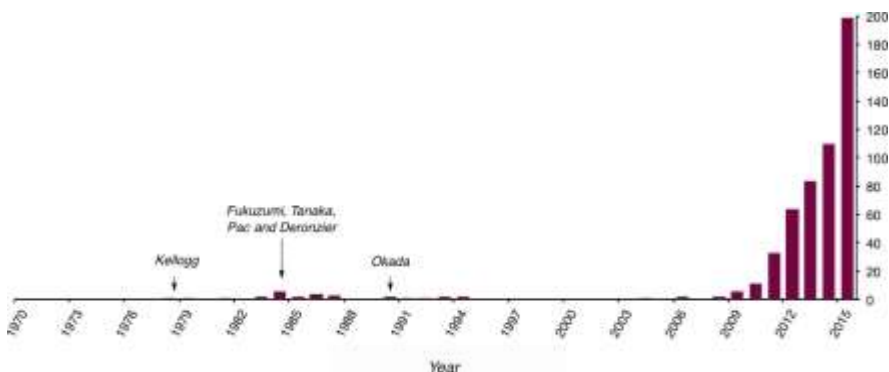


**Ilustración 1.** Artículos publicados por año en el campo de la catálisis fotorredox en síntesis orgánica

Durante el capítulo III observaremos la reactividad del oxindol en el campo de la fotoquímica. De hecho, usaremos los 3-bromoxindoles como sustratos adecuados para este tipo de reacciones.

Por otra parte, y siguiendo esta introducción es necesario conocer el concepto de metalafotocatálisis. Consiste en la combinación de la catálisis debida a metales de transición con la fotocatalisis que recientemente está emergiendo como una plataforma versátil para el desarrollo de nuevas y capaces metodologías sintéticas.

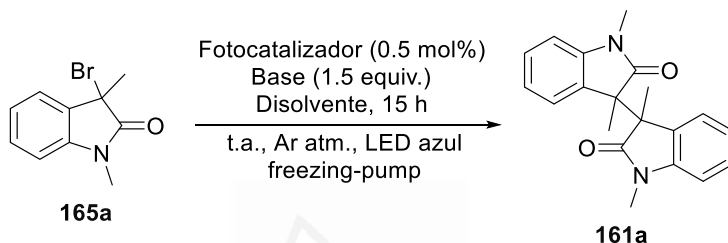
Una de las ventajas de la catálisis foto-redox es que proporciona acceso a especies de radicales reactivas en condiciones suaves de abundantes grupos funcionales y, cuando se combina con catálisis de metales de transición, ésta permite el acoplamiento directo de nucleófilos no tradicionales.

Es decir, la metalafotocatálisis proporciona acceso a distintos modos de activación, que son complementarios a los utilizados tradicionalmente en el campo de la catálisis de metales de transición, lo que permite el desarrollo de reacciones a través de nuevos paradigmas mecanicistas.

Este concepto será útil ya que en el capítulo IV de esta tesis se desarrolla una nueva metodología basada en catálisis dual para la preparación de alcoholes homoalílicos.

## Capítulo III: Catálisis foto-redox en la síntesis de 3,3'-bioxindoles

Según la bibliografía, está descrita la unión de 3-clorooxindoles 3-sustituídos por fotocatalísis empleando *fac*-Ir(ppy)<sub>3</sub>. Partiendo de esta transformación, cambiaremos las condiciones de reacción para que sean las adecuadas empleando los bromuros **165** como sustratos de partida.



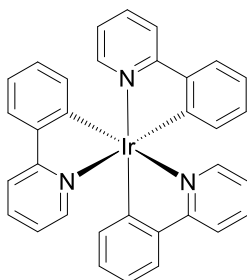
**Esquema 13.** Protocolo general para la síntesis de 3,3'-bioxindoles

En primer lugar, empezaremos buscando el fotocatalizador adecuado, para ello haremos un estudio con distintos fotocatalizadores que se muestran en la Ilustración 2 y compararemos los resultados expuestos en la Tabla 2.

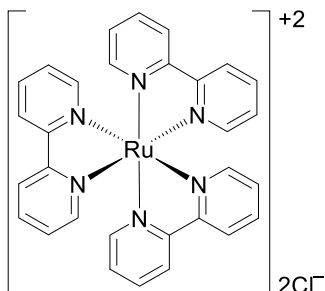
Respecto al fotocatalizador, después de probar con los compuestos descritos en la Ilustración 2, se obtuvo la mejor conversión con el complejo catalítico **232** como se observa en la entrada 6 de la Tabla 2. Es destacable mencionar que este complejo emite en verde con un rendimiento cuántico de 0.87.

En este contexto, cabe mencionar que además de la menor energía de su emisión, el complejo **232** presenta dos diferencias notables con respecto a **234** y **235**. Presenta mayor vida útil en 2-metiltetrahydrofurano, a temperatura ambiente (2,4 y 1,6  $\mu$ s, respectivamente, frente a 7,7  $\mu$ s) además, la presencia de un átomo de oxígeno entre el anillo de piridilo y uno del grupo fenilo hace de ligando de pinza entre C-N-C para estabilizar la geometría octaédrica del catalizador.

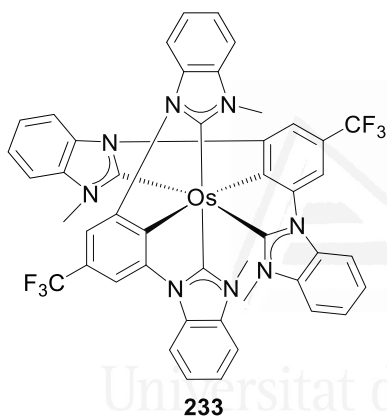
Una vez encontrado el fotocatalizador adecuado, se probaron distintas condiciones de reacción. La fuente de LED azul de 24 W ofreció mejores conversiones que la luz visible, la bombilla fluorescente de 20 W o la bombilla blanca de 20 W (no incluida en la Tabla 2).



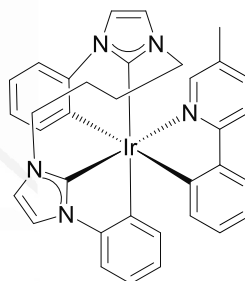
*fac*-Ir(ppy)<sub>3</sub> **185a**



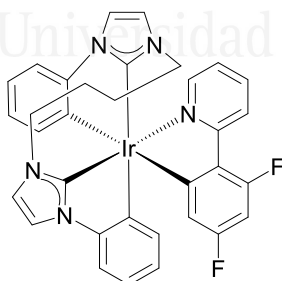
Ru(bpy)<sub>3</sub>Cl<sub>2</sub> **183a**



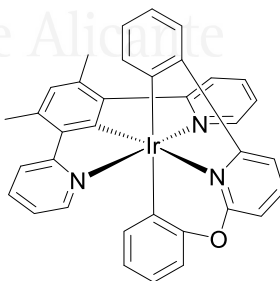
**233**



**234**



**235**



**232**

**Ilustración 2.** Catalizadores foto-redox usados en la optimización de la síntesis de 3,3'-bioxindoles



Tabla 2. Optimización para la preparación del compuesto **161a**

Ent.	Cat.	Base	Disolvente 0.1 M	161a <sup>a</sup>	165a	177	Rto. (%) <sup>b</sup>
1	185a	DBU	MeCN	66	4	30	45
2	183a	DBU	MeCN	trazas	85	15	---
3	233	DBU	MeCN	trazas	90	10	---
4	234	DBU	MeCN	22	65	13	---
5	235	DBU	MeCN	40	36	24	---
6	232	DBU	MeCN	72	16	12	56
7	232 <sup>c</sup>	DBU	MeCN	78	12	10	58
8	232 <sup>c</sup>	DIPEA	MeCN	25	50	25	---
9	232 <sup>c</sup>	DIPEA	THF	85	---	15	68
10	232 <sup>c</sup>	DBU	THF	88	---	12	69
11	232 <sup>c</sup>	DIPEA <sup>d</sup>	THF	93	---	7	73
12	232 <sup>c,e</sup>	DIPEA <sup>d</sup>	THF	93	---	7	73
13	---	DIPEA <sup>d</sup>	THF	10	67	23	---
14	232 <sup>c,f</sup>	DIPEA <sup>d</sup>	THF	trazas	80	10	---
15	232 <sup>c</sup>	---	THF	trazas	19	52	---
16	232	DIPEA <sup>d</sup>	THF	79	---	21	---
17	232 <sup>c</sup>	DIPEA <sup>d,g</sup>	THF	trazas	80	20	---

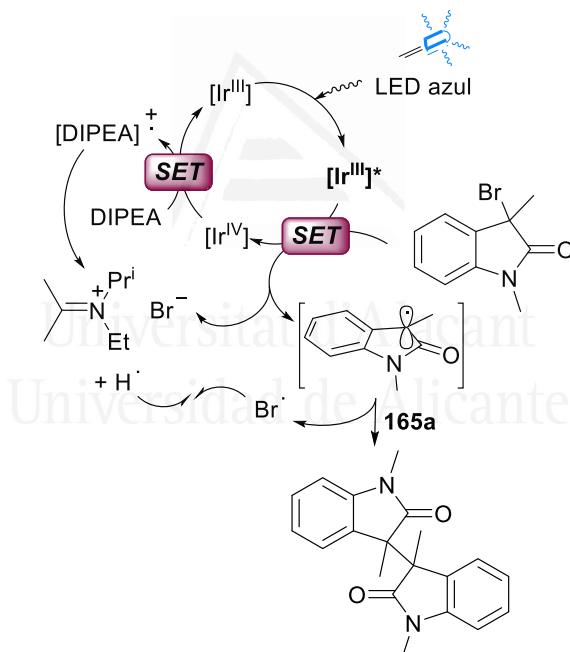
<sup>a</sup> La ratio 1:1 (*R\*,R\**):*meso* diastereomérica se determine con <sup>1</sup>H RMN analizando el crudo de las reacciones. <sup>b</sup> Rendimientos aislados después de cromatografía flash. <sup>c</sup> La reacción se desoxigenó tras ciclos de freezing-pump. <sup>d</sup> Recién destilada y trabajando en condiciones anhidras. <sup>e</sup> 1 mol% del catalizador fue añadido. <sup>f</sup> En ausencia de luz LED azul. <sup>g</sup> Se añadió TEMPO (20 mol%).

A pesar de que la diisopropiletilamina (DIPEA) no dio resultados satisfactorios en acetonitrilo, en THF dio resultados similares a los obtenidos en la reacción con DBU (comparar las entradas 8-10 de la Tabla 2). Aquí, la

operación del freezing-pump resultó ser crucial para disminuir el porcentaje del compuesto **177** oxidado.

Se seleccionó DIPEA como base porque la mezcla de reacción cruda estaba muy limpia (detectada por  $^1\text{H}$  RMN) a diferencia de la reacción cruda generada a partir de DBU. Se mejoraron la conversión y el rendimiento del producto **161a** empleando DIPEA recién destilada (en condiciones anhidras). Se muestran las reacciones en las mejores condiciones (Tabla 2, entrada 11).

Todos los productos **161a** identificados en las mezclas crudas o aislados en esta Tabla 2 resultaron ser mezclas 1: 1 de ( $R^*$ ,  $R^*$ ): *meso* diastereoisómeros de acuerdo con los datos de  $^1\text{H}$  RMN.



**Esquema 14.** Propuesta mecanística para la síntesis de **161a**

Con el objetivo de describir el mecanismo plausible, se realizaron algunos experimentos de control. En presencia de 1 mol% del catalizador, la reacción se produce con la misma conversión y rendimiento que usando 0,5 mol% (Tabla 2, entrada 12). Por otra parte, la ausencia del fotocatalizador presentó

3-bromooxindol **165a** sin reaccionar como un producto principal. (Tabla 2, entrada 13).

Sin DIPEA, luz o freezing-pump, la reacción no se llevó a cabo, por lo que se enfatizan la importancia de estos elementos en la reacción (Tabla 2, entradas 14-16). Finalmente, se añadió TEMPO para demostrar la presencia de radical intermedio. Con estos resultados, se propuso el plausible mecanismo descrito en el Esquema 14.

El complejo **232** en su estado excitado es capaz de hacer una transferencia de electrón (SET) al compuesto **165a** rápidamente de tal forma que la DIPEA actúa como reductor de la especie oxidada de iridio y mediante otra transferencia de electrón es capaz de recuperar el complejo **232** en su estado inicial para cerrar el ciclo catalítico.

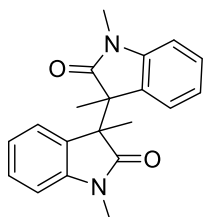
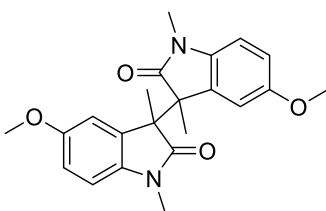
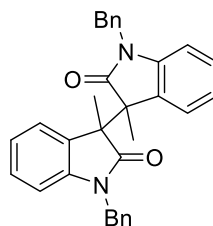
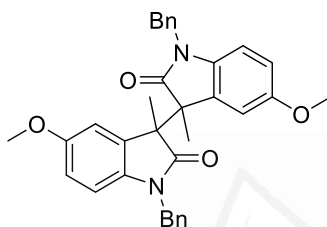
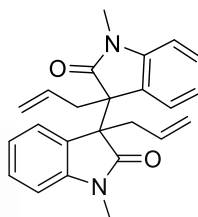
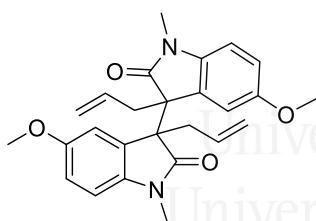
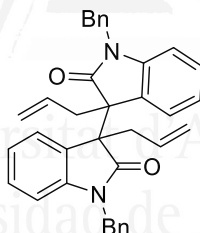
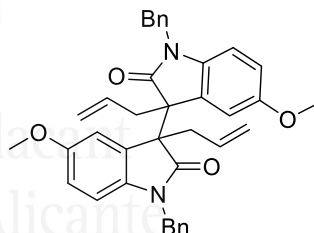
De este modo, se repite el ciclo para formar de nuevo el compuesto **165a** radical que colisiona con la primera molécula formando un enlace C-C del compuesto **161a**.

La eficiente dimerización ocurre bajo condiciones anhidras, en atmósfera de argón, con un 0.5 mol% del catalizador **232** y 1.5 equivalentes de DIPEA después de 15 horas de irradiación con LED azul de 24 W a temperatura ambiente. Previamente, todas las disoluciones que se emplean durante la reacción han sido sometidas al protocolo de freezing-pump.

Seguidamente, se llevó a cabo el estudio del alcance de la reacción. Para ello, se usó como sustratos de partida las 3-bromooxindoles sintetizados en el capítulo anterior.

Como se observa en el Esquema 15, la reacción presenta una diastereoselectividad 1:1 en la mayor parte de los casos, únicamente la ratio aumenta en los compuesto **165b**, **165c** y **165e**. No obstante, a pesar de la buena conversión de la reacción y la diastereoselectividad entre ( $R^*$ ,  $R^*$ ): *meso*, en algunos casos el producto *meso* no pudo ser aislado, como es el caso de los compuestos **161d**, **161f**, **161h** y **161g**.

Por otra parte, los buenos rendimientos que se observan en los compuestos **161a-c** y **161e** son debidos a la contribución de ambos diastereoisómeros aislados.

**161a** 1:1 72%**161b** 1.2:1 51%**161c** 1.2:1 47%**161d** 1:1 30%**161e** 1.2:1 70%**161f** 1:1 25%**161g** 1:1 13%**161h** 1:1 20%**Esquema 15.** Alcance de la reacción

Para finalizar este capítulo se hace un estudio comparativo de las dos técnicas que se describen en el capítulo II y III de esta tesis para la preparación de 3,3'-bioxindoles. Como se puede observar en la ratio ( $R^*$ ,  $R^*$ ): *meso* aumenta desde 1:1 hasta 3:1 empleando la Alquilación Desacilativa (ADa) como metodología, obteniendo el diastereoisómero ( $R^*$ ,  $R^*$ ) después de la purificación con rendimientos moderados.

Respecto a la catálisis foto-redox se observa que en algunos casos el rendimiento es menor, sin embargo, los compuestos **161a-c** y **161e** tienen

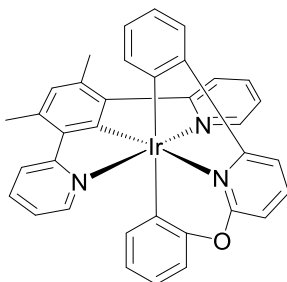
resultados similares e incluso mejores con la ventaja de que ambos diastereoisómeros han sido aislados satisfactoriamente.

**Tabla 3.** Estudio comparativo

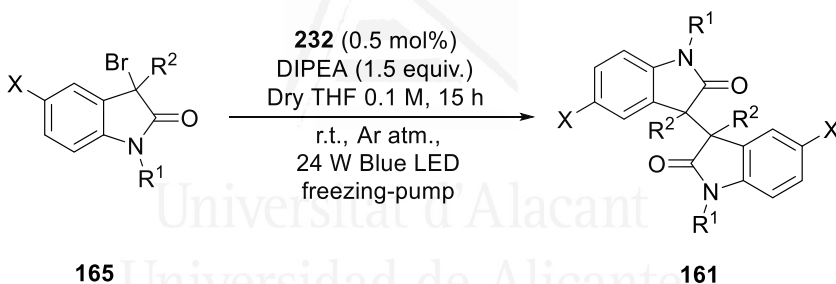
		Alquilación Desacilativa (DAa)		Catálisis Fotorredox	
Ent.	161	$(R^*,R^*): meso$ Rto. (%)		$(R^*,R^*): meso$ Rto. (%)	
<b>1</b>	<b>161a</b>	3:1	80	1:1	72
<b>2</b>	<b>161b</b>	3:1	54	1.2:1	51
<b>3</b>	<b>161c</b>	3:1	48	1.2:1	47
<b>4</b>	<b>161d</b>	3:1	46	1:1	30
<b>5</b>	<b>161e</b>	3:1	40	1.2:1	70
<b>6</b>	<b>161f</b>	3:1	40	1:1	25
<b>7</b>	<b>161g</b>	3:1	26	1:1	13
<b>8</b>	<b>161h</b>	3:1	40	1:1	20

Como resumen del capítulo, 8 bioxindoles han sido sintetizados durante este capítulo empleando la catálisis foto-redox con luz visible. Finalmente, este capítulo se resume con las siguientes conclusiones:

- Las buenas propiedades del complejo **232** (que emite en verde después de su fotoexcitación en estado sólido a temperatura ambiente con un buen rendimiento cuántico de 0.87) hacen adecuado a este fotocatalizador para la síntesis de 3,3'-bioxindoles.

**232**

- Mediante el enfoque foto-redox se logra un procedimiento robusto empleando 0.5 mol% de fotocatalizador, DIPEA como amina orgánica reductora y THF como disolvente con LED azul. La ratio de diastereoselectividad es 1:1 obteniendo de moderados a buenos resultados de rendimiento.



- Dependiendo del incremento de rendimiento o diastereoselectividad de la reacción, ambas metodologías descritas en los capítulos II y II pueden resultar adecuadas para la síntesis de 3,3'-bioxindoles.

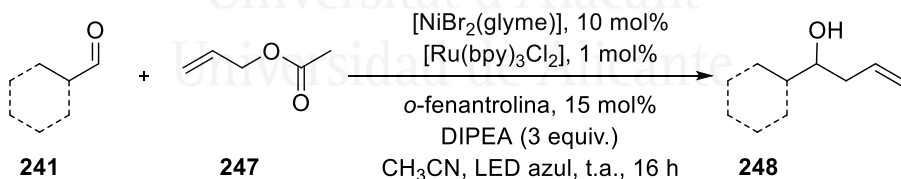
## Capítulo IV: Catálisis fotorredox para la alilación de aldehídos promovida por un complejo de cobalto

La alilación de carbonilos es crucial para la preparación de alcoholes homoalílicos. Las primeras investigaciones sobre la preparación de estos compuestos fueron desarrolladas por Barbier-Grignard, sin embargo, esta metodología es peligrosa ya que requiere condiciones criogénicas y más importante genera cantidades estequiométricas de productos metálicos, lo que dificulta sus aplicaciones a gran escala.

La experimentación con especies de alil-cromo (descritas por Nozaky-Hiyama-Kishi, reacciones NHK) abrieron la posibilidad de emplear ciclos catalíticos en condiciones Barbier. El principal inconveniente de esta metodología es el uso de cromo como reactivo con una toxicidad excesivamente alta.

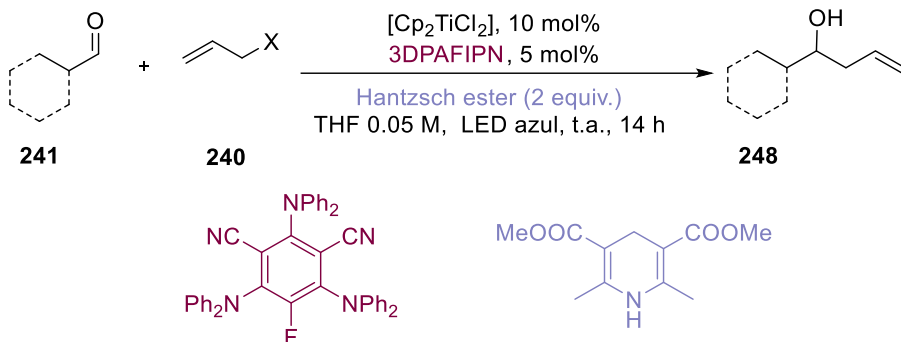
Teniendo en cuenta estos trabajos previos, el grupo de investigación de Cozzi desarrolló una línea referida a la alilación de aldehídos basada en un enfoque de catálisis dual: metalafotocatálisis.

En primer lugar, el grupo publicó un trabajo sobre alilación de aldehídos basada en la combinación entre níquel y foto-redox catálisis. En este trabajo obtuvieron un amplio alcance de productos con gran compatibilidad de grupos funcionales.



**Esquema 16.** Alilación de aldehídos basada en catálisis dual con níquel por el grupo de Cozzi

En este trabajo, se evita el uso de metales como Mg, Zn o Mn sustituyéndolo por una amina terciaria como especie reductora. Más adelante, el grupo de investigación también desarrolló un trabajo basado en un complejo de titanio combinado con un fotocatalizador orgánico. En este caso la abundancia y poca toxicidad del titanio hacen atractivo este trabajo, además su trabajo se basa en el mecanismo de reacción descrito como reacción de cruce radical-polar. Este mecanismo, también será el fundamento teórico en el que basaremos este capítulo.



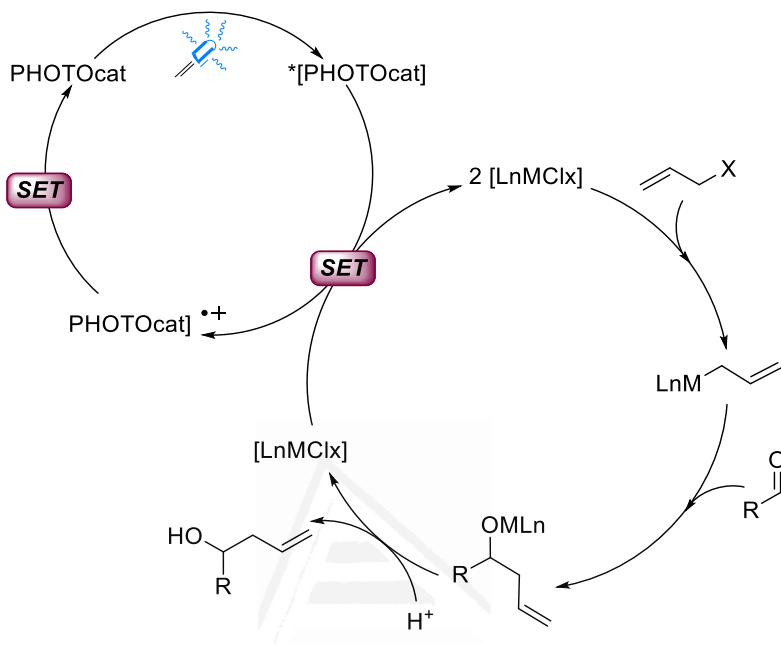
**Esquema 17.** Alilación de aldehídos basada en catálisis dual con titanio por el grupo de Cozzi

Durante este capítulo y continuando con la línea de investigación que empezó el Prof. Cozzi en la Universidad de Bolonia (Italia) se describe una nueva metodología basada en la catálisis dual para la alilación de aldehídos basada en un complejo de cobalto.

El cobalto es el primer elemento del grupo 9 de los metales de transición, comparado con el rodio y el iridio es el elemento del grupo más abundante. Las sales de Co(II) se suelen usar como precatalizadores en muchas reacciones en presencia de zinc o manganeso para reducirse a Co(I) catalíticamente activo. En nuestro caso, el fotocatalizador será el encargado de activar la especie de Co para empezar el ciclo catalítico y así que se produzca la correspondiente adición oxidativa al acetato de alilo que usaremos como sustrato.

Pero antes de empezar a desarrollar la metodología de este capítulo se explicará el mecanismo en el que basamos la reacción que emplearemos.

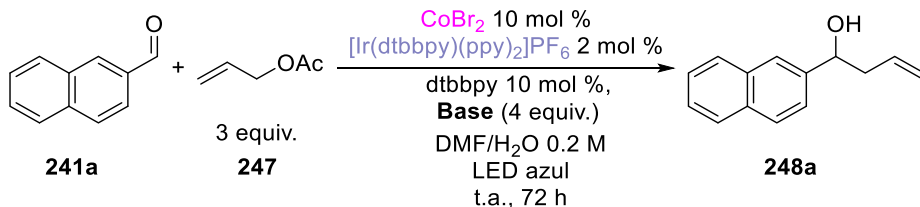




**Esquema 18.** Alilación catalítica basada en RRPC

En esta hipótesis, la combinación de la química polar y radical, en la llamada reacción de cruce radical-polar (RRPC) se ha llevado a cabo. En este mecanismo, un complejo metálico con un bajo estado de oxidación generado por una transferencia de electrón se convierte en una especie organometálica nucleofílica, que mediante una combinación radical-radical o por adición oxidativa reacciona con los sustratos orgánicos adecuados (en nuestro caso el aldehído). El uso de cantidades estequiométricas de metales como Zn o Mn se evita, ya que el catalizador foto-redox en combinación con la luz es el que mantiene el ciclo redox. Por supuesto, sigue siendo necesario el uso de un agente reductor de sacrificio para restaurar el fotocatalizador a su estado elemental, el uso de aminas orgánicas baratas y comercialmente disponibles es una de las principales ventajas de este tipo de reacciones.

Una vez visto el fundamento teórico en el que se basa la reacción que vamos a estudiar, continuamos con el estudio de las condiciones óptimas de reacción. Para ello, se tomó el 2-naftaldehído como sustrato modelo de la reacción. Los resultados obtenidos se muestran en la siguiente tabla:

**Tabla 4.** Modificaciones de los parámetros respecto a la reacción preliminar

Entry <sup>a</sup>	Deviations from standard conditions	Yield (%) <sup>b</sup>
<b>1</b>	None	97 (76)
<b>2</b>	CoBr <sub>2</sub> 5 mol%	28
<b>3<sup>c</sup></b>	Co(OAc) <sub>2</sub>	95 (60)
<b>4<sup>d</sup></b>	TEA	85 (53)
<b>5<sup>e</sup></b>	{Ir[dF(CF <sub>3</sub> )ppy] <sub>2</sub> (dtbbpy)}(PF <sub>6</sub> )	(25)
<b>6<sup>e</sup></b>	[Ru(bpy) <sub>3</sub> ]Cl <sub>2</sub>	0
<b>7</b>	No photocatalyst	0
<b>8</b>	No light	0
<b>9<sup>f</sup></b>	dppe	0
<b>10<sup>f</sup></b>	dppf	0
<b>11<sup>f</sup></b>	PPh <sub>3</sub>	(23)
<b>12<sup>f</sup></b>	Bpy	38
<b>13<sup>g</sup></b>	DMF	97 (60)
<b>14<sup>g</sup></b>	MeCN	55 (33)
<b>15<sup>g</sup></b>	DCE	(50)
<b>16<sup>g</sup></b>	DMSO	(25)

<sup>a</sup> Las reacciones se llevaron a cabo con 0.2 mmol de **241a** en DMF (0.2 mL). <sup>b</sup> Determinado por <sup>1</sup>H RMN análisis del crudo de la reacción. Los rendimientos entre paréntesis son los aislados tras la purificación. <sup>c</sup> En lugar de CoBr<sub>2</sub>. <sup>d</sup> En lugar de DIPEA. <sup>e</sup> Como fotocatalizador. <sup>f</sup> Como liqando. <sup>g</sup> Como disolvente.

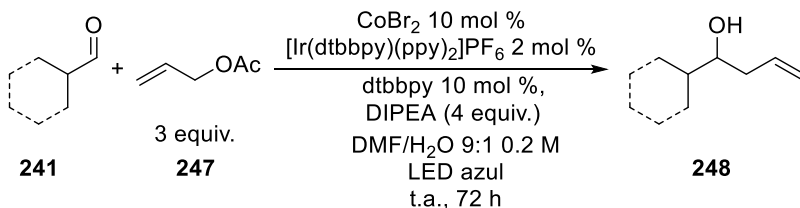
Se probó tanto  $\text{CoBr}_2$  como  $\text{Co}(\text{OAc})_2$  como fuentes apropiadas de  $\text{Co}(\text{II})$  obteniendo resultados similares, pero se eligió el  $\text{CoBr}_2$  ya que es más barato y nos es necesaria una previa deshidratación. Sin embargo, se trató de minimizar la cantidad al 5 mol% dando lugar a malos resultados (Tabla 5, entrada 1-3).

Varios fotocatalizadores fueron probados dando bajos rendimientos o malas conversiones. De hecho, se probó con el mismo catalizador de rutenio del trabajo previo (ver Esquema 16) sin embargo era incapaz de formar un complejo activo de cobalto. Finalmente, el fotocatalizador que se eligió fue  $[\text{Ir}(\text{dtbbpy})(\text{ppy})_2]\text{PF}_6$  (Tabla 5, entradas 5-6).

La reacción no ocurre ni en ausencia de luz ni de fotocatalizador cosa que reafirma el enfoque sinérgico de la metalafotocatálisis (Tabla 5, entradas 7 y 8). Además, se probaron con varias aminas orgánicas dando mejores resultados con DIPEA.

Se probaron distintos disolventes (Tabla 5, entrada 13-16) como medio de reacción y finalmente se observó que, para las condiciones óptimas de reacción, era necesario una mezcla de disolvente con agua DMF/ $\text{H}_2\text{O}$  en una ratio de 9:1 ya que en algunos casos la presencia de agua es crucial para mejorar el rendimiento de la reacción (esto se comentará en el alcance de la reacción). Por último, se observó que la di-*terc*-butilbipiridina era el ligando más apto para la reacción (Tabla 5, entradas 9-12).

Con las condiciones óptimas, se concretó que para llevar a cabo la reacción era necesario 10 mol% de  $\text{CoBr}_2$ , un 2 mol% del fotocatalizador, 10 mol% de dtbbpy como ligando y 4 equivalentes de DIPEA como amina orgánica. La fuente de alilo será acetato de alilo en exceso y será necesario 3 ciclos de freezing-pump para eliminar el posible  $\text{O}_2$  disuelto.



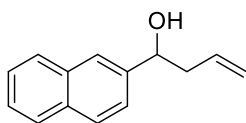
**Esquema 19.** Condiciones óptimas de reacción

Seguidamente, se procedió a hacer el estudio del alcance de la reacción probando con distintos aldehídos como sustrato.

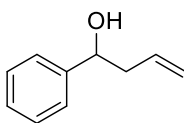
La reacción funciona correctamente con aldehídos aromáticos con grupos electrodonadores de carga. Se observa que en general se obtienen buenos rendimientos. Observando los compuestos sustituidos con el grupo metoxi- se obtienen resultados similares excepto cuando el grupo metoxi- se encuentra en posición *orto*-. Esto puede ser debido al impedimento estérico (compuestos **248e-h**).

Como se puede observar los rendimientos que se expresan entre paréntesis se refieren a las reacciones que se han llevado a cabo únicamente con DMF como disolvente.

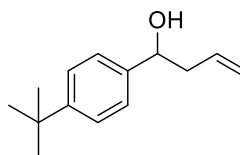
Dada la complejidad del sistema catalítico de la reacción, se deduce que la presencia de agua interviene en la posible hidrólisis del intermedio organometálico. De esta manera se obtiene el alcohol y favorece la recuperación de la especie de cobalto al ciclo catalítico.



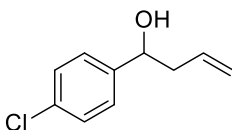
248a 75(60)%



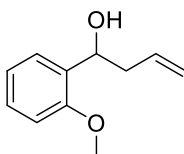
248b 61(40)%



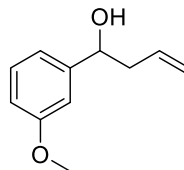
248c 70(33)%



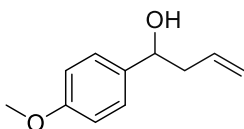
248d (66)%



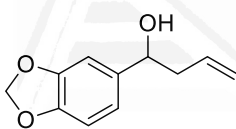
248e 58%



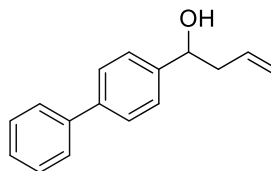
248f 73%



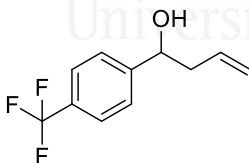
248g (67)%



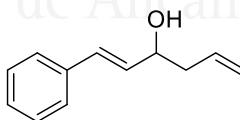
248h (74)%



248i (70)%



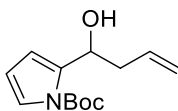
248j 30%



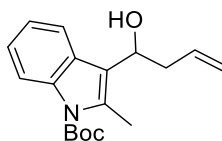
248k 57(21)%

**Esquema 20.** Alcance de la reacción con aldehídos aromáticos

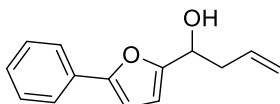
Respecto a los aldehídos heterocíclicos, la reacción ocurre obteniendo rendimientos moderados. Hay que tener en cuenta, que para la purificación de los compuestos **248i** y **248m** se hizo con cromatografía flash de alúmina de este modo se pudo separar correctamente el heterociclo nitrogenado de la biperina que se emplea como ligando de la reacción.



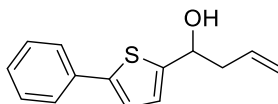
248l 50%



248m 57%



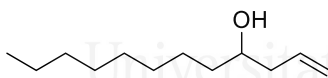
248n 50%



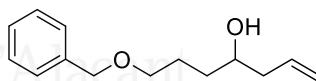
248o 42%

**Esquema 21.** Alcance de la reacción con aldehídos heterocíclicos

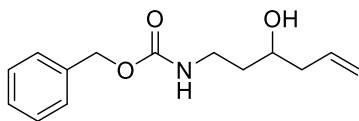
En el caso de los aldehídos alifáticos, los sustratos son generalmente menos reactivos en comparación con los aldehídos aromáticos. Aquí se muestran algunos ejemplos de productos que fueron aislados con un rendimiento bajo en general. En este caso, la presencia de agua era crucial para poder obtener el producto.



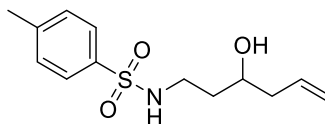
248p 30%



248q 34%



248r <25%



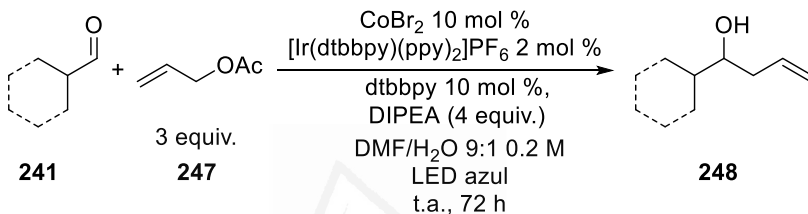
248s <25%

**Esquema 22.** Alcance de la reacción con aldehídos alifáticos

En resumen, 23 alcoholes homoalílicos fueron obtenidos empleando cobalto para promover la reacción foto-redox de alilación de aldehídos orgánicos.

Finalmente, este capítulo se resume con las siguientes conclusiones:

- Un nuevo método foto-redox catalizado por cobalto para la síntesis de alcoholes homoalílicos ha sido desarrollado y optimizado para sustratos selectos.
- El método requiere solamente una cantidad catalítica de dos complejos de metales de transición, una amina básica en cantidad estequiométrica como agente reductor y luz visible común (LED azul 450 nm).



- La reacción es efectiva para sustratos aromáticos y heterociclos, sin embargo, con aldehídos alifáticos la reactividad se reduce.



Universitat d'Alacant  
Universidad de Alicante



A photograph of a desk with various office supplies. In the center, there is a calculator. To the left, there is a stack of books and a yellow notebook. To the right, there are two glass pens holders filled with pens and pencils, and a small wooden desk organizer. The background shows a window with blinds. The word "BIOGRAPHY" is overlaid in the center of the image.

**BIOGRAPHY**

Universitat d'Alacant  
Universidad de Alicante



Universitat d'Alacant  
Universidad de Alicante

I was born in La Nucía (Alicante) on July 1<sup>st</sup>, 1990.

I took my Primary Studies at "C.P. San Rafael" first school in La Nucía. Later I continued my High School Studies at "IES La Nucía" in the same locality finishing them in 2008.

Then, I moved to San Vicente del Raspeig (Alicante) in 2008 to start my bachelor's degree in Chemistry at Faculty of Science, University of Alicante, graduating in 2014.

In 2015, I worked at SIGGO (Quality and Scientific Management) for 3 months as analytical chemist in Altea (Alicante), later I continued my studies with a master's degree in teaching for secondary and high school studies by the University of Miguel Hernández in Elche (Alicante) graduating in 2016.

In September of 2016 I joined to the Department of Organic Chemistry at the University of Alicante to work full-time in the research group of Prof. Carmen Nájera Domingo and José Miguel Sansano Gil.

From September to December 2018 I moved to Bologna (Italy) thanks to 3 months stay abroad fellowship grant from University of Alicante at the Department of Chemistry Giacomo Ciamician at the University of Bologna under supervision of Prof. Pier Giorgio Cozzi.

During this last year, at the end of this thesis, I combined the writing of this thesis with teaching at High School "IES Rafal" in Rafal (Alicante) as teacher of Physics and Chemistry until June 2020.

At the end of 2020 is expected the defense of the Doctoral Thesis.



Universitat d'Alacant  
Universidad de Alicante